

School of Pharmacy

Development of Novel Carriers for Transdermal Delivery of Peptides

Sarika M Namjoshi

**This thesis is presented for the Degree of
Doctor of Philosophy
of
Curtin University of Technology**

December 2009

Declaration

To the best of my knowledge and belief this thesis contains no material previously published by any other person except where due acknowledgment has been made.

This thesis contains no material which has been accepted for the award of any other degree or diploma in any university.

Signature:

Date:

TABLE OF CONTENTS

TABLE OF CONTENTS.....	I
LIST OF FIGURES	VII
LIST OF TABLES	XI
ABSTRACT.....	XII

Chapter 1.	1
------------------------	----------

Introduction.....	1
--------------------------	----------

<i>1.1 Skin barrier properties and function.....</i>	<i>3</i>
--	----------

<i>1.2 Endogenous Peptides – Activity and therapeutic uses in human skin.....</i>	<i>5</i>
---	----------

<i>1.2.1 Human skin diseases and relevant therapeutic peptides.....</i>	<i>5</i>
---	----------

<i>1.2.1.1 Atopic Dermatitis (AD).....</i>	<i>5</i>
--	----------

<i>1.2.1.2 Psoriasis</i>	<i>6</i>
--------------------------------	----------

<i>1.2.1.3 Wound Healing</i>	<i>9</i>
------------------------------------	----------

<i>1.2.1.4 Viral disease.....</i>	<i>15</i>
-----------------------------------	-----------

<i>1.2.1.5 Human epithelial cancer.....</i>	<i>15</i>
---	-----------

<i>1.2.1.6 Peptides as cosmeceuticals.....</i>	<i>15</i>
--	-----------

<i>1.3 Strategies to enhance delivery of peptides across the skin.....</i>	<i>18</i>
--	-----------

<i>1.3.1 Skin penetration of peptides</i>	<i>19</i>
---	-----------

<i>1.3.2 Optimisation of formulation and peptide characteristics.....</i>	<i>19</i>
---	-----------

<i>1.3.2.1 Percutaneous Penetration Enhancers.....</i>	<i>19</i>
--	-----------

<i>1.3.2.2 Encapsulation</i>	<i>20</i>
------------------------------------	-----------

<i>1.3.2.3 Chemical modification.....</i>	<i>21</i>
---	-----------

<i>1.3.2.4 Effect of hydration</i>	<i>22</i>
--	-----------

<i>1.3.3 Physical Energy Application.....</i>	<i>23</i>
---	-----------

<i>1.3.3.1 Iontophoresis</i>	<i>23</i>
------------------------------------	-----------

<i>1.3.3.2 Electroporation.....</i>	<i>25</i>
-------------------------------------	-----------

<i>1.3.3.3 Sonophoresis</i>	<i>26</i>
-----------------------------------	-----------

<i>1.3.3.4 Photomechanical waves</i>	<i>27</i>
--	-----------

<i>1.3.3.5 Magnetic energy.....</i>	<i>27</i>
-------------------------------------	-----------

<i>1.3.4 Minimally invasive strategies for enhancing delivery.....</i>	<i>29</i>
--	-----------

1.3.4.1	Microneedles	29
1.3.4.2	Jet injectors	30
1.3.5	<i>Stratum corneum ablation</i>	30
1.3.5.1	Laser ablation	30
1.3.5.2	Radiofrequency (RF) thermal ablation.....	30
1.3.5.3	Suction blister ablation.....	31
1.3.5.4	Thermal poration.....	31
1.3.5.5	Combination of technologies	31
1.4	<i>Lipopeptides and lipoamino acid conjugation approaches to enhance the stability and delivery of peptides across biological barriers</i>	32
1.5	<i>Peptides as dermatological and cosmetic agents</i>	41
1.5.1	<i>Small peptides as cosmeceuticals</i>	41
1.5.2	<i>Small peptides as dermatologicals</i>	42
1.6	<i>Tetrapeptide conjugates as treatment options in psoriasis</i>	44
1.7	<i>Anti-inflammatory peptides in skin diseases</i>	46
1.8	<i>Significance and objective</i>	48

Chapter 2.50

Permeability of a Model Dipeptide (Ala-Trp) Across Human Epidermis: Effect of Pulsed Electromagnetic Energy50

2.1	<i>AIM</i>	51
2.2	<i>Materials and Methods</i>	51
2.2.1	<i>Chemicals</i>	51
2.2.2	<i>HPLC instrumentation and conditions</i>	51
2.2.3	<i>HPLC analysis and validation</i>	52
2.2.4	<i>Stability study</i>	52
2.2.5	<i>Human skin preparation</i>	53
2.2.6	<i>Skin permeation of Ala-Trp</i>	53
2.2.7	<i>Extraction of Ala-Trp from the epidermis and mass balance</i> ...	54
2.2.8	<i>Statistical Analysis</i>	55
2.3	<i>Results and Discussion</i>	55
2.3.1	<i>Chromatography</i>	55

2.3.2	<i>Stability of the dipeptide in solution</i>	58
2.3.3	<i>Permeation of Ala-Trp through human epidermis with Dermaportation</i>	61
2.4	<i>Conclusion</i>	64

Chapter 3.67

Skin Permeability and Biological Activity of a Therapeutic Peptide and its Lipoamino Acid Conjugates67

3.1	<i>Aim and Brief Background</i>	68
3.2	<i>Materials and Methods</i>	68
3.2.1	<i>Chemicals</i>	68
3.2.2	<i>Peptide synthesis</i>	69
3.2.2.1	General.....	69
3.2.2.2	Lipoamino acid synthesis.....	69
3.2.2.3	Synthesis of Nle(C6-Laa)-Ala-Ala-Pro-Val-NH ₂	70
3.2.3	<i>HPLC instrumentation and conditions</i>	75
3.2.4	<i>HPLC analysis</i>	76
3.2.4.1	Linearity.....	76
3.2.4.2	Precision.....	76
3.2.4.3	Intra-day repeatability.....	77
3.2.4.4	Inter-day repeatability.....	77
3.2.4.5	Lower limit of detection (LOD).....	77
3.2.4.6	Lower limit of quantification (LOQ).....	77
3.2.5	<i>Formulation approaches and duration of skin hydration</i>	78
3.2.5.1	Selection of vehicle and effect of concentration.....	78
3.2.5.2	Skin hydration.....	78
3.2.6	<i>Skin Stability (metabolism) experiment</i>	78
3.2.7	<i>Human skin preparation</i>	79
3.2.8	<i>Skin permeation of tetrapeptide and lipoamino acid conjugates</i>	79
3.2.9	<i>Mass balance and recovery</i>	80
3.2.10	<i>Surface tension measurement</i>	81
3.2.11	<i>Elastase inhibition assays</i>	82
3.2.12	<i>Assay optimization</i>	82

3.2.12.1	Dilution of reaction buffer	82
3.2.12.2	Preparation of standard concentration of the Inhibitors.....	83
3.2.12.3	Preparation of DQ elastin working standard solution.....	83
3.2.12.4	Preparation of enzyme working solution	83
3.2.12.5	Reaction mixture	83
3.2.13	<i>Statistical analysis</i>	84
3.3	<i>Results and discussion</i>	84
3.3.1	<i>Chromatography</i>	84
3.3.1.1	AAPV.....	84
3.3.1.2	C6(D), C6(L) and C6(D,L)-LAA-AAPV.....	85
3.3.1.3	C8(D,L)-LAA-AAPV	89
3.3.1.4	C10 (D,L)-LAA-AAPV	91
3.3.2	<i>Skin stability of tetrapeptide and lipoamino acid conjugates of the tetrapeptide</i>	97
3.3.3	<i>In-vitro skin diffusion of tetrapeptide and lipoamino acid conjugates across human epidermis</i>	98
3.3.3.1	Preliminary experiments to determine final protocol.....	99
3.3.3.2	AAPV, C6(L)-LAA-AAPV, C6(D)-LAA-AAPV and C6(D,L)-LAA-AAPV	102
3.3.3.3	C8(D,L)-LAA-AAPV	107
3.3.3.4	C10(D,L)-LAA-AAPV and C10(D)-LAA-AAPV.....	111
3.3.3.5	Consolidated comparison of skin permeation enhancement by lipoamino acid conjugated tetrapeptide	114
3.3.4	<i>Recovery of tetrapeptide and lipoamino acid conjugates from skin</i>	116
3.3.5	<i>Surface activity</i>	119
3.3.6	<i>Enzyme inhibitory activity</i>	121
3.4	<i>Conclusions</i>	124

Chapter 4. 126

Trans-epidermal Permeation of a Cosmetic Peptide and its Lipoamino Acid Conjugate 126

4.1	<i>Aim and Background</i>	127
4.2	<i>Materials and methods</i>	127
4.2.1	<i>Chemicals</i>	127

4.2.2	<i>HPLC instrumentation and conditions</i>	128
4.2.3	<i>HPLC analysis</i>	129
4.2.3.1	Assay precision	129
4.2.3.2	Minimum detectable limits and low limit of quantitation.....	129
4.2.4	<i>Preparation of human skin</i>	129
4.2.5	<i>In-vitro skin permeation of acetyl hexapeptide-3 and its lipoamino acid conjugate</i>	130
4.2.6	<i>Skin accumulation, mass balance and recovery of peptides from the skin</i>	130
4.3	<i>Results and discussion</i>	131
4.3.1	<i>Chromatography and resolution</i>	131
4.3.1.1	Linearity	133
4.3.1.2	Assay precision	134
4.3.1.3	LOD and LOQ	134
4.3.2	<i>Permeation of acetyl hexapeptide-3, C12(A) and C12(B) conjugated hexapeptide across human epidermis</i>	135
4.3.3	<i>Recovery and skin extraction of acetyl hexapeptide-3 and C12-LAA from the epidermis</i>	136
4.4	<i>Conclusions</i>	139

Chapter 5.....140

Skin Permeation of an Anti-inflammatory Peptide and Analogues Exhibiting Improved Biological Efficacy and Specificity.....140

5.1	<i>Aim</i>	141
5.2	<i>Materials and methods</i>	141
5.2.1	<i>Chemicals</i>	141
5.2.2	<i>HPLC instrumentation and conditions</i>	142
5.2.3	<i>HPLC analysis</i>	142
5.2.3.1	Assay precision	142
5.2.3.2	Lower limit of detection (LOD) and quantitation (LOQ)	143
5.2.4	<i>Skin stability study</i>	143
5.2.5	<i>Preparation of human skin</i>	144
5.2.6	<i>Formulation optimization</i>	144

5.2.7	<i>In-vitro skin diffusion of C1, C1-L and CP</i>	145
5.2.8	<i>Recovery of the peptides from the epidermis</i>	145
5.2.9	<i>Statistical analysis</i>	146
5.3	<i>Results and discussion</i>	146
5.3.1	<i>Chromatography</i>	146
5.3.1.1	<i>Linearity</i>	148
5.3.1.2	<i>Assay precision</i>	149
5.3.1.3	<i>Low limit of detection and low limit of quantitation</i>	150
5.3.2	<i>Stability of C1, C1-L and CP</i>	150
5.3.3	<i>In-vitro permeation of C1, C1-L and CP across human epidermis</i>	151
5.3.4	<i>Recovery and mass balance</i>	157
5.4	<i>Conclusions</i>	158

Chapter 6.	159
Summary and Conclusions.	159
Chapter 7.	165
References.	165
Chapter 8.	191
Appendix.	191

LIST OF FIGURES

Figure 1.1	Sites of solute action below the skin after topical application ⁷	3
Figure 1.2	Structure of human skin	4
Figure 1.3	Development of psoriatic skin lesions ³⁰	7
Figure 1.4	Diagrammatic representation of the stratum corneum and the intercellular and transcellular routes of penetration ⁸⁹	18
Figure 1.5	How hydration increases the fluidity of the stratum corneum lipids by insertion of water molecules between polar head groups ¹⁰⁷	22
Figure 1.6	Infosys system: patient controlled analgesia by iontophoresis enhanced transdermal fentanyl delivery (Alza corp)	24
Figure 1.7	The basic design of ultrasonic delivery devices (A) Drug is placed on the skin beneath the ultrasonic probe. Ultrasound pulses are passed through the probe and drug molecules are hypothesized to move into the skin through a combination of physical wave pressure and permeabilisation of intercellular bilayers. (B) The formation of bubbles in the intercellular lipid space caused by cavitation increases bilayer fluidisation and resultant permeability ⁹⁶	26
Figure 1.8	Schematic of PEMF Dermaportation waveform.....	28
Figure 1.9	Images of microneedles used for transdermal drug delivery ¹³³	29
Figure 1.10	Lipoamino acid conjugate of methotrexate ¹⁴⁹	37
Figure 1.11	Structure of Endo 1 and C12-LAA-Endo 1 ¹⁵¹	38
Figure 1.12	Phe-Gly and its acyl derivatives ¹⁵³	40
Figure 2.1	Schematic of skin diffusion experimental cell with Dermaportation coil in place.....	54
Figure 2.2	Chromatograms for Ala-Trp analyzed after 8h (a) Dermaportation (96.49 $\mu\text{g}/\text{cm}^2$) and (b) Passive (2.77 $\mu\text{g}/\text{cm}^2$).....	57
Figure 2.3	Chromatogram for Ala-Trp and degradation product analyzed after 3h when the sample was incubated with skin.....	59
Figure 2.4	Ala-Trp degradation profile in solution at varying conditions.....	60
Figure 2.5	Cumulative penetration of dipeptide (1 mg/mL) across human epidermis for passive (\blacktriangle) or Dermaportation (\bullet) applied from 0-4h (mean \pm SEM: n=9).....	62
Figure 3.1	Chemical structure of AAPV.....	72
Figure 3.2	Chemical structure of L-C6-LAA-AAPV conjugate.....	72
Figure 3.3	Chemical structure of L-C8-LAA-AAPV conjugate.....	73

Figure 3.4	Chemical structure of L-C10-LAA-AAPV conjugate.....	73
Figure 3.5	Molecular models of (a) (R) C6-LAA-AAPV, (b) (S) C8-LAA-AAPV and (c) (R) C10-LAA-AAPV.....	75
Figure 3.6	Chromatogram of 125 µg/mL standard of AAPV	85
Figure 3.7	Chromatogram of 15.62 µg/mL standard of C6(D)-LAA-AAPV	86
Figure 3.8	Chromatogram of 25 µg/mL standard of C6(L)-LAA-AAPV from UQ.....	87
Figure 3.9	Chromatogram of 30 µg/mL standard of C6(D,L)-LAA-AAPV	89
Figure 3.10	Chromatogram of 100 µg/mL standard of C8(D,L)-LAA-AAPV from UQ.....	90
Figure 3.11	Chromatogram of 62.5 µg/mL standard of C8(D,L)-LAA-AAPV from GLS Biochem.....	91
Figure 3.12	Chromatogram of 100 µg/mL standard of C10(D,L)-LAA-AAPV from UQ.....	92
Figure 3.13	Chromatogram of 50 µg/mL standard of C10(D,L)-LAA-AAPV from GLS Biochem.....	93
Figure 3.14	Degradation profile of tetrapeptide and its lipoamino acid conjugates.....	97
Figure 3.15	Permeation profile of cumulative amount vs. time of C6(D,L)-LAA-AAPV (racemic mixtures) vs. AAPV across human epidermis. Results are expressed as mean (±SEM).....	100
Figure 3.16	Cumulative amount vs. time of AAPV and its C10 lipoamino acid conjugate across human epidermis at a donor concentration of 3 mg in 300 µL propylene glycol. Results are expressed as mean (±SEM: n=6).....	101
Figure 3.17	Permeation profiles for individual C6(D) and C6(L) diastereomers (3mg in 300µL propylene glycol) across human epidermis from 0-24h. Results are expressed as mean (±SEM: n=3).....	102
Figure 3.18	Comparison of cumulative permeation of C6(L)-LAA-AAPV and C6(D)-LAA-AAPV vs. AAPV across human epidermis. Mean (±SEM: n=3).....	104
Figure 3.19	Cumulative amount vs. time of C6(D)-LAA-AAPV, C6(L)-LAA-AAPV (racemic mixture) and AAPV across human epidermis Results are expressed as mean (±SEM: n=9).....	105
Figure 3.20	Comparison of cumulative permeation of C6(D) and C6(L) individual diastereomers (n=3) vs. C6(D,L)-LAA-AAPV racemic mixture (n=9) and AAPV (n=7) across human epidermis at a donor concentration of 3mg in 300 µL propylene glycol. Results are expressed as mean (±SEM).....	106

Figure 3.21	Permeation profiles of the tetrapeptide and lipotetrapeptide [C8(D,L)-LAA-AAPV) racemic mixture across human epidermis at a donor concentration of 3mg in 300 μ L propylene glycol. Results are expressed as mean (\pm SEM: n=3 for C8(D,L)-LAA-AAPV and n=7 for AAPV).....	108
Figure 3.22	Cumulative permeation of C8(D,L)-LAA-AAPV (n=7) and AAPV (n=4) across human epidermis with 24h hydration. Mean (\pm SEM)	109
Figure 3.23	Permeation profiles of C8(D,L)-LAA-AAPV racemic mixture and AAPV at a donor concentration of 6 mg in 300 μ L PG. Results are expressed as mean (\pm SEM:n=4)	110
Figure 3.24	Cumulative amount vs. time permeation of C10(D,L)-LAA-AAPV and AAPV at a donor concentration of 6 mg in 300 μ L PG across human epidermis. Results are expressed as mean (\pm SEM, n=4).....	112
Figure 3.25	Cumulative penetration of C10(D,L)-LAA-AAPV and AAPV across human epidermis with 24h hydration. Results are expressed as mean (\pm SEM: n=4).....	113
Figure 3.26	Permeation profiles of AAPV and its lipoamino acid conjugates across human epidermis. Results are expressed as mean (\pm SEM)	114
Figure 3.27	Amount of AAPV and its lipoamino acid conjugates in the skin after the permeation experiments (Donor concentration of 3mg peptide/lipopeptide in 300 μ L PG) and 1 h hydration. Results are expressed are mean (\pm SEM: n=4)	117
Figure 3.28	Amount of AAPV and its lipoamino acid conjugates in the skin after the permeation experiments (Donor concentration of. 3mg peptide/lipopeptide in 300 μ L PG) and 24 h hydration. Results are expressed are mean (\pm SEM: n=4)	118
Figure 3.29	Amount of AAPV and its lipoamino acid conjugates in the skin after the permeation experiments (Donor concentration of. 6mg peptide/lipopeptide in 300 uL PG) and 24 h hydration. Results are expressed are mean (\pm SEM: n=4)	118
Figure 3.30	Surface tension measurement of the native tetrapeptide and the conjugated lipopeptides. Results are expressed as mean (\pm SEM) of 3 measurements.....	120
Figure 3.31	Percent inhibition of elastase by tetrapeptide and its lipoamino acid conjugates. (a) and (C) inhibition at 6.25 μ g/mL of substrate and 0.25 U/mL elastase, (B) inhibition at 25 μ g/mL of substrate and 0.5 U/mL elastase	123
Figure 4.1	Chemical structure of acetyl hexapeptide-3 and C12-LAA conjugates.....	128
Figure 4.2	Typical chromatograms of (a) acetyl hexapeptide-3 (10.4 μ g/mL in PBS) eluted at 9.8 min (b) C12(A)-LAA-hexapeptide-3 (83.3 μ g/mL in PBS) eluted at 12.1 min and (c) C12(B)-LAA-hexapeptide-3 (83.3 μ g/mL in PBS) eluted at 13.2 min.....	133
Figure 4.3	Permeation profile of acetyl hexapeptide-3 across human epidermis. Results are expressed as mean (\pm SEM: n=5).....	135

Figure 4.4	Amount of native peptide and conjugates remaining in epidermal membrane at 48 h.....	137
Figure 5.1	Chromatograms for (a) CP at 62.5 µg/mL, (b) C1-L at 64.5 µg/mL and (c) C1 at 60.93 µg/mL.....	148
Figure 5.2	Degradation profiles of CP, C1 and C1-L	150
Figure 5.3	Permeation profiles for individual C1, C1-L and CP across human epidermis from 0-48h. Results are expressed as mean (±SEM: n=6 for C1, n=4 for C1-L and n=6 for CP).....	152
Figure 5.4	Permeation profiles for C1, C1-L and CP across human epidermis from 0-154h. Results are expressed as mean (±SEM: n=3 for C1-L and C1, n=4 for CP)	154
Figure 5.5	Amount of C1-L, CP and C1 in the skin after (a) 8 h (n=3) and (b) 48 h (n=4). Results are expressed as mean (± SEM).....	157
Figure 6.1	Optimization of peptide delivery	161

LIST OF TABLES

Table 1-1	Biological activity of various endogenous and synthetic peptides ...	11
Table 1-2	Lipoamino acid/lipophilic conjugation of peptides.....	34
Table 2-1	Rate of degradation of Ala-Trp at different temperatures and conditions	64
Table 2-2	Rate of permeation of dipeptide and degradation product with Dermaportation and passive diffusion. Data are mean (\pm sem, n=9).....	65
Table 2-3	...in permeation of Ala-Trp with Dermaportation and passive diffusion.....	65
Table 3-1	Correlation coefficient of tetrapeptide and its conjugates	93
Table 3-2	Assay precision, Intra-day and Inter-day variations of AAPV and its lipoamino acid conjugates	94
Table 3-3	Percent degradation of AAPV and its lipoamino acid conjugates (Mean, n=3, \pm SEM).....	97
Table 3-4	Comparison of permeation parameters of the native and conjugated peptides(flux calculated till 8 and 24 h for C6(D) and C6(L)-LAA-AAPV individual diastereomers).....	114
Table 4-1	Correlation coefficients of the native peptide and its lipoamino acid conjugates	132
Table 4-2	Intra-day and Inter-day variations of acetyl hexapeptide-3 and its lipoamino acid conjugates	133
Table 5-1	Peptide sequences and code.....	141
Table 5-2	Correlation coefficient of C1, C1-L and CP	148
Table 5-3	Assay precision, Intra-day and Inter-day variations of C1, C1-L and CP.....	148
Table 5-4	Comparison of permeation parameters of C1, C1-L and CP over 48 h.....	152
Table 5-5	Comparison of permeation parameters of C1, C1-L and CP over 6 days.....	153

ABSTRACT

Recent developments in genetic engineering and biotechnology have resulted in an increase in availability of therapeutic peptides and small anti-cytokines. Oral administration is inappropriate as these molecules are unstable in the gastrointestinal tract and are subject to hepatic first-pass effect. Transdermal delivery is an attractive alternative as the skin exhibits less enzymatic activity and allows for a controlled, sustained local therapeutic drug concentration over a prolonged period of time. However, the skin's lipophilic *stratum corneum* acts as a major barrier to the delivery of hydrophilic molecules, including peptides, resulting in lack of efficacy of these compounds if applied topically. Considerable research effort has been focussed on the development of skin penetration enhancement techniques. However, many of these techniques have been limited by insufficient penetration enhancement and/or induced irritancy.

We have investigated three approaches to enhance the delivery of peptides that have therapeutic or cosmetic effect in the skin. These approaches include the use of physical energy to enhance the delivery of Alanine-Tryptophan (Ala-Trp), lip amino acid (LAA) conjugation to increase the permeability of a HNE inhibitor Ala-Ala-Pro-Val (AAPV) and a cosmetic peptide, acetyl hexapeptide-3 and cyclisation to enhance the delivery of a core peptide (CP) which has anti-inflammatory activity.

In vitro permeation studies across human epidermis were performed in Pyrex glass Franz-type diffusion cells. Ala-Trp was selected as a small molecular weight model dipeptide to study the penetration enhancement effects of Dermaportation, which is a newly developed pulsed electro magnetic field (PEMF) technology. The dipeptide was found to be unstable on exposure to skin at 37°C and Dermaportation (Pulsed electromagnetic field technology) *significantly* increased the *in vitro* permeability coefficient of Ala-Trp across human epidermis from 7.7×10^{-4} cm/h with passive diffusion to 1.94×10^{-2} cm/h with Dermaportation over an 8 h period. Dermaportation thus may provide an effective means of delivering molecules that are highly susceptible to degradation like dipeptides, in higher amounts and in a relatively short duration.

The effectiveness of coupling a short chain lipoamino acid to enhance trans-epidermal delivery of a model human neutrophil elastase (HNE) inhibitor (Ala-Ala-Pro-Val) was assessed. The optimal conjugate structure for skin penetration and biological activity of this therapeutic peptide with anti-inflammatory activity was determined. In order to enhance the trans-epidermal delivery of the peptide, lipophilic derivatives with LAAs of chain length C6, C8, and C10 were prepared by solid phase synthesis. Conjugation to a C6-LAA enhanced epidermal permeability of the tetrapeptide. Stereoselective permeation of the lipopeptide diastereomers across the human epidermis was observed. The amount of C6(D)-LAA-AAPV ($467.94 \mu\text{g}/\text{cm}^2$) was *significantly* higher than C6(L)-LAA-AAPV ($123.04 \mu\text{g}/\text{cm}^2$). The same was observed with C8(D)-LAA-AAPV. The effect of donor concentration and skin hydration on skin permeability of C8(D,L)-LAA-AAPV and C10(D,L)-LAA-AAPV was also assessed and it was observed that there was higher permeation of C10(D,L)-LAA-AAPV at a higher donor concentration. The lipoamino acid conjugates were more stable than the native tetrapeptide and biological activity was retained after coupling of the tetrapeptide to C6, C8 and C10 LAA.

A cosmetic peptide, acetyl hexapeptide-3 was coupled to individual diastereomers of C12 (A)-LAA and C12 (B)-LAA. The preliminary study was designed to assess the effect of coupling of a LAA of higher molecular weight on the transepidermal permeation and accumulation of this hexapeptide. Accumulation of these peptides in the skin was also quantified. Detectable amounts of C12(A)-LAA-hexapeptide-3 and C12(B)-LAA-hexapeptide-3 were not found in the receptor solution but higher quantities of these conjugates were found to be retained in the skin. The amount of C12(B)-LAA-hexapeptide-3 ($59.92 \mu\text{g}/\text{cm}^2 \pm 10.64$) in the epidermis was highest followed by C12(A)-LAA-hexapeptide-3 ($33.06 \mu\text{g}/\text{cm}^2 \pm 3.70$) and acetyl hexapeptide-3 ($12.64 \mu\text{g}/\text{cm}^2 \pm 1.48$).

Lastly, skin permeability and in skin stability of an anti-inflammatory peptide (core peptide: CP) and two analogues that have demonstrated improved biological efficacy and specificity: a cyclic peptide sequence (C1) and its linear sequence counterpart (C1-L) were assessed. The stability of C1 and C1-L was *significantly* higher as compared to CP when placed in contact with skin at 37°C . The epidermal penetration of the core anti-inflammatory peptide improved after cyclisation. The order of

permeation of the analogues was C1>C1-L>CP after 48h and 6 days. The amount of peptide retained in the skin was higher after 48h as compared to 8h due to greater partitioning of these peptides in the skin.

This work demonstrates the enhancement effects of these three techniques to optimize the transdermal/topical permeation of therapeutic and cosmetic peptides.

Chapter 1.
Introduction

The advances in synthetic chemistry and molecular biology techniques over the past years have resulted in the application of peptides or peptide-like drugs becoming a growing field in therapeutics.¹ A number of peptides and proteins have been approved by the regulatory authorities for medical use in cardiovascular disorders, incontinence, cancer, viral infections, calcium metabolism, immunity, inflammation, diabetes, homeostasis and obesity. Currently parenteral injection is the most frequent mode of administration for protein and peptide drugs as they are unstable if given orally. Most proteins and peptides have short plasma half-lives, thus requiring frequent injections therefore an alternative delivery mode that can offer controlled release is more attractive. Hence current research is focused on finding alternative routes of delivery, including inhaled, buccal, intranasal and transdermal routes as well as novel delivery systems.² Transdermal delivery is an attractive option for the delivery of peptides for a number of reasons: it avoids first-pass degradation in the liver or GIT and the skin exhibits less enzymatic activity than the other routes of administration. In addition, whilst most proteins and peptides are intended for systemic action, many peptides have potential therapeutic or cosmetic value if they can be locally administered to target sites within the skin.³ Figure 1.1 describes the various sites of solute action after topical application to the skin. Therapeutic targets within the skin and underlying tissues vary according to disease localization and other factors. For instance, penetration of active ingredient to the depth of *stratum corneum* only is desired for sunscreens and insect repellants⁴. Treatment of acne requires drug targeting of pilosebaceous structures and in psoriasis therapeutic drug levels should be attained in deeper epidermal layers.⁵ Antimicrobial peptides (AMPs) are one class of peptides which may have potential in the management of atopic dermatitis, psoriasis and skin infections. A number of peptides are incorporated in cosmeceutical products, particularly those marketed for anti ageing. To be effective as either therapeutic or cosmetic skin care products or for systemic action, the applied peptide must reach its target site, either within the skin or systemically, in sufficient quantity to generate a therapeutic response and this requires overcoming the considerable barrier properties of the skin.⁶

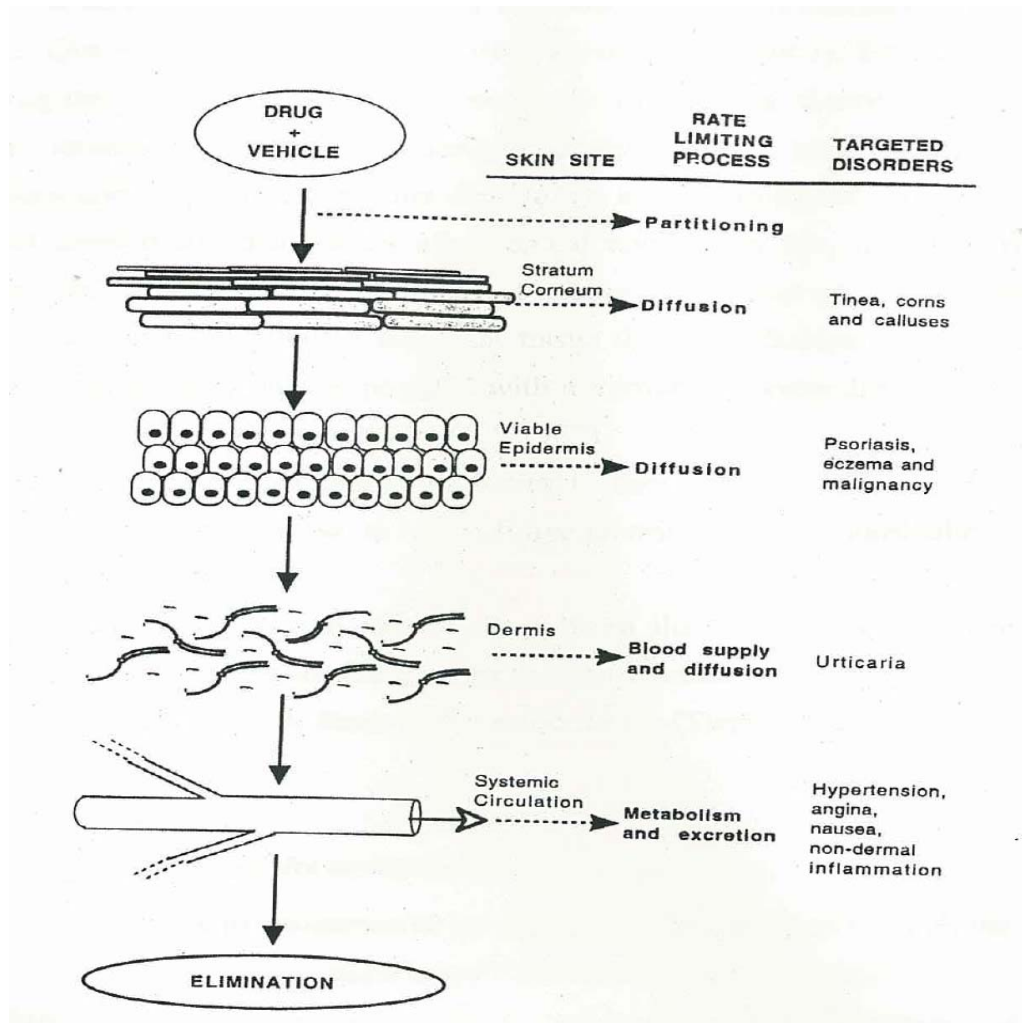


Figure 1.1 Sites of solute action below the skin after topical application⁷

1.1 Skin barrier properties and function

The skin is one of the most extensive and readily accessible organs of the human body with at least five different cell types contributing to its structure, and other cell types from circulatory and immune systems being transient residents of the skin.⁸ It receives about one-third of the blood circulation through the body.⁹ Its primary function is protection, including physical, chemical, immune, pathogen, UV radiation and free radical. For the purpose of transdermal drug delivery, human skin can be categorised into four main layers: the innermost hypodermis or subcutaneous fat layer, the overlying dermis, the viable epidermis and the outermost layer of the skin, the *stratum corneum* (Figure 1.2).

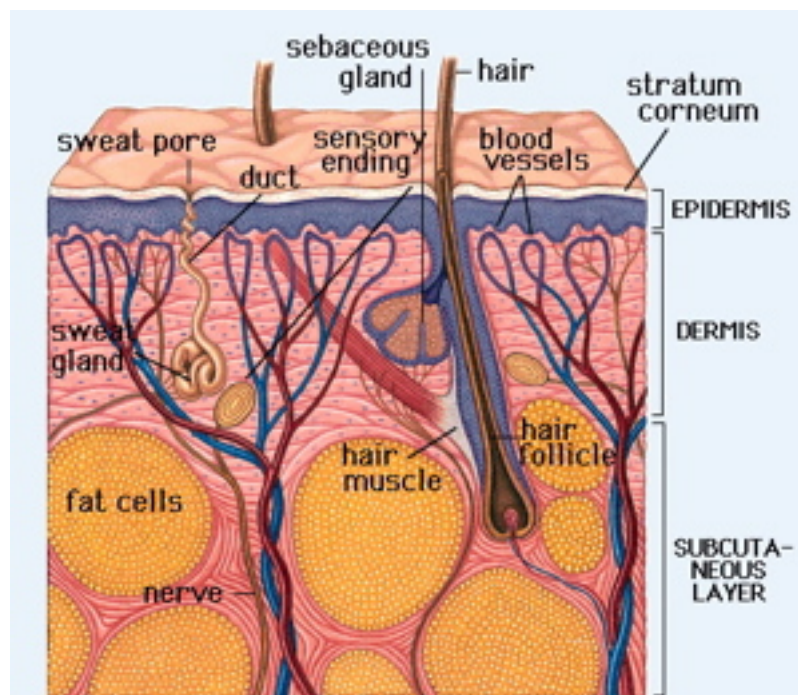


Figure 1.2 Structure of human skin

The dermis (or corium) is typically 3–5 mm thick and is the major component of human skin. It is composed of a network of connective tissue, predominantly collagen fibrils providing support and elastic tissue providing flexibility, embedded in a mucopolysaccharide gel. In terms of transdermal drug delivery, this layer is often viewed as essentially gelled water, and thus provides a minimal barrier to the delivery of most polar drugs, although the dermis may be significant when delivering highly lipophilic molecules.¹⁰

The epidermis, is approximately 100 to 150 μm thick and contains four histologically distinct layers which, from the inside to the outside, are the stratum germinativum, stratum spinosum, stratum granulosum and the *stratum corneum*.¹⁰ The *stratum corneum* (or horny layer) is the final product of epidermal cell differentiation, and though it is an epidermal layer it is often viewed as a separate membrane in topical and transdermal drug delivery studies. Typically, the *stratum corneum* is around 10 μm thick when dry, although it may swell to several times this thickness when hydrated.¹⁰ It is a nonviable, desiccated layer that acts as a first line of defense against invading microorganisms¹¹ and contributes significant resistance to molecular transport both from and into the body.¹² It is 10–15 cell layers thick over much of the body and, although histologic sections demonstrate wide separations

between corneocytes (the so-called "basket-weave" appearance), this is an artifact and the cells are actually tightly held to each other. The intercellular spaces between corneocytes are filled with stacked sheets of lipid bilayers whose organization and chemical composition confer a high degree of water impermeability. It is these lipid lamellae that constitute the epidermal permeability barrier, both to water and to other foreign materials.¹³

1.2 Endogenous Peptides – Activity and therapeutic uses in human skin

This physical skin barrier is susceptible to injuries or may be compromised by some diseases that allow the entry of opportunistic microbial agents into the skin.¹⁴ When these microorganisms gain access to the otherwise sterile internal environment, they activate a complex immune defence system.¹⁵ Human skin is also known to produce antimicrobial agents that form an innate epithelial chemical shield.¹⁶ These endogenous antimicrobial peptides (AMPs) are produced by the epithelial surface of the host.¹⁵ Two major classes of peptides have been identified in mammalian skin: defensins and cathelicidins. These peptides act as effector molecules and exhibit activity against a broad range of microorganisms such as bacteria, fungi and viruses.¹⁷⁻¹⁹ They are also involved in host repair and adaptive immune responses. Many AMPs have recently been isolated, including lysozyme, RNase 7, elafin, psoriasin, dermicidin1L, granulysin, antileukoprotease and human cationic antimicrobial protein (hCAP18).^{17, 20} The AMP activity in the skin is summarised in Table 1-1.

1.2.1 Human skin diseases and relevant therapeutic peptides

1.2.1.1 Atopic Dermatitis (AD)

Atopic Dermatitis is a chronic inflammatory skin disease with abnormal expression or processing of AMPs.²¹ It is characterised by dry skin and involves non lesional skin and increased transepidermal water loss. *Staphylococcus aureus* can be isolated from skin lesions. The bacterium gains access to underlying viable skin layers due to skin barrier dysfunction, reduced skin lipid content, alkaline pH of the skin and increased deposition of fibrinectin and fibrinogen. About 30% of patients with AD

have bacterial or viral infections of the skin, which is more than the 7% infection rate with psoriasis.²² LL-37 and H β D-2 expression is greatly increased in patients with inflammatory skin conditions.^{19, 23} Furthermore, the AMPs that are normally induced in keratinocytes by inflammation show good antimicrobial activity against *S. aureus*, herpes simplex virus (HSV) and vaccinia virus.²⁴ This suggests that lack of AMP expression in AD might contribute to bacterial and viral infections associated with the disease. Keratinocytes in lesional AD exhibit evidence of cytokine and lymphokine modulation.²⁵ In addition, AD patients show reduced expression of DCD in their sweat. A marked reduction in viable bacterial cells on the skin surface of healthy individuals was observed after sweating, but not in patients with AD. Thus decreased DCD expression correlated with infection and therefore may contribute to the propensity of AD skin to recurrent bacterial and viral skin infections, and altered skin colonisation.²⁶

1.2.1.2 Psoriasis

Psoriasis is a condition of unknown aetiology characterized by epidermal hyperplasia, vascular alterations and inflammation.²⁷ Almost 2% of the population in western countries is affected by this disease and genetic factors are thought to be of fundamental importance in the expression of the disease. Many studies have been directed towards understanding the involvement of cytokines, growth factors and arachidonic acid derived mediators as potential candidates with a pathogenic role in cutaneous inflammation.^{27, 28} The protein psoriasin is highly upregulated in psoriatic epidermis and is most likely linked to the inflammatory stimuli.²⁷ Identification of the receptor or cellular target for this protein will facilitate the development of new strategies to block the local epidermal inflammatory response that characterizes psoriasis.²⁹

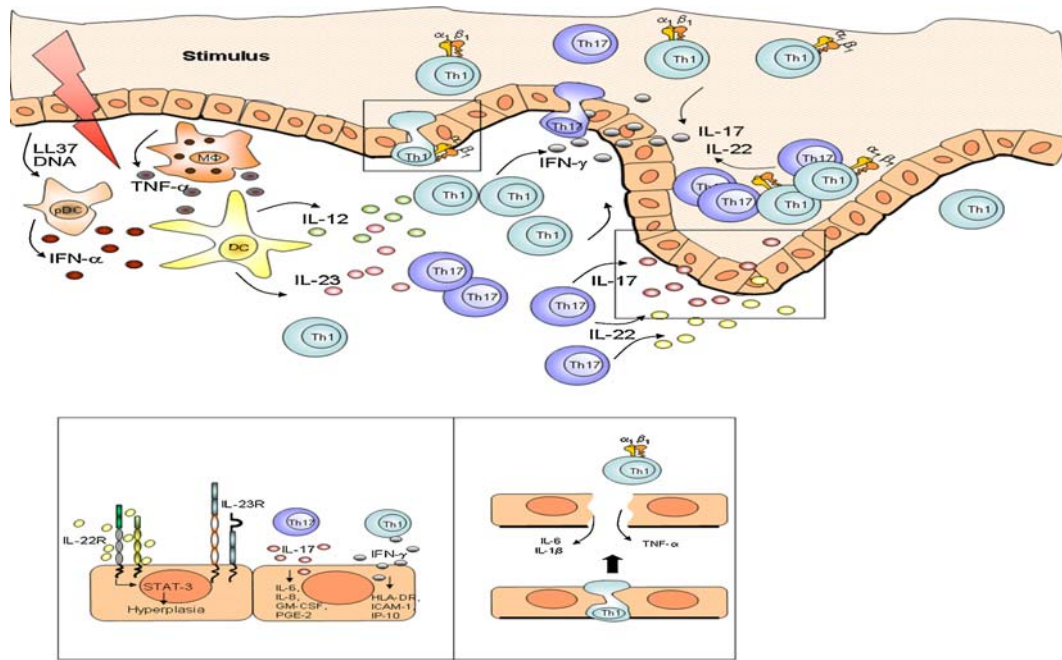


Figure 1.3 Development of psoriatic skin lesions³⁰

Expression of the peptide elafin is also elevated in the spinous layers of psoriatic skin.³¹ IL-1 β and TNF- α are thought to be the major inflammatory cytokines released from PMN in the early stages of acute inflammation³² (Figure 1.3) and it is suggested that over-expression of elafin may be caused by IL-1 β and TNF- α released by dermal neutrophils. In psoriatic skin this peptide functions as a protective agent against damage of the epidermis caused by neutrophil elastase.³³ Antileukoprotease like elafin, a potent serine protease inhibitor, is also present in psoriatic scales with a role in protecting the psoriatic epidermis against proteolytic degradation.

Peptide T analogue, D-[Ala]-Ser-Thr-Thr-Thr-Asn-Tyr-Thr-amide (DAPTA) has been shown to clear psoriasis lesions in clinical trials.³⁴ In this study it was seen that DAPTA significantly inhibited the monocyte and lymphocyte chemotactic properties of RANTES (a beta chemokine found in increased amount in psoriatic lesions).³⁴

ALP is present in psoriatic scales in concentrations sufficient for inhibition of neutrophil derived serine proteases human leukocyte elastase and cathepsin G.³⁵ Chronic inflammatory skin disorders could benefit from the development of serine protease inhibitors for use in therapy. The restitution of the HLE-HLE inhibitory balance in psoriasis may be of therapeutic value given that bathing in hypertonic solutions is known to remove HLE from the surface of psoriatic lesions.³⁵ In

microbiocidal assays recombinant ALP exhibited antimicrobial activity against several human skin associated microorganisms like *Pseudomonas aeruginosa*, *Staphylococcus aureus*, *Staphylococcus epidermidis* and *Candida albicans* indicating that ALP may actively participate in mechanisms allowing homeostasis of bacterial and yeast colonization on human skin.³⁶

IL-1 is of particular interest in psoriasis because of its ability to stimulate production of chemotactic cytokines. IL-6 and IL-8 may directly contribute to the epidermal hyperplasia seen in psoriatic lesions. TGF- α , which is required for the normal growth of epithelial cells, is over-expressed in psoriasis.³⁷ In addition EGF/TGF- α receptor expression is also increased in lesional epidermis.³⁸ LTB4 levels are also seen to be increased in lesional psoriatic skin. Neutrophil activating peptide-1/IL-8, which is responsible for the release of LTB4 has been isolated from psoriatic skin. This peptide shares homology with a number of peptides which have pro-inflammatory or growth stimulating activities, such as β thromboglobulin, platelet factor 4, γ -interferon and a peptide with melanoma growth stimulatory activity.³⁹

H β D 2 and H β D 3 have also been isolated from extracts of lesional scales of psoriatic skin¹⁸. In keratinocytes the expression of H β D2 is induced by IL-1 α , IL-1 β or *Pseudomonas aeruginosa*.¹⁸ IL-1 and H β D2 have a key role in epidermal defence during inflammation. It is known that secondary infection is rare in psoriasis. This has been attributed to the presence of a number of AMPs including granulysin which is known to be expressed in psoriatic plaques.^{40, 41} In addition, antimicrobial activity of lesional cytokines,⁴² defensin expression by keratinocytes and increased numbers of NK-T cells in lesions is likely to contribute to the bacterial resistance in psoriasis plaques. RNase 7 is another broad spectrum AMP present in normal skin and in elevated levels in psoriatic skin. Support for its antimicrobial defence action is strengthened by the observation that contact of keratinocytes with bacteria induced RNase 7 gene expression. In addition, peptide T analogue DAPTA, which inhibits the lymphocyte/monocyte chemotactic activities of RANTES, is expressed in high amounts in the keratinocytes of psoriatic tissue.³⁴

A better understanding of the role of these peptides may provide new strategies for the treatment of diseases like psoriasis and to prevent secondary infection in a number of skin conditions.⁴³ For example, the development of peptides structurally

related to AMPs and/or with a similar mode of action as psoriasin (Table 1-1) could be utilised. Antimicrobial peptides can also be artificially induced to fight skin infections. Another strategy could be to apply substances known to induce AMP synthesis or activity such as L-isoleucine and some structurally related molecules.⁴⁴

1.2.1.3 Wound Healing

The wound healing process involves four stages: inflammation, which involves the release of chemotactic agents; migration, where keratinocytes migrate from the wound edge towards the centre of the wound; deposition, which involves deposition of the matrix components in the dermis by fibroblasts and; maturation which involves contraction of the dermis and squamous differentiation of the keratinocytes on the wound surface. Cytokines act as mediators in all four phases of wound healing.⁴⁵ EGF, TGF and several other growth factors have been isolated from wounds and are known to promote keratinocyte growth and migration both in culture and in wounds.⁴⁶ In a murine model, the EGF-receptor-mediated signalling systems played an active part in epidermal wound repair: an increase in the number of EGF receptors precedes the hypertrophic response, and a decrease precedes the attenuation of this response.⁴⁷ Combinations of platelet derived growth factor (PDGF) with either IGF-1 or TGF- α have been shown to enhance connective tissue deposition, angiogenesis and collagen content and maturity.⁴⁸ Potent activators of keratinocytes such as IL-1 have an important role to play in the wound healing process. IGF-1 and TGF- α also induce or enhance the expression of the antimicrobial peptides/polypeptides hCAP-18, h β D-3, NGAL and SLPI in human keratinocytes thereby fighting potential secondary infection. TGF- α has also been shown to induce the expression of the same number of antimicrobial peptides/ polypeptides as the proinflammatory cytokine IL-1.⁴⁹ PMN-specific α -chemokine IL-8 is a major biologically active PMN attractant in wound fluid but prolonged IL-8 levels may also contribute to additional healing activities in the later phases of wound healing. A strong correlation between TNF- α levels and IL-8 levels in wound fluid has been found.⁵⁰

During the proteolytic remodelling of the extra cellular matrix, small soluble RGD-containing peptides are released into the matrix milieu.⁵¹ As these peptides are known to directly activate apoptosis they are likely to be especially helpful in

situations in which leukocyte accumulation and resistance to apoptosis contribute to disease pathology.⁵² They are useful in wound repair as they are internalized into a cell and are able to bind and activate caspase 3 inducing apoptosis.⁵¹

Copper peptides have also been used as wound healing agents.^{53, 54} For example, glycyl-L-histidyl-L-lysine-Cu (GHK) accelerates wound healing and stimulates biological events important in tissue repair such as angiogenesis, nerve outgrowth and chemoattraction of cells critical to healing (e.g., macrophages, monocytes, mast cells, capillary endothelial cells). A stimulating effect of GHK-Cu on collagen synthesis by fibroblasts has been reported.⁵⁴ Copper peptides have also been used in combination with retin A to reduce inflammation.⁵⁵ These agents improve healing after cosmetic procedures such as chemical peels, laser and dermabrasion procedures, where they are reported to decrease skin inflammation by increasing skin nutrient density.⁵⁵

Table 1-1 Biological activity of various endogenous and synthetic peptides

Peptide	Abbreviation	Source	Biological Activity	Reference
THERAPEUTIC PEPTIDES				
Adrenomedullin	AM	Keratinocytes of the epidermis and hair follicles, cells of the glands and secretory ducts of normal skin and in skin tumours of different histologies	Antibacterial and antifungal activity. May be involved in the wound repair process and functions as a growth regulator. Role in skin homeostasis, carcinogenesis and acne vulgaris	56
Alpha defensins	HNP-(1, 2, 3 and 4)	Neutrophil granules, macrophages, monocytes, T cells, paneth cell granules	Antimicrobial effect, macrophage phagocytosis, complement activation	57
Antileukoprotease	ALP	Human callus and detected in supernatants of cultured human primary keratinocytes	Antimicrobial activity against several microorganisms and maintains homeostasis	35, 36
Antiflammin-1 and Antiflammin-2		Synthetic nonapeptides	Potent anti-inflammatory action	58
Cathelicidin	LL37	Keratinocytes, epithelial cells, neutrophils, monocytes, T cells, Mast cells	Antimicrobial effect, cytokine and chemokine production by monocytes and keratinocytes	59
Copper peptides	e.g. Gly-His-Lys-Cu	Synthetic	Antioxidant, growth and regulation of hair follicles and increases collagen disposition	53

Dermicidin 1L	DCD 1L	Synthetic: recombinant dermcidin-1L was expressed in <i>Escherichia coli</i> as a fusion protein and purified by affinity chromatography	New class of potential broad-spectrum antimicrobial and anti-tumour drug	60
Elafin	SKALP	Isolated from psoriatic skin	Specific inhibitor of human leukocyte elastase (HLE), porcine pancreatic elastase (PPE), proteinase3	33, 61
Granulysin		Psoriatic plaques	Broad spectrum antimicrobial	62
Growth hormone	GH	Expressed in whole human skin (normal and BCC)	Associated with fibroblast activity, sebum production and induction of IGF-1 production.	63
Human beta defensin	HβD (1-4)	Suprabasal keratinocytes of the skin and sweat ducts within the dermis	wound healing and skin diseases such as atopic eczema	16, 64
Human neutrophil elastase	HNE	Detected in psoriatic lesions	Physiological functions in host defence against bacterial infections and matrix remodelling following tissue injury	65
Interleukins	IL	Released from an intracellular preformed pool in kaeratinocytes	Involved in wound healing	50
Peptide T		Synthetic	Anti-chemotactic activity – therapeutic efficacy in psoriasis	34

Proopiomelanocortin and melanocortin peptides	POMC	Found in the basal layer of the intermolecular epidermis.	Stimulate eumelanin synthesis, antipyretic and antiinflammatory	66, 67
Psoriasin		Discovered in psoriatic skin lesions and constitutive expression in healthy skin keratinocytes	Psoriasin preferentially kills <i>E. coli</i> , but has a weak antimicrobial activity against <i>S. aureus</i> , <i>P. aeruginosa</i> and <i>Staph. epidermidis</i>	68
RNase 7		Expressed in healthy skin (isolated from skin derived <i>stratum corneum</i>).	Broad spectrum antimicrobial	43
Skin peptide tyrosine-tyrosine	SPYY	Isolated from the amphibian skin	Antifungal and antiparasitic activity	69 70
Soluble RGD peptides	RGD	Released during the proteolytic remodelling of the extracellular matrix	Wound healing - internalized into a cell and able to bind and activate caspase 3 inducing apoptosis	51
Transforming growth factor	TGF- α , TGF- β	Intercellular space of all the layers of the epidermis and the subepidermal area of the dermis.	Regulator of both cell growth and differentiation	71
COSMETIC PEPTIDES				
Pal-KTTS		Pentapeptide fragment	Stimulates collagen I and III and fibronectin production	72

Acetyl hexapeptide- 3		Synthetic peptide	Improvement in periorbital rhytides	73
Palmitoyl pentapeptide-3		It is a fatty acid mixed with amino acids	Superior anti-wrinkle effects	(www.sederma.fr)
Syn-Ake		Synthetic tri-peptide	Anti-wrinkle/anti-aging effect	(www.centerchem.com)
Antioxidative collagen derived peptides	e.g. Arg-Ser-Arg-Lys	Tetrapeptide	Antioxidant and decreases cellular activity	74
Carnosine		Naturally occurring histidine containing dipeptide	Wound healing and acts as an anti-ageing peptide	75,76

1.2.1.4 Viral disease

Alterations in the skin barrier can lead to infection with bacteria and selected viruses, including herpes simplex virus, varicella-zoster virus and vaccinia virus. Evidence of the protective effect of AMPs in skin is demonstrated by the induction of epidermal cathelicidin LL37 during the development of verruca vulgaris and condyloma accuminatum, two human papilloma virus infections responsible for common cutaneous warts.⁷⁷ The effects of cathelicidin, α -defensins, β -defensins and control peptides on vaccinia virus replication *in vitro* have been investigated. Cathelicidins but not defensins demonstrated antibacterial activity which caused a reduction in vaccinia viral plaque formation.²⁴ It was observed that mice deficient in the murine LL-37- equivalent showed less effective wound healing upon infection with group A Streptococci. Thus LL-37 is an attractive candidate as a novel therapeutic agent. A cathelicidin based indolicidin like peptide has been developed for acne treatment and is currently in phase 2 clinical trials (Migenix Inc., Vancouver, BC, Canada). LL-37-versions for topical treatment of atopic dermatitis are in preclinical research stages (Ansata Therapeutics Inc., La Jolla, CA).⁴⁴

1.2.1.5 Human epithelial cancer

Adrenomedullin (AM), a calcitonin gene related peptide is found to be present in normal and malignant skin. AM may be involved with the wound repair process, sustaining normal epidermal turnover and influencing tumour initiation and proliferation.⁷⁸ It plays an important role in skin homeostasis and carcinogenesis. Some metastatic melanomas showed strong expression of AM at the periphery of the metastasis, whereas the majority of melanoma cells at the centre showed little or no expression. Keratoacanthoma showed a similar pattern of AM distribution. Thus, AM is a possible growth regulatory factor of the skin and malignant tissue, therefore targeted delivery to induce inhibition in malignant tissue could be a treatment option.

1.2.1.6 Peptides as cosmeceuticals

Cosmeceuticals are topical cosmetic- pharmaceutical hybrids lying on the spectrum between drugs and cosmetics.^{72, 79} There is an increasing trend towards the use of these agents in skin care regimens. There are numerous cosmeceutically active

products on the market which can be broadly classified into the following categories: antioxidants, amino-peptides, growth factors, anti-inflammatories, polysaccharides and pigment lightening agents.⁷² In most cases the overall purpose is antiageing but the method by which this is achieved varies. With the advances in biotechnology various peptides are now being used as cosmeceuticals. Examples include copper peptides, amino-peptides, acetyl hexapeptide-3 and dimethylaminoethanol.⁷² Copper peptides such as GHK-copper complex are included in products to improve skin firmness and texture, fine lines and hyperpigmentation.⁸⁰ Pal-KTTS is a pentapeptide fragment that stimulates collagen I and III and fibronectin production *in vitro* and functions in wound healing. Another synthetic peptide, acetyl hexapeptide-3 when tested in an open label trial demonstrated improvement in periorbital rhytides (wrinkles on the face and near eyes).^{72,73} It is claimed to have muscle-relaxing effects similar to Botox injections (www.centerchem.com). Palmitoyl pentapeptide-3 (Matrixyl) is a fatty acid mixed with amino acids (www.sederma.fr). Sederma conducted three different "half-face" studies with a total of about 45 participants showing the palmitoyl pentapeptide-3 product to have superior anti-wrinkle effects than a retinol or vitamin C product. Similar claims have been made for Syn-Ake, a synthetic tri-peptide based on Waglerin 1, a peptide derived from the venom of the Temple Viper (www.pentapharm.com). It reduces the contraction frequency of muscle cells in the face thereby decreasing expression lines to provide an anti-wrinkle/anti-aging effect.

Antioxidative collagen derived peptides are present in human placenta where they protect the embryo from oxidative stresses. The antioxidant activity of these collagen peptides accounted for approximately 15% of the total antioxidant activity of human placenta extract (PLX).⁸¹ A number of patents have been filed on the use of peptides for cosmetic products. These include the tripeptide Lysine-proline-valine for stimulating or inducing hair growth.⁸² Another patent describes topical compositions containing the tetrapeptide Arg-Ser-Arg-Lys for reducing wrinkles.⁷⁴ This tetrapeptide is a fibroblast growth factor derived peptide which slows down or decreases cellular activity. Carnosine and related naturally occurring histidine containing dipeptides such as anserine, exhibit antioxidative properties by quenching free radicals.^{75,83,76} Carnosine also accelerates healing of wounds and ulcers and is reported to act as an anti-ageing peptide.^{75,76} Fibroblast collagen production has been

reported to be stimulated by a pentapeptide fragment (Lys-Thr-Thr-Lys-Ser) of the collagen molecule. It is a potent stimulator of collagen and fibronectin synthesis, which are both important components of the interstitial matrix⁸⁴ and if enhanced can decrease signs of ageing in the skin.

Growth factors act as regulatory proteins to mediate inter- and intra-cellular signalling pathways. They play an active role in wound healing and are involved in the induction of collagen, elastin and glycosaminoglycan formation. A study conducted by Fitzpatrick *et al* (2003) showed their efficacy in improving wrinkles through stimulation of epidermal thickening.⁸⁵

The use of chemically modified peptides for healing, hydrating and improving skin appearance has stimulated substantial patent activity. A combination of peptides with the general sequence X-Thr-Thr-Lys-Y was reported to have activity against the formation or deterioration of wrinkles.⁸⁶ Cosmetic compositions have been formulated with at least one ceramide compound and one peptide attached to a fatty acid chain. Ceramides and their analogues have been known to protect and repair skin or hair fibres from damage caused by various agents and hair treatments. They provide a barrier effect which minimizes the leakage of proteins.⁸⁷ Protein hydrolysates such as wool keratin hydrolysate were included in the formulation to improve ceramide binding to the skin or hair fibre.

It is thus clear that many peptides play a wide variety of roles in normal skin and many are present or increased in skin disease. As we further develop our understanding of the role of these peptides in normal function and disease, the potential to exploit them for therapeutic or cosmetic purposes becomes clearer. This requires the synthesis of these peptides, or in some cases chemicals capable of inhibiting their action. In addition an efficient means of delivering them in an active form to their target sites within the skin is required. As many of these peptides are greater than 500 Da and hydrophilic in character they will not diffuse passively across intact skin, therefore their delivery will require an enhancement system. The potential for new treatment options, particularly for chronic skin diseases that are often poorly controlled by available therapeutics, is a priority in dermatological research.

1.3 Strategies to enhance delivery of peptides across the skin

Recent developments in genetic engineering and biotechnology have resulted in an explosion in availability of therapeutic peptides and small anti-cytokines. Oral administration is inappropriate as these molecules are unstable in the gastrointestinal tract and are subject to hepatic first-pass effect.⁸⁸ Currently only a small number of transdermally delivered drugs are commercially available despite the potential advantages of this route of administration.

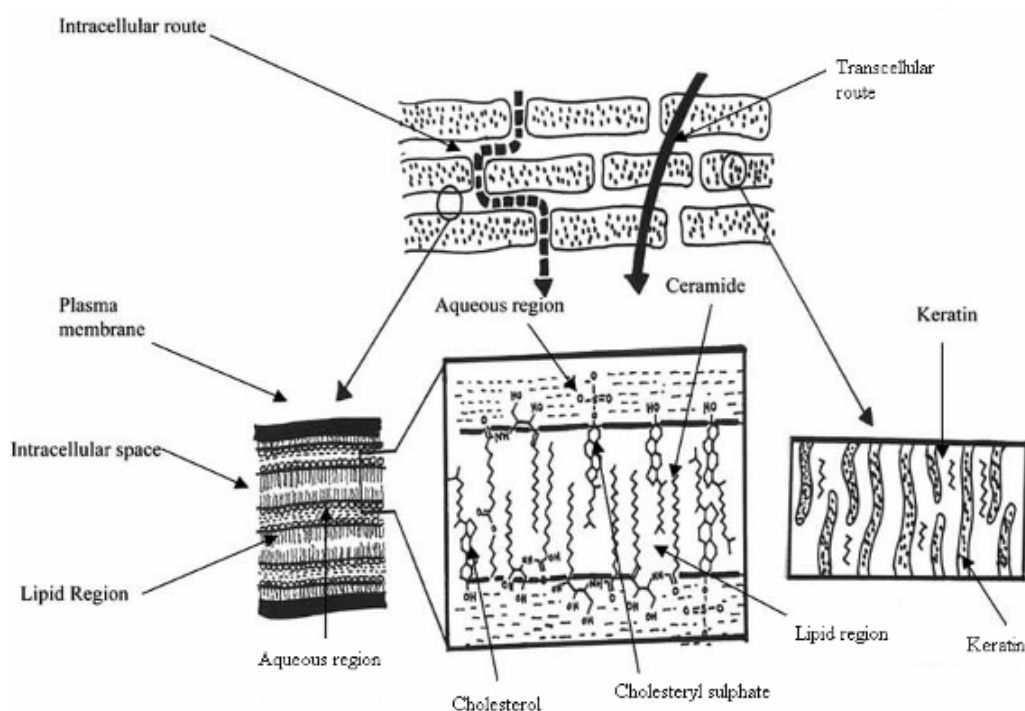


Figure 1.4 Diagrammatic representation of the stratum corneum and the intercellular and transcellular routes of penetration⁸⁹

Ideal characteristics for successful transdermal delivery are a relatively low molecular weight (<500 Da) and melting point (<200°C), moderate lipophilicity (log P 1–3) and aqueous solubility (>1 mg/mL) and high pharmacological potency. A penetrant applied to the skin surface has three potential pathways across the epidermis: via the hair follicles and associated sebaceous glands; through sweat ducts; or across the continuous *stratum corneum* (Figure 1.4). The fractional surface area of the appendages is only about 0.1%⁹⁰ therefore it is generally accepted that this route makes a negligible contribution to steady state drug flux into and across the

skin. It may, however, contribute in the early time period between drug application and establishment of steady state flux and could be a more important route for large polar molecules, polymers and colloidal particles that do not readily diffuse across the *stratum corneum*. This barrier layer is composed of primarily long chain ceramides, free fatty acids, triglycerides, cholesterol, cholesterol sulphate and sterol/wax esters.^{91, 92} It is generally accepted that the intercellular lipid matrix is the predominant route through the *stratum corneum* for the majority of penetrant molecules. Within the viable epidermis and dermis a number of proteases may exert enzymic degradation of peptides and proteins.^{93, 94} However the proteolytic enzyme activity in the skin is substantially less than GIT or hepatic enzymatic metabolism⁹⁵ and a transdermal delivery system tends to expose the peptide to a relatively small application area. The potential for metabolic activity in the skin must be considered in the design of the transdermal device and dose of active peptide required to be delivered to the target site.

1.3.1 Skin penetration of peptides

Peptides are hydrophilic and often charged molecules at physiological pH. They range in molecular weight from 300 Da to greater than 1000 kDa. Consequently their skin permeation is poor and despite generally having high potency, they are ineffective if administered transdermally. Several penetration enhancement techniques have been developed to overcome the skin barrier and facilitate the permeation of peptides and proteins through the skin. Strategies include chemical modification to form a conjugate with increased lipophilicity, encapsulation into hydrophobic carriers and administration with penetration enhancers which chemically or physically reduce the *stratum corneum* barrier.^{89,96}

1.3.2 Optimisation of formulation and peptide characteristics

1.3.2.1 Percutaneous Penetration Enhancers

The most widely researched approach to enhance transdermal delivery of drugs is formulation with chemical penetration enhancers (sorption promoters or accelerants). These enhancers increase the diffusivity of the drugs by *stratum corneum* lipid fluidisation thus decreasing barrier function. This approach has been successful for enhancing the permeation of a wide range of small molecules but many of these

chemical penetration enhancers are of limited clinical application due to irritation. Magnusson and Runn⁹⁷ reported enhanced transdermal penetration of M-TRH, an analogue of the endogenous tripeptide, thyrotrophin releasing hormone (TRH), in the presence of a terpene and ethanol vehicle. Steady state flux values for M-TRH across human epidermis from PBS were 0.34 mg/cm²/h. In the presence of 50% ethanol the flux increased threefold and a combination of 47% ethanol and 3% cineole resulted in a flux of 1.60 mg/cm²/h. Hence substantial enhancement was achieved for this small peptide but this approach is of limited value for larger peptides and care needs to be taken that enhancer chemicals do not denature the peptide. Karande *et al* reported the skin permeation enhancing properties of an anionic surfactant, sodium lauroylsarcosinate (NLS) and a non-ionic surfactant, sorbitan monolaureate (S20) in 1:1 phosphate buffered saline (PBS):ethanol solvent. It was observed from the results that combinations of NLS and S20 exhibited significantly higher enhancement of skin permeability compared to that induced by individual surfactants. It was thus concluded based on the data generated from nuclear magnetic resonance (NMR) and fourier transform infra red (FTIR) studies that NLS acts as a strong extractor of stratum corneum lipids and S20 behaves as a weak fluidizer.⁹⁸ The author also undertook a study to uncover the fundamental mechanisms that define the potency and irritation of chemical penetration enhancers and reported that the irritation behavior of chemical penetration enhancers is related to the ratio of hydrogen bonding to polar interactions.⁹⁹

1.3.2.2 Encapsulation

Encapsulation involves the entrapment of a peptide drug within a polymeric, phospholipid or carbohydrate particulate delivery system such as microspheres, liposomes, or nanoparticles. Liposomes are phospholipid based vesicles which have been extensively investigated in transdermal delivery. It is generally acknowledged that whilst they are useful for local delivery to superficial skin layers they do not penetrate the epidermis intact. Encapsulation of interferon (IFN)- α into liposomes has been shown to increase deposition in the skin¹⁰⁰ but increased penetration of macromolecules through the skin has not been demonstrated. A number of other liposome like vesicles with increased structural flexibility have been developed including transfersomes, niosomes and ethosomes. Ethosomes have been evaluated

with a number of small molecules and with insulin. When the effect of skin application of an ethosomal insulin formulation on blood glucose levels (BGL) *in vivo* in normal and diabetic rats was investigated, it was found that insulin delivered from the ethosomal patch significantly decreased (up to 60%) blood glucose level in both normal and diabetic rats. A prolonged plateau effect of at least 8h was also observed using the ethosomal insulin patch.¹⁰¹ Niosomes are vesicles composed of non-ionic surfactants that have been evaluated as carriers for a number of cosmetic and drug applications. Gupta *et al* studied the relative potential of transfersomes, niosomes and liposomes in non-invasive delivery of tetanus toxoid (TT). They observed that the entrapment efficiency, elasticity and topical effect with these encapsulated forms were higher than intramuscular administration of alum-adsorbed tetanus toxoid.¹⁰² In another study, conducted on trans-retinoic acid or tretinoin, the potential of niosomes as topical delivery systems capable of improving the cutaneous delivery of tretinoin was assessed. Tretinoin cutaneous delivery was strongly affected by vesicle composition and thermodynamic activity of the drug with negatively charged niosomal formulations showing higher cutaneous drug retention than both liposomes and commercial formulations.¹⁰³ Transfersomes are composed of phospholipids such as phosphatidylcholine, but also contain surfactant which acts as an 'edge activator' conferring deformability on the vesicle.^{104, 105} However, in all cases scale up of these delivery systems to provide therapeutic peptide levels in humans is yet to be demonstrated.

1.3.2.3 Chemical modification

Lipophilic derivatives of peptides can be made either to increase the encapsulation efficiency into liposomes or directly increase their delivery through skin. The approach has been used successfully to enhance peptide permeability across intestinal and rectal barriers.¹⁰⁶ Recently this approach has been applied to skin delivery. Foldvari *et al*¹⁰⁰ reported cutaneous absorption of IFN- α with fatty acids with increasing chain length (C12, C14, C16, C18 and C18:1). The skin absorption of acylated IFN α derivatives was tested in a gel-type pharmaceutical formulation. The cutaneous and percutaneous absorption of acylated IFN- α was, overall, 2.5–5 times greater than IFN- α . Increasing fatty acid chain length from 12 to 16 resulted in increased palmitoyl substitutions to lysine residues in the protein compared with the

parent IFN- α while further fatty acid chain increase lead to a decrease in absorption. In the early 1970's it was shown that conjugating fatty acids to bovine serum albumin changed the immune response from humoral to a mainly delayed type hypersensitivity response. Subsequently, it was shown that dipalmitoyl-peptide conjugates in combination with Freund's complete adjuvant were able to induce antibodies and cytolytic T cells (CTL) and lipopeptides were used.¹⁰⁷ The major priority to improve the transmembrane absorption of poorly-absorbed compounds was to impart them with increased membrane-like character, by conjugation to lipidic amino acids and their oligomers. However, the resultant underderivatised hydrophobic conjugates were often poorly soluble in water. The problem of maintaining the balance between the lipophilic and hydrophilic properties of the conjugates was addressed by modifying the lipidic amino acids themselves and secondly by conjugating the lipidic amino acids with hydrophilic molecules.¹⁰⁸ Lipoamino acid conjugated peptides and lipopeptides have been discussed in detail in section 1.5.

1.3.2.4 Effect of hydration

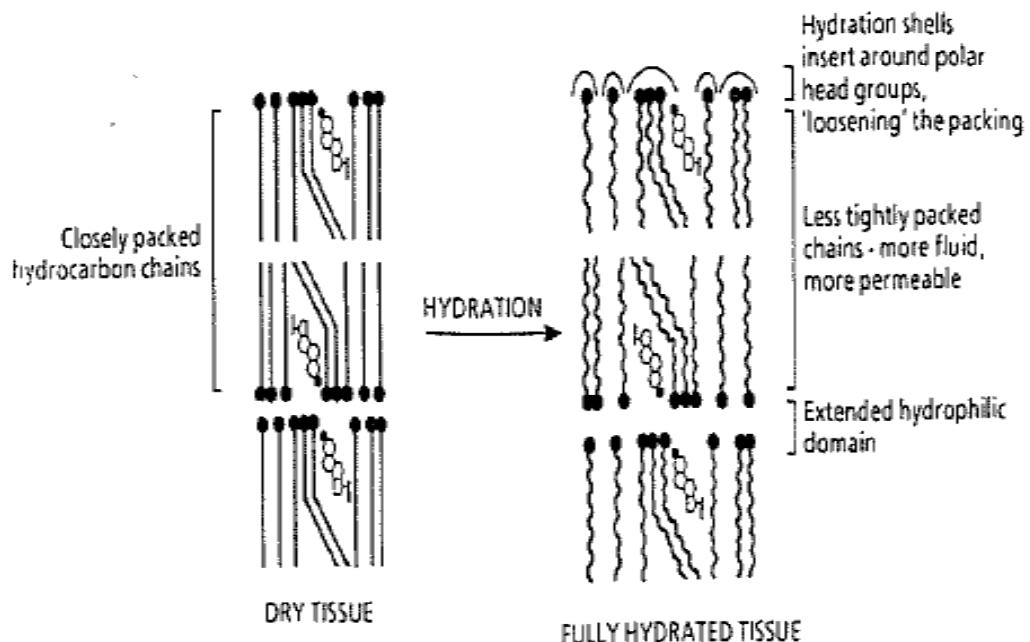


Figure 1.5 How hydration increases the fluidity of the stratum corneum lipids by insertion of water molecules between polar head groups¹⁰⁹

The state of hydration of the *stratum corneum* may influence the percutaneous absorption of a drug. The *stratum corneum* water content at normal relative humidity is between 15 and 20% of dry weight. Increased water content results in increased elasticity and permeability of the *stratum corneum*, whereas reducing water content will lead to opposite effect.¹¹⁰ One of the proposed mechanisms for the increase in transport of the drug is by water being absorbed into the *stratum corneum* where it acts as a plasticiser in its bound state (Figure 1.5). Other studies suggest that the *stratum corneum* not only swells, but also develops multiple folds, resulting in a 37% increase in surface area.¹¹⁰ Increase in water content of the *stratum corneum* is associated with a decrease in lipid/protein phase transition temperature indicating lipid disruption and protein denaturation.¹¹¹ Hydration does not always increase permeation and in case of molecules with strong lipophilic character there was no effect on the absorption rate.

1.3.3 Physical Energy Application

1.3.3.1 Iontophoresis

Iontophoresis uses small voltage constant current (up to 0.5 mA/cm²) to push charged molecules into the skin. The main mechanism of enhancement is electrorepulsion whereby a solute with the same charge as an electrode placed on the skin surface is repelled into the skin.¹¹² The applied current also has a direct effect on skin permeability and causes electroosmosis, the convective flow of water molecules which enhances the permeability of neutral solutes.¹¹³ Iontophoretic transdermal delivery of a number of peptides has been demonstrated, including luteinising hormone releasing hormone (LHRH), TRH, cyclosporin, nafarelin, arginine vasopressin (AVP), octreotide, calcitonin and insulin.¹⁰⁵



Figure 1.6 Infosys system: patient controlled analgesia by iontophoresis enhanced transdermal fentanyl delivery (Alza corp)

Iontophoretic delivery of peptides has been extensively investigated by Guy's group who have generated an understanding of the primary mechanism of enhancement for peptides and attempted to develop peptide structure-penetration relationships. Computational studies that generated 3D quantitative structure-permeation relationships predicted that iontophoresis was favoured by peptide hydrophilicity and hindered by voluminous, localized hydrophobicity.¹¹⁴ This was particularly the case where the bulky lipophilic moiety was directly adjacent to a positively charged residue, as occurs in nafarelin and leuprolide. It has been suggested that this structure inhibits electroosmosis, thereby reducing iontophoretic transport.¹¹⁵ Interestingly, the molecular characteristics that favour electrotransport are the converse of those that favour passive diffusion. Combinations of iontophoresis with chemical enhancers and formulation modifications have been investigated. For example, Boinpally *et al*¹¹⁶ reported that the *in vitro* transport of cyclosporine from lecithin vesicles under anodal iontophoresis was greater than when applied in combination with a microemulsion. Pillai and coworkers¹¹⁷ have systematically investigated the iontophoretic delivery of insulin with a range of solvents and chemical penetration enhancers. Whilst increased skin penetration could be achieved this was frequently associated with increased skin irritation. To date, iontophoretic transdermal delivery of large peptides and proteins sufficient to achieve therapeutic outcomes in humans has not been demonstrated. However the technique may be useful for local delivery of small peptides (less than 10 kDa) in the treatment of skin conditions or lesions.¹⁰⁵

1.3.3.2 Electroporation

Electroporation involves the application of high voltages (100–1000 V) in short pulses (1–100 ms) to induce transient structural changes in the *stratum corneum* lipid bilayers which manifest as aqueous pores.¹¹⁸ The electrical pulses cause a transient drop in skin resistance of up to three orders of magnitude which is associated with an increase in permeability up to three to four orders of magnitude for small and macromolecules. Enhancement of peptide permeation by electroporation has been shown to be substantially greater than by iontophoresis. For example, Prausnitz *et al*¹¹⁹ demonstrated *in vitro* skin permeation of heparin by electroporation at amounts equivalent to therapeutic levels (100–500 mg/cm² h). This was an order of magnitude greater than the heparin flux achieved with iontophoresis. Sen *et al*¹²⁰ reported a 20-fold increase in transport of fluorescence- labelled insulin across porcine epidermis when applied in the presence of an anionic phospholipid (1,2-dimyristoyl-3-phosphatidylserine) with electroporation compared with electroporation alone. The main question associated with electroporation is patient tolerance. Many of the studies of electroporation to date have involved *in vitro* or animal experimentation with few clinical studies. In a study of electrochemotherapy of melanoma lesions, local injection of bleomycin followed by electroporation was applied to multiple lesions on 12 patients. All patients reported discomfort during electroporation with mild pain and/or muscle spasms.¹²¹ Recent studies have indicated that it may be possible to modify the applied electroporation parameters to reduce muscle spasms whilst maintaining electrochemotherapeutic efficacy. If these side effects can be overcome, the potential clinical applications of electroporation in transdermal delivery are worthy of further investigation.¹⁰⁵

1.3.3.3 Sonophoresis

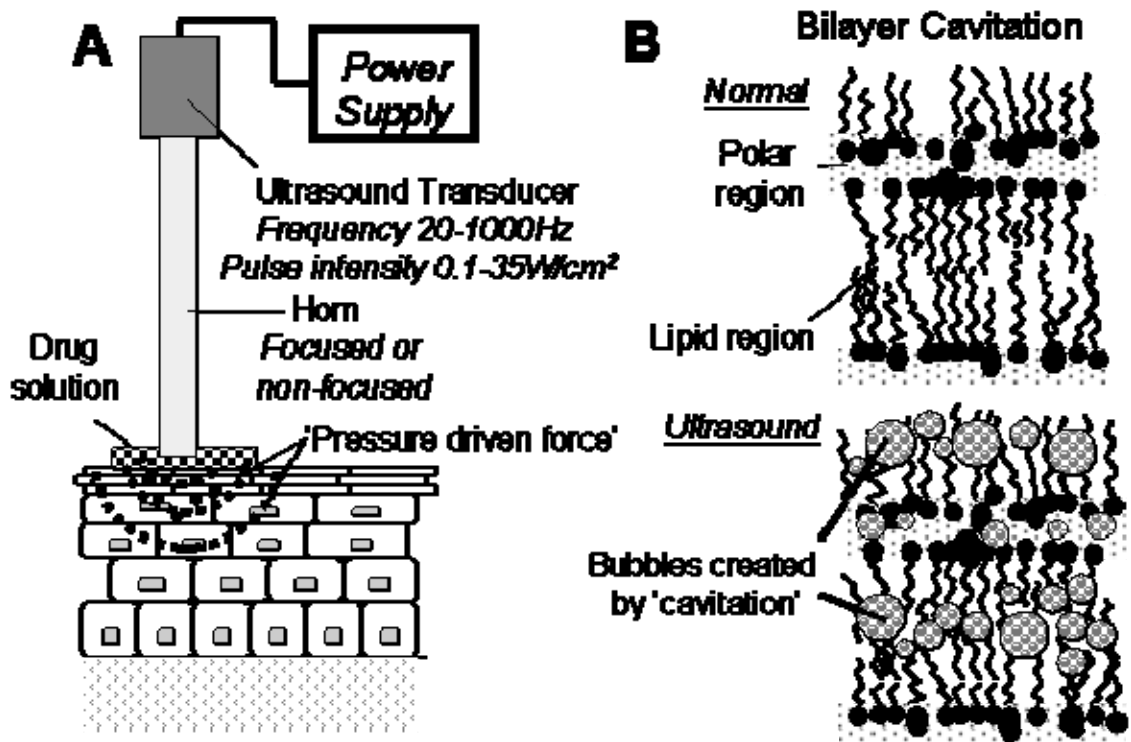


Figure 1.7 The basic design of ultrasonic delivery devices (A) Drug is placed on the skin beneath the ultrasonic probe. Ultrasound pulses are passed through the probe and drug molecules are hypothesized to move into the skin through a combination of physical wave pressure and permeabilisation of intercellular bilayers. (B) The formation of bubbles in the intercellular lipid space caused by cavitation increases bilayer fluidisation and resultant permeability ⁹⁶

Ultrasound at therapeutic frequencies (1–3 MHz) as used in physical therapy was first applied to enhance the skin penetration of small drugs in the 1980s. More recently low frequency ultrasound (<100 kHz) has been used to provide greater enhancement and has been extended to the delivery of macromolecules across intact skin.¹²² The mechanism by which the acoustic waves enhance permeability through the skin is not fully understood but it is hypothesized that these waves cause microcavitation in the skin which disorders the *stratum corneum* lipid bilayers, thereby promoting drug diffusion (Figure 1.7). In addition, it has been reported that ultrasound causes *stratum corneum* lipid extraction which contributes to increased permeability.¹²³ Ultrasound enhanced transdermal delivery of a number of peptides and proteins has been reported including insulin, erythropoietin, IFN- γ and

heparin.¹⁰⁵ These studies utilised a range of ultrasonic transducers and baths. Recently, a miniaturised ultrasound system was developed and investigated. This system involves an array of ultrasound transducers and offers the potential of development as a transdermal patch. For example, following application of insulin with or without ultrasound to six pigs blood glucose decreased by 72 ± 5 mg/dL at 60 min ($p<0.05$) and 91 ± 23 mg/dL at 90 min compared with an increase of 31 ± 21 mg/dL in the control animals ($p<0.05$) from baseline glucose level (146 ± 13 mg/dL).¹²⁴ The authors concluded that their cymbal array ultrasound system has potential for noninvasive transdermal insulin delivery for diabetes management. Patient acceptance and safety of therapeutic ultrasound in physical therapy applications is well established. Short periods of low frequency ultrasound pulses as used for the SonoPrep local anaesthetic application (10 sec 55 kHz of ultrasound pretreatment) also seem to be well tolerated,¹²⁵ however these very short pretreatments and low intensities are unlikely to be sufficient to generate therapeutically relevant transdermal delivery of large molecules.

1.3.3.4 Photomechanical waves

Photomechanical waves are generated by the impact of laser radiation on a target material (e.g., polystyrene) that is then directed towards the skin surface. Lee and coworkers¹²⁶ have hypothesised that these stress waves cause transient permeabilisation of the *stratum corneum* sufficient to permit the diffusion of macromolecules. Delivery of insulin through the skin of diabetic rats by this technique caused a reduction in blood glucose of $80\pm 3\%$, with the level maintained below 200 mg/dL for 3 h.¹²⁷ Delivery of oligonucleotides, DNA and 100 nm microspheres has been reported, though the recently introduced technique has yet to be tested on human subjects.

1.3.3.5 Magnetic energy

Limited work has been undertaken to investigate the ability of magnetic fields to move diamagnetic substances through skin.¹²⁸ Langer discussed the interesting idea of employing intelligent systems based on magnetism or microchip technology to deliver drugs in controlled, pulsatile mode.¹²⁹ An alternative method for achieving pulsatile release involves using microfabrication technology to develop active

devices that incorporate micrometre- scale pumps, valves and flow channels to deliver liquid solutions.¹²⁹

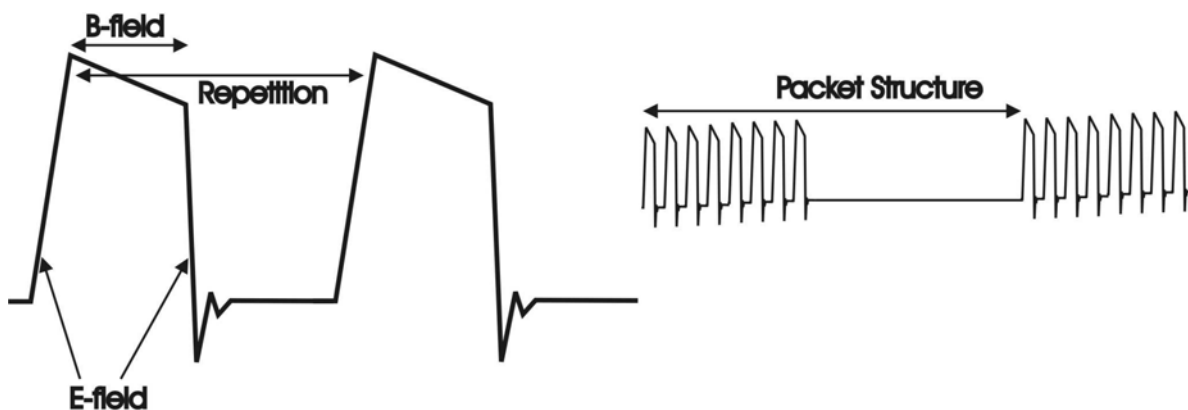


Figure 1.8 Schematic of PEMF Dermaportation waveform

In this study a novel physical skin penetration enhancement technology was investigated for peptide delivery. Dermaportation (OBJ Ltd) is a Pulsed Electro Magnetic Field (PEMF) platform technology that applies electromagnetic pulses to enhance skin permeation and push target molecules away from the field. The technique utilizes a time varying electromagnetic field that is believed to interact with the skin to enhance transdermal delivery. At the heart of the Dermaportation system is a low energy time varying quasi-rectangular PEMF. Each pulse has a rapidly rising and falling edge (Figure 1.8) that is hypothesised to induce localized electromagnetic field effects in the *stratum corneum* environment. Biological and therapeutic effects of electromagnetic fields and inductive effects on biological tissues have been widely reported, for example, enhancement of healing of venous ulcers and bone fractures and effects on a range of cellular functions.^{130, 131} Dermaportation uses a low voltage (3V) and does not require direct physical contact with the skin to produce diffusion enhancement. This offers potential advantages, particularly in wound management and drug delivery into the skin. In addition, the fabrication of small self contained Dermaportation patches is possible due to the low energy requirements. The standard Dermaportation system (DP1001) generates a specific pattern of energy pulses that have been shown to induce transdermal flux increases during field exposure of a number of small molecules, such as 5-aminolevulinic acid¹³², diclofenac diethylammonium salt¹³³ and lidocaine

hydrochloride.¹³⁴ . It is proposed that Dermaportation energy influences both the molecular movement of drug molecules in the epidermis and the ordered structure of the *stratum corneum* lipid bilayers but the precise mechanism of enhancement is an area of continuing investigation.

1.3.4 Minimally invasive strategies for enhancing delivery

1.3.4.1 Microneedles

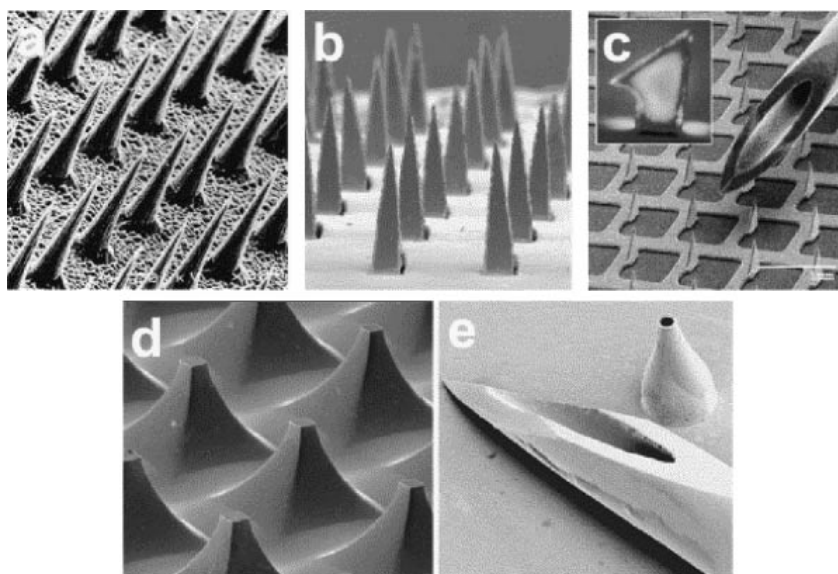


Figure 1.9 Images of microneedles used for transdermal drug delivery¹³⁵

Microneedles are an application of the microfabrication technology whereby an array of needles is used to pierce the skin in a minimally invasive manner to create a physical pathway for drug diffusion.¹³⁶ The microneedle array (Figure 1.9) is applied to the skin surface so that the needles (usually about 150 μm in length) penetrate the epidermis to bypass the *stratum corneum* and deliver drug directly to the viable epidermis. As the epidermis is devoid of nociceptors and the microneedles do not penetrate to the nociceptors of the dermis, a pain sensation is not elicited. The microneedle technology has been applied to the transdermal delivery of a number of macromolecules. Martanto *et al*¹³⁷ reported decreased plasma glucose levels of up to 80% in diabetic rats following administration of insulin solution for 4 h preceded by a 10 min application of a 105 stainless steel solid microneedle array. However the insulin delivery levels achieved in laboratory animals are considerably lower than those required by humans and the technique has yet to be tested clinically. Safety has

been one of the main concerns raised since microneedles were first introduced. However it has been reported that breakage of silicon microneedles is minimal if the array is inserted gently and carefully.¹³⁶

1.3.4.2 Jet injectors

A number of devices are commercially available which propel solid particles or liquid droplets into the skin at high velocity. They offer a needle-less alternative to the traditional injection. The current applications are for the administration of recombinant human growth hormone (hGH), insulin and vaccination. There has also been interest for small molecules, other proteins, gene delivery and immunotherapeutics. The premise that jet propulsion is less painful than conventional needles has not been substantiated.¹⁰⁵

1.3.5 *Stratum corneum* ablation

It is well known that the *stratum corneum* is the main skin barrier therefore its removal will dramatically enhance skin penetration and water loss. A number of techniques have been developed to provide a controlled removal of the SC. These techniques are discussed below:

1.3.5.1 Laser ablation

A high energy laser directed at the skin surface can remove the *stratum corneum* to increase drug permeability to subsequently applied drugs. Nelson *et al*¹³⁸ first described the technique in 1991 when they reported a 2.1 times increase in the permeability coefficient of IFN- γ across pig skin that had been exposed to a laser at 2790 nm. The safety and reversibility of the technique is yet to be established and it is likely that laser ablation would be restricted to the clinical setting with limited application. Laser ablation is also widely used by beauticians to improve skin tone.

1.3.5.2 Radiofrequency (RF) thermal ablation

TransPharma Medical's application of its RF-microchannel technology is the ViaDerm system which consists of a microarray of radiofrequency electrodes which create microchannels in the epidermis by cell ablation thereby permitting drug diffusion via the microchannels. The technology has been evaluated for transdermal

delivery of small hydrophilic drugs, peptides and genes. Bioavailability of hGH applied by ViaDerm to rats was 75% of the subcutaneous injection and recently the delivery of 100 nm nanoparticles and gene therapy vectors was demonstrated. The technique also appears to be well tolerated with only mild erythema reported and as the energy is restricted to the upper epidermis, dermal nociceptors are not affected therefore minimal pain would be expected.¹⁰⁵

1.3.5.3 Suction blister ablation

A mechanical device exerts a vacuum to cause a small blister on the skin which is then removed to expose a site for drug application.¹³⁹ According to Svedman *et al* only the epidermis is split off by this suctioning and it does not cause bleeding or discomfort because the effect is superficial to the dermal capillaries and nociceptors. They reported the application of the antidiuretic peptide 1-deamino-8-D-arginine vasopressin with close to 100% bioavailability in healthy human subjects with recovery of the skin spot to normal after 6 weeks. However, further research into this technique has been undertaken in the past 10 years or by other groups so it is unlikely that this technique will progress further for peptide delivery.¹⁰⁵

1.3.5.4 Thermal poration

Thermal poration involves the application of pulsed heat to form micron scale aqueous pathways across the *stratum corneum*. Badkar *et al*¹⁴⁰ recently demonstrated transdermal delivery of interferon alpha in hairless rats using thermal poration alone and a twofold increase when combined with iontophoresis. Iontophoresis alone and passive application did not result in transdermal flux of interferon.

1.3.5.5 Combination of technologies

The combination of two or more of these enhancement techniques to generate a synergistic enhancement effect has been extensively explored and offers promise for the future development of transdermal products.¹⁴¹ For example, Srinivasan *et al*¹⁴² reported several-fold enhancement of transdermal leuprolide delivery by application with iontophoresis after a pretreatment with ethanol. Choi *et al*¹⁴³ suggested that pretreatment with chemical enhancers dilated intercellular spaces and reduced skin impedance thereby increasing the effectiveness of iontophoresis of insulin.

Synergistic effects between physical enhancement techniques have also been reported. The application of a single electroporation pulse prior to iontophoresis increased the transdermal flux of LHRH by five to ten times as compared to iontophoresis alone. This combination also increased the transdermal flux of human parathyroid hormone (hPTH) up to 10 times greater than electroporation alone. These studies do raise the possibility of using combinations of enhancement approaches to achieve therapeutically relevant delivery of proteins and peptides to and across the skin. Whilst the safety and patient tolerability of these combinations must be fully established they do offer opportunities for effective delivery alternatives.¹⁰⁵

1.4 Lipopeptides and lipoamino acid conjugation approaches to enhance the stability and delivery of peptides across biological barriers

The problem with most peptides is delivering them to the specific site, in an intact and biologically active form and without the peptide being integrated into other tissues.¹⁰⁷ In order for a peptide to be of significant value as a drug, there are several potential problems that must be overcome as discussed in previous sections. Novel drug-delivery systems for the oral administration of drugs and peptides, which are normally poorly absorbed or biologically unstable have been developed by combining the peptide or drug with a lipoamino acid (LAA) or liposaccharide (LS), lipopeptides, liposomes and polyethylene glycol (PEG) conjugates which can act as a carrier.¹⁰⁷

Increasing lipophilicity by addition of long aliphatic chains or lipid moieties is an established method of increasing bioavailability. This technique increases the permeability across the epithelial barriers or can increase uptake by the lymphatic system. Passive diffusion is the major route for compounds crossing the epithelial barrier and so is the most important target for increasing bioavailability. Presence of lipid groups on peptides has been shown to significantly increase the biological half life of peptides.¹⁴⁴ LAAs combine the properties of amino acids with those of lipids; thus combining them with a peptide or drug provides a means of transporting the compound into the body in a stable and biologically active form.^{145, 146} The linkage

between drug and lipidic unit may either be biologically stable (such that a new drug is formed) or possess biological or chemical instability (when the conjugate will be a pro-drug). In either case, the resulting conjugates would be expected to possess a high degree of membrane-like character, which may be sufficient to facilitate their passage across membranes. The long alkyl side chains may also have the additional effect of protecting a labile parent drug from enzymatic attack. The LAA system has also been used to increase the oral absorption of various drugs including peptides, β lactam antibiotics¹⁴⁷ and benzoquinolizine alkaloids.¹⁰⁸ Conjugation to lipidic peptides increased the half-life of LHRH and TRH with the peptides subsequently being released from Caco-2 cell homogenates. The released LHRH or TRH subsequently demonstrated a longer half-life than when present alone in the incubation mixture, suggesting that the cleaved lipidic peptide is capable of inhibiting enzymes.¹⁴⁸ Table 1-2 lists some of the examples of peptides conjugated to lipoamino/fatty acids

Research has been carried out to investigate the effect of lipoamino acid and liposaccharide conjugation on the activity of a somatostatin analogue TT-232.¹⁴⁹ The combination of LAA's with TT-232 resulted in bifunctional conjugates where the long alkyl side chains were lipophilic and the peptide part was hydrophilic (Table 1-2). Conjugation with LAA's resulted in higher lipophilicity which is essential for crossing biological membranes but the conjugate has to have a certain degree of water solubility for absorption through the gut. Sugars were hence conjugated to TT-232 to increase the water solubility. This not only improved physicochemical properties of parent compounds, such as solubility, but also allowed the conjugate to utilize active transport uptake systems (e.g. the Na⁺-dependent D-glucose transporter) and help target the compound (e.g. sialyl Lewis-X sugars, elevated α -glucuronidase expression in some tumours). The results indicated that there was no clear correlation between the biological activity and the length of the side chain of the LAA, or the presence of a spacer between the N-terminus of the molecule and the ligand, or the presence of an additional carbohydrate moiety. It was thus concluded that modification of the N- and C- termini of TT-232 with LAA or LS resulted in amphipathic surfactant-like molecules with higher bioavailability and stability.

Toth *et al*¹⁴⁶ also synthesized and evaluated LAA and carbohydrate modified enkephalins. These centrally acting anti-nociceptive agents are ideal molecular templates for the development of novel analgesics which may not produce the undesired side effects exhibited by opioids currently utilised in the clinic. However, as with most other peptides, the native compounds are rapidly catabolised via enzymatic degradation following administration, and the amount remaining in the blood stream displays poor BBB permeation due to its highly polar nature. The *in vitro* data suggested that C- terminal modifications of the leu-enkephalin structure were more favourably tolerated than the N- terminal modifications. The *in vitro* activities of the peptide conjugates were established using MVD (mouse vas deferens) and GPI (Guinea pig ileum) assays. However, C-terminal conjugation of one or two glucuronic acid analogues to the native peptide via amide linkages led to a dramatic increase in activity. Thus, it can be concluded that conjugation of the native peptide with a lipoamino acid did not lead to any significant decrease in the biological activity of the peptide (Table 1-2).¹⁴⁶ In addition a novel lipid core peptide (LCP) system was developed by incorporating lipid amino acids to the poly lysine system to enhance lipophilicity and membrane binding effects and the stability of the LCP system.¹⁵⁰

Table 1-2 Lipoamino acid/lipophilic conjugation of peptides

Peptide	Experimental detail	Outcome	Reference
Somatostatin analogue TT 32	A somatostatin construct with lipid and sugar moieties at opposite ends was synthesized so that the entire molecule could be considered as an amphipathic surfactant	Conjugation with LAA's resulted in higher lipophilicity and the conjugated sugars increased water solubility and no loss of anti proliferative activity was observed	149
Enkephalins	LAA and carbohydrate modified enkephalins were synthesized	The C – terminal analogues of the LAA peptide conjugates displayed activity whilst the dimers were inactive. Inclusion of a glucose or glucuronic acid moiety into the lipopeptide structure decreased activity.	144
Methotrexate	MTX was conjugated through one or both of its glutamate carboxyl groups to LAA with varying side chain lengths to alter the lipophilicity and solubility of the adducts	The results indicated that the carboxylic conjugates showed higher encapsulation in neutral and positive liposomes whereas the DPPS-containing negative vesicles gave lower encapsulation	151
Thymogen (IM862)	A library of eight novel derivatives of the dipeptide IM862 was designed and synthesized by conjugating dodecanoic α -amino acid (C12) and/or β -D-glucuronic acid (GlcA).	Nearly all the synthesized lipid and glycoside conjugates displayed greater permeation due to increase in lipophilicity	152
Endorphins (opoid peptides)	Endo 1 and lipopeptides (C12 LAA-endo-1) loaded liposomes were examined for their stability and membrane permeability via Caco 2 cells	Endo-1 was in a homogenate of Caco-2 cells with a short half life while a 3-fold increase in stability was observed with liposomal formulation. The apparent permeability of C12 LAA-Endo-1 was similar to that of Endo-1. An increase in apparent permeability was observed for shorter LAA conjugates (C8 and C10).	153

Occludin peptide	Lipopeptide derivatives of one of the active occludin peptides (OPs), were synthesized by adding a C14-LAA the N terminus.	The L- and D-diastereomers of C14-OP ₉₀₋₁₀₃ had distinctly different effects. The D-isomer, which released intact OP ₉₀₋₁₀₃ from the lipoamino acid, displayed a rapid and transient increase in tight junction permeability. The L-isomer, which released OP ₉₀₋₁₀₃ more rapidly, was seen to have a more sustained increase in tight junction permeability	154
Phenylalanine-Glycine	Butyric acid (C4), caproic acid (C6) and octanoic acid (C8) was conjugated to Phe-Gly	No permeation of parent peptide observed and skin permeation of C6 acyl derivative was found to be highest. Acyl Phe-Gly derivatives increased the stability of the dipeptide	155
DADLE (Tyr-D-Ala-Gly-Phe-D-Leu)	Derivatives were synthesized with various fatty acids by conjugation at the C terminus to increase their stability and permeability in the intestine.	Higher permeability for DADLE-C2, DADLE-C4, and DADLE-C6 was observed in comparison to native DADLE, and DADLE-C4 showed the highest permeability across the jejunum and colon. The permeation of DADLE-C8 was lower than native DADLE despite being the most lipophilic derivative.	156
Cyclosporine (CsA)	Arginine oligomers were conjugated to CsA to facilitate transdermal delivery	The amount of conjugate delivered and the free drug released was therapeutically effective in an animal model of contact dermatitis in which preparations containing 1, 0.1 and 0.01% of a chemically releasable CsA conjugate reduced ear inflammation.	157

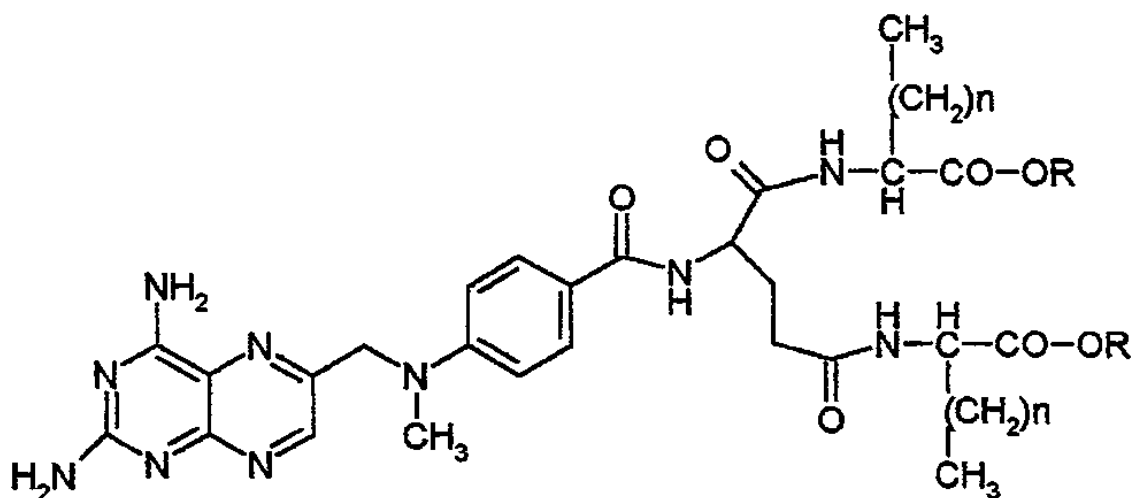


Figure 1.10 Lipoamino acid conjugate of methotrexate¹⁵¹

In 2003, Pignatello *et al*¹⁵¹ studied the effect of liposomal delivery on *in vitro* antitumor activity of lipophilic conjugates of methotrexate (MTX) with lipoamino acids (Figure 1.10). In previously published studies, they had described the synthesis and preliminary biological evaluation of a series of conjugates of methotrexate with lipoamino acid residues (Table 1-2). The activity exhibited *in vitro* by the liposomal formulations was found to be comparable to or lower than that of one of the free drugs after the same times of incubation. Therefore, inclusion in the phospholipid vesicles did not further improve the penetration through cell membranes by passive diffusion of these lipophilic conjugates. The highest improvement of activity with respect to the free compounds was generally observed by encapsulating the conjugates in positively charged (Stearylamine containing) liposomes.

Another study was undertaken to investigate the use of liposomes for the delivery of the lipopeptide antigens, with the intention of enhancing uptake and subsequent cellular expression of the entrapped antigen. Synthetic lipopeptides were synthesized by conjugating C8, C12 and C16 LAA to the antigens. This conjugation enhanced the immune stimulatory capacity of peptide antigen. However, encapsulation of lipopeptides within liposomes appears to compromise their immune stimulatory capacity at least at a loading of 10% when tested in cell culture. Only the C12 lipopeptide encapsulated in liposomes showed enhanced activity over unmodified peptide either alone or

encapsulated in liposomes.¹⁵⁸ Research has also been undertaken on a naturally occurring thymic peptide, Thymogen, is a dipeptide shown to possess immunomodulating and anti-angiogenic properties. It is highly hydrophilic in nature and hence demonstrates low permeability across the gastrointestinal tract. The dipeptide L-Glu-L-Trp-OH is under development for potential treatments of certain cancers and immunodeficiency disorders. Intestinal permeability was studied using Caco 2 cell layers and it was observed that the permeability of IM862 alone could not be determined as its concentration was below the limit of quantification, hence confirming the poor oral absorption of the dipeptide (Table 1-2). In comparison, nearly all the synthesized lipid and glycoside conjugates displayed greater permeation values.¹⁵²

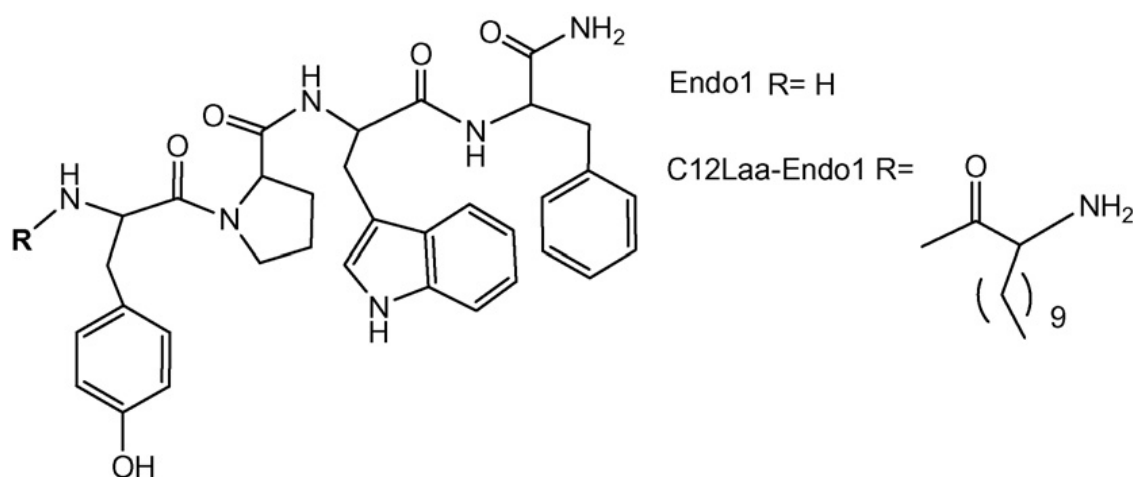


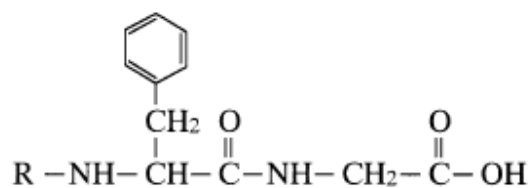
Figure 1.11 Structure of Endo 1 and C12-LAA-Endo 1¹⁵³

Endorphins (opioid peptides) were isolated from mammalian brain tissue and are widely distributed in the human CNS. These peptides were not favourable drug candidates due to low stability and poor membrane permeability. To fulfill their potential as pharmaceutically relevant pain-modulating compounds, pharmacokinetics of these peptides must be improved. LAA residues (8,12,18 carbons) were introduced as a racemic mixture of both the L- and D-stereoisomers.¹⁵³ These modified endorphin peptides overcame the poor metabolic stability and the low membrane permeability *in vitro*. In a follow on study the endo 1 and lipopeptides (C12 LAA-endo-1) (Figure 1.11) loaded liposomes were examined for their stability and membrane permeability and it was concluded that the liposomal formulation of endo 1 and C12 LAA-Endo-1 formed

stable emulsions in buffer and the liposomal preparation of the lipopeptide had higher metabolic stability than the liposomal formulation of the native peptide (Table 1-2). The permeability across Caco-2 cell monolayers of both peptides was also improved 2-fold with the liposomal formulation.¹⁵⁹ Staffan *et al* also investigated the effect of LAA conjugation to long chain peptides such as occludin (Table 1-2). It was concluded from this study that there can be clear differences in the permeability/stability of the D- and L-diastereomers after conjugation to a peptide.¹⁵⁴

Polysaccharides have also been used for delivering drugs to colon. The rationale for using polysaccharides as a delivery system is the presence of a number of polysaccharidases in the colon which degrade the carrier and release the drug. Some of the polysaccharides that have been studied for delivering drugs to colon include chitosan, pectin, cyclodextrin, dextrans and inulin.¹⁶⁰ One example of polysaccharides is dextrans which have varying molecular weights. These compounds have been used most widely to modify the pharmacokinetics of drugs. Examples of their use include the local delivery of anticancer and chemisensitiser drugs using biodegradable dextran ion-exchange microspheres.¹⁶¹

Fatty acid addition to peptides can enhance bioavailability and membrane permeability of peptides that are poorly absorbed.¹⁶² Whittaker *et al*¹⁶³ used 2-amino-2-hydroxy-methyl-1,3-propanediol (tris) a common laboratory reagent to link fatty acyl groups to peptides. Improvement in the transdermal delivery of tetragastrin by lipophilic modification with fatty acids (acetic acid and butyric acid) has also been studied. The flux of these acyl derivatives was in the order of acetyl > butyroyl > caproyl. The stability of tetragastrin in skin homogenate was also significantly improved by chemical modification with fatty acids. These results suggested that chemical modification of tetragastrin with fatty acids increases its lipophilicity, which makes it permeable across the skin. Moreover, it also reduced the degradation in the viable skin, resulting in increase in permeation of tetragastrin across the *stratum corneum*.¹⁶⁴



R = C4, C6 or C8

Figure 1.12 Phe-Gly and its acyl derivatives¹⁵⁵

Lipophilic derivatives of Phe-Gly have also been synthesized by chemical modification with butyric acid (C4), caproic acid (C6) and octanoic acid (C8) (Figure 1.12). The *in vitro* stability, permeability and accumulation of this peptide were investigated in rat skin. The native peptide rapidly degraded in the skin homogenates but the acyl-Phe-Gly derivatives were more stable than the parent peptide. Also no significant difference was observed in the stability of the acyl-Phe-Gly derivatives. All the three derivatives permeated across the skin and the permeation of the C6 acyl derivative was the highest. No permeation of the parent peptide was observed. These results thus, suggested that it was possible to adjust the lipophilicity of Phe-Gly derivatives by conjugating them with fatty acids and higher the carbon number of the fatty acids higher is the stability and the transdermal absorption (Table 1-2).¹⁵⁵ Chemical modification of peptide and protein drugs is a potentially useful approach because it can alter the various physicochemical properties of peptides and proteins, such as an increase in their molecular weights and lipophilicity and alter their *in vivo* pharmacokinetic behaviour. Furthermore, Fujita *et al* found that acyl peptides were more permeable across the intestine than the native peptides while retaining their biological activities. They studied the intestinal absorption of chemically modified of hCT (human calcitonin) and investigated the synergistic effects of acylation and absorption enhancers on its intestinal absorption.¹⁶⁵

In a study conducted by Uchiyama *et al* DADLE (Tyr-D-Ala-Gly-Phe-D-Leu), an enkephalin analogue, was chosen as a model peptide, and new lipophilic derivatives of DADLE were synthesized by chemical modification (Table 1-2). It was found that the derivatives had at least 75% activity of the native DADLE. DADLE was also found to be relatively stable and is resistant to aminopeptidases, carboxypeptidases and

enkephalinases. The higher permeability of these derivatives across jejunum and colon in comparison with native DADLE might be accounted for by their lipophilicity.¹⁵⁶

Another interesting study was published by Rothbard *et al* where they studied the conjugation of arginine oligomers to cyclosporine to facilitate transdermal delivery through the skin. Orally administered CsA is effective against a broad range of inflammatory skin diseases, including widespread conditions such as psoriasis and atopic dermatitis; however, systemic administration is limited by considerable side effects, including nephrotoxicity and many drug interactions. Topical application of CsA has been proven ineffective in a range of inflammatory disorders due to poor topical absorption. Short oligomers of arginine efficiently cross biological membranes and can be used to facilitate the uptake of a variety of small molecules to which they are attached (Table 1-2). The results indicated that short oligomers of arginine facilitated transport across the cutaneous barrier when applied topically.¹⁵⁷ Lipoamino acid and lipid conjugation thus, holds promise in modifying the properties of different therapeutic peptides by increasing their stability, lipophilicity, permeability across biological barriers and in some cases the activity of these molecules which are of therapeutic significance in the treatment of various diseases.

1.5 Peptides as dermatological and cosmetic agents

A number of small peptides have been identified for their therapeutic or cosmetic potential in the skin. In this project we have investigated the skin permeation of Alanine-Tryptophan (Ala-Trp) as a model dipeptide.

1.5.1 Small peptides as cosmeceuticals

For example, carnosine (β -Ala-His), a widely researched peptide is implicated in biological activities such as wound healing and as an antioxidant. The native peptide has very low affinity for the skin and does not permeate beyond the first layer of the *stratum corneum*, the outermost region of the epidermis. However, when a palmitoyl chain is attached to the terminal $-NH_2$ group the lipopeptide has been shown to diffuse into the *stratum corneum*, epidermal and dermal skin layers and remain localized without any

systemic activity.¹⁶⁶ Lys-Thr and Lys-Ser dipeptides have been used in personal care compositions to improve the cosmetic appearance of skin, hair and nails.¹⁶⁷ Lys-Thr and N-acyl derivatives and esters have also been used to treat or minimize signs of skin ageing such as wrinkles, skin lines and large pores.¹⁶⁸ The dermatological use of the citrullinylarginine dipeptide as a skin and phanera care and treatment agent has also been studied and is said to have repairing and revitalizing properties.¹⁶⁹ Acetyl-dipeptide-1 cetyl ester is another such dipeptide which is used as a hair conditioning and skin conditioning agent.¹⁷⁰ Dipeptide-2 consists of amino acids, valine and tryptophan and is believed to improve lymphatic circulation and is used in eye creams for dark circles and puffy eyes. The peptide's structure resembles that of the lipid content of the epidermis and is considered to be a natural moisurizing factor as it helps in the skin's healing process and prevents dermal irritation.¹⁷¹ A number of other small peptides are also formulated or under investigation for their anti-ageing potential.¹⁷²

1.5.2 Small peptides as dermatologicals

Similarly dipeptides also have therapeutic potential in the treatment of Herpes simplex virus type 2 infection (HSV-2). These immunotherapeutic agents induce cytokine production that can lead to potent antimicrobial activity.¹⁷³ Immunomodulating dipeptides such as muramyl dipeptides have shown antiviral activity against pathogens including murine cytomegalovirus and human immunodeficiency virus type 1 (HIV-1).^{174, 175} In other work, a bacterially derived dipeptide, SCV-07 (gamma-d-glutamyl-l-tryptophan), significantly increased the efficacy of antituberculosis therapy, stimulated thymic and splenic cell proliferation, and improved macrophage function.¹⁷³ Two commercially available dipeptides of glutamine are DIPEPTIVEN™, which is an alanyl-glutamine (Fresenius Laboratories, Germany) and GLAMIN™ (Pharmacia and Upjohn Laboratory, Sweden). Arginyl-glutamine dipeptide inhibits the over-proliferation of unwanted blood vessels and is advantageous in retinopathy because it is safe for human and animal use and can be readily formulated in an aqueous solution.¹⁷⁶ Use of the dipeptides, alanyl-glutamine (Ala-Gln) and glycyl-glutamine (Gly-Gln) has also been suggested as an alternative to the use of free Gln as a supplement in total parenteral nutrition (TPN), owing to their better pharmaceutical properties.¹⁷⁷ The antihypertensive

effects of dipeptides such as Ile-Tyr, Lys-Trp, Val-Tyr, and Ile-Trp have been demonstrated to be derived from their inhibitory effect on angiotensin-I-converting enzyme.¹⁷⁸ In a study conducted by Lin *et al*, the penetration of various amino acids and dipeptides through porcine skin was measured *in vitro* to examine the effect of lipophilicity and molecular weight of the compounds on the permeability of passive diffusion. The results indicated that the effect of lipophilicity was a more dominant factor than the molecular weight. The permeability of Ala-Leu, Ala-Phe, Ala-Trp, Gly-Gly and Trp-Ala was also predicted and the permeability was comparable to that of other experimental systems in the same molecular weight range.¹⁷⁹ Abla *et al* studied the effect of charge and molecular weight on the transdermal delivery of peptides by iontophoresis. Two series of dipeptides were selected for this study: the first was a group of unblocked lysine-containing dipeptides, the second, a series of (unblocked and partially blocked) tyrosine-containing dipeptides. The results demonstrated that for the amino acids and dipeptides studied the transdermal flux was governed by the charge/MW ratio. It was also shown that ionic mobility decreases with increasing molecular weight.¹⁸⁰ In a study by Babizhayev *et al* it was shown that, *N* - acetylcarnosine may pass through the lipid membranes of the corneal and skin cells more easily than carnosine. *N* – acetylcarnosine can be gradually broken down to carnosine which then exerts its beneficial effects. *N* – acetylcarnosine containing eye drops have demonstrated efficacy in treating a variety of ophthalmic conditions including corneal diseases, cataracts and glaucoma. Due to its relative hydrophobicity as compared to L-carnosine, it might cross the cornea of the treated eye gradually and maintain the concentration of L- carnosine for a longer time in the aqueous humor. Data also demonstrated that the topical administration of 1% L-carnosine to the rabbit eye does not lead to the accumulation of this compound in the aqueous humor. It was thus concluded, that using *N* – acetylcarnosine or its pharmacologically acceptable salt in combination with a cellulose compound can be used to increase the intraocular (or transepidermal) permeation of L-carnosine in mammals upon ophthalmic or cosmetic application.¹⁸¹

1.6 Tetrapeptide conjugates as treatment options in psoriasis

The second group of peptides we looked at in our project was the native tetrapeptide, Alanine-Alanine-Proline-Valine (Ala-Ala-Pro-Val) and its lipoaminoacid conjugates which act as Human neutrophil elastase (HNE) inhibitors. HNE is a member of the chymotrypsin family of serine proteases and is primarily located in the azurophil granules of polymorphonuclear leucocytes. It can cause the degradation of a wide variety of biomacromolecules such as elastin, which plays a major structural function in the lungs, arteries, skin and ligaments, collagen types I, II, III, IV, VIII, IX and XI, fibrin, fibronectin, cartilage proteoglycans, cytokines, the platelet IIb/IIIa receptor and cadherins.¹⁸² Human neutrophil elastase (HNE; EC 3.4.21.37) has physiological functions in host defense against bacterial infections and extracellular matrix (ECM) remodeling following tissue injury.¹⁴⁵ During acute inflammatory disorders, the local concentration of HNE exceeds those of its natural inhibitors such as α_1 -proteinase inhibitor, leading to ECM degradation.¹⁴⁵ Insufficient levels of protease inhibitors has been therefore suggested as a contributing factor in a number of diseases including, among others, acute lung injury, cystic fibrosis, ischemic reperfusion injury, rheumatoid arthritis, atherosclerosis, psoriasis, and malignant tumors.¹⁴⁵ Active HNE is detected in psoriatic lesions and induces keratinocyte hyperproliferation via the EGFR signaling pathway.¹⁸³ This imbalance can be restored by administration of natural inhibitor (α_1 Pi) or low molecular weight peptidic reversible or irreversible inhibitors.^{184, 185} Thus, the involvement of HNE in such pathological processes makes it an interesting target for the development of anti-inflammatory drugs. Attempts to develop useful therapeutic HNE and elastase inhibitors are therefore in progress.

Hassall *et al* synthesized a new family of water soluble, reversible HLE inhibitors which had potential use in the treatment of inflammatory conditions.¹⁸⁵ In another study done in the same year, Hornebeck *et al* synthesized fatty acid peptide derivatives as model compounds to protect elastin against degradation by elastases. Peptide sequences which fit the extended binding sites of porcine pancreatic elastase and human leukocyte elastase were covalently coupled to oleic acid. The coupling of a fatty acid moiety to the peptide greatly decreased its inhibitor constant (Ki) vs. human leukocyte elastase (Ki for

Oleoyl(Ala)₂ProValine: 3.0 (10⁻⁶M). The modifications of the carboxylic end group of the peptide to an aldehyde further greatly enhanced the inhibition capacity of the compound towards leukocyte elastase (K_i for Oleoyl(Ala)₂ProAlaninal: 0.7 μM). It was thus shown that, Oleoyl(Ala)₂Pro-Valine was also capable of inhibiting elastases in their adsorbed form to insoluble elastin.¹⁸⁶ The effect of oleoyl peptide, oleoyl-alanyl-alanyl-prolyl-valine (Ol-Ala-Ala-Pro-Val-OH) conjugates against elastolysis by neutrophil elastase and kappa elastin-induced monocyte chemotaxis was investigated by Rasoamanantena *et al.* The results indicated that when the -COOH terminal of the oleoyl peptide was derivatized to amide forms, the compound lost its ability to interact with HNE while keeping its elastin-protecting function. In addition, the HNE-inhibitory capacity of Ol-Ala-Ala-Pro-Val-OH was only reduced 2-fold by using elastin as a substrate. This decrease was much lower than those determined with other HNE inhibitors of similar potency and could be accounted for by the ability of oleoyl peptide to bind to elastin.¹⁸⁷

The role of plant derived phenolics as HNE inhibitors was investigated by Hrenn *et al.* Several phenolics of different sizes were tested and it was found that the ellagitannins, agrimoniin and pedunculagin were the most potent direct HNE inhibitors (IC₅₀ = 0.9 and 2.8 μM, respectively). Agrimoniin also showed anti-proliferative effects in the ATP assay (IC₅₀ = 3.2 μM), suggesting that this type of tannin could have beneficial effects in the treatment of diseases such as psoriasis.¹⁸⁸ In a study conducted on some Yemeni medicinal plants it was found that 14 extracts at various concentrations inhibited the activity of HNE¹⁸² Steinbrecher *et al* reported the binding affinity prediction, organic synthesis, and activity measurement for bornyl (3,4,5-trihydroxy)-cinnamate. This compound was a cinnamic acid ester derivative found to have IC₅₀ value in the μM range. Free energy calculations predicted that the ligand would inhibit HNE with an IC₅₀ value in the nanomolar range.¹⁸³ Many other studies have investigated compounds such as alpha-ketooxadiazole, for their role in HNE inhibition in psoriasis and in different disease states.¹⁸⁹

Peptidic HNE inhibitors have a common hydrophobic sequence which partially mimics certain amino acid sequences found in elastin. The Ala-Ala-Pro-Val sequence fits the P-

P1 subsites of elastase and inhibits HNE competitively. Toth *et al* synthesized a series of lipopeptides of increasing lipophilic character keeping the peptide moiety (Ala-Ala-Pro-Val) constant and their HNE inhibitory capacity was then analysed. Enzyme inhibition increased with increased lipophilicity of the substances; all compounds were more potent HNE inhibitors than N-oleoyl-(Ala)₂Pro-Val-OH.¹⁴⁵ We have investigated the approach of lipoamino acid conjugation to increase the lipophilicity of the tetrapeptide and assess its transdermal delivery and biological activity. In an earlier study we had assessed the effectiveness of coupling a short chain lipoamino acid (LAA) to enhance transepidermal delivery of a model HNE (human neutrophil elastase) inhibitor. HNE was coupled to a racemic mixture of a short chain LAA resulting in two diastereomers of the lipoamino acid modified tetrapeptide. The penetration of the lipopeptide mixture was assessed across human epidermis *in vitro*. The cumulative amount (μg : mean \pm SEM; n=6) penetrating to the receptor over 8 h was approximately $80 \mu\text{g}/\text{cm}^2$ for the D-LAA conjugate, $30 \mu\text{g}/\text{cm}^2$ for the L-LAA conjugate, compared to 0 for the peptide. It was concluded that the D-diastereomer was more stable than the L-diastereomer and penetrated the human epidermis more than the L-diastereomer.¹⁹⁰ The application of this approach to cutaneous delivery is relatively new and has merit on a scientific basis but may be less convenient from a regulatory viewpoint as chemical modification generating a new compound is involved.

1.7 Anti-inflammatory peptides in skin diseases

Inflammation is mediated by a series of events that are mediated by cellular and soluble components of the immune system.¹⁹¹ Lymphomononuclear cells play important role in inflammatory process. Intraepidermal localization of activated T-lymphocytes and dermal infiltration of monocytes are unique histologic features of psoriasis. These cells have important role in initiation and maintenance of the inflammatory process via several cascade mechanisms including cytokines (IL-2, IFN- γ) and chemokines (IL-8, RANTES).¹⁹² Extensive research has been undertaken to study the effects of anti-inflammatory peptides on the proinflammatory cytokines and the T cell function. In a study conducted by Rayachaudhri *et al*, the anti-inflammatory actions of peptide T were investigated. Peptide T (Ala-Ser-Thr-Thr-Thr-Asn-Tyr-Thr) is a ligand for the CD3:T3

receptor and is a part of the HIV envelope protein gp120. The study reported that, peptide T analogue (DAPTA) inhibited the lymphocyte, monocyte chemotactic activities of RANTES and fmlp. Thus DAPTA may help to decrease the cellular infiltrates which in turn may decrease the intraepidermal chemokine and cytokine cascade activities.³⁴ Manlios *et al*¹⁹³ explored the role of core peptide (CP; G-L-R-I-L-L-L-K-V) to inhibit IL-2 production in T cells following antigen recognition. This peptide had protective effects of induction on adjuvant induced arthritis in rats. In this study, the tris technology was used as a delivery system for core peptide. To increase biological availability of CP, the peptide was conjugated to tris-glycine-tripalmitate and then injected in rats. When tested in acute adjuvant induced arthritis the lipopeptide had a therapeutic effect on inflammation.¹⁹⁴ Babu *et al* studied the *in vitro* permeation and distribution of spantide II with or without cysteine HCl (CH) as a penetration enhancer through hairless rat skin. The anti-inflammatory effect of spantide II was studied by measuring the reduction of allergic contact dermatitis (ACD) in C57BL/6 mice after application of spantide II as a topical solution. The *in vitro* permeation studies indicated no detectable levels of spantide II permeated through hairless rat skin. However accumulation of the peptide was seen in the different skin layers making it suitable for topical drug delivery. The anti-inflammatory activity of SP antagonist spantide II was also demonstrated by topical application.¹⁹¹

A new class of anti-inflammatory peptides being researched are the α -MSH (melanocyte stimulating hormone) and related peptides. α -MSH is a tridecapeptide which, upon proteolytic cleavage, is generated from its precursor ACTH. The anti-inflammatory effects of α -MSH which have been observed at subpicomolar, concentrations have been attributed to modulation of proinflammatory cytokine and adhesion molecule expression. α -MSH and related tripeptides have been shown to possess promising *in vitro* as well as *in vivo* anti-inflammatory effects. In particular the α -MSH-related tripeptides appear to be suited to being developed as anti-inflammatory drugs. Their small molecular size further provides advantages especially for local therapy of inflammatory diseases of skin and mucous membranes.¹⁹⁵ Granulysin is another antimicrobial peptide that was modified by shortening the length of the peptide to 20 amino acids. It was observed that even after chemically modifying the structure it

retained both antimicrobial and anti-inflammatory activity.¹⁹⁶ The potential of an anti-inflammatory peptide (antiflammin I) to reduce irritation when delivered transdermally by iontophoresis has been examined by Mize *et al.* These nonapeptides have been reported to have potent anti-inflammatory activity *in vivo* without any of the known side effects of corticosteroids. Transdermal delivery of antiflammin I significantly decreased drug-induced inflammatory response in hairless guinea pig skin, demonstrating retention of the peptides biological activity after delivery *in vivo*.¹⁹⁷ In this project we have evaluated the transdermal delivery of 3 anti-inflammatory peptides, core peptide (CP) and two analogues that have demonstrated improved biological efficacy and specificity: a cyclic peptide sequence (C1) and its linear sequence counterpart (C1-L).

1.8 Significance and objective

An effective transdermal application is expected to provide a new therapeutic approach for psoriasis and other inflammatory disorders associated with the skin and underlying tissues. In many cases these conditions are poorly controlled with currently available products. Several peptides and synthetic small molecules are now available that can inhibit specific pathways in the development of psoriasis.^{8, 9} Examples include peptide T, RNase 7, granulysin and psoriasin. An effective delivery system that targets therapeutic compounds to their sites of action, preferably following a convenient application to the skin surface, will provide a major advancement in the management of psoriasis and other skin related disorders.

The overall objective of this research was to investigate novel technologies for the enhanced transdermal delivery of peptides, particularly those with therapeutic or cosmetic application in skin. The major objective of this research was to assess different enhancement strategies (Dermaportation and lipoamino acid conjugation) for the delivery of small and high molecular weight peptides for cosmetic and therapeutic uses. Our hypothesis is that Dermaportation and lipoamino acid conjugation will enhance the delivery of small and high molecular weight peptides through the skin. We also hypothesize that, the skin permeability of a core peptide (CP), which has anti-

inflammatory activity will also increase upon cyclization. The project was divided into following parts:

- Assessment of stability and skin permeability of a model dipeptide (Ala-Trp) across human epidermis with Dermaportation
- Assess the stability, skin permeability, accumulation and biological activity of the native tetrapeptide (Ala-Ala-Pro-Val) and its lipoamino acid conjugates
- Assess the skin permeability and accumulation of Acetyl hexapeptide 3 and its lipoamino acid conjugates
- Assess the stability and skin permeability of the core peptide with anti-inflammatory activity and two analogues, a cyclic peptide sequence (C1) and its linear sequence counterpart (C1-L)

Chapter 2.

Permeability of a Model Dipeptide (Ala-Trp) Across Human Epidermis: Effect of Pulsed Electromagnetic Energy

2.1 AIM

The aim of the present study was to assess the effect of pulsed electromagnetic field (PEMF) energy (Dermaportation DP1001; OBJ Ltd) on the permeation of a model dipeptide (Ala-Trp) through human epidermis using an *in vitro* skin diffusion model. The stability of the dipeptide was also assessed at different temperatures and conditions. As discussed in section 1.5 dipeptides have potential as cosmetic and therapeutic agents. To exert either of these actions, the peptide should permeate through the lipophilic *stratum corneum* and accumulate in the viable epidermis or dermis depending on its target site of action. Ala-Trp was selected as a small molecular weight model dipeptide to study the penetration enhancement effects of Dermaportation, which is a newly developed PEMF technology.

2.2 Materials and Methods

2.2.1 Chemicals

Alanine-Tryptophan (Ala-Trp), a model dipeptide with a molecular weight 275.30 Da was purchased from Sigma Aldrich (USA). Acetonitrile, HPLC solvent was supplied by JT Baker (USA) and phosphate buffered saline solution (PBS) was prepared according to the United States Pharmacopoeia.

2.2.2 HPLC instrumentation and conditions

The samples were analysed by reverse phase HPLC Agilent 1100 system which consisted of a quaternary pump (G1311A), autosampler (G1313A), degasser (G1312A) and photo diode array detector (G1321A). Separation was achieved on a Phenomenex Jupiter C18, 300A column (5 μ m, 4.6mm \times 150mm). Integration was undertaken using Chemstation software B.03.01 [317]. Elution was performed at ambient temperature using a mobile phase gradient at a flow rate of 1 mL/min and the wavelength of detection was 210 nm. Buffer A was 0.1% TFA and Buffer B was 0.1% TFA in acetonitrile. The dipeptide was eluted using a combination of isocratic and linear gradient protocol; Buffer B was held at 10% for 5 min followed by a linear gradient

from 10 to 100% over 10 min. All samples were analysed by HPLC using injection volumes of 20 μL .

2.2.3 HPLC analysis and validation

Calibration curves were obtained using 0.9, 1.9, 3.9, 7.81, 15.62 and 31.25 $\mu\text{g/mL}$ of Ala-Trp standard solutions in PBS at pH 7.4. Linearity (quoted as R^2) was evaluated by linear regression analysis, which was calculated by the least square regression method. The precision of the assay was determined by injecting three standard concentrations (0.9, 7.8 and 31.25 $\mu\text{g/mL}$ Ala-Trp) six times on the HPLC column. The intra-day repeatability was assessed by injecting 7.8 and 15.62 $\mu\text{g/mL}$ Ala-Trp standards six times at different times in a day. The inter-day repeatability was determined by injecting 7.8 and 15.62 $\mu\text{g/mL}$ Ala-Trp standards six times on 3 different days. The intra- and inter-day repeatability were quoted as the coefficient of variance. The minimum detectable and quantifiable limits (LOD and LOQ) were measured by diluting Ala-Trp in PBS to give a concentration range from 0.9 to 31.3 $\mu\text{g/mL}$ and then injected on the HPLC. Accuracy of the analytical method was determined for *in vitro* skin diffusion studies as follows. Two separate samples of PBS which had been incubated with human epidermis for 24h at 37°C were spiked with Ala-Trp standards to give final concentrations of 7.8 and 15.6 $\mu\text{g/mL}$ Ala-Trp. Each spiked sample and standard was injected six times on the HPLC column and the percentage difference between each standard and the corresponding spiked sample was calculated.

2.2.4 Stability study

The stability of Ala-Trp was determined at different temperatures and with having the dipeptide in contact with skin to provide an estimate of the stability of the drug during the skin diffusion experiments. The following temperatures were used: 37°C, room temperature (ambient light), room temperature (dark) and at 4°C. Vials containing 3 mL of 1 mg/mL dipeptide solution were stored under these conditions. 100 μL samples were withdrawn at 0, 20, 45, 60 min, 2h, 3h, 4h, 5h and 6h. The samples were then diluted to give a final theoretical concentration of 20 $\mu\text{g/mL}$ and were analysed by HPLC.

2.2.5 Human skin preparation

Full thickness human skin samples excised from female patients (30 year old female abdominal section was used in the present study) undergoing abdominoplasty at Perth hospitals were refrigerated immediately after surgery. Sampling was approved by the Human Research Ethics Committee of Curtin University (Approval numbers HR132/2001, HR 70/2007 and HR 129/2008) and was conducted in compliance with the guidelines of the National Health and Medical Research Council of Australia. The following procedure was used to obtain epidermal sheets. The subcutaneous fat was removed by dissection, the full thickness skin then immersed in water at 60°C for 1 min, allowing the epidermis to be teased off the dermis.¹⁹⁸ The epidermis was placed onto aluminum foil, air dried, then placed in a zip-lock bag and stored at -20°C until required.

2.2.6 Skin permeation of Ala-Trp

In vitro permeation studies across human epidermis were performed in Pyrex glass Franz-type diffusion cells (enabling permeation across skin sections of cross sectional area 1.18 cm²; receptor volume approximately 3.5 mL: Figure 2.1). Epidermal membrane was placed between the donor and receptor compartments and allowed to equilibrate for 30 min with the receptor solution (PBS pH 7.4) which was stirred continuously with a magnetic stirrer bar. The receptor compartment of the cell was immersed in a water bath at 37±0.5°C. PBS (1 mL) was placed in the donor compartment, allowed to equilibrate for 30 min and the conductivity across the epidermis was measured using a digital multimeter to determine membrane integrity. The PBS solutions were then removed from the donor and receptor compartments and the receptor refilled with approximately 3 mL of fresh pre-warmed PBS. The donor solution, which consisted of 1mL of 1mg/mL Ala-Trp in PBS was added. 200 µL samples of the receptor phase were withdrawn and replaced with an equal volume of fresh pre-warmed (37°C) PBS over an 8 h period to maintain sink conditions. The Ala-Trp content in the samples was determined using HPLC.

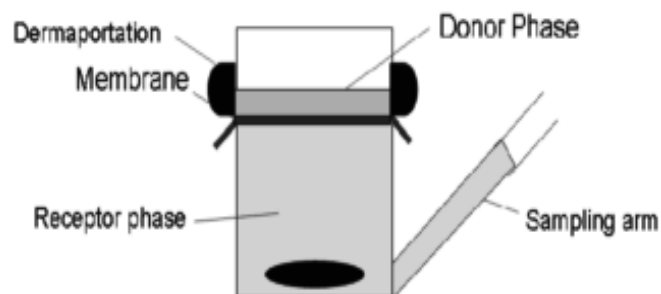


Figure 2.1 Schematic of skin diffusion experimental cell with Dermaportation coil in place

Dermaportation coils were added to the exterior of the donor compartment and energy applied for 8 h (Dermaportation cells), whilst other cells had no external Dermaportation energy applied. 9 replicates were conducted for passive and Dermaportation experimental protocols. The cumulative amount of drug permeated through the epidermis ($\mu\text{g}/\text{cm}^2$) versus time (h) was plotted. The cumulative amount was calculated by taking into account the amount of peptide present at the previous time points plus the amount present in the 200 μL sample and the amount present at the time point at which the cumulative amount is calculated. The flux of Ala-Trp through the human epidermis for both passive and Dermaportation cells was determined from the slope of the plot of cumulative amount versus time and expressed as $\mu\text{g}/\text{cm}^2/\text{h}$. Permeability coefficients (cm/h) were calculated for Ala-Trp for both passive and Dermaportation using the following equation:

$$\text{Permeability coefficient } K_p \text{ (cm/h)} = \text{Flux (J)} / \text{Concentration in the donor (C)} \dots \text{(Eq 1)}$$

2.2.7 Extraction of Ala-Trp from the epidermis and mass balance

The uptake of Ala-Trp into the epidermis was also investigated. To validate the extraction procedure a 1 mg/mL solution of Ala-Trp was allowed to equilibrate with the epidermis for 8 hours. After 8 hours the epidermis was removed, four water washes were completed and 50 μL from each extract was analysed by HPLC. This extraction procedure was undertaken on each epidermal membrane on termination of the skin

diffusion experiment. The donor solution was removed from the donor compartment and the skin sample soaked in 1 mL water. Four water washes were completed and 50 μL from each extract was analysed by HPLC. The donor solution was also diluted 10 times and the diluted solution analysed by HPLC to quantify the amount of the peptide left in the donor at the end of the experiment.

2.2.8 Statistical Analysis

The cumulative amount of target drug in the receptor chamber was determined over the entire period of testing, and the differences between the diffusion by passive and Dermaportation were analyzed using ANOVA with the Factors Treat and Time (GLM procedures, SAS Institute). Further, flux rates ($\mu\text{g}/\text{cm}^2\cdot\text{h}$) were calculated from the slope of the linear relationship between the cumulative amount and time per group. Two separate flux rates were calculated, (i) the rate of the active drug diffusion or transport in the first 20 min, and (ii) the average diffusion rate over the first 2 h. An ANOVA with Fisher LSD post hoc comparisons on the Factors Treat and Experiment was used for the flux rates. A result was considered significant with $p < 0.05$. Enhancement Ratios with respect to passive diffusion were calculated from statistically significant flux values only.

2.3 Results and Discussion

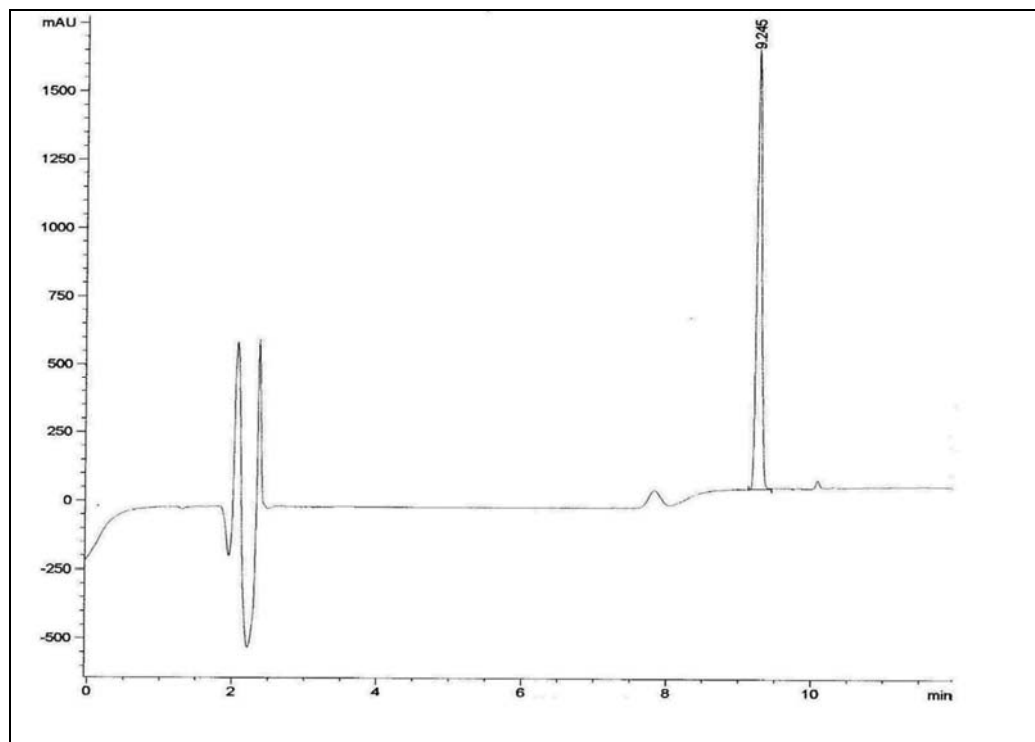
2.3.1 Chromatography

Ala-Trp was analysed by UV detection using HPLC. The dipeptide eluted without any interfering peaks at a retention time of 9.1 min. The linearity obtained by the HPLC method was 0.9999 over the range of the calibration curve (0.975-31.25 $\mu\text{g}/\text{mL}$) for Ala-Trp standard solutions. Figure 2.2 is a typical HPLC chromatogram of Ala-Trp analysed 8 h after (a) passive and (b) Dermaportation administration to human epidermis.

A calibration curve was obtained by plotting the peak area versus concentration of standards injected. The coefficient of variation (CV) for precision, determined from the relative standard deviation ($n = 6$), was 0.27% for 0.98 $\mu\text{g}/\text{mL}$, 0.15% for 7.80 $\mu\text{g}/\text{mL}$

and 0.13% for 31.25 $\mu\text{g/mL}$ Ala-Trp standard solutions in PBS. The intraday variation was 0.69% and 0.43% and the interday variation was 0.55% and 0.38% at 7.80 and 15.63 $\mu\text{g/mL}$ Ala-Trp standard solutions in PBS, respectively. These are within the acceptable criteria for intra and inter-day repeatability of R.S.D. < 2%.

(a)



(b)

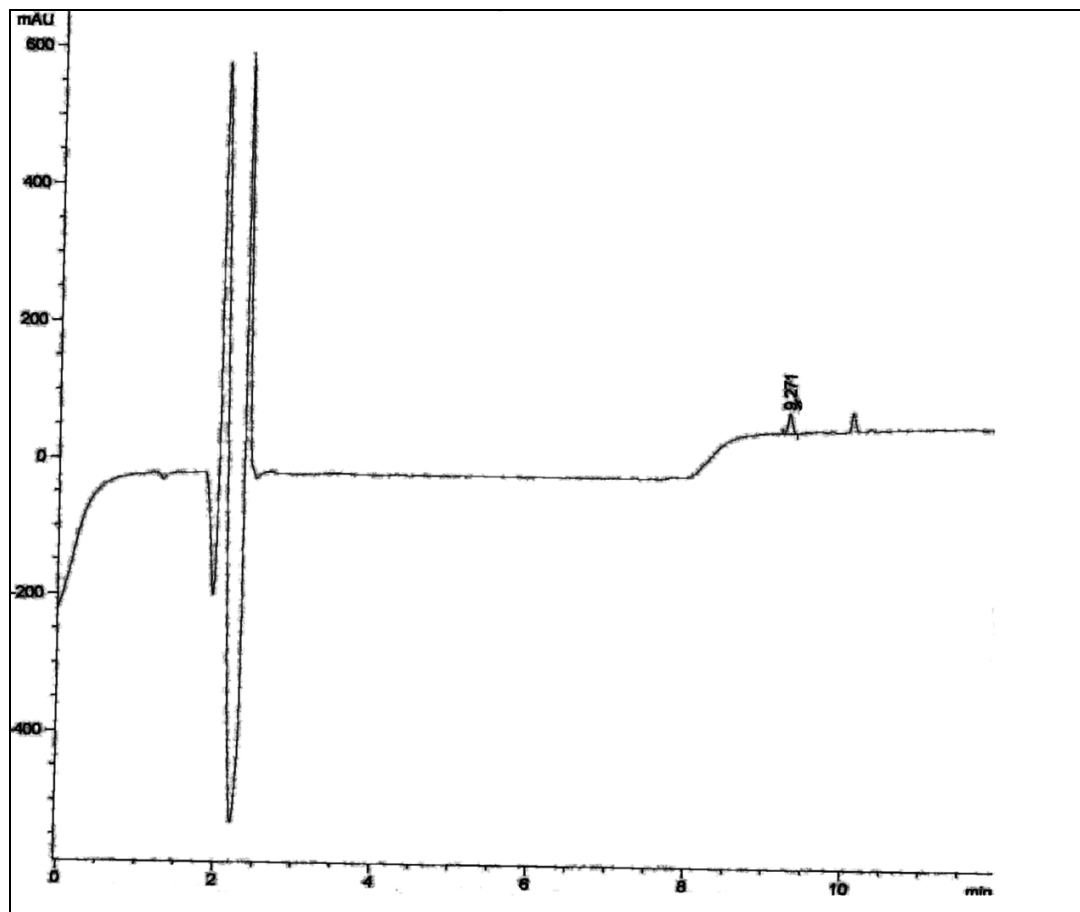


Figure 2.2 Chromatograms for Ala-Trp analyzed after 8h (a) Dermaportation ($96.49\mu\text{g}/\text{cm}^2$) and (b) Passive ($2.77\mu\text{g}/\text{cm}^2$)

The limit of detection (LOD), calculated as greater than three times the baseline noise level in the assay, was 49 ng/mL. The limit of quantitation (LOQ), calculated as greater than 10 times the baseline noise level in the assay, was 165 ng/mL. The suitability of the assay with a simulated diffusion cell receptor solution (PBS solution which had been in contact with skin for 4 h) was demonstrated, with no interfering peaks detected. The HPLC method permitted the detection of 7.8 $\mu\text{g}/\text{mL}$ of Ala-Trp sample with 92.11% accuracy and 15.63 $\mu\text{g}/\text{mL}$ of Ala-Trp sample with 93.16% accuracy.

2.3.2 Stability of the dipeptide in solution

The degradation profile of Ala-Trp at different temperatures is shown in Figure 2.4. The stability data was presented as the percent peptide remaining over time at varying temperatures and conditions. It was observed that when the dipeptide solution was placed at 37°C in contact with the skin about 11% of the peptide was lost in 6 h. This is in agreement with previous reports that lysine and tyrosine containing dipeptides are unstable when in contact with the skin.¹⁸⁰ This compares with only 4.6% loss of dipeptide in the same conditions but without skin present. In our experiment the skin was previously frozen therefore much of the enzymatic activity was lost, yet substantial degradation was still observed. It is expected that the dipeptide would be more extensively degraded where the cutaneous enzymes were preserved. The dipeptide was most stable at 4°C with 3% degraded over the 6 h period, and was relatively stable at room temperature in dark and light conditions with 4% loss over the 6 h period. A separate preliminary study was conducted to assess the stability during Dermaportation and passive diffusion and it was found that the dipeptide collected from the receptor was relatively stable during the time of the experiment. No significant amounts of degradation products, which were present in samples in contact with the skin, were detected. Figure 2.2 is a typical HPLC chromatogram of Ala-Trp analysed 8 h after (a) passive and (b) Dermaportation suggesting that either Dermaportation does not alter the Ala-Trp structure or the degraded products may have a very strong affinity to the skin therefore may not diffuse through the skin. The possibility of the latter is under further investigation.

Dipeptides have previously been shown to degrade in the skin due to the presence of cutaneous enzymes.¹⁷⁹ Skin proteases have been isolated and characterized however it is not known which peptide sequences or peptides are most susceptible to enzymatic degradation in human skin.^{199,200} Previous studies have suggested that peptides can undergo extensive enzymatic metabolism in the viable skin and hence it is particularly desirable to increase the rate and extent of permeation of these drugs across the skin and thereby reduce the potential effects of skin enzymes.²⁰¹

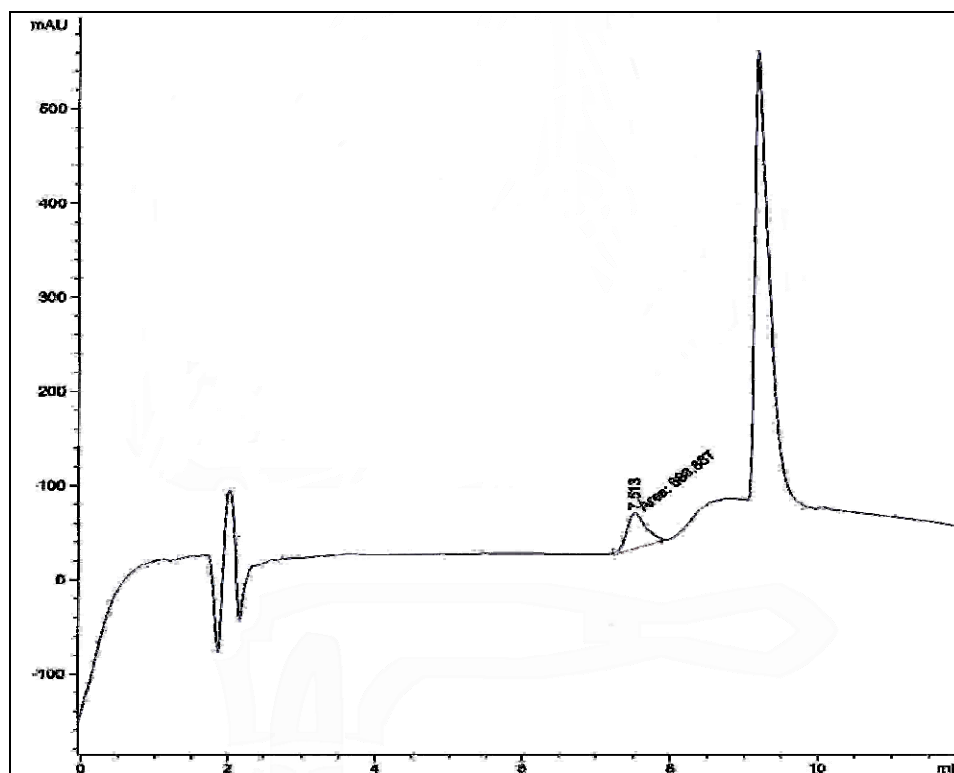


Figure 2.3 Chromatogram for Ala-Trp and degradation product analyzed after 3h when the sample was incubated with skin

In the stability study the rate of degradation of the dipeptide at 37°C without skin was about 9.4 times lower than the rate of degradation at 37°C when the dipeptide solution was left in contact with skin. Figure 2.3 is a typical chromatogram of Ala-Trp and the degradation product analysed after 3h. At lower temperatures (i.e. at room temperature, room temperature and dark and at 4°C) the mechanism of degradation was different than at higher temperatures and it was assumed to follow a biphasic degradation pattern (Figure 2.4). The amount of product that eluted at about 7.5 min, which was suspected to be the degradation product, steadily increased till about 6 h. The total amount of the dipeptide and the percentage of degradation product were plotted against time and the rate was determined from the slope of the linear portion of the curve from 0.33 to 3 h. The rate of degradation as determined in both studies, showed a higher level in the stability study than that of the skin diffusion experiment with Dermaportation. This may

be because the samples in the skin diffusion studies were collected from the receptor compartment that has a lower concentration of the dipeptide and is affected by the skin permeability of the dipeptide and degradation product. A lower percentage of degradation product was detected with passive diffusion since very low amounts of the dipeptide actually traversed the skin, which led to a lower amount of both dipeptide and degradation products in the receptor chamber.

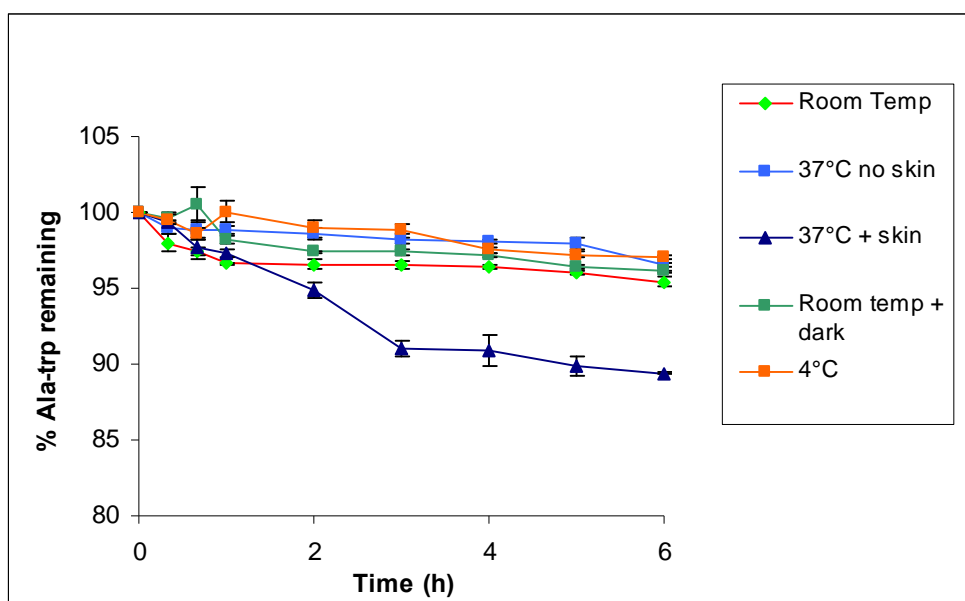


Figure 2.4 Ala-Trp degradation profile in solution at varying conditions

Previous studies on the characterization of aminopeptidases showed that Ala-Trp was susceptible to hydrolysis by aminopeptidase-I but no definite structures of the degradation products were reported.²⁰² Although tryptophan was suspected to be one of the likely degradation products, tryptophan residues in peptides or proteins can also undergo oxidation. Few studies have focussed on identification of compounds formed from these peptides. Simat *et al* attempted to identify tryptophan degradation compounds by subjecting the amino acid itself and peptides containing tryptophan to an oxidising agent.²⁰³ Comparing the transepidermal flux values in this study, it was seen that the permeation of the degradation product is lower than that of the native dipeptide. We have speculated that Ala-Trp may undergo hydrolysis or enzymatic degradation which results in the formation of a degradation product which could be an alanine or

tryptophan related compound. This compound was detected after the diffusion of the native peptide through human epidermis at a lower level than expected, suggesting that this degradation product may have a tendency to remain in the skin. In addition, it was also observed that its permeation through the skin was enhanced by Dermaporation. Fast permeation of the dipeptide by Dermaporation could also mean less contact time for the peptide with the skin enzymes and more rapid delivery to the target site, both of which would benefit the therapeutic outcome.

2.3.3 Permeation of Ala-Trp through human epidermis with Dermaporation

In this study the influence of the novel penetration enhancement technology, Dermaporation on epidermal penetration of Ala-Trp *in vitro* was determined. Dermaporation appears to permit a substantial amount of native dipeptide to penetrate through the skin structure over the 8 h application period. The cumulative amount of Ala-Trp penetrating the human epidermis to the receptor solution over time for Dermaporation and passive application is demonstrated in Figure 2.5. We used the general guideline of accepting skin sections which had conductivity lower than 20k Ω . The conductivity was measured at the start and end of the experiment and cells which had a high conductivity value were not included in cumulative amount calculation. The cumulative amount of dipeptide permeated after 8 hours with Dermaporation was 96.5 $\mu\text{g}/\text{cm}^2$ and the amount permeated with passive diffusion was 2.77 $\mu\text{g}/\text{cm}^2$. The results indicated an increase in the rate and extent of Ala-Trp diffusion through human epidermis over 8 h in cells where Dermaporation was applied, as compared to cells where the dipeptide solution was applied without Dermaporation (Treat: F1,16 = 23.97, $p < 0.001$; Treat by Time interaction: F13,208 = 10.33, $p < 0.001$). An analysis per time point, demonstrated that the Dermaporation-treated cells had already a significantly higher amount of the dipeptide in the receptor compartment at 10 min (Treat=10m: F1,16 = 12.93; $p < 0.005$). At $t = 0$, all groups were equal (Treat=0: F1,16 = 0, $p < 0.001$), demonstrating that no dipeptide was present in the receptor compartment before the experiment was started. The lag time was approximately 0.33h with Dermaporation.

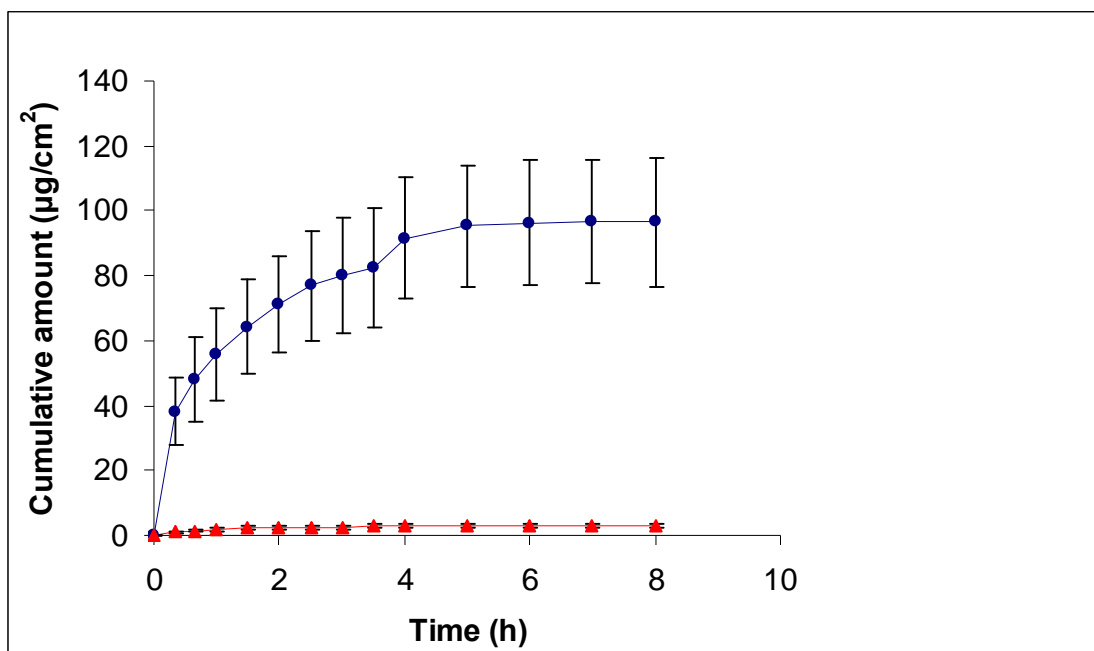


Figure 2.5 Cumulative penetration of dipeptide (1 mg/mL) across human epidermis for passive (▲) or Dermaportation (●) applied from 0-4h (mean \pm SEM: n=9)

The estimated transdermal flux was calculated over the linear portion (0.33-2h) of the curve as $19.427 \mu\text{g}/\text{cm}^2/\text{h}$ for Dermaportation and $0.778 \mu\text{g}/\text{cm}^2/\text{h}$ for passive diffusion. Approximately 35 fold enhancement was observed with Dermaportation as compared to passive diffusion. The estimated permeability coefficient for Ala-Trp was $1.94 \times 10^{-2} \text{ cm}/\text{h}$ with Dermaportation and $7.7 \times 10^{-4} \text{ cm}/\text{h}$ with passive diffusion (Table 2-3). The transdermal permeability coefficient (kp) of the dipeptide in porcine skin when measured for passive diffusion has been reported to be $1.39 \times 10^{-2} \text{ cm}/\text{h}$ by Lin *et al*¹⁷⁹, in comparison with the current study value of $7.7 \times 10^{-4} \text{ cm}/\text{h}$. However it is not valid to directly compare the two permeability coefficients since they were determined using different skin models. In the current study Dermaportation was applied for the first 4 h and a steep increase in cumulative amount permeating to the receptor was observed in 20 mins (38.23 and $1.02 \mu\text{g}/\text{cm}^2$ for Dermaportation and passive application respectively). This difference may be due to an initial push into the skin due to the applied electromagnetic field. There was a steady increase in the amount of dipeptide permeating over the entire period of the experiment (Figure 2.5). Over the first 20 mins, the first 2 h, the first 4 h, and the entire 8 h period, the Ala-Trp diffusion flux in

Dermaportation diffusion cells was larger than for the passive cells (TreatFlux20: $F_{1,16} = 12.93$, $p < 0.005$; TreatFlux120: $F_{1,33} = 20.79$, $p < 0.005$; TreatFlux4hr: $F_{1,16} = 13.50$, $p < 0.005$; TreatFlux8hr: $F_{1,16} = 12.58$, $p < 0.005$). Dermaportation enhanced the permeability of Ala-Trp in the first 20 min by up to 37.3-fold over the passive diffusion rate. This finding is in agreement with previous reports in which Dermaportation was shown to increase the transdermal diffusion of a low molecular weight hydrophilic compound, 5-aminolevulinic acid and the local anaesthetics lignocaine and tetracaine hydrochloride in similar *in vitro* experiments with human epidermis.^{132, 133} Tables 2-1 and 2-2 list the flux and correlation coefficients for the stability study and the skin diffusion experiments.

The efficiency of the solvent extraction method used to recover the peptide from the epidermal membrane at the conclusion of each experiment was approximately 85%. The amount of dipeptide remaining in the epidermis after 8h application period was approximately $0.85 \mu\text{g}/\text{cm}^2 (\pm 0.07)$ with passive diffusion and $0.54 \mu\text{g}/\text{cm}^2 (\pm 0.06)$ with Dermaportation. The comparably lower amount in the skin with Dermaportation as compared to passive diffusion may be due to the increased delivery of the dipeptide to the receptor compartment after 8h.

There have been limited reports on skin penetration enhancement of dipeptides. Altenbach *et al* observed no iontophoretic and passive transport of Tyr-Phe across human skin *in vitro* without the addition of an enzyme inhibitor at 37°C .²⁰⁴ Human cadaver skin of postmortem biopsies excised within 24 h of death from the abdominal region of female donors was used in this study. Epidermal membrane including the *stratum corneum* and the viable epidermis was isolated from the underlying dermis by heat treatment and mechanical separation. The results indicated that there was substantial metabolism of Tyr-Phe in human cadaver epidermis during permeation. The metabolism of Tyr-Phe was potentially catalyzed by enzymes such as dipeptidase, carboxypeptidase and aminopeptidase that have been found in the epidermis. Metabolic degradation of Tyr-Phe at both pH values was found to be completely suppressed at 4°C . Tyr and Phe were found in the receiver solution and recovered from the epidermis. Also, Tyr-Phe permeation was measurable and the amount of intact Tyr-Phe extracted

from the tissue was larger compared to the experiments at 37 °C at the same pH where no permeation of the dipeptide was observed.

We cannot directly compare the transdermal flux values from this study to literature data since there has been very limited work done on Ala-Trp as a model dipeptide. This preliminary study indicates that the delivery rate of the peptide can be enhanced with Dermaportation when compared to passive diffusion. Dermaportation may provide an effective means of delivering molecules that are highly susceptible to degradation like dipeptides, in higher amounts and in a relatively short duration.

2.4 Conclusion

Dermaportation significantly enhanced the delivery of Ala-Trp through human epidermis *in vitro* over an 8 h period when compared to passive diffusion. The dipeptide was shown to be unstable on exposure to human epidermis with an increasing amount of degradation product evident in the receptor phase over the 8 h period. Given the susceptibility of peptides to degradation in the skin it is essential that they are delivered rapidly across the skin in order to maximise the opportunity for delivery of the native peptide. Dermaportation offers a potential new delivery method for skin delivery of peptides for dermatological and cosmetic applications.

Table 2-1 Rate of degradation of Ala-Trp at different temperatures and conditions

Dipeptide						Degradation product	
	Room temperature	37°C without skin	37°C with skin	Room temperature and dark	4°C	37°C with skin	% of Degradation product
Rate ($\mu\text{g}/\text{cm}^2/\text{h}$)	4.9	2.98	28.34	10.64	1.89	6.61	0.66
Correlation coefficient (R^2)	0.643	0.981	0.981	0.679	0.115	0.982	0.983

Table 2-2 Rate of permeation of dipeptide and degradation product with Dermaportation and passive diffusion. Data are mean (\pm SEM, n=9)

	<i>Dipeptide</i>		<i>Degradation product</i>		<i>% of degradation product</i>	
	Dermaportation	Passive	Dermaportation	Passive	Dermaportation	Passive
Flux ($\mu\text{g}/\text{cm}^2/\text{h}$)	19.42	0.77	2.36	0.13	2.39	0.021
Correlation coefficient or rate (slope) (R^2)	0.978	0.940	0.993	0.931	0.996	0.001

Table 2-3 Skin permeation of Ala-Trp with Dermaportation and passive diffusion over 2h

Treatment	Cumulative amount ($\mu\text{g}/\text{cm}^2$)	Transdermal flux ($\mu\text{g}/\text{cm}^2/\text{h}$)	Permeability coefficient (k_p) (cm/h)	Enhancement ratio (0-2h)
Dermaportation	96.49	19.42	1.94×10^{-2}	34.67
Passive	2.77	0.77	7.7×10^{-4}	

Chapter 3.

Skin Permeability and Biological Activity of a Therapeutic Peptide and its Lipoamino Acid Conjugates

3.1 Aim and Brief Background

This study was designed to investigate the lipoamino acid (LAA) conjugation approach for enhanced skin permeability of small peptides, particularly those with therapeutic application in skin diseases. The choice of the Human Neutrophil Elastase (HNE) inhibitor peptide offers the potential for application as a new therapeutic approach for psoriasis and other inflammatory disorders associated with the skin. The effectiveness of coupling a short chain LAA to enhance transepidermal delivery of a model HNE inhibitor tetrapeptide (Ala-Ala-Pro-Val or AAPV) was assessed. The optimal conjugate structure for skin penetration and biological activity of this therapeutic peptide with anti-inflammatory activity was also determined. When HNE inhibitor was coupled to a racemic mixture of a short chain LAA, two diastereomers of the LAA modified tetrapeptide were formed. Preliminary *in vitro* skin penetration studies with C8-LAA conjugated AAPV had shown that, in general, the delivery through the skin of the D-diastereomer was higher than the L-diastereomer. In this study the effect of conjugation of C6, C8 and C10 LAAs was assessed on the skin permeation, stability and biological activity of the native HNE inhibitor. Accumulation of these peptides in the skin was quantified using solvent extraction and recovery (mass balance) was calculated. Permeability coefficients were calculated for each peptide and conjugate and HNE inhibition studies were undertaken to determine the differences in activity of the conjugates on elastase enzyme as compared to the parent peptide. Preliminary investigations to elucidate the mechanism for enhanced permeation of these conjugated peptides in the skin were also conducted.

3.2 Materials and Methods

3.2.1 Chemicals

AAPV (MW 355.4) (Figure 3.1), C6(D)-LAA-AAPV (MW 468.6), C6(L)-LAA-AAPV (MW 468.6) (Figure 3.2), C6(D,L)-LAA-AAPV (MW 468.6), C8(D,L)-LAA-AAPV (MW 496.6) (Figure 3.3) and C10(D,L)-LAA-AAPV (MW 524.4) (Figure 3.4) were supplied by our collaborators in University of Queensland (Brisbane, Australia) and GLS Biochem (Shanghai, China). Propylene glycol (PG) and dimethyl sulphoxide

(DMSO) were obtained from BDH Chemical Pvt Ltd and Ajax FineChem respectively. HPLC grade acetonitrile and methanol were used and all other chemicals were of analytical grade. Phosphate buffered saline solution (PBS) was prepared according to the United States Pharmacopoeia.

3.2.2 Peptide synthesis

3.2.2.1 General

The following information describing the synthesis, purification and validation of the peptides was supplied by Professor Toth's group at the University of Queensland. Dimethylformamide (DMF) and trifluoroacetic acid (TFA) of peptide synthesis grade were purchased from Auspep (Parkville, Australia). HPLC grade acetonitrile was purchased from Labscan Asia Co. Ltd. (Bangkok, Thailand). Fmoc-protected amino acids (Ala, Pro, Val, Nle) and Rink amide MBHA resin (100-200 mesh, 0.78 mmol/g loading) were obtained from Novabiochem (Melbourne, Australia). Piperidine was purchased from Auspep. All other chemicals were purchased from the Aldrich Chemical Company unless otherwise stated.

3.2.2.2 Lipoamino acid synthesis

N-tert-Butoxycarbonyl-2-amino-D,L-octanoic acid (C8-LAA) and *N-tert*-Butoxycarbonyl-2-amino-D,L-dodecanoic acid (C10-LAA) were synthesized from diethyl acetamido malonate and the appropriate alkyl bromide followed by *N*-Boc protection using published procedures and the spectral data for these compounds matched the reported data.

Peptide synthesis

The parent peptide, AAPV and C8- and C10-LAA derivatives were assembled on Rink amide MBHA resin (100-200 mesh, 0.78mmol/g loading) on a 0.5 mmol scale using HBTU/DIPEA activation and the *in situ* neutralization protocol. The efficiency of each amino acid coupling was determined by the quantitative ninhydrin reaction and couplings repeated until an efficiency > 99.6% was achieved. When construction of the

peptide was complete, the resin was washed with DMF, dichloromethane and methanol and dried. The peptide was deprotected and cleaved from the resin by treatment with TFA:water:triisopropylsilane (TIS) (95:2.5:2.5 v/v, 25 mL) for 6 hours. The resin was removed by filtration and washed with TFA. The solvent was removed from the peptide solution under a stream of nitrogen and the crude peptide precipitated with cold diethyl ether, collected and dissolved in 20% acetonitrile and lyophilized.

The purification of peptide analogues was achieved by preparative RP-HPLC on a Grace Vydac C18, 25 cm preparative column using a Shimadzu SCL-10AVP controller and pump with an SPD 10AVP UV-Vis detector set at a wavelength of 214nm. The peptides were purified using a gradient elution profile from 100% Solvent A (0.1% TFA in H₂O) to 90% solvent B (90% CH₃CN in water with 0.1% TFA) over 35 minutes at a flow rate of 5mL/min. The peptides were purified to a single peak in the case of AAPV and two peaks in the case of the C8-LAA and C10-LAA-derivatives corresponding to the two diastereomers of the peptide, by analytical RP-HPLC. The purity of peptide analogues was determined by analytical RP-HPLC on a Vydac C18, 25cm analytical column using the Shimadzu SCL-10AVP system described above and a gradient of 100% Solvent A to 90% Solvent B over 30 minutes at a flow rate of 1 mL/min, electrospray ionization MS (ESI-MS; Perkin-Elmer Sciex API 3000) and LC/MS (Shimadzu LC-10AT HPLC, Perkin-Elmer Sciex API 3000).

3.2.2.3 Synthesis of Nle(C6-Laa)-Ala-Ala-Pro-Val-NH₂

Both D- and L-norleucine (C6-LAA) were coupled to purified AAPV peptide in a solution phase coupling procedure described below:

Solution Phase Coupling of Fmoc Protected Lipoamino acids

Fmoc-D-Nle-OH (27.14 mg, 0.077 mmol) was activated by HBTU (30.28 mg, 0.08 mmol) and hydroxybenzotriazole (HOBt) (14.89 mg, 0.11 mmol) in DMF (5mL). This solution was stirred for 25 min before being added to a stirred solution of AAPV (22.28 mg, 0.063 mmol), N,N-Diisopropylethylamine (DIPEA) (40 μ L, 0.23 mmol) in DMF (10 mL) under anhydrous conditions. The reaction was stirred at room temperature for 21 hr. The solution was concentrated to dryness *in vacuo* at 40°C with residual DMF

azeotropically removed using toluene to give a dark yellow oil. The residue was dissolved in water (10 mL), the product extracted with ethyl acetate (3 × 25 mL) and combined layers successively washed with 10% citric acid (2 × 20 mL), 10% sodium bicarbonate (2 × 20 mL), brine (3 × 20 mL), dried magnesium sulfate (MgSO₄), filtered, and concentrated to dryness *in vacuo* at 35°C.

Fmoc deprotection:

20% Piperidine solution (20% in DMF) (40 mL) was added to the crude lipoamino acid and stirred at room temperature for 3 hr. The resultant solution was concentrated to dryness *in vacuo* at 35°C to give a yellow oil and dissolved in 1:1 CH₃CN/H₂O, filtered and lyophilized overnight to afford crude C6-AAPV.

Purification of C6-AAPV

Crude lipoamino acid was purified on strata-X-C 33 um polymeric strong cation 200 mg/ 3mL sep-pack. The crude lipoamino acid was dissolved in H₂O (2 mL). Sep-pack was flushed with 2 mL H₂O before crude lipoamino acid was loaded. Sep-pack was successively flushed with H₂O (4 mL) and fractions collected and lyophilized from the following gradients; 20% CH₃CN /H₂O (6 mL), 50% CH₃CN /H₂O (6 mL) and 100% CH₃CN /H₂O (6 mL) to give purified C6-AAPV **1** as a white solid: LRESIMS *m/z* 1457 [M + H⁺]⁺; HRESIMS *m/z* 1456.8700 (M + H⁺, C₆₂H₁₁₄N₂₁O₁₉ requires 1456.8594).

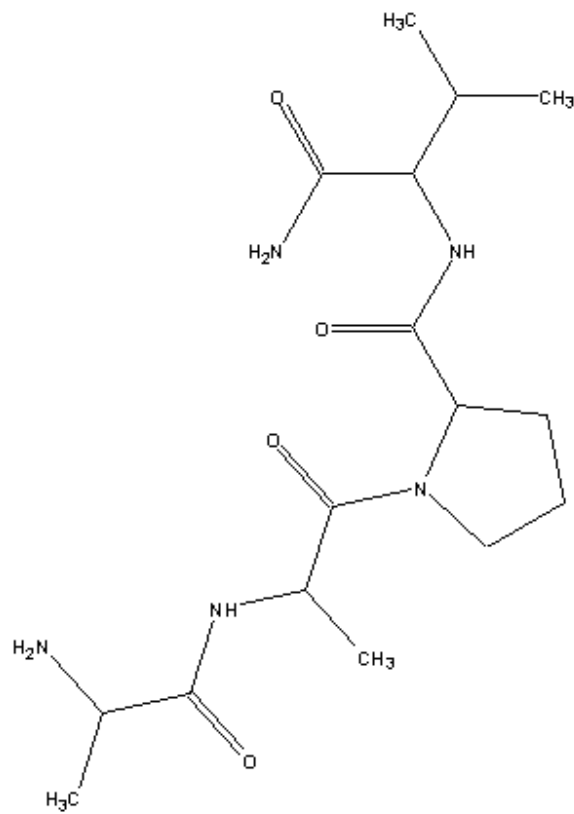


Figure 3.1 Chemical structure of AAPV

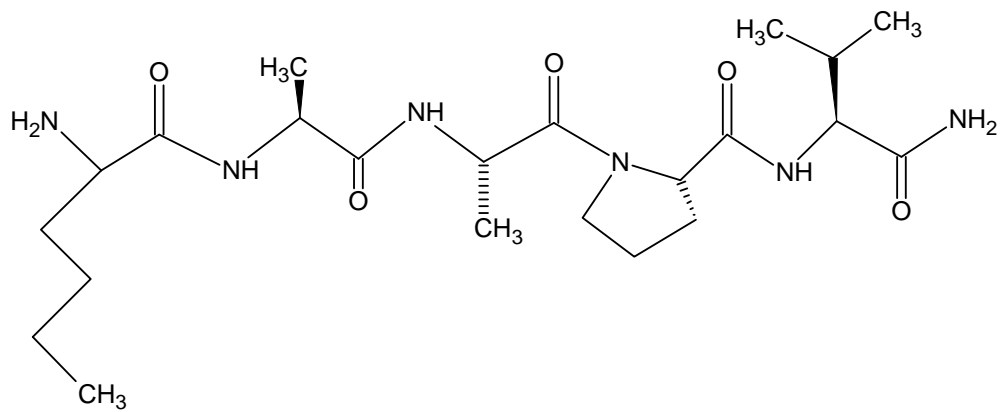


Figure 3.2 Chemical structure of L-C6-LAA-AAPV conjugate

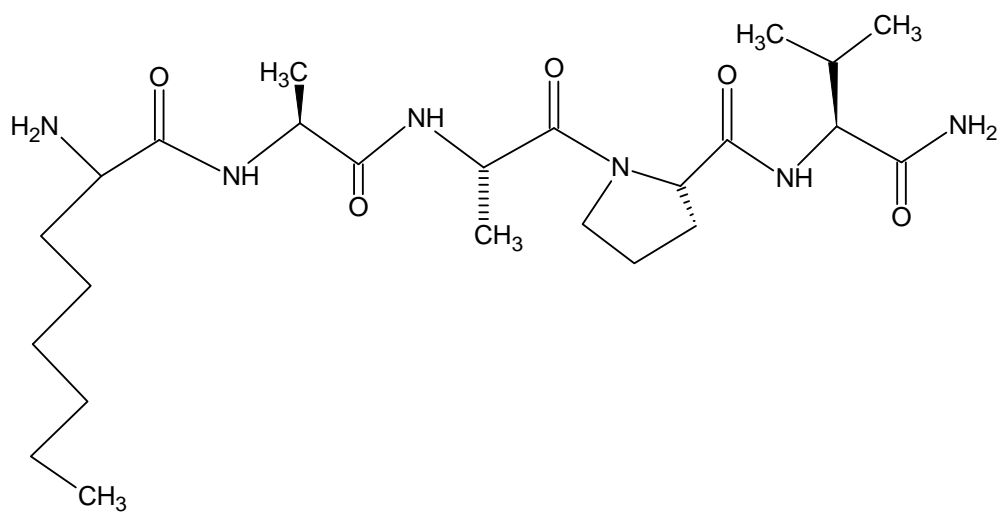


Figure 3.3 Chemical structure of L-C8-LAA-AAPV conjugate

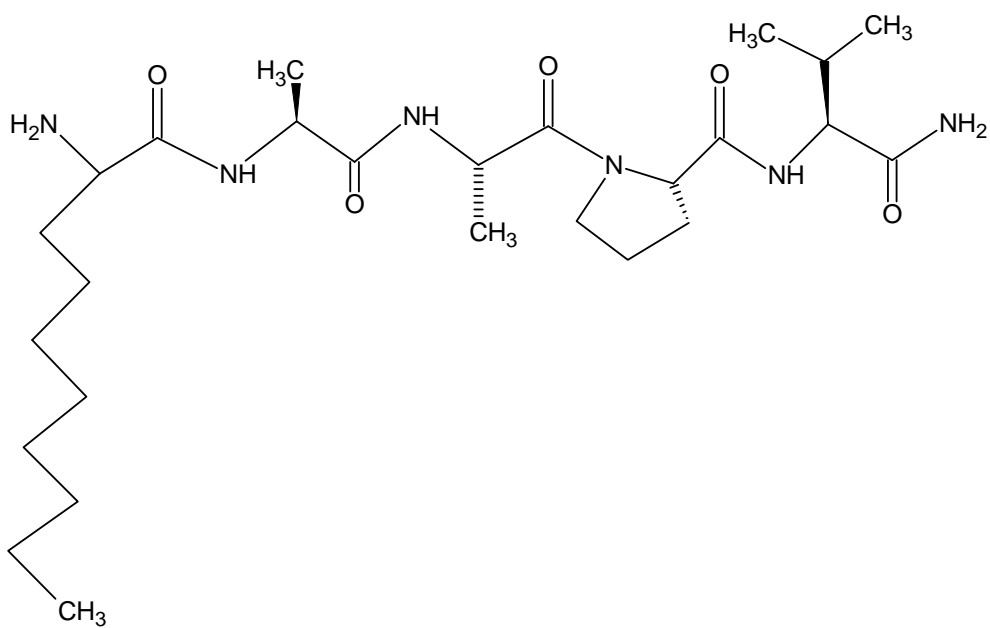
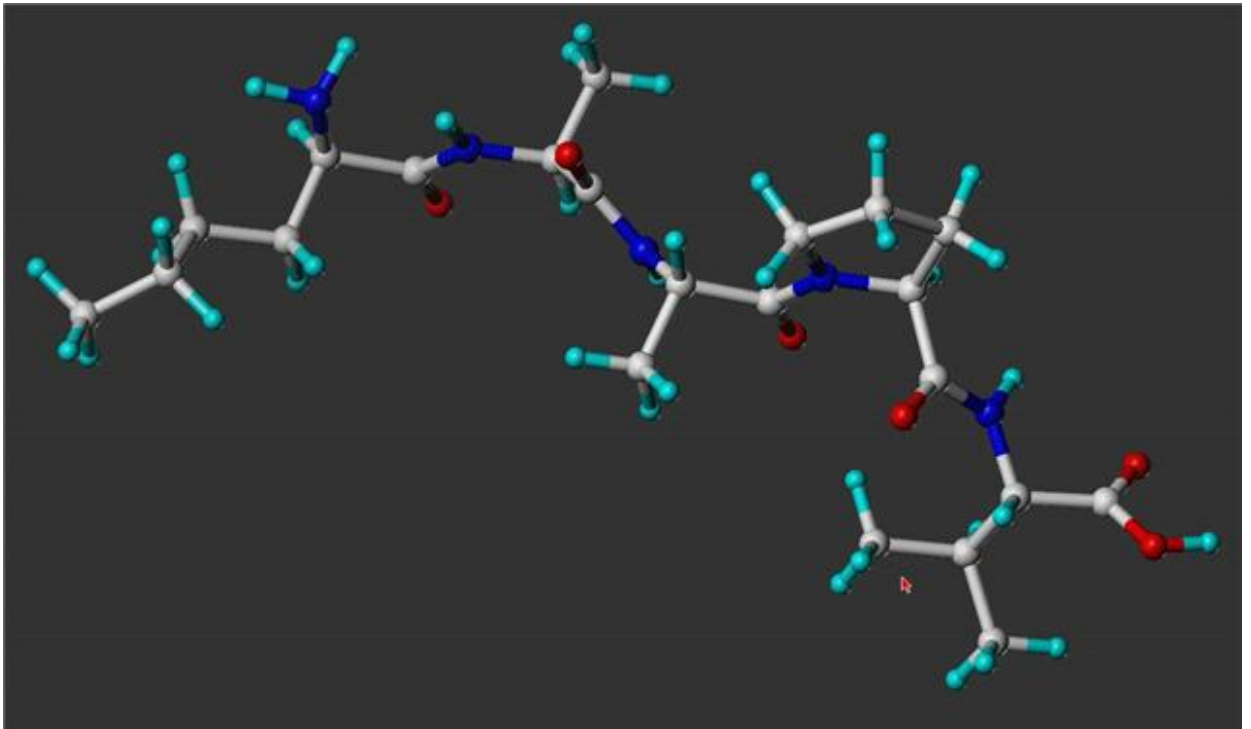
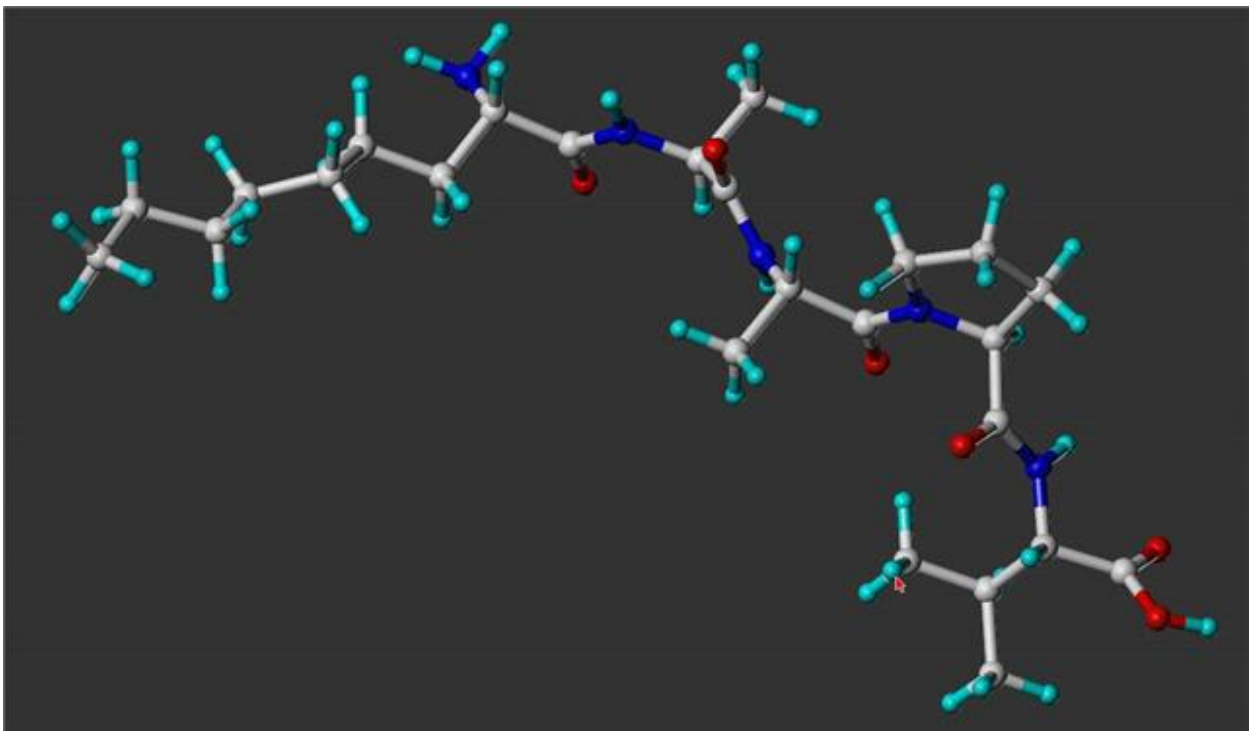


Figure 3.4 Chemical structure of L-C10-LAA-AAPV conjugate

(a)



(b)



(c)

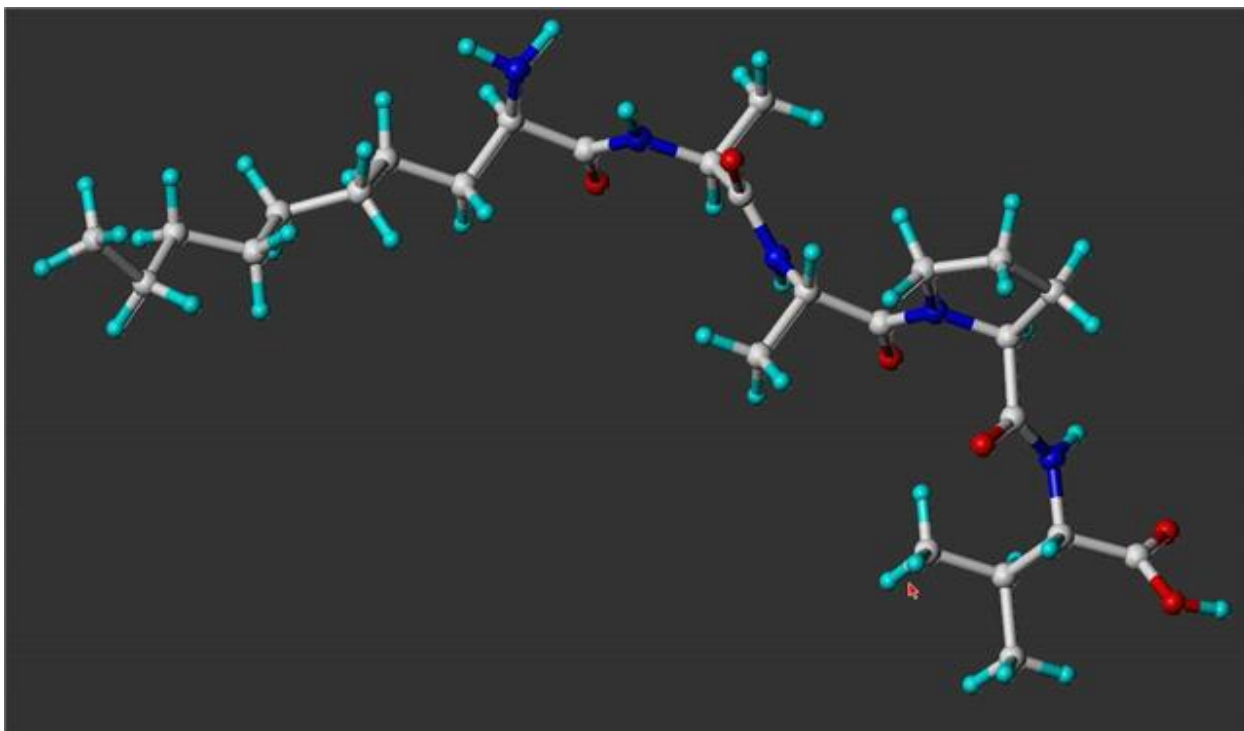


Figure 3.5 Molecular models of (a) (R) C6-LAA-AAPV, (b) (S) C8-LAA-AAPV and (c) (R) C10-LAA-AAPV

3.2.3 HPLC instrumentation and conditions

The general HPLC method for the analysis of the tetrapeptide and lipophilic conjugates was supplied by our collaborators but it had to be modified according to the available HPLC instrument. The experimental samples were analysed by reverse phase HPLC (Agilent 1200 system) which consisted of a binary pump (G1312A), autosampler (G1329A), degasser (G1379B) and diode array detector (G1365B). Separation was achieved on a Phenomenex C18 column (5 μm , 4.6 mm \times 50 mm) using a mobile phase gradient. Calibration curves of tetrapeptide and lipopeptides in PBS were obtained to ensure consistency with samples from the *in vitro* permeation experiments. Buffer A was 0.1% TFA and buffer B was 0.1% TFA in acetonitrile. Elution was performed at a flow rate of 1.0 ml/min with the column temperature held at 25°C and the injection volume was 50 μL . The tetrapeptide and lipopeptides were eluted using a combination of

isocratic and linear gradient protocol; buffer B was held at 10% for 5 min followed by a linear gradient from 10 to 100% B over 10 min for C8(D,L)-LAA-AAPV, C10(D,L)-LAA-AAPV and C6(L)-LAA-AAPV. For C6(D,L)-LAA-AAPV, buffer B was held at 10% for 5 min followed by a linear gradient from 10 to 20% over 10 min. For C6(D)-LAA-AAPV, buffer B was held at 10% for 2.5 min followed by a linear gradient from 25 to 100% over 12.5 min. Each sample analysed was automatically followed by a post-wash for 5 min. Absorbance was simultaneously monitored at 205, 210 and 214 nm using a photo diode array detector. All calculations were carried out in comparison with external standards using areas acquired at 210 nm.

3.2.4 HPLC analysis

3.2.4.1 Linearity

A 1 mg/mL stock solution of the parent peptide, AAPV and conjugated peptides [C6(L), C6(D), C6(D,L), C8(D,L) and C10(D,L)] was prepared by dissolving 5 mg peptide in 5 mL propylene glycol. Linear dilution was performed using PBS and calibration curves were obtained using 3.9, 7.81, 15.62, 31.25, 62.5 and 125 µg/mL for AAPV, C6 (D)-LAA-AAPV, C6(D,L)-LAA-AAPV and C10(D,L)-LAA-AAPV; 3.12, 6.25, 12.5, 25, 50 and 100 µg/mL for C6(L)-LAA-AAPV; 1.95, 3.9, 7.81, 15.62, 31.25, 62.5 and 125 µg/mL for C8(D,L)-LAA-AAPV obtained from UQ; 3.67, 7.34, 14.68, 29.36, 58.72 and 11.5 µg/mL for C8(D,L)-LAA-AAPV obtained from GLS Biochem solutions in PBS at pH 7.4. Linearity (quoted as R^2) was evaluated by linear regression analysis, which was calculated by the least square regression method.

3.2.4.2 Precision

The precision of the assay was determined by injecting three standard concentrations of 7.80 and 31.25 5 µg/mL AAPV, 1.95, 15.625 and 62.5 µg/mL C6(D,L)-LAA-AAPV and C8(D,L)-LAA-AAPV from UQ; 0.975, 7.80 and 31.25 µg/mL C6(D)-LAA-AAPV; 6.25, 50.0 and 100.0 µg/mL C6(L)-LAA-AAPV; 7.34, 29.37 and 117.50 µg/mL C8(D,L)-LAA-AAPV from UQ; 3.06, 12.50 and 50 µg/mL C10(D,L)-LAA-AAPV from

GLS Biochem and 3.90, 15.62 and 62.50 µg/mL C10(D,L)-LAA-AAPV from UQ six times on the HPLC.

3.2.4.3 Intra-day repeatability

The intra-day repeatability was assessed by injecting 7.80 and 31.25 µg/mL AAPV; 1.95 and 62.5 µg/mL C6(D,L)-LAA-AAPV; 1.95 and 15.62 µg/mL C8(D,L)-LAA-AAPV from UQ; 7.80 and 31.25 µg/mL C6(D)-LAA-AAPV; 6.25 and 50.0 µg/mL C6(L)-LAA-AAPV; 7.34 and 29.37 µg/mL C8(D,L)-LAA-AAPV from GLS Biochem; 3.90 and 15.62 µg/mL C10(D,L)-LAA-AAPV from UQ and 3.06 and 50.0 µg/mL C10(D,L)-LAA-AAPV from GLS Biochem standards six times at different times in a day.

3.2.4.4 Inter-day repeatability

The inter-day repeatability was determined by injecting 7.80 and 31.25 µg/mL AAPV; 1.95 and 62.5 µg/mL C6(D,L)-LAA-AAPV; 1.95 and 15.62 µg/mL C8(D,L)-LAA-AAPV from UQ; 7.80 and 31.25 µg/mL C6(D)-LAA-AAPV; 6.25 and 50.0 µg/mL C6(L)-LAA-AAPV; 3.90 and 15.62 µg/mL C10(D,L)-LAA-AAPV from UQ and 3.06 and 50.0 µg/mL C10(D,L)-LAA-AAPV from GLS Biochem standards six times on 3 different days. The intra- and inter-day repeatabilities were quoted as the coefficient of variance.

3.2.4.5 Lower limit of detection (LOD)

The minimum detectable and quantifiable limits (LOD and LOQ) were measured by diluting the stock solution of AAPV and conjugated peptides with PBS to give a concentration range from 3.9 to 125 µg/mL and then injected on the HPLC. The LOD was calculated as greater than 3 times the baseline noise level by the following formula: $LOD = 3 \times SD \text{ of peak area of standard} / \text{slope}$.

3.2.4.6 Lower limit of quantification (LOQ)

The LOQ was calculated as 10 times the baseline noise level. The LOQ was calculated by the following formula: $LOQ = 10 \times SD \text{ of peak area of standard} / \text{slope}$.

3.2.5 Formulation approaches and duration of skin hydration

3.2.5.1 Selection of vehicle and effect of concentration

Based on the preliminary data for C8 (D,L) conjugated AAPV, it was decided to use propylene glycol as the vehicle. Due to limited availability of the peptides it was first decided to assess the effect of a lower concentration on the delivery of the peptide across the skin. Experiments were also conducted using a 75:25 mixture of propylene glycol: PBS as the donor vehicle and 25:75 propylene glycol: PBS as the receptor for C6(D,L)-LAA-AAPV, C8(D,L)-LAA-AAPV and C10(D,L)-LAA-AAPV. Based on this preliminary study 3 mg peptide dissolved in 300 μ L propylene glycol was used as the vehicle and phosphate buffered saline as the receptor medium for the skin diffusion studies. To assess the effect of concentration on skin permeation of the native and conjugated peptides a comparison was also made by using 6 mg peptide in 300 μ L propylene glycol in the donor.

3.2.5.2 Skin hydration

As discussed in the introduction, skin hydration can improve the delivery of drugs across the continuous *stratum corneum*. This hypothesis was investigated by hydrating the epidermal membranes to be used in the diffusion study with phosphate buffered saline (receptor medium) for 1h and overnight. Before the start of the experiment, the receptor medium was withdrawn and a fresh sample of pre-equilibrated PBS at 35°C was replaced in the receptor compartment.

3.2.6 Skin Stability (metabolism) experiment

The influence of human skin on the stability of the native tetrapeptide and the lipoamino acid conjugates of the tetrapeptide was determined by placing skin in a vial containing peptide solution to provide an estimate of their stability during the skin diffusion experiments. Vials containing 2 mL of 20 μ g/mL AAPV, 250 μ g/mL C6(D)-LAA-AAPV, 10 μ g/mL C6(D,L)-LAA-AAPV, 100 μ g/mL C8(D,L)-LAA-AAPV and 30 μ g/mL C10(D,L)-LAA-AAPV solutions were stored at 37°C. The concentrations of each peptide for the stability study were chosen based on the amount of peptide found in

the receptor after skin permeation. 150 μ L samples were withdrawn at 0, 2, 4, 6 and 24h. In the case of C6(D,L)-LAA-AAPV the samples were diluted to give a final theoretical concentration of 125 μ g/mL and were analysed by HPLC. The percentage of intact peptide was calculated as follows:

$$\text{Intact peptide} = \frac{\text{Final amount of peptide}}{\text{Initial amount of peptide}} \times 100 \%$$

3.2.7 Human skin preparation

Full thickness human skin samples excised from female donors undertaking abdominoplasty surgery at Perth hospitals were refrigerated immediately after surgery. Sampling was approved by the Human Research Ethics Committee of Curtin University (Approval numbers HR132/2001, HR 70/2007 and HR 129/2008) and was carried out under the Guidelines of the National Health and Medical Research Council of Australia. The subcutaneous fat was removed by dissection and whole skin was frozen at -20°C within 24 h of surgery. When required for a permeation study the skin samples were thawed at room temperature. Epidermis was detached from the dermis by heat separation as described previously.¹⁹⁸ Permeation of the tetrapeptide and lipoamino acid conjugates of the tetrapeptide was assessed across epidermis prepared by heat separation from the dermis.

3.2.8 Skin permeation of tetrapeptide and lipoamino acid conjugates

The epidermal membrane was mounted on a Franz-type diffusion cell (effective diffusion surface area approximately 1 cm^2 and receptor volume approximately 3 ml) with the *stratum corneum* layer facing the donor compartment. The receptor compartment was filled with phosphate buffered saline pH 7.4 (PBS) or 25:75 propylene glycol: PBS and allowed to equilibrate in a 35°C water bath with the receptor phase stirring continuously for approximately 1h or overnight depending on the experimental protocol. 35°C was used for the diffusion experiments because water bath temperature of 35°C will give a skin surface temperature of 32°C . The donor compartment was loaded with 300 μ L of either propylene glycol or propylene glycol and PBS mixture containing

3 mg or 6 mg of peptide (tetrapeptide or lipoamino acid conjugated tetrapeptide) and sealed with Parafilm. These amounts were completely soluble at these concentrations. The apparatus was maintained at 35°C throughout the 24 h duration of the experiment. 200 µL aliquots were taken from the receptor compartment at 0, 0.5, 1, 1.5, 2, 3, 4, 6, 8, and 24 h and replaced immediately with 200 µL of receptor medium pre-equilibrated at 35°C to maintain skin conditions. At the termination of the experiment (24 h) samples were also taken from the donor compartment. Samples collected were kept at 4°C in the injecting tray for analysis by reverse phase HPLC. All samples from individual experiments were assayed together in the same run. The D- and L-diastereomers of the lipopeptide were identified by comparison with synthesised standards of the individual diastereomers of known configuration.

3.2.9 Mass balance and recovery

The uptake of peptide and conjugates in the epidermis was also investigated. Different solvents were tested for their extraction efficiency of the peptide and conjugates from the skin. As C6(L)-LAA-AAPV and C6(D)-LAA-AAPV were available in greatest amount, these conjugates were used for testing extraction efficiency with a number of solvents. DMSO, methanol and propylene glycol were compared as extraction solvents for the peptides and conjugates from the skin. The protocol for DMSO and methanol extraction was as follows:

1. The absolute recovery of C6(D)-LAA-AAPV and C6(L)-LAA-AAPV from skin tissue was determined by spiking skin sections with the conjugates in propylene glycol. The skin sections were allowed to rest in 500 µL methanol and agitated for 2 min.
2. The sample was then transferred to a second Eppendorf tube containing 500 µL methanol and agitated for another 2 min.
3. The skin sample was then extracted with 1 mL 50:50 DMSO: water for 2 hours with agitation.
4. After 2 hours the methanolic and DMSO extracts with skin were centrifuged at 10,000 RPM for 10 mins. The supernatants were withdrawn and injected on HPLC to quantify the amount of peptide in the skin.

The protocol for propylene glycol and methanol extraction was as follows:

1. The absolute recovery of AAPV, C6(D,L)-LAA-AAPV, C8(D,L)-LAA-AAPV and C10(D,L)-LAA-AAPV from skin tissue was determined by spiking skin sections with the conjugates in propylene glycol. The skin sections were allowed to rest in 500 μ L methanol and vortexed for 2 min.
2. The skin section was then transferred to a second Eppendorf tube containing 500 μ L methanol and vortexed for another 2 min.
3. The skin sample was then placed in 1 mL propylene glycol for 2 hours with agitation.
4. After centrifuging each extract at $10,000 \times g$ for 10 min, the resultant supernatants were diluted appropriately and quantified by HPLC.

The extraction method using methanol and propylene glycol was most efficient and therefore used for experimental samples.

To determine mass balance/recovery purpose in the skin permeation experiments, the donor solution was removed from the donor compartment and diluted appropriately to quantify the amount of peptide in the donor at the end of the experiment. The donor compartment with the skin was rinsed with 300 μ L PBS and the wash was collected. The receptor compartment was emptied and washed with 500 μ L PBS. Samples from both washes were injected on HPLC to quantify the peptides and conjugates present in the washes.

3.2.10 Surface tension measurement

The surface tension of AAPV, C6(D,L)-LAA-AAPV, C8(D,L)-LAA-AAPV and C10(D,L)-LAA-AAPV was measured by the ring method using a Du Nouy ring tensiometer at room temperature. A 1 mg/mL standard solution of each peptide was first prepared by dissolving 10 mg of peptide in 10 mL PBS. Linear dilution was carried out to give final concentrations of 0.5, 0.25, 0.125 and 0.0625 mg/mL in PBS. The surface tension was first measured for PBS and it was used as a control. The surface activity of the peptides and conjugates was compared to the control.

3.2.11 Elastase inhibition assays

Inhibition of HNE by the synthesized conjugates and the parent tetrapeptide was assessed using an EnzChek® Elastase Assay Kit (E-12056, Molecular Probes). The native peptide, AAPV was used as a standard to which the lipoamino acid conjugates were compared. The kit contained DQ™ elastin (component A) from bovine neck ligament that was labeled with BODIPY® FL, a 10 times concentrated reaction buffer containing 1 M Tris-HCL at pH 8 and 2mM sodium azide (component B) and elastase from pig pancreas (component C). Digestion products from the DQ elastin substrate had absorption maxima at approximately 505 nm and fluorescence emission maxima at 515 nm.

3.2.12 Assay optimization

The activity of the tetrapeptide and its LAA conjugates from both the sources (University of Queensland and GLS Biochem, China) was assessed at 2 different concentrations of the elastin substrate and porcine elastase. The activity of the peptides at different concentrations was tested at a final concentration of 6.25 and 25 µg/mL DQ elastin substrate and 0.25 and 0.5 U/mL elastase. A two hour incubation period and a fluorescence microplate reader equipped with standard fluorescein filters were used to detect the activity of elastase from porcine pancreas down to a final concentration of 5×10^{-3} U/mL (40 ng protein/mL). Because the assay is continuous, kinetic data can be obtained easily and a comparison was made between 0.5 and 0.25 U/mL elastase at a specific concentration of the substrate.

3.2.12.1 Dilution of reaction buffer

To prepare a 1X reaction buffer, 6 mL of the 10X reaction buffer was diluted in 54 mL deionized water (dH₂O). This 60 mL volume of working 1X reaction buffer was sufficient to prepare working solutions of elastase and inhibitors.

3.2.12.2 Preparation of standard concentration of the Inhibitors

A 1 mM solution of inhibitor standards was prepared by dissolving 0.354 mg AAPV, 0.468 mg C6(L)-LAA-AAPV and C6(D,L)-LAA-AAPV, 0.497 mg C8 (D,L)-LAA-AAPV and 0.534 mg C10 (D,L)-LAA-AAPV in 1 mL propylene glycol. Further linear dilution was carried out with 1X reaction buffer to give 0.5, 0.25, 0.125, 0.062, 0.031 and 0.015 mM working standard concentrations.

3.2.12.3 Preparation of DQ elastin working standard solution

A 1.0 mg/mL stock solution of the DQ elastin substrate was prepared by adding 1.0 mL of deionized water (dH₂O) directly to a vial containing the lyophilized substrate. It was mixed thoroughly to dissolve. A 100 µg/mL working solution of the DQ elastin substrate was prepared by diluting the DQ elastin stock solution ten-fold in 1X Reaction Buffer. Appropriate concentrations of the substrate were prepared by linearly diluting the 100 µg/mL solution with 1X Reaction Buffer.

3.2.12.4 Preparation of enzyme working solution

A 100 U/mL stock solution by of porcine pancreatic elastase was prepared by dissolving the contents of the vial (Component C) in 0.5 mL dH₂O. A 1 U/mL solution was prepared by diluting the 100 U/mL stock solution 100 times with 1X Reaction Buffer. A 0.5 U/mL solution can be prepared by linearly diluting the 1 U/mL solution with 1X Reaction Buffer.

3.2.12.5 Reaction mixture

- 1) 50 µL of the diluted inhibitors in the concentration range of 0.031 to 1mM (or no-inhibitor control) was added to each assay well.
- 2) Either 50 µL of 100 µg/mL or 25 µg/mL DQ elastin working solution was then added to each assay well. This gave a final concentration of 25 and 6.25 µg/mL DQ elastin in the final reaction mixture.

- 3) Porcine pancreatic elastase was diluted in 1X Reaction Buffer. 100 μ L of the diluted enzyme, or 100 μ L of 1X Reaction Buffer as a blank, was added to the sample wells preloaded with substrate and inhibitor.
- 4) The samples were incubated at room temperature, protected from light, for an appropriate time, e.g. 1–2 hours. Because the assay is continuous (not terminated), fluorescence may be measured at multiple time points.
- 5) The fluorescence intensity was measured in a fluorescence microplate reader equipped with standard fluorescein filters.
- 6) Correction was made for background fluorescence by subtracting the values derived from the no-enzyme control.

3.2.13 Statistical analysis

Differences in the permeation of AAPV and the lipoamino acid conjugates were analysed for statistical significance ($p < 0.05$) using an Analysis of Variance (ANOVA) at each of the prescribed time points. The ANOVA model was implemented using the GENMOD procedure in the SAS software system, with the control group being the reference group in each model. Because of the skewness in the concentrations, the regression model was applied to the log-transformed data (in order to obtain the p-values for comparison of treatments). The overall p-values were found to be significant for most of the comparisons.

3.3 Results and discussion

3.3.1 Chromatography

3.3.1.1 AAPV

The current HPLC method was an extension of that established previously in our laboratory.²⁰⁵ The method provided good selectivity and specificity and the tetrapeptide eluted at approximately 2.8 min. The linearity shown by the HPLC method was 1.00 and the precision was 0.22% for 31.25 μ g/mL and 0.56% for 7.8 μ g/mL. The lowest amount

of AAPV that could be detected (LOD) by this method was 200 ng and the amount that could be quantified (LOQ) accurately was 700 ng. The method showed intra-day repeatability of 0.40% for 31.25 $\mu\text{g/mL}$ and 0.60% for 7.8 $\mu\text{g/mL}$ (both within the acceptable criteria for intraday repeatability which is $\text{RSD} < 5\%$) and the inter-day repeatability of 0.76 % for 31.25 $\mu\text{g/mL}$ and 1.05 % for 7.8 $\mu\text{g/mL}$. Thus the method was validated to be used as a detection method for AAPV after permeation through skin. A typical chromatogram for AAPV is shown in Figure 3.6 below.

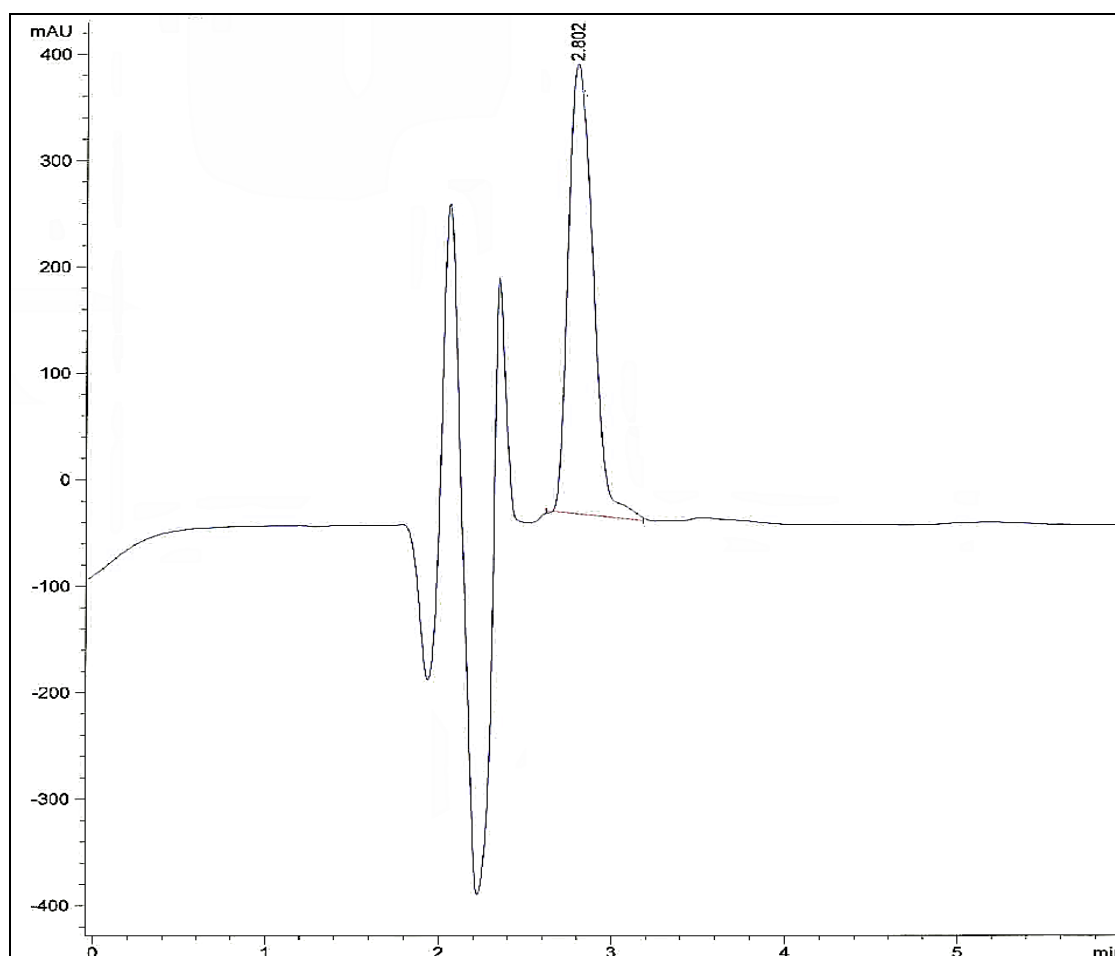


Figure 3.6 Chromatogram of 125 $\mu\text{g/mL}$ standard of AAPV

3.3.1.2 C6(D), C6(L) and C6(D,L)-LAA-AAPV

The HPLC method developed for AAPV enabled co-analysis of both the tetrapeptide and the lipopeptide diastereomers in the same run. The retention time for the lipopeptide

[C6(D)-LAA-AAPV] was approximately 9.1 min. This peptide was obtained from University of Queensland and stating the source was important since there are minor differences in the chromatographic conditions of the same peptides from 2 different sources. The linearity shown by the HPLC method was 1.0 and the precision was 0.74% for 0.975 $\mu\text{g/mL}$, 0.63% for 7.8 $\mu\text{g/mL}$ and 0.24% for 31.25 $\mu\text{g/mL}$. The LOD and LOQ of C6(D)-LAA-AAPV was 0.3 μg and 0.99 μg respectively. The method showed intra-day repeatability of 0.68% for 7.8 $\mu\text{g/mL}$ and 0.37% for 31.25 $\mu\text{g/mL}$ (both within the acceptable criteria for intra-day repeatability which is $\text{RSD} < 5\%$) and the inter-day repeatability of 0.85% for 7.8 $\mu\text{g/mL}$ and 0.40% for 31.25 $\mu\text{g/mL}$. A typical chromatogram for C6(D)-LAA-AAPV is shown in Figure 3.7 below.

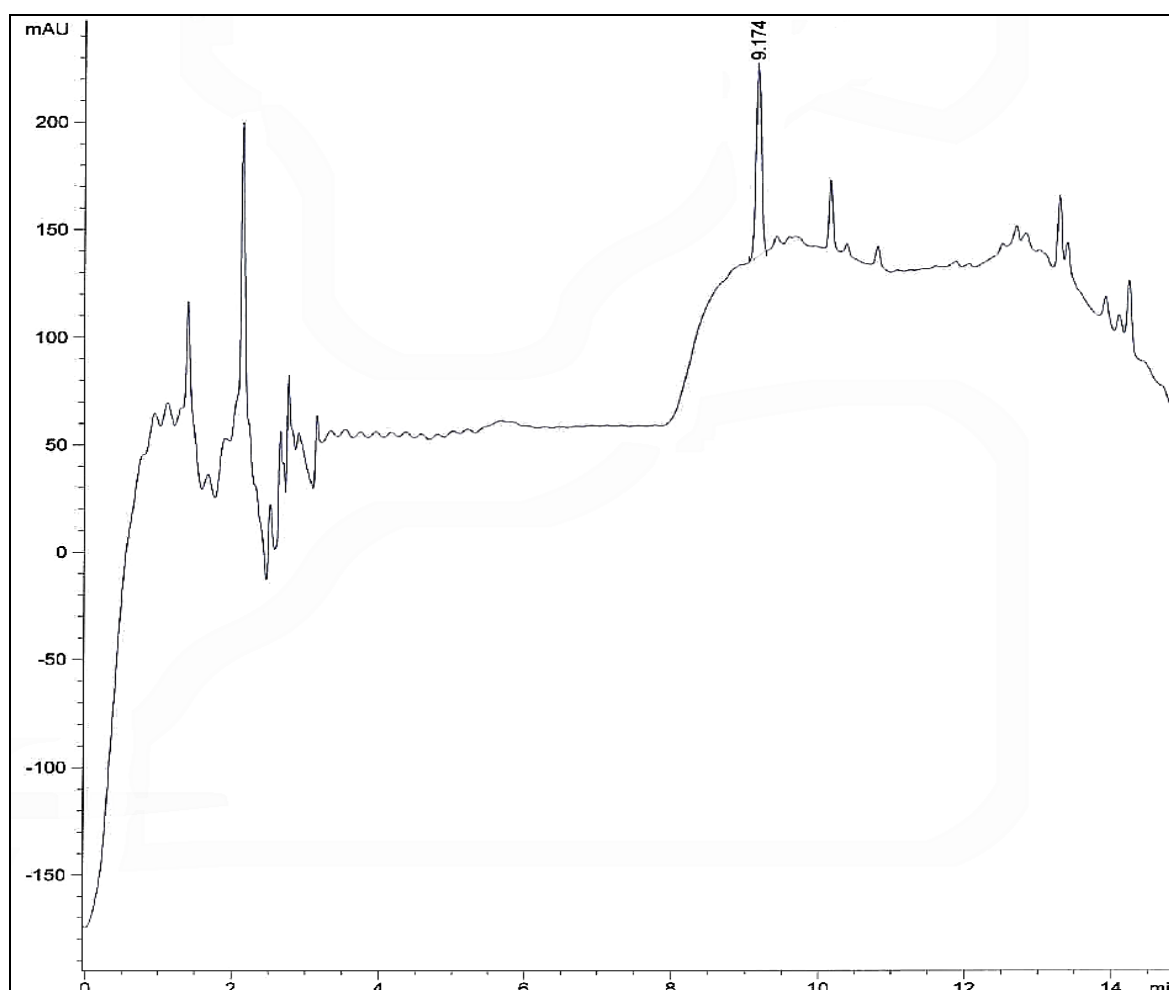


Figure 3.7 Chromatogram of 15.62 $\mu\text{g/mL}$ standard of C6(D)-LAA-AAPV

The retention time of C6(L)-LAA-AAPV was 4.6 min. The linearity obtained by the HPLC method was 0.9994 and the precision was 0.90% for 6.25 $\mu\text{g/mL}$, 0.46% for 50 $\mu\text{g/mL}$ and 0.47% for 100 $\mu\text{g/mL}$. The LOD and LOQ of C6(L)-LAA-AAPV was 0.11 μg and 0.38 μg respectively. The method showed intra-day repeatability was 1.04% for 6.25 $\mu\text{g/mL}$ and 0.61 % for 50 $\mu\text{g/mL}$ and the inter-day repeatability was 1.09% for 6.25 $\mu\text{g/mL}$ and 0.62% for 50 $\mu\text{g/mL}$. A typical chromatogram for C6(L)-LAA-AAPV is shown in Figure 3.8 below.

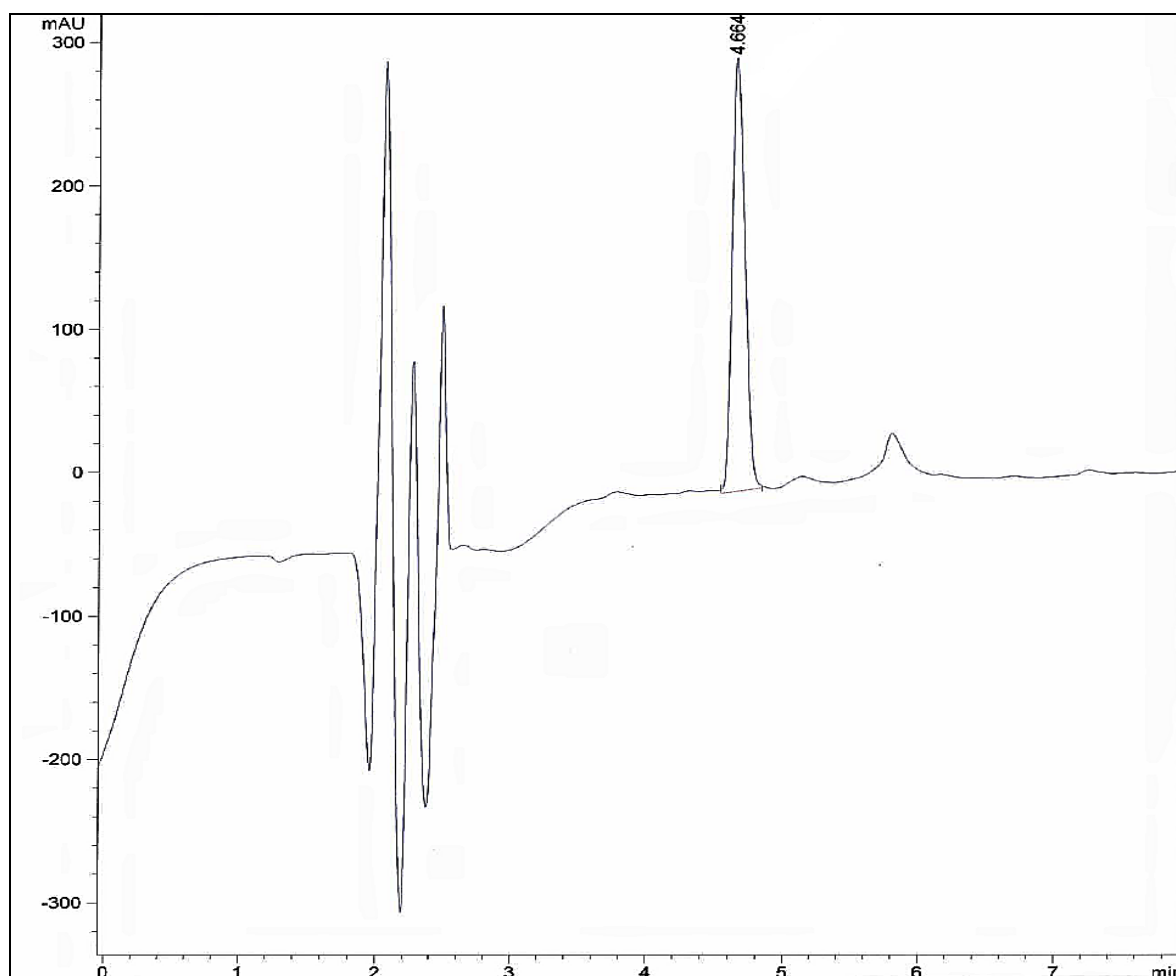


Figure 3.8 Chromatogram of 25 $\mu\text{g/mL}$ standard of C6(L)-LAA-AAPV from UQ

The HPLC method for the racemic mixture of C6(D,L)-LAA-AAPV obtained from GLS Biochem varied in comparison to the method used for C6(D) and C6(L) individual diastereomers, in terms of the mobile phase gradient used to elute the two peaks

corresponding to the D- and L- diastereomers. The lipopeptide gave a twin peak, which is typical of diastereomeric mixtures; the L-diastereomer peak eluted at approximately 11.2 min and the D-diastereomer at 11.5 min. The linearity obtained by the HPLC method was 0.9999 for the D- isomer and 1.00 for the L- diastereomer. For the D-diastereomer the precision was 0.74% for 1.95 µg/mL, 0.25% for 15.625 µg/mL and 0.17% for 62.5 µg/mL; LOD was 44 ng and LOQ was 147 ng. The method showed intra-day repeatability of 1.10% for 1.95 µg/mL and 0.16 % for 62.5 µg/mL and inter-day repeatability of 1.10% for 1.95 µg/mL and 0.18% for 62.5µg/mL. For the L-diastereomer the precision was 0.86% for 1.95 µg/mL, 0.19% for 15.625 µg/mL and 0.19% for 62.5 µg/mL, the LOD was 34 ng and the LOQ was 113 ng. The method showed intra-day repeatability of 1.10% for 1.95 µg/mL and 0.10 % for 62.5 µg/mL and the inter-day repeatability of 1.22% for 1.95 µg/mL and 0.18% for 62.5µg/mL. A typical chromatogram for C6(D,L)-LAA-AAPV is shown in Figure 3.9 below.

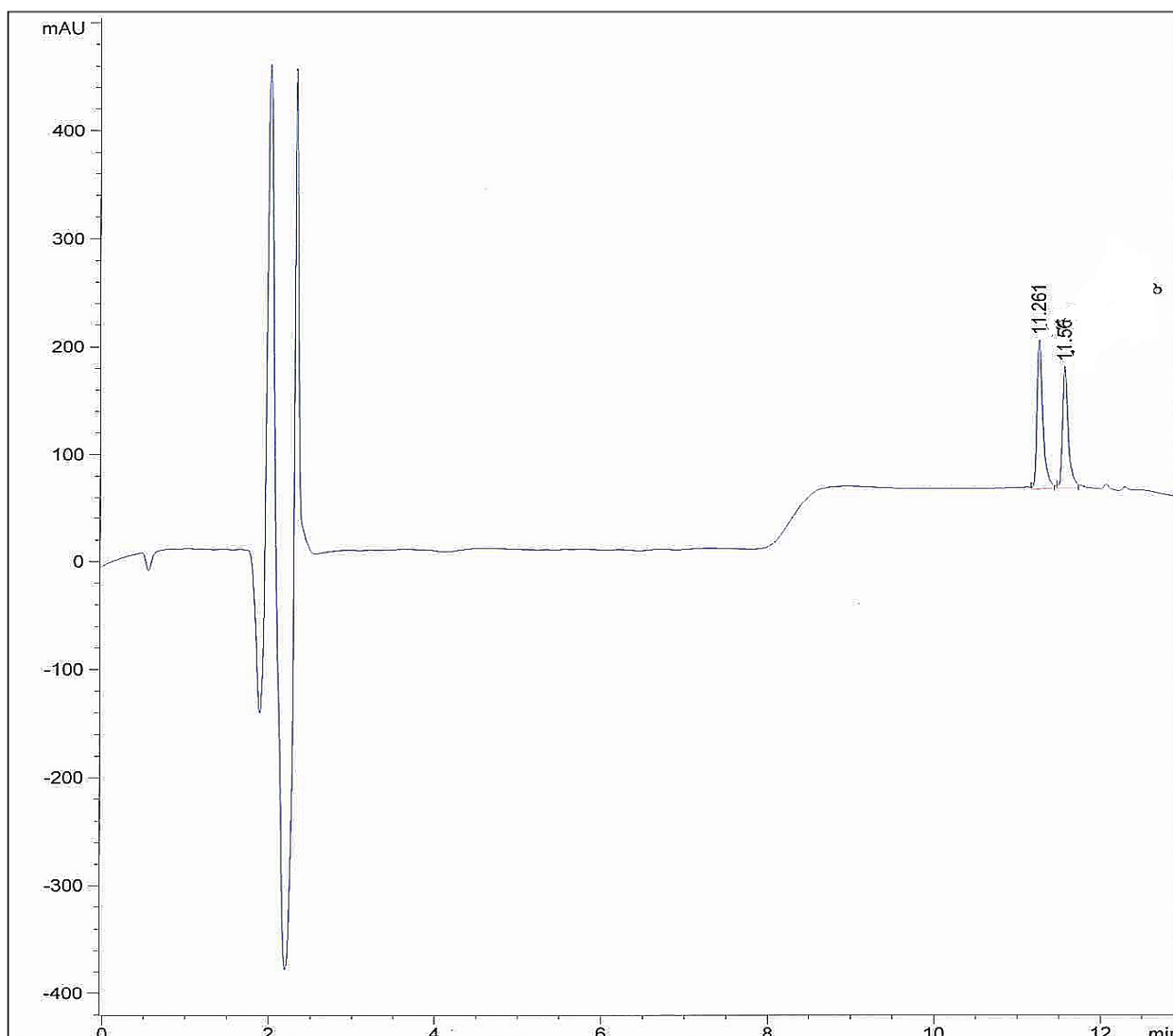


Figure 3.9 Chromatogram of 30 µg/mL standard of C6(D,L)-LAA-AAPV

3.3.1.3 C8(D,L)-LAA-AAPV

C8(D,L)-LAA-AAPV was obtained from two sources. C8(D,L) from UQ gave a twin peak after HPLC analysis (Figure 3.10) whereas the C8(D,L) from GLS Biochem, eluted as a single sharp peak under the same chromatographic conditions. The HPLC method was validated for C8(D,L) obtained from both the sources. For the UQ sourced lipopeptide L-diastereomer peak eluted at approximately 10.2 min and the D-diastereomer at approximately 10.4 min. The linearity for the L- diastereomer and the D-diastereomer was 0.9998 and 0.9999 respectively. For the C8(L) diastereomer the

precision was, 1.35% for 1.95 $\mu\text{g/mL}$; 0.38% for 15.625 $\mu\text{g/mL}$ and 0.11% for 62.5 $\mu\text{g/mL}$. The LOD was 88 ng and the LOQ was 293.23 ng. The method showed intra-day repeatability of 2.40% for 1.95 $\mu\text{g/mL}$ and 0.61 % for 15.625 $\mu\text{g/mL}$ and inter-day repeatability of 2.12% for 1.95 $\mu\text{g/mL}$ and 0.83% for 15.625 $\mu\text{g/mL}$. For the C8(D)-LAA-AAPV diastereomer, the precision was 1.40% for 1.95 $\mu\text{g/mL}$, 0.56% for 15.625 $\mu\text{g/mL}$ and 0.33% for 62.5 $\mu\text{g/mL}$. The LOD was approximately 67.90 ng and the LOQ was 226.34 ng. The method showed intra-day repeatability of 2.0% for 1.95 $\mu\text{g/mL}$ and 0.94 % for 15.625 $\mu\text{g/mL}$ and the inter-day repeatability of 2.28% for 1.95 $\mu\text{g/mL}$ and 0.90% for 15.625 $\mu\text{g/mL}$.

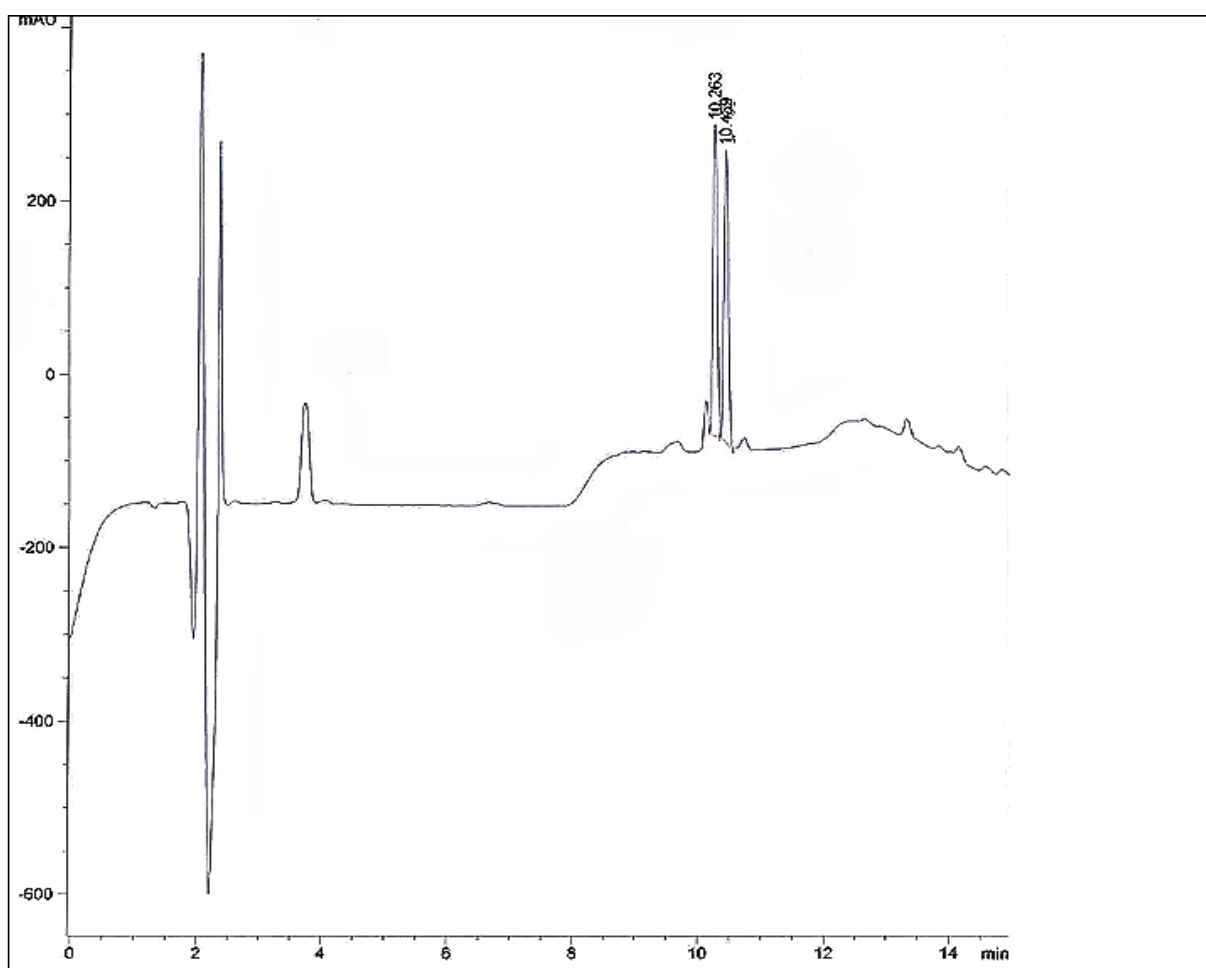


Figure 3.10 Chromatogram of 100 $\mu\text{g/mL}$ standard of C8(D,L)-LAA-AAPV from UQ

C8(D,L)-LAA-AAPV obtained from GLS Biochem eluted at approximately 10.7 min and variation of the HPLC conditions did not permit elucidation of two peaks

corresponding to the diastereomers. The linearity by this method was 1.0 and the precision was 0.94% for 7.34 $\mu\text{g/mL}$, 0.25 % for 29.37 $\mu\text{g/mL}$ and 0.21% for 117.5 $\mu\text{g/mL}$. The LOD was approximately 30 ng and the LOQ was 102 ng. The method showed intra day repeatability of 0.68% for 7.34 $\mu\text{g/mL}$ and 0.51 % for 29.37 $\mu\text{g/mL}$ and the inter day repeatability of 0.63% for 7.34 $\mu\text{g/mL}$ and 0.40% for 29.37 $\mu\text{g/mL}$. A typical chromatogram for C8(D,L)-LAA-AAPV is shown in Figure 3.11 below.

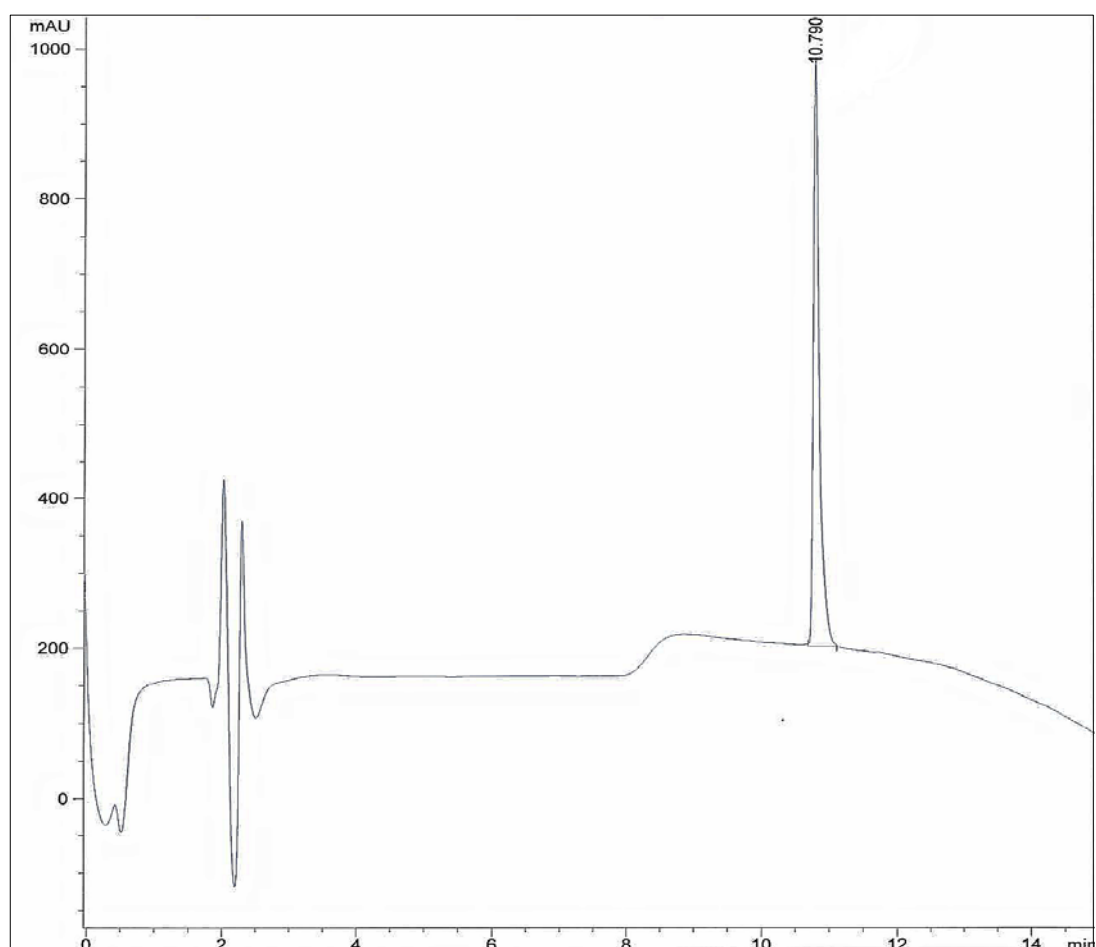


Figure 3.11 Chromatogram of 62.5 $\mu\text{g/mL}$ standard of C8(D,L)-LAA-AAPV from GLS Biochem

3.3.1.4 C10 (D,L)-LAA-AAPV

C10(D,L)-LAA-AAPV obtained from UQ eluted as twin peaks, one corresponding to the L- diastereomer and the other D- diastereomer while the same compound obtained from GLS Biochem eluted as a single peak. The peak corresponding to the L-

diastereomer eluted at 11.3 min and the peak corresponding to the D- diastereomer eluted at 11.6 mins (Figure 3.12). The linearity obtained by the HPLC method for C10(D,L) from UQ was 0.9996 for the L- distereomer and 0.9998 for the D- diastereomer. For C10(L)-LAA-AAPV the precision of the assay was 1.31% for 3.9 $\mu\text{g/mL}$, 0.52% for 15.625 $\mu\text{g/mL}$ and 0.22% for 62.5 $\mu\text{g/mL}$, and the LOD and LOQ were 61.68 ng and 205.60 ng respectively. The intra-day repeatability was 1.05% for 3.9 $\mu\text{g/mL}$ and 0.33% for 15.625 $\mu\text{g/mL}$ and the inter-day repeatability was 1.05 % for 3.9 $\mu\text{g/mL}$ and 0.28% for 15.625 $\mu\text{g/mL}$. For C10(D)-LAA-AAPV, the precision was 1.51% for 3.9 $\mu\text{g/mL}$, 0.76% for 15.625 $\mu\text{g/mL}$ and 0.13% for 62.5 $\mu\text{g/mL}$. The intra-day repeatability was 1.27% for 3.9 $\mu\text{g/mL}$ and 0.35% for 15.625 $\mu\text{g/mL}$ and the inter-day repeatability was 1.26% for 3.9 $\mu\text{g/mL}$ and 0.46% for 15.625 $\mu\text{g/mL}$. The LOD and LOQ were approximately 30 ng and 100 ng respectively.

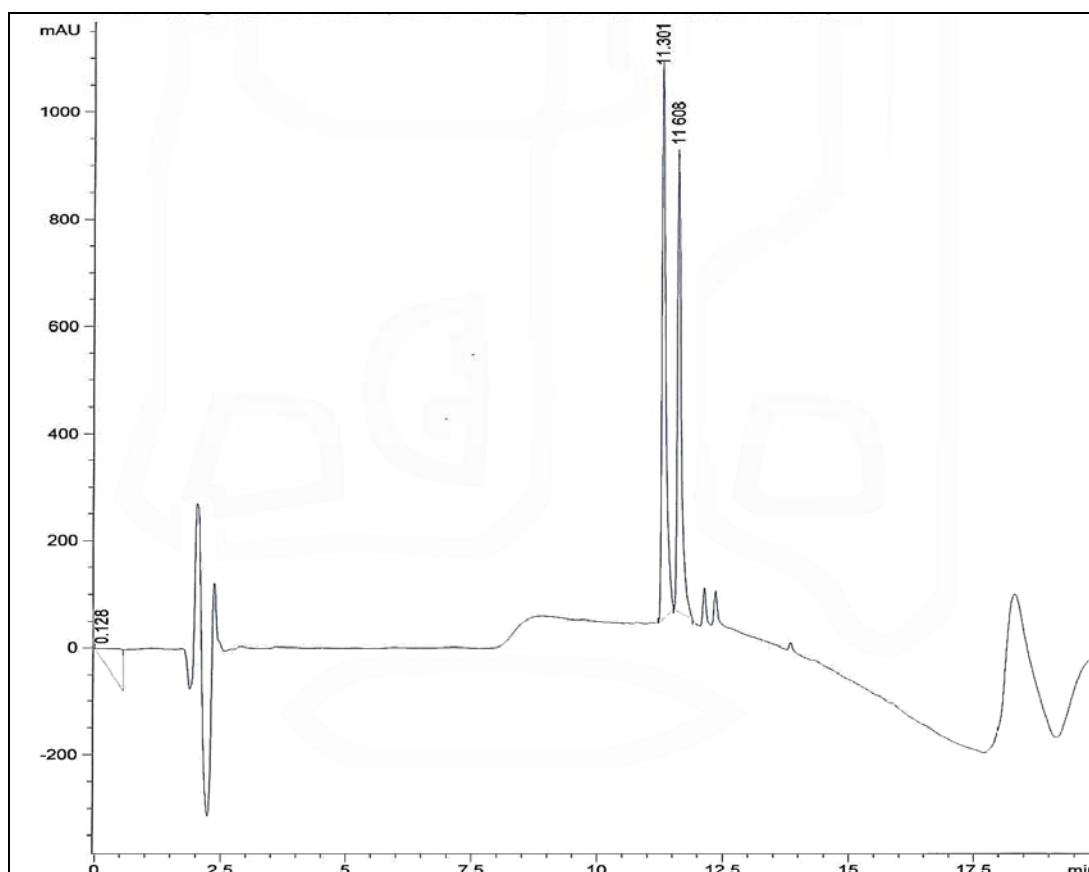


Figure 3.12 Chromatogram of 100 $\mu\text{g/mL}$ standard of C10(D,L)-LAA-AAPV from UQ

C10(D,L)-LAA-AAPV obtained from GLS Biochem eluted as a single peak at 11.3 min and variation of the HPLC conditions did not permit elucidation of two peaks corresponding to the diastereomers. The linearity by the assay method was 1 and precision was 1.02% for 3.06 $\mu\text{g/mL}$, 0.41% for 12.5 $\mu\text{g/mL}$ and 1.64% for 50 $\mu\text{g/mL}$. The LOD of C10(D,L)-LAA-AAPV was approximately 120 ng and the LOQ was 400 ng. The method showed intra-day repeatability of 0.70% for 3.06 $\mu\text{g/mL}$ and 0.63 % for 50 $\mu\text{g/mL}$ and the inter day repeatability of 0.82% for 3.06 $\mu\text{g/mL}$ and 0.56% for 50 $\mu\text{g/mL}$. A chromatogram for C10(D,L)-LAA-AAPV is shown in Figure 3.13 below.

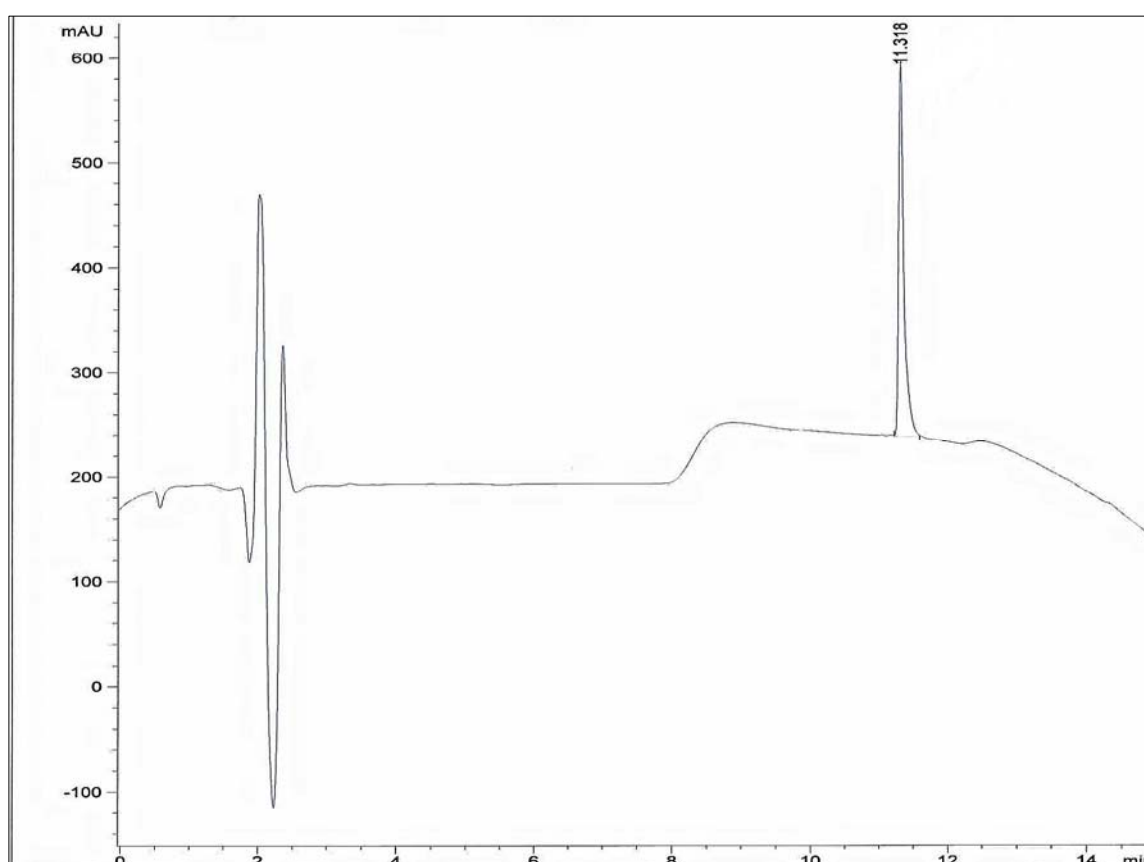


Figure 3.13 Chromatogram of 50 $\mu\text{g/mL}$ standard of C10(D,L)-LAA-AAPV from GLS Biochem

We evaluated several validation parameters to demonstrate that the analytical procedure is suitable for analyzing AAPV and its lipoamino acid conjugates in skin samples. The HPLC method described in the study also has the advantage of a rapid and sensitive

quantification of AAPV and its conjugates in the skin. Validation parameters such as linearity and assay precision of the peptides obtained from UQ and GLS Biochem were found to be similar with minimal difference in the correlation coefficient and coefficient of variance (Table 3-1 and 3-2). The only difference between C8(D,L)-LAA-AAPV and C10(D,L)-LAA-AAPV obtained from GLS Biochem as compared to UQ was that it was not possible to separate them into individual diastereomers chromatographically. *In-vitro* skin diffusion studies were conducted on the peptides from both sources and similar results were obtained verifying that peptides from both the sources showed similar permeation characteristics. The only drawback was that we were not able to compare the diffusion of the individual diastereomers in the diffusion studies undertaken with the peptides from GLS Biochem.

Table 3-1 Correlation coefficient of tetrapeptide and its conjugates

Peptide	Correlation coefficient (r ²)	Linear range(µg/mL)
AAPV	1.000	3.9-125
C6(D)-LAA-AAPV-UQ	1.000	3.9-125
C6(L)-LAA-AAPV-UQ	0.9994	3.12-100
C6(D,L)-LAA-AAPV- GLS Biochem	0.999 –D diastereomer 1.000- L diastereomer	3.9-125 3.9-125
C8(D,L)-LAA-AAPV- UQ	0.9999 –D diastereomer 0.9998- L diastereomer	1.95-125 1.95-125
C8(D,L)-LAA-AAPV- GLS Biochem	1.000	3.67-117.5
C10(D,L)-LAA-AAPV- UQ	0.9998 –D diastereomer 0.9996- L diastereomer	3.9-125 3.9-125
C10(D,L)-LAA-AAPV- GLS Biochem	1.000	3.06-100

Table 3-2 Assay precision, Intra-day and Inter-day variations of AAPV and its lipoamino acid conjugates

Peptide	Precision (n=5)			Intra-day variation (n=5)		Inter-day variation (n=9)	
Coefficient of Variance (CV,%)	7.8 µg/mL	31.25 µg/mL		7.8 µg/mL	31.25 µg/mL	7.8 µg/mL	31.25 µg/mL
AAPV (%)	0.56	0.22		0.60	0.40	0.76	1.05
C6(D)-LAA-AAPV,UQ	0.975 µg/mL	7.8 µg/mL	31.25 µg/mL	7.8 µg/mL	31.25 µg/mL	7.8 µg/mL	31.25 µg/mL
(%)	0.74	0.63	0.24	0.68	0.37	0.85	0.40
C6(L)-LAA-AAPV, UQ (%)	6.25 µg/mL	50 µg/mL	100 µg/mL	6.25 µg/mL	50 µg/mL	6.25 µg/mL	50 µg/mL
	0.90	0.46	0.47	1.04	0.61	1.09	0.62
C6(D,L)-LAA-AAPV, GLS Biochem, D diastereomer (%)	1.95 µg/mL	15.62 µg/mL	62.5 µg/mL	1.95 µg/mL	62.5 µg/mL	1.95 µg/mL	62.5 µg/mL
	0.74	0.25	0.17	1.10	0.16	1.10	0.18
C6(D,L)-LAA-AAPV, GLS Biochem, L diastereomer (%)	1.95 µg/mL	15.62 µg/mL	62.5 µg/mL	1.95 µg/mL	62.5 µg/mL	1.95 µg/mL	62.5 µg/mL
	0.86	0.19	0.19	1.10	0.10	1.22	0.18

C8(D,L)-LAA-AAPV, UQ, D diastereomer (%)	1.95 µg/mL	15.62 µg/mL	62.5 µg/mL	1.95 µg/mL	15.62 µg/mL	1.95 µg/mL	15.62 µg/mL
	1.40	0.56	0.33	2.00	0.94	2.28	0.90
C8(D,L)-LAA-AAPV,UQ, L diastereomer(%)	1.95 µg/mL	15.62 µg/mL	62.5 µg/mL	1.95 µg/mL	15.62 µg/mL	1.95 µg/mL	15.62 µg/mL
	1.35	0.38	0.11	2.40	0.61	2.12	0.83
C8(D,L)-LAA-AAPV, GLS Biochem, (%)	7.34 µg/mL	29.37 µg/mL	117.5 µg/mL	7.34 µg/mL	29.37 µg/mL	7.34 µg/mL	29.37 µg/mL
	0.94	0.25	0.21	0.68	0.51	0.63	0.40
C10(D,L)-LAA-AAPV, UQ, D diastereomer (%)	3.9 µg/mL	15.62 µg/mL	62.5 µg/mL	3.9 µg/mL	15.62 µg/mL	3.9 µg/mL	15.62 µg/mL
	1.51	0.76	0.13	1.27	0.35	1.26	0.46
C10(D,L)-LAA-AAPV, UQ, L diastereomer (%)	3.9 µg/mL	15.62 µg/mL	62.5 µg/mL	3.9 µg/mL	15.62 µg/mL	3.9 µg/mL	15.62 µg/mL
	1.31	0.52	0.22	1.05	0.33	1.05	0.28
C10(D,L)-LAA-AAPV, GLS Biochem, (%)	3.06 µg/mL	12.5 µg/mL	50 µg/mL	3.06 µg/mL	50 µg/mL	3.06 µg/mL	50 µg/mL
	1.02	0.41	1.64	0.70	0.63	0.82	0.56

3.3.2 Skin stability of tetrapeptide and lipoamino acid conjugates of the tetrapeptide

The degradation profiles of AAPV, C6(D,L)-LAA-AAPV, C8(D,L)-LAA-AAPV and C10(D,L)-LAA-AAPV are shown in Figure 3.14. The stability data was presented as the percentage of the peptide remaining at 37°C over time.

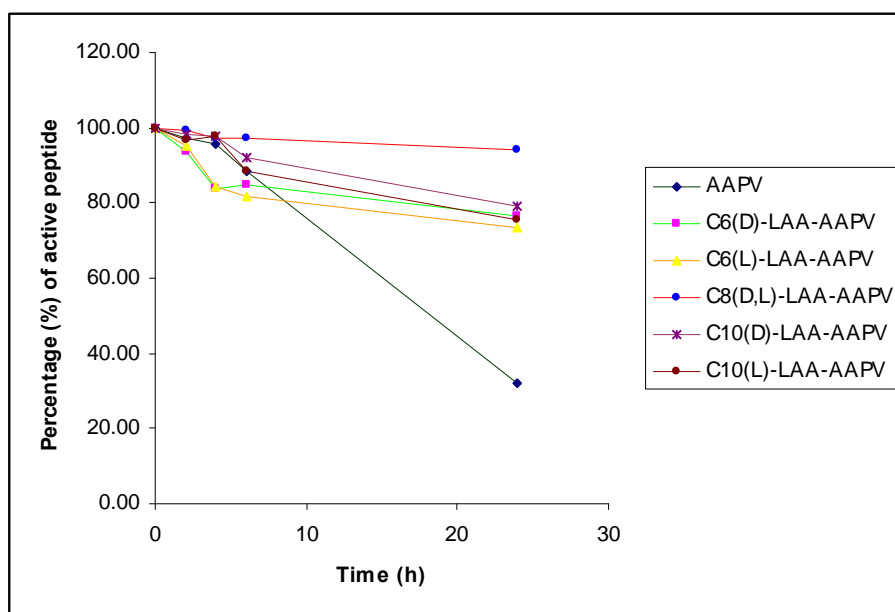


Figure 3.14 Degradation profile of tetrapeptide and its lipoamino acid conjugates

It was observed that when the tetrapeptide and its conjugates were placed at 37°C in contact with human skin about 70% of the native peptide was lost in 24 h while the stability of all the conjugated peptides was higher in comparison. (Table 3-3)

Table 3-3 Percent degradation of AAPV and its lipoamino acid conjugates (Mean, n=3, ± SEM)

Time	% AAPV	% C6(D) diastereomer	% C6(L) diastereomer	% C8(D,L)	% C10(D) diastereomer	% C10(L) diastereomer
0	100.00	100.00	100.00	100.00	100.00	100.00
2	97.43 (±2.06)	93.56 (±2.60)	95.06 (±5.31)	99.23(±0.05)	98.39 (±1.69)	96.71 (±0.23)
4	95.85 (±1.62)	83.96 (±5.30)	84.21 (±6.52)	97.38 (±0.05)	97.53 (±0.49)	97.57 (±)
6	88.31(±4.63)	84.81 (±6.40)	81.58 (±5.64)	97.24 (±0.03)	91.93 (±2.40)	88.54 (±0.68)
24	31.93 (±7.73)	76.43 (±5.0)	73.60 (±3.88)	94.30 (±0.02)	79.37 (±7.78)	75.57 (±7.43)

C6(D)-LAA-AAPV, C6(L)-LAA-AAPV, C10(D)-LAA-AAPV and C10(L)-LAA-AAPV diastereomers showed similar degradation profiles whereas C8(D,L)-LAA-AAPV was the most stable of the conjugated peptides with just 6% loss in activity at the end of 24h period. The rank order of peptides from most to least stable was C8(D,L)-LAA-AAPV > C10(D)-LAA-AAPV > C6(D)-LAA-AAPV > C10(L)-LAA-AAPV > C6(L)-LAA-AAPV though there was no significant difference in the stability between these conjugates. A significant difference ($p < 0.0001$) was observed when stability of each of these conjugates was compared to AAPV at 24h. It has been reported in the literature that conjugation of a native peptide with long alkyl side chains may protect a labile parent drug from enzymatic attack. This was demonstrated for the enzymatically labile model peptides LHRH and TRH which when conjugated to various lipidic peptides showed increased metabolic stability during incubation with Caco 2 cell homogenates.¹⁰⁸

3.3.3 In-vitro skin diffusion of tetrapeptide and lipoamino acid conjugates across human epidermis

In this study lipoamino acid conjugation was used as an enhancement strategy to improve transdermal delivery of the HNE inhibitor, AAPV. LAAs are α -amino acids

with a hydrocarbon side chain. They are a convenient method of incorporating lipid groups into peptides as they can be coupled to the peptide during solid phase synthesis using standard coupling techniques and can be incorporated at any place in the sequence. The results of all human skin permeability experiments were plotted as cumulative amount of conjugated peptide/tetrapeptide permeated through the epidermis ($\mu\text{g}/\text{cm}^2$) versus time (h). The steady-state flux of each of these conjugated/native peptide through the human epidermis was determined using equation 2 and expressed as $\mu\text{g}/\text{cm}^2\cdot\text{h}$. Permeability coefficients (cm/h) were calculated for each of these peptides using the equation 1 in section 2.2.6

3.3.3.1 Preliminary experiments to determine final protocol

Preliminary investigations were carried out on C6(D)-, C6(L)-, C6(D,L)-, C8(D,L)- and C10(D,L)-LAA-AAPV lipoamino acid conjugates. It is important to note that experiments were conducted based on the availability of these peptide conjugates. Synthetic procedures are time consuming and expensive therefore we were only able to get very small and limited quantities of peptides. In some cases experiments could not be repeated if a portion of the available compound was required for other assessment procedures. Experiments were undertaken to determine the final donor concentration, donor vehicle, receptor vehicle and period of epidermal membrane hydration.

The first set of studies was carried out with racemic mixture of C6(D,L)-LAA-AAPV. A solubility study was first undertaken with racemic mixture of C6(D,L)-LAA-AAPV where 2 mg C6(D,L)-LAA-AAPV was dissolved in four different solvent mixtures (100% PG, 75:25 PG:PBS, 50:50 PG:PBS and 25:75 PG:PBS). The results indicated that the racemate had good solubility in both 100% PG and 75:25 PG: PBS mixture. For the purpose of formulation optimization to assess the effect of a particular donor vehicle/receptor medium on the skin diffusion of C6 (D,L)-LAA-AAPV a 75:25 mixture of propylene glycol: PBS was used as the donor vehicle and 25:75 PG:PBS was used as the receptor medium. In preliminary work done in our laboratory on stereoselective permeation of C8(D,L)-LAA-AAPV, a concentration of 3mg peptide in 300 μL PG was applied to epidermal sections which had been hydrated with PBS for 1h before starting the experiment. Keeping in line with this study, we decided to use a donor concentration

of 3 mg. 3 mg peptide was dissolved in 300 μ L vehicle (75:25 PG:PBS) and the epidermis was hydrated for 1 h before starting the experiment. The receptor compartment contained 25:75 PG: PBS.

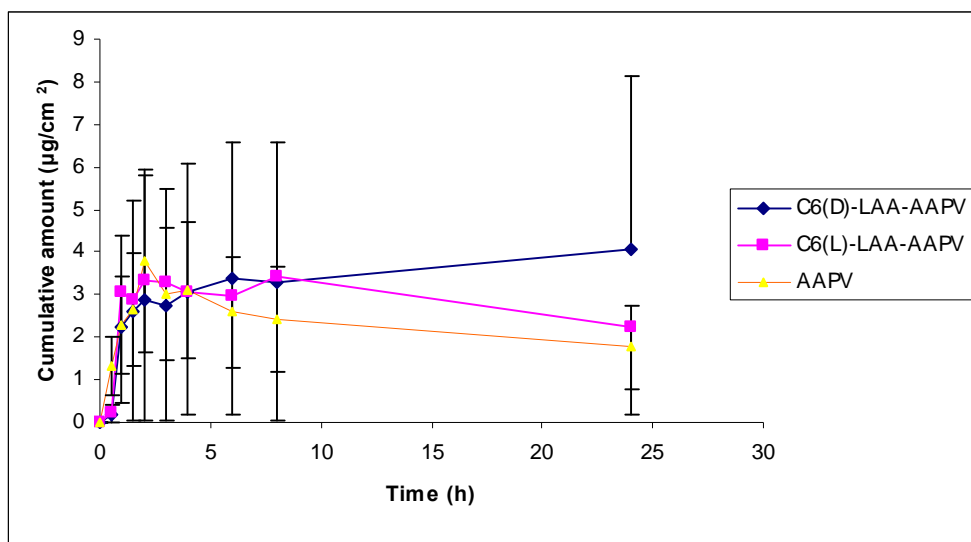


Figure 3.15 Permeation profile of cumulative amount vs. time of C6(D,L)-LAA-AAPV (racemic mixtures) vs. AAPV across human epidermis. Results are expressed as mean (\pm SEM), n=8

The results showed that there was decreased permeation of the racemic mixture as compared to the individual diastereomers across the human epidermis (Figure 3.15). Significant difference was not found in the permeation of the D- and the L- diastereomers except at 24 h where the cumulative amount of D- and L- diastereomers in the receptor compartment was 4 μ g/cm² and 2.24 μ g/cm². A large variability was also observed in the data which may be due to considerable intra-donor differences. Based on these studies it was thus decided to evaluate the permeation of C6(D,L)-LAA-AAPV using the same (3mg) donor concentration dissolved in 100% propylene glycol.

After evaluation of skin permeation with C6-LAA-AAPV, higher carbon chain length lipoamino acids conjugated to AAPV were evaluated. Skin permeation of C8(D,L)-LAA-AAPV was assessed at different conditions by altering the donor vehicle, receptor medium and concentration of the peptide in the donor. A preliminary study was then conducted by changing the donor vehicle to 75:25 PG:PBS and the receptor to 25:75

PG:PBS. However there was no observed permeation of the lipopeptide across the human epidermis under these conditions.

The last set of lipoamino acid conjugates we investigated was a racemic mixture of C10-(D,L)-LAA-AAPV. In an initial study, 3mg of C10(D,L)-LAA-AAPV was dissolved in 300 μ L propylene glycol.

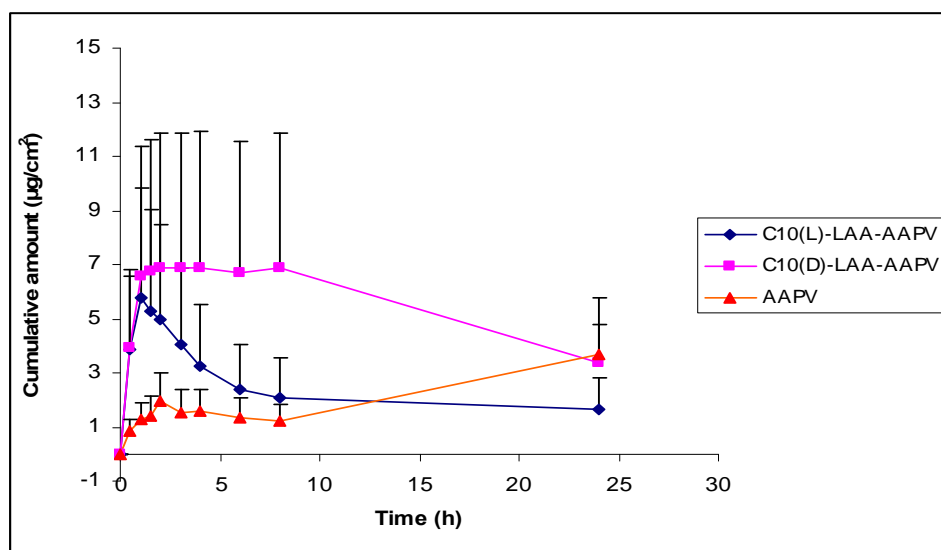


Figure 3.16 Cumulative amount vs. time of AAPV and its C10 lipoamino acid conjugate across human epidermis at a donor concentration of 3 mg in 300 μ L propylene glycol. Results are expressed as mean (\pm SEM; n=6).

The above results suggest that there was a steady increase in the permeation of the D-diastereomer of the lipopeptide till 8h (Figure 3.16). The permeation of the L-diastereomer started to decrease after approximately 2h and this may be due to the stability of the L- diastereomer as observed for C6(D,L)-LAA-AAPV. The maximum cumulative amounts in the receptor for C10(D)-LAA-AAPV and C10(L)-LAA-AAPV diastereomers were approximately 7 and 6 μ g/cm² respectively. Interestingly, the amount of D- diastereomer and the native peptide at 24h was almost similar, with the tetrapeptide being marginally higher than the lipopeptide. Also, a large variability was observed in skin sections from the same donor which may have contributed to the above results and hence this study was considered inconclusive. In the next set of optimization

studies, experiments were conducted at donor concentration of 3mg and 6 mg peptide in 300 μ L of propylene glycol.

Based on the preliminary data obtained for all the LAA conjugates a final protocol for the skin permeation studies was designed. It was decided to assess the skin permeation at two different peptide concentrations (3mg and 6 mg in 300 μ L) wherever possible. The donor vehicle was fixed as 100% propylene glycol as this permitted adequate solubility of all LAA conjugates at the required donor concentration and the receptor medium as PBS (pH 7.4)

3.3.3.2 AAPV, C6(L)-LAA-AAPV, C6(D)-LAA-AAPV and C6(D,L)-LAA-AAPV

Conjugation of the tetrapeptide to a C6-LAA substantially enhanced the ability of the tetrapeptide to cross the epidermis (Figure 3.17). We evaluated the skin permeation of C6(L), C6(D) individual diastereomers and its racemic mixture C6(D,L)-LAA-AAPV. The skin permeation of individual diastereomers of C6(D) and C6(L) was compared to determine if there were differences in permeation of the lipopeptide diastereomers across human epidermis.

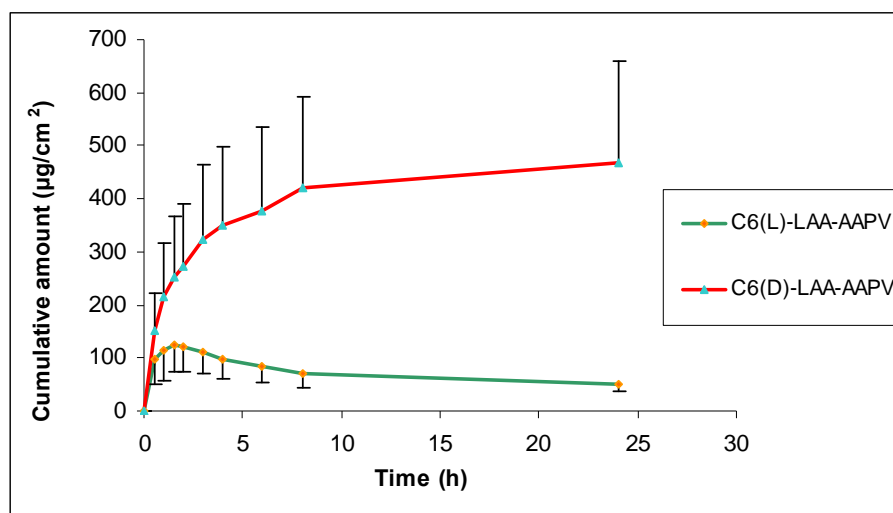


Figure 3.17 Permeation profiles for individual C6(D) and C6(L) diastereomers (3 mg in 300 μ L propylene glycol) across human epidermis from 0-24h. Results are expressed as mean (\pm SEM; n=3).

Permeation of L- diastereomer was substantially lower than that of D-diastereomer and was consistent with our earlier work with C8(D,L)-LAA-AAPV racemate where the D-diastereomer was found to permeate the epidermis to a greater extent than the L-diastereomer. The cumulative amount of C6(D)-LAA-AAPV and C6(L)-LAA-AAPV penetrated across skin was plotted against time. The pseudo-steady state flux was determined from the gradient of the linear portion over 8 and 24h of the cumulative amount-time plot by equation 2.

$$J = V(C/t)/A \dots\dots\dots(\text{Equation 2})$$

where J is the steady-state flux ($\mu\text{g}/\text{cm}^2/\text{h}$), V is the receptor volume (ml), C is the concentration of peptide in the receptor ($\mu\text{g}/\text{ml}$), t is the time (h), and A is the active diffusional area (cm^2). Over the 24h experimental period the transdermal flux of C6(D)-LAA-AAPV was calculated to be $58.5 \mu\text{g}/\text{cm}^2/\text{h}$ as compared to $15.37 \mu\text{g}/\text{cm}^2/\text{h}$ for C6(L). Over 8h the flux increased to $157.69 \mu\text{g}/\text{cm}^2/\text{h}$ for C6(D)-LAA-AAPV and $26.22 \mu\text{g}/\text{cm}^2/\text{h}$ for C6(L)-LAA-AAPV. This may be due to higher stability of both the diastereomers at the 8h time period. A significant difference was observed in the permeation of C6(D)-LAA-AAPV and C6(L)-LAA-AAPV as compared to AAPV at 8h and 24h with $p < 0.0001$ for C6(D)-LAA-AAPV and C6(L)-LAA-AAPV at 8h and $p < 0.0001$ for C6(D)-LAA-AAPV and $p < 0.05$ for C6(L)-LAA-AAPV at 24h. The permeability coefficient was also found to be higher (5.25×10^{-2} and $1.94 \times 10^{-2} \text{ cm/h}$ over 8 and 24h) in case of C6(D)-LAA-AAPV as compared to C6(L)-LAA-AAPV (8.7×10^{-3} and $1.9 \times 10^{-2} \text{ cm/h}$ over 8 and 24h). The approximate lag times for both the diastereomers were 0.5h. There was variability in permeation of each compound between the cells as shown by the standard error of the mean. The variability may be due to the intra-donor differences in skin permeation. The passive permeation of native tetrapeptide AAPV without conjugation to lipoamino acid was found to be very low (Figure 3.18). Conjugation with C6(D) ($p < 0.0001$) and C6(L) ($p < 0.05$) diastereomers enhanced the permeation of the tetrapeptide approximately 104 and 27-fold over 24h and 349 and 58 fold over 8h respectively.

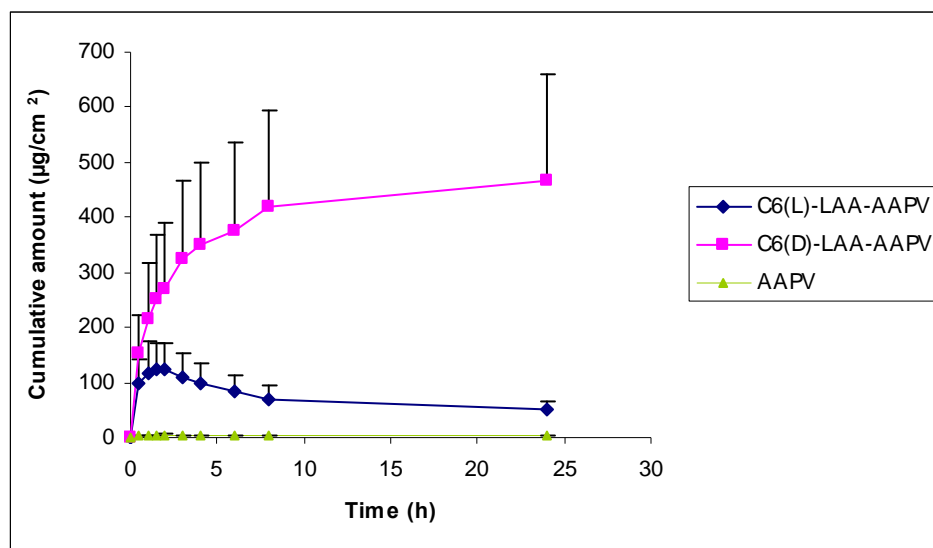


Figure 3.18 Comparison of cumulative permeation of C6(L)-LAA-AAPV and C6(D)-LAA-AAPV vs. AAPV across human epidermis. Mean (\pm SEM: n=3)

The current data demonstrates stereo selective permeation of the lipopeptide diastereomers across human epidermis (Figure 3.18). These observations of diastereoselective permeation of the lipopeptide across human epidermal sections are in line with other reports of stereoselective percutaneous permeation of enantiomers and racemates. The components of the *stratum corneum* are proposed to serve as potential sources of chiral discrimination that may result in differential diffusion rates, dependent on the stereochemistry of the solute ²⁰⁶. Furthermore, the stereochemistry of drug molecules can influence physicochemical properties such as solubility and melting point.²⁰⁷ and such differences can affect skin permeability. The results from the stability study also showed that there is approximately 25% loss in the activity of the C6(L) diastereomer i.e. 5% more than the C6(D) diastereomer. This combined with less permeation of the L- diastereomer could be a factor contributing to decreased flux of the C6(L) diastereomer. We therefore hypothesise that the observed decreased trans-epidermal delivery of the L-diastereomer, in comparison with the D-diastereomer, may be related to increased degradation of the L-diastereomer in the receptor and/or stereoselective permeability of the diastereomers. The percentage of applied dose penetrating to the receptor over 24 h following administration was 4.67% for the D-diastereomer conjugate and 1.23% for the L-diastereomer, compared to 0.04% for the

peptide. We envisage that these concentrations will be sufficient to inhibit HNE activity since this tetrapeptide may also show an increased inhibitory capacity with lipidation.¹⁴⁵

In the next set of experiments, diffusion of the racemic mixture of C6(D,L)-LAA-AAPV was investigated. The skin diffusion studies were conducted on 2 different skin donors and the data was pooled to calculate the cumulative amount permeating the receptor at the end of 24 hours. The donor concentration used in the study was 3mg peptide in 300 μ L propylene glycol and the epidermis was hydrated for 1 h before starting the experiment.

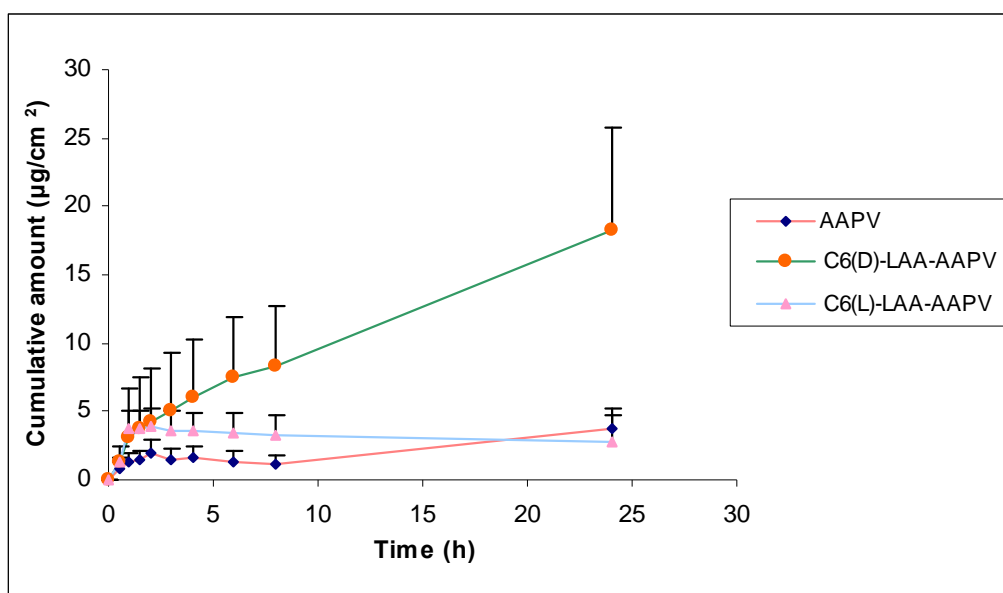


Figure 3.19 Cumulative amount vs. time of C6(D)-LAA-AAPV, C6(L)-LAA-AAPV (racemic mixture) and AAPV across human epidermis. Results are expressed as mean (\pm SEM; n=9).

The results showed that in accordance with the individual diastereomer there was more permeation of the D-diastereomer from the racemic mixture as compared to the L-diastereomer. The estimated transdermal flux was calculated over 24h using equation 2 as $2.29 \mu\text{g}/\text{cm}^2/\text{h}$ for the C6(D) and $0.5 \mu\text{g}/\text{cm}^2/\text{h}$ for the C6(L) isomer. The flux of the D-diastereomer in the racemate was approximately 4.6-fold higher than the L-diastereomer. In comparison with the individual diastereomers it was found that the permeation of the racemate across the epidermis was lower (Figure 3.20).

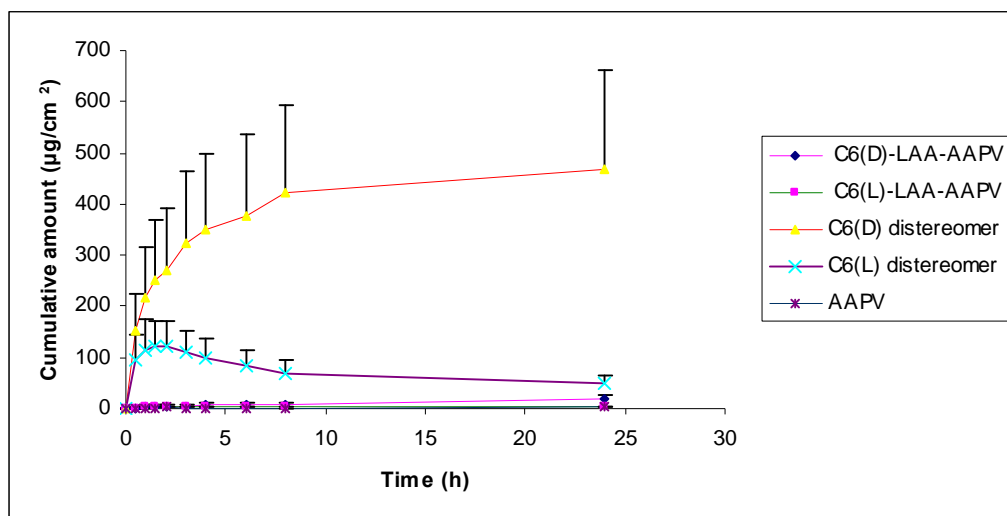


Figure 3.20 Comparison of cumulative permeation of C6(D) and C6(L) individual diastereomers (n=3) vs. C6(D,L)-LAA-AAPV racemic mixture (n=9) and AAPV (n=7) across human epidermis at a donor concentration of 3 mg in 300 µL propylene glycol. Results are expressed as mean (\pm SEM).

The major barrier to transdermal drug delivery is the outermost layer of the skin, the *stratum corneum*. Drug-skin interactions may be of a stereo selective nature since the *stratum corneum* components form essentially a chiral environment²⁰⁸. Considering the intercellular diffusion pathway, an interaction with ceramides is possible. Ceramides are chiral substances having two (ceramides 1 and 2), three (ceramides 3, 4 and 5) or four chiral carbons (ceramide 6) within the polar head. Stereo selective interaction with ceramides has been shown in ephedrine enantiomers²⁰⁸, although not connected with differences in permeation ability. In addition, in the case of intracellular permeation, an interaction with keratin can take place. Various stereo selective processes in the skin have been investigated.²⁰⁹ Significant differences in rates of skin transport between a racemate and pure enantiomers have previously been demonstrated from saturated solutions. This phenomenon has been attributed to the crystallinity of the solid: the greater solubility and hence greater flux relative to the racemate. One important reason for higher permeation of the pure enantiomers is the inherent differences in physicochemical properties of the two.²¹⁰ For example, stereoselective skin permeation of organic nitrates was reported to be due to differences in solubility, lipophilicity and

diffusivity and these properties were closely related to the stereochemistry of the diastereomers.¹⁹⁰

Miyazaki *et al* reported different permeation rates of propranolol enantiomers through rat skin, indicating a stereoselective interaction with the *stratum corneum*.²¹¹ The *in vitro* human skin permeation of racemic and enantiomerically pure R- and S-propranolol HCl from topical formulations containing a chiral cellulose derivative as excipient was determined. In the case of the pure enantiomers, there was a significant difference between the penetration rates of R- and S-propranolol. The flux of the R- and D- isomers was 1.20 and 0.58 $\mu\text{g}/\text{cm}^2/\text{h}$ respectively and flux ratio was 2.06. In the case of racemic propranolol, however, the flux of the R- and S- isomers was 0.59 and 0.49 $\mu\text{g}/\text{cm}^2/\text{h}$ respectively and the flux ratio was decreased to 1.2.²¹⁰ The more lipophilic pro-drugs of propranolol appear to show more notable stereoselective permeation profiles. In full thickness skin, (R)- caproyl-propranolol showed the highest permeability which was about 52-fold greater than that of propranolol.²¹²

3.3.3.3 C8(D,L)-LAA-AAPV

We had previously determined that the *stratum corneum* acts as a barrier to the delivery of the N-acetylated tetrapeptide (Ac-AAPV-NH₂) across human skin.²⁰⁵ The current research was aimed at enhancing the transepidermal delivery of this potentially therapeutically useful tetrapeptide. We also demonstrated that coupling of a tetrapeptide to a short chain C8-LAA enhanced its trans-epidermal delivery.¹⁹⁰ The lipopeptide was present as a mixture of the D- and L-diastereomers of the LAA with greater sub-epidermal availability of the D-diastereomer. This is in agreement with the results for C6(D,L)-LAA-AAPV.

We replicated the published study using a new batch of C8(D,L)-LAA-AAPV supplied by University of Queensland and by using a different skin donor. The donor concentration of C8(D,L)-LAA-AAPV was 3mg in 300 μL propylene glycol and the epidermis was hydrated for 1h. The skin diffusion of C8(D,L)-LAA-AAPV was then compared to the native tetrapeptide. Based on the preliminary studies done with C6(D,L)-LAA-AAPV in different solvents and receptor medium propylene glycol was

used as a vehicle to dissolve the peptide and PBS as the receptor medium. The data was plotted as the cumulative amount ($\mu\text{g}/\text{cm}^2$) of the peptide permeating in the receptor vs. time. Transdermal flux was calculated using equation 2.

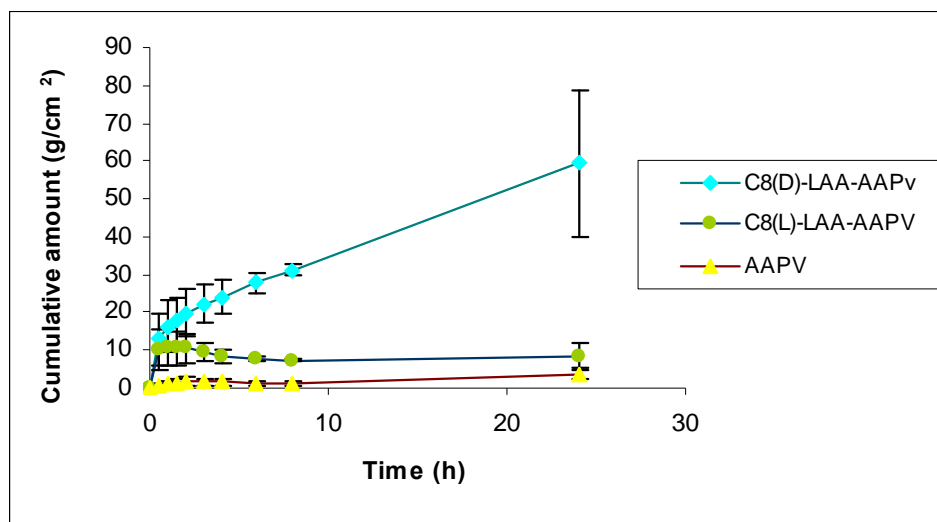


Figure 3.21 Permeation profiles of the tetrapeptide and lipotetrapeptide [C8(D,L)-LAA-AAPV] racemic mixture across human epidermis at a donor concentration of 3 mg in 300 μL propylene glycol. Results are expressed as mean ($\pm\text{SEM}$; $n=3$ for C8(D,L)-LAA-AAPV and $n=7$ for AAPV)

The results indicated that conjugation of the tetrapeptide to a C8-LAA enhances the ability of the tetrapeptide to cross the epidermis (Figure 3.21). The percentage of applied dose penetrating to the receptor over 24 h following administration was approximately 2% for the D-LAA conjugate and 0.36% for the L-LAA conjugate, compared to 0.12% for the peptide. The estimated transdermal flux for the D- diastereomer and L- diastereomer was $7.42 \mu\text{g}/\text{cm}^2/\text{h}$ and $1.37 \mu\text{g}/\text{cm}^2/\text{h}$ respectively. The cumulative amount of the D- diastereomer increased linearly in the receptor with the maximum of 60 μg at the end of 24h. The permeation of C8(D)-LAA-AAPV diastereomer was significantly increased as compared to AAPV permeation over the time period of the experiment ($p<0.05$). With regards to C8(L)-LAA-AAPV a significant difference in permeation as compared to AAPV was observed at 4h and 8h ($p<0.05$). The approximate lag times for both the diastereomers were 0.5h. The amount obtained for the D- diastereomer was comparable to our previously published results though the values for the L- diastereomer were substantially lower. No degradation peak was observed for the L- diastereomer in

spite of a slight downward trend over the 24h experimental period. The reason may be attributed to stereo selective permeation across the epidermis and to a different skin sample used in the present study.

The hydration time was increased from 1 to 24h and the donor concentration was kept constant (3mg in 300 μ L PG). The peptide was dissolved in propylene glycol and the receptor medium was PBS. Results were expressed as mean (\pm SEM) of sections taken from two different female volunteers comparing tetrapeptide to lipotetrapeptide.

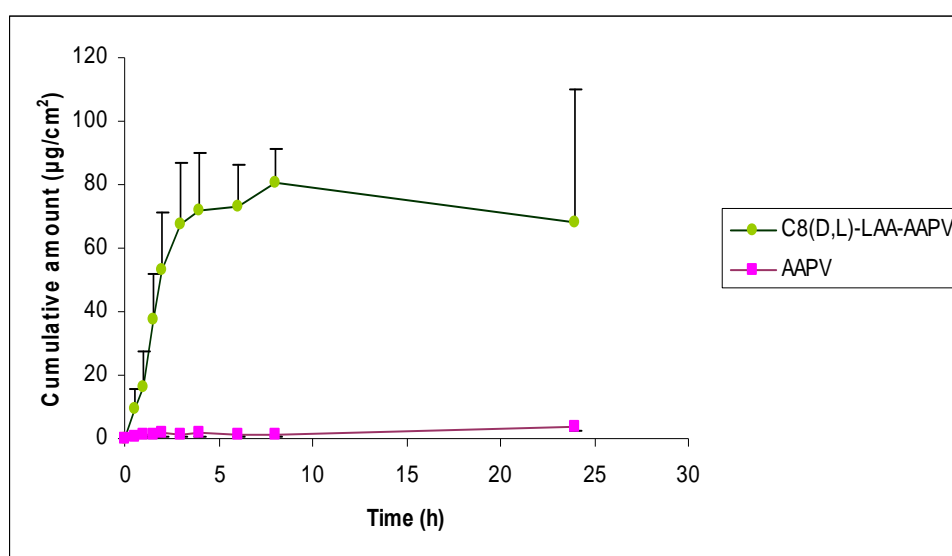


Figure 3.22 Cumulative permeation of C8(D,L)-LAA-AAPV (n=7) and AAPV (n=4) across human epidermis with 24h hydration. Mean (\pm SEM)

The data suggests that, there was a marginal increase in the amount of lipidated peptide traversing the skin with skin hydrated for 24 h compared to 1 h hydration (Figure 3.22). The maximum cumulative amount of the tetrapeptide and lipo-tetrapeptide was approximately 80 μ g/cm² and 4 μ g/cm² ($p < 0.05$). The estimated transdermal flux calculated over the linear portion of the curve was 10.08 μ g/cm²/h for the lipo-tetrapeptide while 0.5 μ g/cm²/h for the native peptide. The amount of C8(D)-LAA-AAPV increased from 60 to 80 μ g/cm² for skin hydrated for 24h but this effect was not seen with a racemic mixture of C10 (D,L)-LAA-AAPV.

The effect of increasing concentration was also assessed on skin permeation of C8(D,L)-LAA-AAPV and the native peptide. A donor concentration of 6 mg native/lipo-peptide in 300 μ L propylene glycol was used and the skin was hydrated/equilibrated was 24h. Cumulative amount of lipopeptide and native peptide permeating to the receptor was calculated and the results showed that increase in concentration did not have a major impact on skin permeation (Figure 3.23). The cumulative amount at 24h for C8(D,L)-LAA-AAPV and AAPV were approximately 60.0 μ g/cm² and 2.0 μ g/cm² respectively ($p < 0.05$). These values were similar to those obtained at lower concentration and shorter equilibration time.

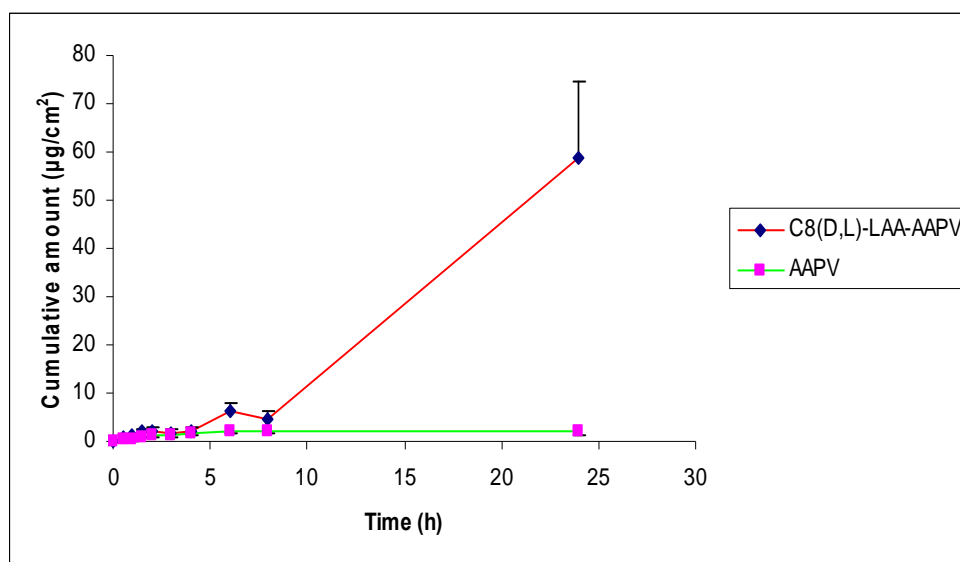


Figure 3.23 Permeation profiles of C8(D,L)-LAA-AAPV racemic mixture and AAPV at a donor concentration of 6 mg in 300 μ L PG. Results are expressed as mean (\pm SEM;n=4)

Acylation of peptides and proteins has been investigated for drug delivery via a number of routes of administration including transdermal. Yamamoto and colleagues examined the transdermal delivery of acyl derivatives (C4, C6 and C8) of a dipeptide (Phe-Gly) across full-thickness abdominal skin excised from a male rat and reported that the stability and permeability of the dipeptide was improved by the chemical conjugation with short chain fatty acids. The permeability of the C6-Phe-Gly across intact skin was the highest and the amount of C8-Phe-Gly remaining in the intact skin was highest of all the acyl derivatives studied, likely due to its high binding characteristics to the skin.¹⁵⁵

Although the transfer characteristics of many compounds have been investigated, differences that may exist in the transfer rates of individual stereoisomers of chiral compounds have received scant attention. Stereoselective processes have also been reported within the viable epidermis and dermis, including those involved in contact dermatitis and skin metabolism. It is also possible that inter conversion of stereoisomers could occur due to enzyme activity. However, as the rate-limiting step in percutaneous penetration is diffusion across the *stratum corneum*, the significance of these substratum corneum effects is difficult to assess.²⁰⁸

In this study, the tetrapeptide sequence was synthesised to generate the active conformation (using all L-amino acids) and the addition of the LAA is what generated the two stereoisomer's, therefore we do not expect a decrease in activity for either of the lipopeptide isomers generated but possibly a difference in efficacy which will be discussed in the following section.

3.3.3.4 C10(D,L)-LAA-AAPV and C10(D)-LAA-AAPV

This conjugate was more lipophilic than the C6-LAA-AAPV and C8-LAA-AAPV conjugated peptides. The skin permeation of this lipopeptide was compared with the native peptide. The effect of donor concentration and time of hydration on skin permeability of peptides was also evaluated.

Based on the low skin permeation results obtained in the preliminary study with donor concentration of 3 mg in 300 μ L, it was then decided to increase the donor concentration and study its effect on skin permeability. A concentration of 6 mg peptide in 300 μ L propylene glycol was used in the donor and the equilibration period was 1 h. From the skin permeation studies (Figure 3.24), the human epidermis was more permeable to the lipopeptide than to the less lipophilic native tetrapeptide but there was a longer lag time seen than with the shorter LAA conjugates.

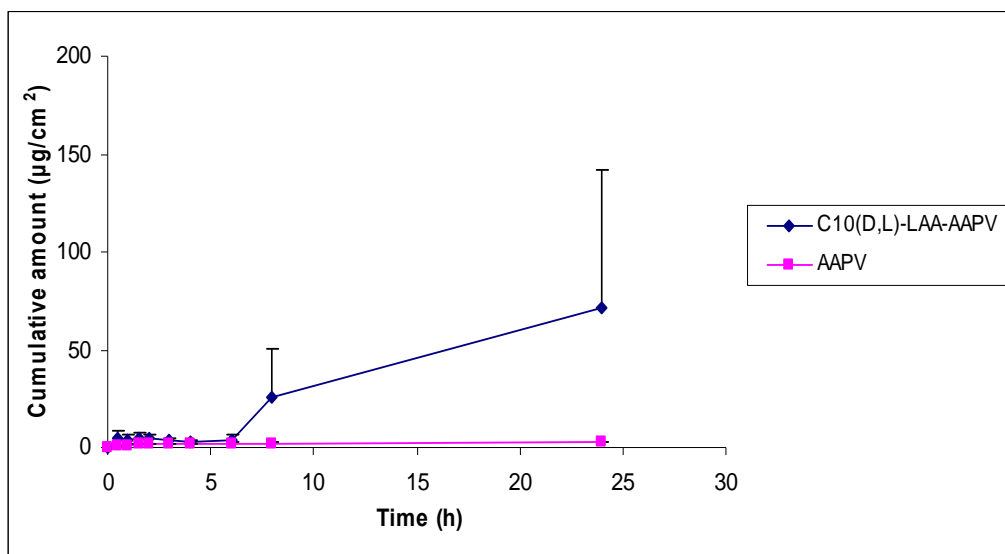


Figure 3.24 Cumulative amount vs. time permeation of C10(D,L)-LAA-AAPV and AAPV at a donor concentration of 6 mg in 300 µL PG across human epidermis. Results are expressed as mean (\pm SEM, n=4)

The flux value for AAPV was 0.24 µg/cm²/h compared to 8.92 µg/cm²/h for the lipopeptide. The C10(D,L)-LAA conjugate thus increased the permeation of the native peptide 37-fold. The cumulative amounts for AAPV and C10(D,L)-LAA-AAPV transported after 24 hours were approximately 2.2 and 71.43 µg/cm². The difference in permeation between C10(D,L)-LAA-AAPV and AAPV was significant at the 24h time point ($p < 0.05$).

The next objective was to study the effect of increasing skin hydration on transdermal delivery of this lipopeptide. Experiments were conducted at donor concentration of 6 mg in 300 µL propylene glycol and the skin hydration/equilibration period was increased from 1 to 24h.

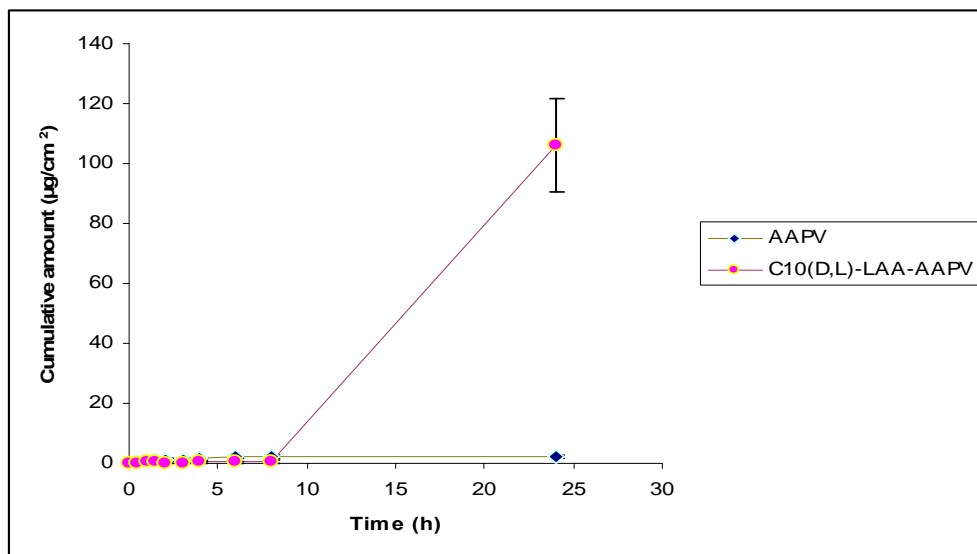


Figure 3.25 Cumulative penetration of C10(D,L)-LAA-AAPV and AAPV across human epidermis with 24h hydration. Results are expressed as mean (\pm SEM; n=4)

It can be concluded from these experiments that a higher donor concentration improved the skin permeability of a high molecular weight and more lipophilic peptide, C10 (D,L)-LAA-AAPV. Initially the skin permeation of the lipopeptide was slow due to its high molecular weight and lipophilic nature. But, after 24 h the cumulative amount in the receptor was approximately 106 $\mu\text{g}/\text{cm}^2$ as compared to 2.13 $\mu\text{g}/\text{cm}^2$ for the tetrapeptide. C10(D,L)-LAA-AAPV permeation was significantly increased as compared to AAPV permeation at 24h ($p < 0.0001$). The rate of permeation of the lipopeptide and native tetrapeptide was 13.25 and 0.26 $\mu\text{g}/\text{cm}^2/\text{h}$ respectively. The permeability coefficient for lipopeptide and native tetrapeptide was 2.2×10^{-3} cm/h and 4.5×10^{-5} cm/h respectively. Conjugation with C10(D,L)-LAA-AAPV thus resulted in 48-fold enhancement in the transdermal delivery of the tetrapeptide when used at a higher concentration (Figure 3.25). On comparison of this data with the results obtained with a donor concentration of 6 mg and skin hydration of 1 h it was observed that a 1.5 fold enhancement in the delivery of C10(D,L)-LAA-AAPV was observed with longer period of hydration. The data follows the same pattern where minimal permeation was observed till 8h and the amount increased at the 24h time period. The only concern though is its lipophilic nature due to which the skin permeation begins only after 8 h in contrast to the other lipoamino acid conjugates investigated. Skin hydration/equilibration

also may have played a role in increasing transport of this lipophilic peptide across the lipid barrier.

3.3.3.5 Consolidated comparison of skin permeation enhancement by lipoamino acid conjugated tetrapeptide

The skin delivery results clearly indicate that, at a lower concentration of 3mg peptide/lipopeptide in 300 μ L in propylene glycol the order of permeation was C6(D)>C6(L)>C8(D)>C8(L)>C6(D)>C6(L)>C10(D)>C10(L).

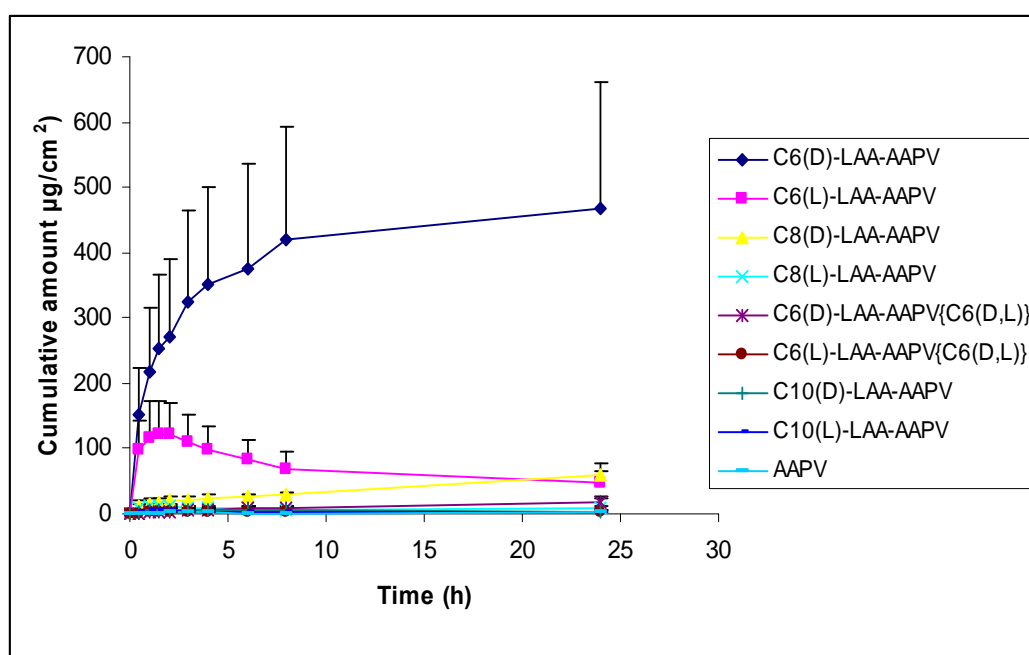


Figure 3.26 Permeation profiles of AAPV and its lipoamino acid conjugates across human epidermis. Results are expressed as mean (\pm SEM)

The D- diastereomers of each of these peptides showed higher flux as compared to the L- diastereomers. Permeation of native AAPV across intact skin was very low during the period of observation. In contrast, the three derivatives, C6-LAA-AAPV, C8-LAA-AAPV and C10-LAA-AAPV permeated through the epidermis, with the individual diastereomers of C6-LAA-AAPV as the most permeable (Fig 3.26, Table 3-4). When the concentration was increased to 6 mg in 300 μ L propylene glycol with 1 h hydration, the amount of C10(D,L) permeating the skin increased.

Table 3-4 Comparison of permeation parameters of the native and conjugated peptides (flux calculated till 8 and 24 h for C6(D) and C6(L)-LAA-AAPV individual diastereomers)

Peptide	Cumulative amount ($\mu\text{g}/\text{cm}^2$)	Transdermal flux ($\mu\text{g}/\text{cm}^2/\text{h}$)	Permeability coefficient $K_p(\text{cm}/\text{h})$
AAPV (3mg in 300 μL)	3.70 (\pm 1.09)	0.46	1.50×10^{-3}
C6(D)-LAA-AAPV (3mg in 300 μL)	467.94 (\pm 192.6)	157.69 – 8 h	5.25×10^{-2} - 8 h
		58.50- 24 h	1.94×10^{-2} - 24 h
C6(L)-LAA-AAPV (3mg in 300 μL)	123.04 (\pm 48.89)	26.22- 8 h	8.70×10^{-2} - 8 h
		15.37- 24 h	5.70×10^{-2} - 24 h
C6(D,L)-LAA-AAPV (3mg in 300 μL)			
C6(D)-LAA-AAPV	18.32 (\pm 7.40)	2.29	2.29×10^{-3}
C6(L)-LAA-AAPV	3.93 (\pm 1.32)	0.50	4.90×10^{-3}
C8(D,L)-LAA-AAPV (3mg in 300 μL)			
C8(D)-LAA-AAPV	59.38 (\pm 19.14)	7.42	1.90×10^{-2}
C8(L)-LAA-AAPV	10.99 (\pm 5.20)	1.37	4.50×10^{-4}
C8(D,L)-LAA-AAPV (6mg in 300 μL)- 1h	60.00 (\pm 15.71)	7.50	1.20×10^{-3}
C10(D,L)-LAA-AAPV (6mg in 300 μL)	106.03 (\pm 15.74)	13.25	2.2×10^{-3}

Overall, the permeability of the lipoamino acid conjugates of Ala-Ala-Pro-Val was much higher than the native tetrapeptide, Ala-Ala-Pro-Val. The permeability of the more lipophilic conjugates such as C10-LAA was less than that of native peptide in the initial time period of transport studies, but was higher than that of native at the end of the transport studies. These results for the skin permeability experiments are in good agreement with previous finding that the transdermal absorption of tetragastrin was enhanced by its chemical modification with fatty acids.¹⁶⁴ Similar results were also observed in the intestinal absorption of various acyl derivatives of peptides and proteins including insulin, calcitonin and DADLE, an enkephalin derivative.²¹³ The lack of permeability of native Ala-Ala-Pro-Val across the epidermis maybe mainly attributed to its metabolism in the skin and low lipophilicity. The reason why the permeability of C6 (D)-LAA-AAPV distereomer was the highest of all the lipoamino acids used in the study is not clearly understood but it may be due to the intrinsic stereoselectivity of the skin for enantiomers of chiral molecules and extrinsic factors such as differences in physicochemical properties between enantiomers and racemate.²¹⁴

It has also been demonstrated previously that the permeability of the acyl-tetragastrin derivatives was not correlated with their lipophilicity. That is, the permeability of acetyl-tetragastrin was higher than that of butyryl- and caproyl-derivatives across the intact and stripped skin.¹⁶⁴ Therefore, the low initial permeability of higher lipophilic derivatives of Ala-Ala-Pro-Val [C10(D,L)-LAA-AAPV] in certain experimental conditions may be due to its strong partitioning and binding to the *stratum corneum*. From these findings, it may be considered that there is an optimal lipophilicity (length of lipoamino acid chain) of the derivatives for improving their transdermal delivery.

3.3.4 Recovery of tetrapeptide and lipoamino acid conjugates from skin

Figures 3.27, 3.28 and 3.29 indicates the amounts of native tetrapeptide and its lipoaminoacid conjugates in the skin after the permeation experiments. As shown in this figure, the amount of AAPV in the skin increased as the carbon number of fatty acid attached to the AAPV molecule increased in the intact skin. Initially extraction was carried out with DMSO and methanol for C6 (D)-LAA-AAPV and C6 (L)-LAA-AAPV.

The recovery of C6(D)-LAA-AAPV with DMSO was approximately 60% whereas 70% in case of C6(L)-LAA-AAPV. It was thus decided to optimize the extraction procedure by substituting DMSO with propylene glycol. The recovery of AAPV, C6(D,L), C8(D,L) and C10(D,L) was validated using the extraction procedure with PG and methanol. After three successive extractions with methanol and propylene glycol the recovery was 97%, 93 %, 90%, 96% and 95% for AAPV, C6(D)-LAA-AAPV, C6(L)-LAA-AAPV, C8(D,L)-LAA-AAPV and C10(D,L)-LAA-AAPV respectively of the theoretical input. The possible loss of about 5–10% of tetrapeptide and its conjugates might be due to skin enzyme activity, metabolism and handling of the skin tissue, and other processes in the experiment. These peptide accumulation data further attest to the suspected strong interaction between the peptide and lipophilic structures present in the skin. The accumulation may also be the result of peptide to peptide interactions, which result in aggregation of these molecules in the skin and eventually in peptide deposition in the transport pathways.²¹⁵ Figures 3.27, 3.28 and 3.29 shows the amount of peptide in the epidermis in different experimental conditions.

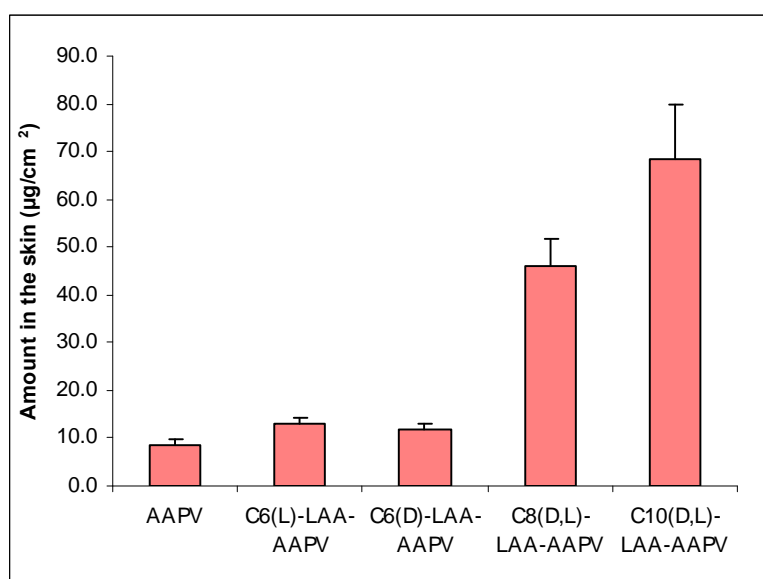


Figure 3.27 Amount of AAPV and its lipoamino acid conjugates in the skin after the permeation experiments (Donor concentration of 3mg peptide/lipopeptide in 300 µL PG) and 1 h hydration. Results are expressed as mean (±SEM; n=4)

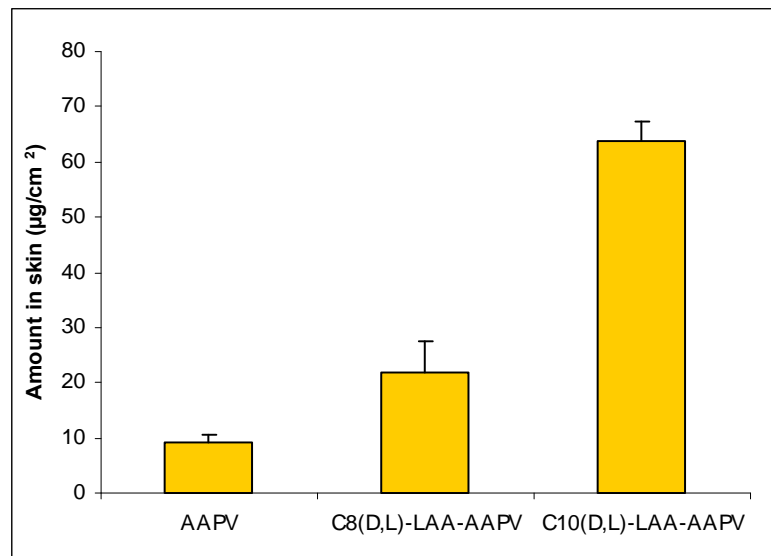


Figure 3.28 Amount of AAPV and its lipoamino acid conjugates in the skin after the permeation experiments (Donor concentration of 3mg peptide/lipopeptide in 300 µL PG) and 24 h hydration. Results are expressed as mean (\pm SEM; n=4)

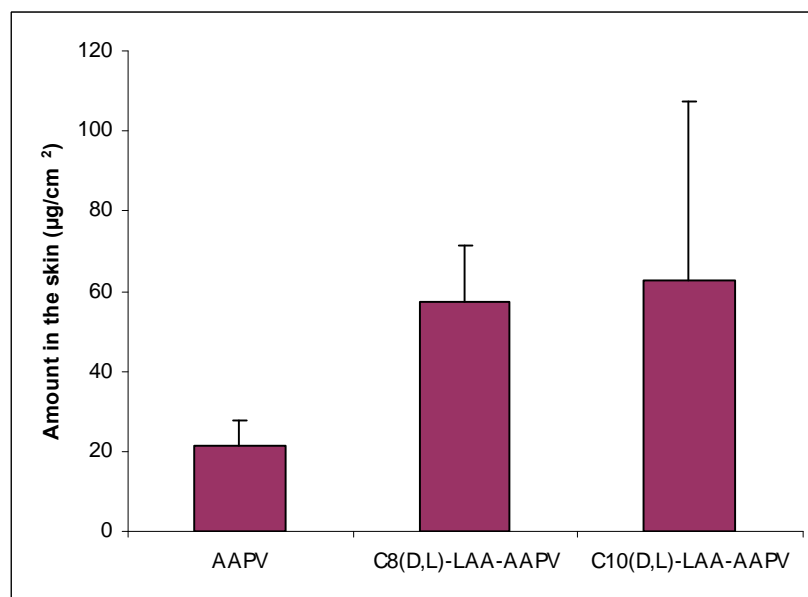


Figure 3.29 Amount of AAPV and its lipoamino acid conjugates in the skin after the permeation experiments (Donor concentration of 6mg peptide/lipopeptide in 300 uL PG) and 24 h hydration. Results are expressed as mean (\pm SEM; n=4)

The amount of drug remaining in the epidermis at 24 h (Figure 3.27) increased as the number of carbons in the fatty acids that were chemically attached to the native Ala-Ala-Pro-Val increased. As expected, the amount of C10(D,L)-LAA-AAPV was the highest of all the lipoamino acid derivatives. Therefore, an optimum lipophilicity (the carbon number of the fatty acids) is thought to exist for the drug accumulation in the skin. For example, Walter and Kurz (1988) reported good correlation between the partition coefficient of 10 different drugs with different physicochemical properties and their skin binding affinity. They concluded that these drugs might bind with skin components such as proteins, but binding with lipids was less likely as their binding was not affected when skin lipids were removed.²¹⁶ These findings were in good agreement with our present finding of the highest accumulation of C10(D,L)-LAA-AAPV. Therefore, we speculate that the longer lag time of C10(D,L)-LAA-AAPV permeation is due to its high binding characteristics to the skin, since C10(D,L)-LAA-AAPV had the highest molecular weight and lipophilicity of all the lipoamino acid derivatives investigated.

3.3.5 Surface activity

A preliminary study was undertaken to assess if lipophilic conjugates of the tetrapeptide possess surface active properties which may be important in determining their permeability. The surface tension activity of tetrapeptide and its lipophilic conjugates was determined in aqueous solutions in the range of 0.0625-1 mg/mL by the ring method using a Du Nouy tensiometer at room temperature. An approximate critical micelle concentration (CMC) was obtained from the graph of surface tension in dyne/cm versus concentration (Figure 3.30). There was a significant decrease in surface tension of phosphate buffered saline with the addition of the AAPV coupled lipopeptides and the tetrapeptide ($p < 0.0001$). In addition a significant difference ($p < 0.0001$) in the surface tension lowering capacity between the lipoamino acid conjugates was also observed with C8 and C10 (D,L)-LAA-AAPV causing highest decrease followed by C6(D,L)-LAA-AAPV and AAPV. The estimated CMC for AAPV, C6(D,L)-LAA-AAPV, C8(D,L)-LAA-AAPV and C10(D,L)-LAA-AAPV was approximately 0.125, 0.25, 0.5, 0.5 mg/mL. This is preliminary data to indicate that the tetrapeptide and its conjugates possess surface activity but more work is required to establish reliable CMC values.

Bio-based surfactants are synthetic amphipathic structures based on natural structures of biosurfactants. Among them, lipoamino acid/peptide and glycolipid analogues have become increasingly important because of their chemical simplicity, surface activity, aggregation properties and broad biological activity.²¹⁷ A well-known example of a biosurfactant is surfactin, a cyclic lipopeptide and powerful surfactant commonly used as an antibiotic.²¹⁸ It has been found to exhibit effective characteristics like anti-bacterial, anti-viral, anti-fungal, anti-mycoplasma and haemolytic activities.

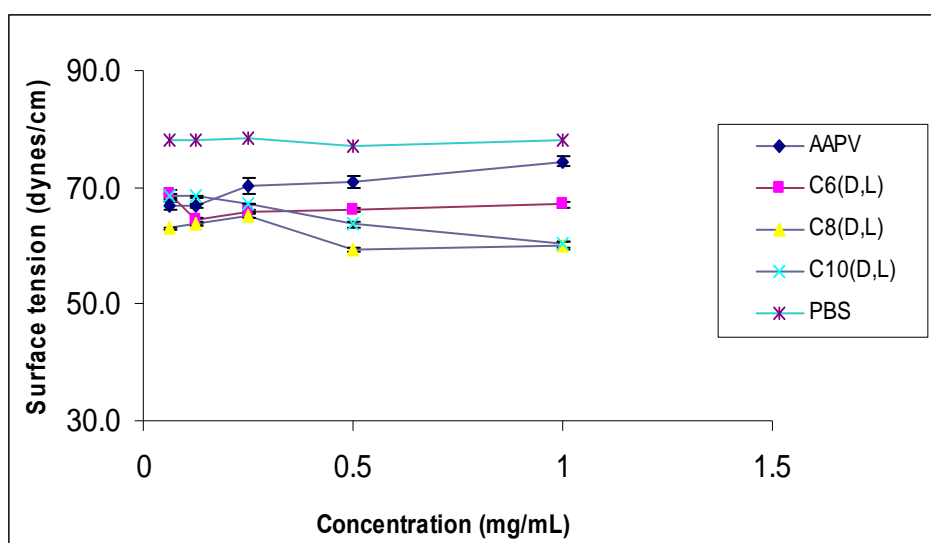


Figure 3.30 Surface tension measurement of the native tetrapeptide and the conjugated lipopeptides. Results are expressed as mean (\pm SEM) of 3 measurements

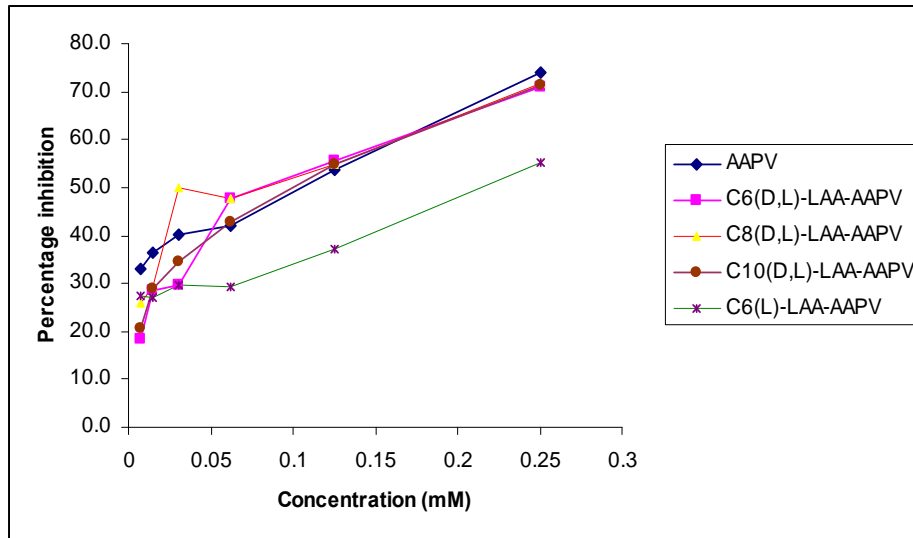
Surfactant analogues of lipoamino acid/peptides have received a great deal of attention due to their multifunctionality, i.e. high efficiency, good aggregation properties and broad biological activity. These properties make them good alternatives for a wide range of applications in personal care, pharmaceutical and food sectors. In a study undertaken by Ashton *et al* the effects of a series of surfactants on the permeability of human skin *in vitro* using methyl nicotinate as a model drug was investigated. It was found that while the ionic surfactants exerted a greater effect on the flux of methyl nicotinate, the non-ionic surfactants had a smaller but more immediate effect on the flux.²¹⁹ We hypothesize that the LAA coupled peptides may have surfactant like properties which aid in skin permeation. They can interact with the *stratum corneum* by either increasing the local

water concentration with consequent swelling of the tissue. They may also interact with the *stratum corneum* through electrostatic and hydrophobic links or may interact with the protein fractions of the *stratum corneum* through hydrophobic interactions with keratin.²²⁰

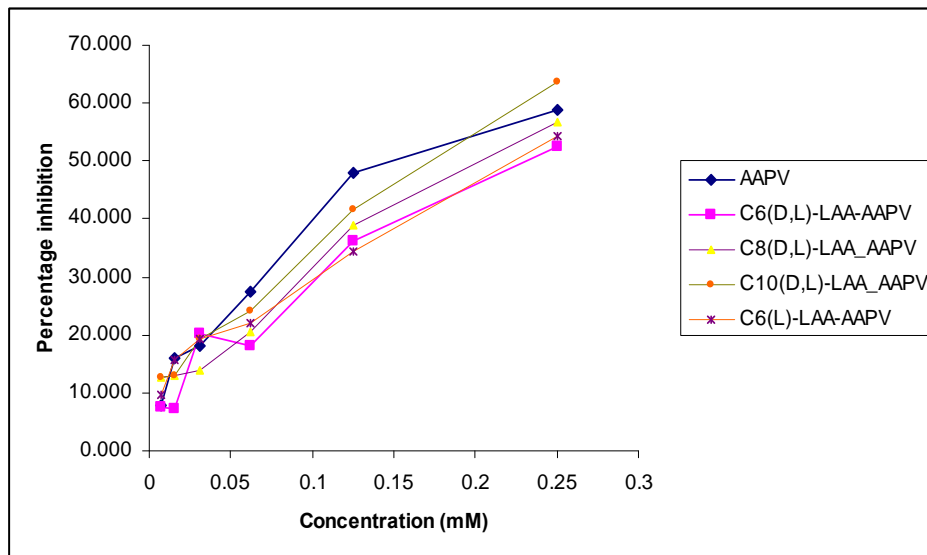
3.3.6 Enzyme inhibitory activity

The main objective of this study was to assess the biological activity of the LAA conjugates and compare it to the native tetrapeptide. The elastase inhibitory activity of these peptides was assessed at two different substrate (6.25 µg/mL and 25 µg/mL) and enzyme concentrations (0.25 and 0.5 U/mL). Figure 3.31 showed that the ability of elastase to digest the substrate decreased as the concentration of each of the inhibitors in the reaction mixture increased. The inhibition caused by synthesised conjugates and the parent tetrapeptide was fairly similar. It was observed that there was approximately 70% reduction in the activity of elastase with the lipopeptides and tetrapeptide at 0.25mM. C6(L)-LAA-AAPV caused an overall inhibition of 55% when the assay was carried out at a lower concentration of elastase and substrate. At a higher concentration of substrate and elastase the results were fairly similar to those obtained at a lower concentration. It was observed that there was approximately 55% reduction in activity with the tetrapeptide and lipopeptides at 0.25mM. In comparison with the control tetrapeptide only C10(D,L) caused a higher level of inhibition at 0.25mM. As the two sets of experiments were carried out on different days there might be differences in the observed percentage of inhibition though the trends are similar. A comparison could not be made with C6(D)-LAA-AAPV since we did not have sufficient compound. In a separate study done earlier, the activity of C6(L)-LAA-AAPV and C6(D)-LAA-AAPV was compared with AAPV and it was observed that the activity of the conjugates was comparable to the tetrapeptide, at concentrations of 0.031, 0.062 and 0.125mM (Figure 3.31). A significant difference was not found in the inhibitory capacity of the tetrapeptide by itself as compared to the LAA conjugates at all experimental conditions.

(a)



(b)



(c)

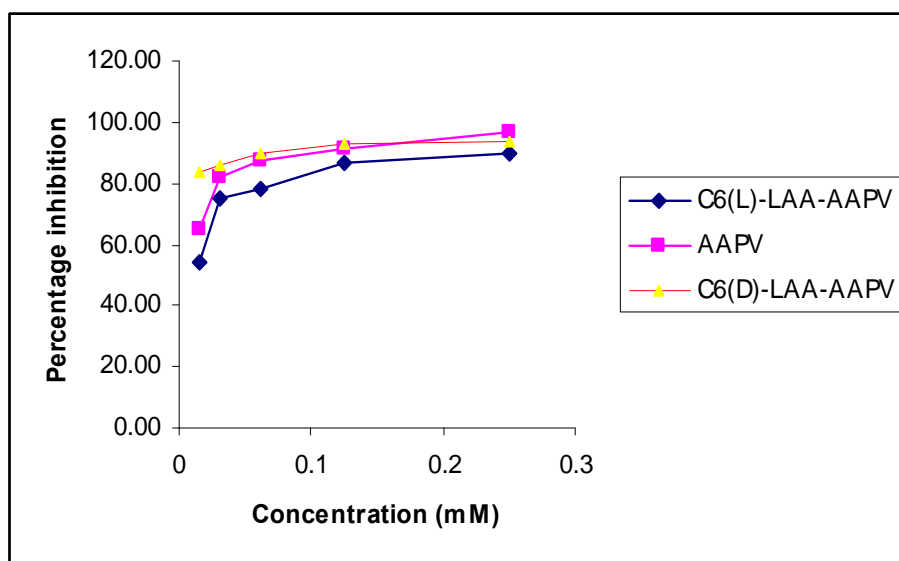


Figure 3. 31 Percent inhibition of elastase by tetrapeptide and its lipoamino acid conjugates. (a) and (C) inhibition at 6.25 $\mu\text{g}/\text{mL}$ of substrate and 0.25 U/mL elastase, (B) inhibition at 25 $\mu\text{g}/\text{mL}$ of substrate and 0.5 U/mL elastase

Peptidic HNE inhibitors have a common hydrophobic peptide sequence, which partially mimics certain amino acid sequences found in elastin. The Ala-Ala-Pro-Val sequence fits the P-P1 subsites of elastase and inhibits HNE competitively with K_i approx. 10^{-4} M. The covalent coupling of lipophilic moieties as long chain *cis* unsaturated fatty acids has been found to increase considerably the inhibitory capacity of the substance, in keeping with the presence of an unusual hydrophobic binding site in HNE located near its active centre.¹⁸⁶ In this project a series of lipopeptides of increasing lipophilic character were synthesized, keeping the peptide moiety (Ala-Ala-Pro-Val) constant and their HNE inhibitory capacity was then analysed. These lipidic peptides combine the physicochemical and biological properties of peptides and proteins with those of lipids and membranes and can also confer protection against enzyme degradation to biologically labile compounds and behave as bifunctional inhibitors.¹⁰⁸ It can be concluded from these elastase inhibition studies that the biological activity of the tetrapeptide is not affected considerably by lipoamino acid conjugation. Indeed the

activity of C10(D,L)-LAA-AAPV was approximately 4.5% higher than the tetrapeptide control but the difference was not statistically significant.

3.4 Conclusions

We have demonstrated that coupling of a tetrapeptide to a short chain LAA enhances its trans-epidermal delivery. The lipopeptide was present as a mixture of the D- and L-diastereomers of the LAA with greater sub-epidermal availability of the D-diastereomer. The stability of the LAA conjugates was found to be higher than the native tetrapeptide with only 20-25% degradation of the conjugates as compared to approximately 40% for the parent peptide. The transepidermal delivery of C6(D)-LAA-AAPV was found to be highest when the experiments were done using a donor concentration of 3 mg in 300 μ L propylene glycol and hydration period of 1 hour. On increasing the hydration period to 24h the flux and permeation rate of C8(D,L)-LAA-AAPV, in particular the C8(D) diastereomer was found to be highest. When the donor concentration was increased to 6 mg in 300 μ L propylene glycol and the hydration period was 24h, the permeability of the most lipophilic conjugate, C10(D,L)-LAA-AAPV was found to be highest. The permeability of this peptide up to 8 h was minimal and this lag time may be due to binding to the *stratum corneum* lipids. The amount of peptide remaining in the skin increased with the increase in carbon chain length that was chemically attached to the native tetrapeptide and C10(D,L)-LAA-AAPV was found to be present in the skin in highest amount. We hypothesize that the skin permeation enhancement with the LAA conjugates may be due to the increase in lipophilic nature of the conjugates. In addition, the interfacial properties conferred by the LAA-peptide structure may also contribute to their skin permeability (lowering of surface tension). The preliminary surface activity study indicated that the LAA conjugates decreased the surface tension indicating that the coupled peptides may have surfactant like properties which aids in skin permeation. Importantly, the elastase inhibition studies concluded that the biological activity was retained after coupling of the tetrapeptide to C6, C8 and C10 (D,L)- LAA.

In conclusion, we have shown that the stability and permeability of Ala-Ala-Pro-Val across the skin was improved by the chemical modification with lipoamino acids. This

chemical modification approach may be useful for the transdermal delivery of peptide drugs as well as the topical delivery of these drugs to the skin in the treatment of skin disorders such as psoriasis and dermatitis.

Chapter 4.

Trans-epidermal Permeation of a Cosmetic Peptide and its Lipoamino Acid Conjugate

4.1 Aim and Background

Wrinkles represent the more evident outcome of cutaneous ageing. Their onset is linked to a variety of events, among which are dermo-epidermal junction thinning due to decrease of laminine and loss of collagen.²²¹ Acetyl hexapeptide-3 (Ac-EEMQRR) is a six-amino-acid peptide derived from SNAP-25 that has been shown to produce the desired interference with the neurosecretion. Ac-EEMQRR is described as a mimic of botulinum neurotoxin (Botox), which functions by inhibiting neurotransmitter release, thus exerting muscle relaxing effects involved in defining facial wrinkles.²²² This hexapeptide is marketed under the name Argireline[®] (Lipotec, Barcelona, Spain). The objective of this study was to investigate the *in vitro* skin permeation of acetyl hexapeptide-3 and its C12 lipoamino acid conjugate. The cosmetic peptide was coupled to individual diastereomers of C12 (A)-LAA-hexapeptide-3 and C12 (B)-LAA-hexapeptide-3. This preliminary study was designed to assess the effect of coupling of a LAA of higher molecular weight on the transepidermal permeation and accumulation of this hexapeptide. Accumulation of these peptides in the skin was also quantified.

4.2 Materials and methods

4.2.1 Chemicals

Acetyl hexapeptide-3 (MW-889.99), C12(A)-LAA-Glu-Glu-Met-Gln-Arg-Arg (MW 1044.27) and C12(B)-LAA-Glu-Glu-Met-Gln-Arg-Arg (MW 1044.27) (Figure 4.1) were synthesised by Professor Toth's group at the University of Queensland (Brisbane, Australia). Propylene glycol (PG) was obtained from BDH Chemicals Pty Ltd. HPLC grade acetonitrile and methanol were used and all other chemicals were of analytical grade. Phosphate buffered saline solution (PBS) was prepared according to the United States Pharmacopoeia.

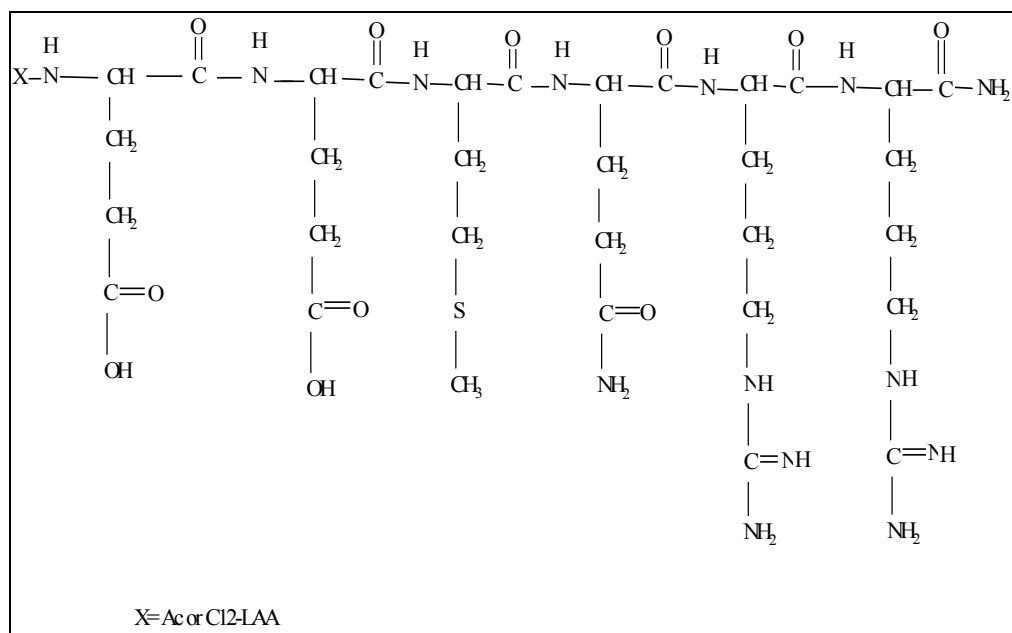


Figure 4.1 Chemical structure of acetyl hexapeptide-3 and C12-LAA conjugates

4.2.2 HPLC instrumentation and conditions

The samples were analysed by reverse phase HPLC (Agilent 1200 system) on a Grace Vydac C18 column (4.6 mm×250 mm) using a mobile phase gradient. Calibration curves of hexapeptide and its LAA conjugate in PBS were obtained to ensure consistency with samples from the *in vitro* permeation experiments. Buffer A was 0.1% TFA and buffer B was 0.1% TFA in 90% acetonitrile and 10% water. Elution was performed at a flow rate of 1.0 ml/min with the column temperature held at 25°C and the injection volume was 50 µL. The hexapeptide and its LAA conjugate were eluted using a combination of isocratic and linear gradient protocols; buffer B was held at 10% for 5 min followed by a linear gradient from 10 to 100% B over 10 min. Each sample analysed was automatically followed by a post-wash for 5 min. Absorbance was simultaneously monitored at 205, 210 and 214 nm using a photo diode array detector. All calculations were carried out in comparison with external standards using areas acquired at 214 nm.

4.2.3 HPLC analysis

4.2.3.1 Assay precision

Stock solutions were prepared by accurately weighing the peptides and dissolving in 75:25 propylene glycol: PBS. Working solutions of the three peptides were freshly prepared from their stock solutions.

- Working solution for C12(A)-LAA-hexapeptide-3 was prepared by a 1:5 dilution of the stock with PBS. Appropriate dilution of this working solution gave concentrations of 1.56 to 100 µg/mL.
- C12 (B)-LAA-hexapeptide-3 working solution was prepared by 1:20 dilution of the stock with PBS. Appropriate dilution of this working standard gave concentrations of 5.20 to 166.5 µg/mL.
- Acetyl hexapeptide-3 working solution was prepared by 1:20 dilution of the stock with PBS. Appropriate dilution of this working standard gave concentrations of 4.55 to 145.8 µg/mL.

The entire procedure was repeated on three different days to test inter-day variation and repeated six times at low and high concentrations to test intra-day variation. Volumes of 50 µL of the standards were used for the assay.

4.2.3.2 Minimum detectable limits and low limit of quantitation

The LOD and LOQ were measured by diluting C12(A)-LAA-hexapeptide-3, C12(B)-LAA-hexapeptide-3 and acetyl hexapeptide-3 in 75:25 PG:PBS to give a concentration range from 1.56 to 50 µg/mL, 5.20 to 166.5 µg/mL and 4.55 to 145.8 µg/mL respectively and then injected on the HPLC. The LOD was calculated by the following formula: $LOD = 3 \times \text{average height of noise} / \text{slope}$. The LOQ was calculated by the following formula: $LOQ = 10 \times \text{average height of noise} / \text{slope}$.

4.2.4 Preparation of human skin

Ethical approval was obtained from the Curtin University Human Research Ethics Committee (Approval numbers HR132/2001, HR 70/2007 and HR 129/2008) for the

collection and use of human skin obtained from abdominoplasties. The *in vitro* transdermal experiments for acetyl hexapeptide-3, C12(A)-LAA-hexapeptide-3 and C12(B)-LAA-hexapeptide-3 were performed by using heat separated human epidermis prepared following the method of Kligman and Christophers¹⁹⁸ as previously described.

4.2.5 In-vitro skin permeation of acetyl hexapeptide-3 and its lipoamino acid conjugate

Skin samples were allowed to thaw at room temperature. The epidermal membrane was mounted on a Franz-type diffusion cell (effective diffusion surface area approximately 1 cm² and receptor volume approximately 3 ml) with the *stratum corneum* layer facing the donor compartment. The receptor compartment was filled with 25:75 propylene glycol: PBS and allowed to equilibrate in a 35°C water bath with the receptor phase stirring continuously for approximately 1h before the addition of the peptide to the donor compartment. The donor compartment was loaded with 300 µL of propylene glycol and PBS mixture containing 2 mg peptide (acetyl hexapeptide-3 or lipoamino acid conjugated hexapeptide) and covered with Parafilm. These amounts were completely soluble at these concentrations. The apparatus was maintained at 35°C throughout the 48h duration of the experiment. Aliquots (200 µL) were taken from the receptor compartment at 0, 0.5, 1, 1.5, 2, 3, 4, 6, 8, 24 and 48 h then replaced immediately with 200 µL of receptor medium pre-equilibrated at 35°C. At the termination of the experiment samples were also taken from the donor compartment and analysed. Samples collected were kept at 4°C in the injecting tray while awaiting analysis by reverse phase HPLC.

4.2.6 Skin accumulation, mass balance and recovery of peptides from the skin

A suitable method for recovery of peptide remaining in the epidermal membrane at the conclusion of the experiment was developed and validated as follows. Human epidermal membranes were immersed in 2 mL of standard solution of peptides for 48h at 35°C. At the end of 48h, the skin samples were placed in 500 µL methanol in an Eppendorf tube and agitated for 2 min. The sample was then transferred to a second Eppendorf containing 500 µL methanol and agitated for another 2 min. The skin sample was then

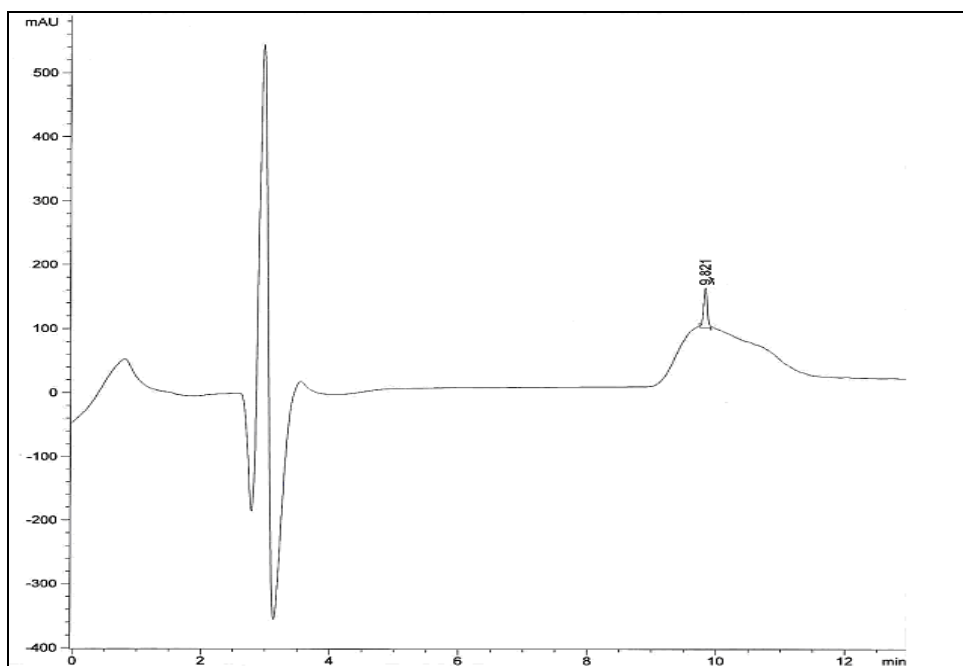
extracted with 1 mL 75:25 PG:PBS for 2 hours with agitation. After 2 hours the methanolic and PG: PBS extracts with skin were centrifuged at 10,000 RPM for 10 min. The supernatants were withdrawn and injected on HPLC to quantify the amount of peptides in the skin. For mass balance/recovery purposes, the donor solution was removed from the donor compartment and diluted appropriately to quantify the amount of peptide in the donor at the end of the experiment. The donor compartment with the skin was rinsed with 300 μ L PBS and the wash was collected. The receptor compartment was emptied and washed with 500 μ L PBS. Samples from both the washes were injected on HPLC to quantify the peptides present in the washes.

4.3 Results and discussion

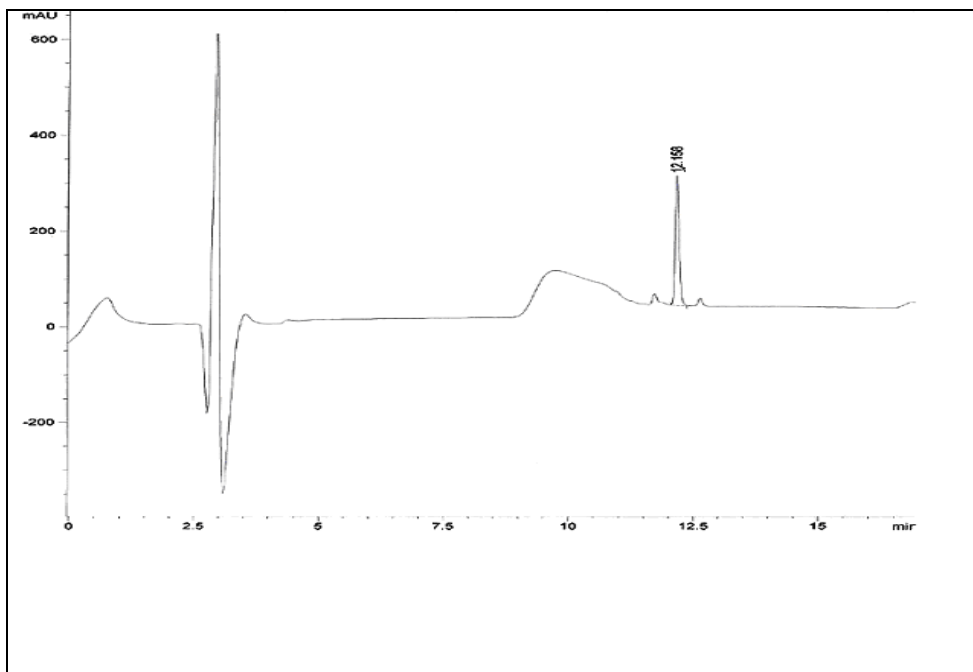
4.3.1 Chromatography and resolution

HPLC chromatograms of the parent hexapeptide and its lipoamino acid conjugates are shown in Figure 4.2. Good resolution of the peptides on the column was achieved with elution times of 9.82, 12.15 and 13.23 mins for acetyl hexapeptide-3, C12(A)-LAA-hexapeptide-3 and C12(B)-LAA-hexapeptide-3 respectively.

(a)



(b)



(c)

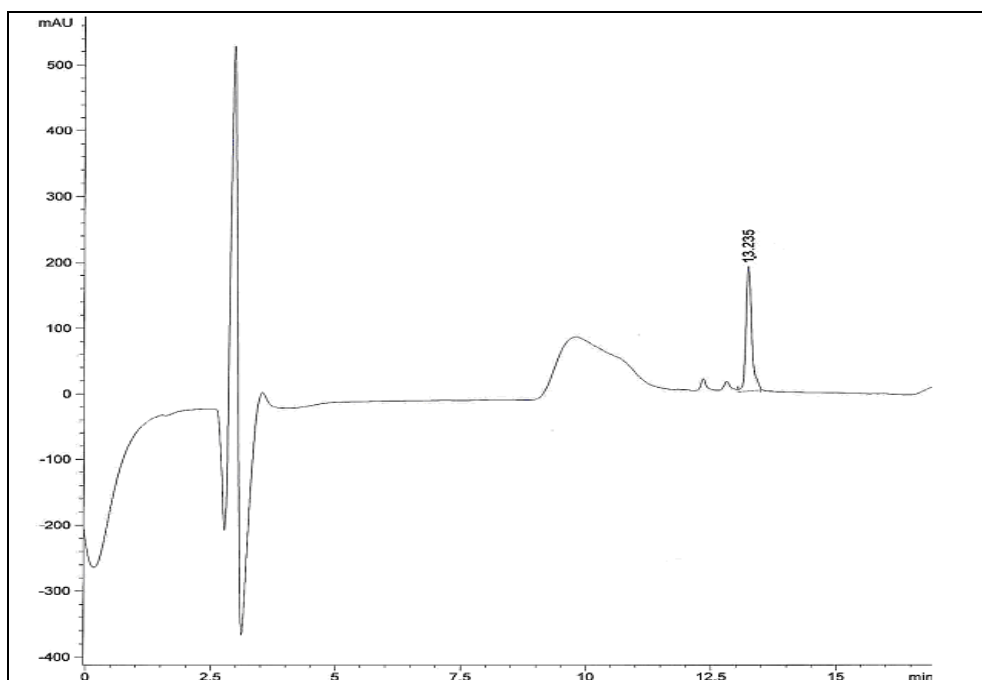


Figure 4.2 Typical chromatograms of (a) acetyl hexapeptide-3 (10.4 $\mu\text{g/mL}$ in PBS) eluted at 9.8 min (b) C12(A)-LAA-hexapeptide-3 (83.3 $\mu\text{g/mL}$ in PBS) eluted at 12.1 min and (c) C12(B)-LAA-hexapeptide-3 (83.3 $\mu\text{g/mL}$ in PBS) eluted at 13.2 min

4.3.1.1 Linearity

Excellent linearity was obtained for all the three peptides over the concentration range studied (Table 4-1).

Table 4-1 Correlation coefficients of the native peptide and its lipoamino acid conjugates

Peptide	Correlation coefficient (r^2)	Linear range ($\mu\text{g/mL}$)
Acetyl hexapeptide-3	0.9999	4.55-145.8
C12(A)-LAA-hexapeptide-3	0.9997	1.56-100
C12(B)-LAA-hexapeptide-3	0.9999	5.20-166.5

4.3.1.2 Assay precision

Calibration graphs were constructed by plotting the peak area versus concentration of standards injected. The best-fit straight lines were determined using the method of least squares. All plots passed through the origin. To obtain a satisfactory UV response for all peptides, the detection wavelength was selected at 214 nm. The intra-day and inter-day precision of the assay are summarised in Table 4-2. Intra and inter day coefficients of variation (C.V.) of the assay for the three peptides were below 5%

Table 4-2 Intra-day and Inter-day variations of acetyl hexapeptide-3 and its lipoamino acid conjugates

Peptide	Intra-day variation (n=5)		Inter-day variation (n=9)	
Acetyl hexapeptide-3	4.55 µg/mL	72.91 µg/mL	4.55 µg/mL	72.91 µg/mL
C.V.(%)	1.24	0.84	1.57	1.11
C12(A)-LAA-hexapeptide-3	3.125 µg/mL	50 µg/mL	3.125 µg/mL	50 µg/mL
C.V. (%)	1.80	0.13	2.38	0.52
C12(B)-LAA-hexapeptide-3	10.40 µg/mL	83.25 µg/mL	10.40 µg/mL	83.25µg/mL
C.V. (%)	1.04	0.85	0.95	0.83

4.3.1.3 LOD and LOQ

The LOD calculated as greater than 3 times the baseline noise in the assay was 25 ng for acetyl hexapeptide-3, 31 ng for C12(A)-LAA-hexapeptide-3 and 44.80 ng for C12 (B)-LAA-hexapeptide-3. The LOQ calculated as greater than 10 times the baseline noise in the assay was 83ng for acetyl hexapeptide-3, 103.6 ng for C12(A)-LAA-hexapeptide-3 and 149 ng for C12 (B)-LAA-hexapeptide-3.

4.3.2 Permeation of acetyl hexapeptide-3, C12(A) and C12(B) conjugated hexapeptide across human epidermis

In this study, the effect of lipoamino acid (C12-LAA) conjugation on the skin permeation of acetyl hexapeptide-3 was studied. The cumulative amount of acetyl hexapeptide-3 penetrating the human epidermis to the receptor solution over time is demonstrated in Figure 4.3.

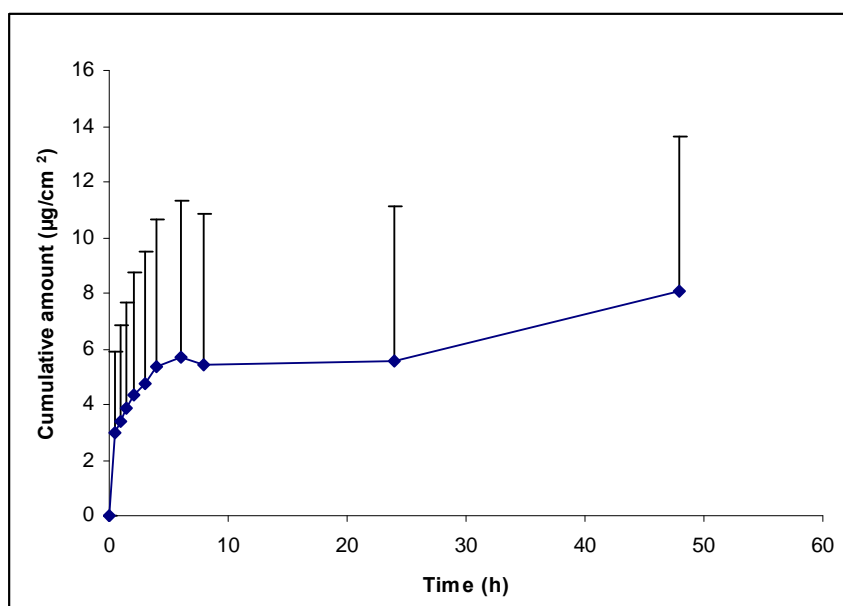


Figure 4.3 Permeation profile of acetyl hexapeptide-3 (donor concentration of 2mg in 300µL propylene glycol) across human epidermis. Results are expressed as mean (\pm SEM; n=5)

No skin permeation was observed for the C12(A) and C12(B) lipoamino acid conjugates. The maximum cumulative amount of acetyl hexapeptide-3 in the receptor was 8 $\mu\text{g}/\text{cm}^2$ after 48 h and there was considerable variability between cells. The estimated transdermal flux was calculated using equation 2 (Section 3.3.3.2) as $2.5 \times 10^{-4} \mu\text{g}/\text{cm}^2/\text{h}$. The estimated permeability coefficient for acetyl hexapeptide-3 was $1.26 \times 10^{-7} \text{ cm}/\text{h}$. The lack of permeation of the conjugates may be due to the chain length of the lipoamino acid attached to the peptide. The molecular weight of hexapeptide-3 is 889 and it increases to 1044.27 with the addition of a C12 lipoamino acid chain. The high molecular weight of the conjugated peptides may be one of the

reasons for its poor transepidermal delivery. In addition, the low permeability of higher lipophilic derivatives of acetyl hexapeptide may be due to its strong partitioning into and binding to the *stratum corneum*. Yamamoto *et al* investigated the skin permeation and distribution of fatty acid conjugates of Phe-Gly and observed that the epidermal diffusion of C8-Phe-Gly was very low as compared to C4 and C6-Phe-Gly but the amount of C8-Phe-Gly in the skin was much higher than the native Phe-Gly and the other acyl derivatives. We can thus speculate from these findings that there is an optimal lipophilicity (length of acyl chain) of the acyl derivatives for improving their transdermal delivery. It may be that the optimal chain length is dependent on balancing desired lipophilicity with not markedly increasing molecular weight.¹⁵³

4.3.3 Recovery and skin extraction of acetyl hexapeptide-3 and C12-LAA from the epidermis

Figure 4.4 indicates the amounts of native hexapeptide and its lipoamino acid conjugates in the skin after the permeation experiments. Native acetyl hexapeptide-3, C12(A)-LAA-hexapeptide-3 and C12(B)-LAA-hexapeptide-3 were recovered from the epidermis at the end of the experiment. The epidermal extraction procedure was validated and the recovery of acetyl hexapeptide-3, C12(A)-LAA-hexapeptide-3 and C12(B)-LAA-hexapeptide-3 was 96%, 93% and 94% respectively.

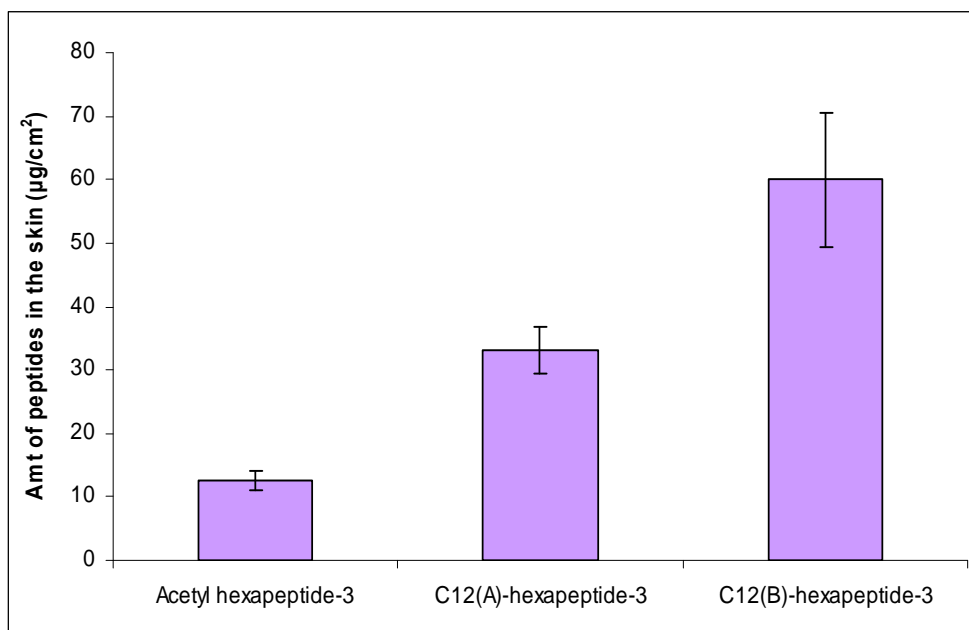


Figure 4.4 Amount of native peptide and conjugates remaining in epidermal membrane at 48 h

The results indicate that the amount of C12(B)-LAA-hexapeptide-3 ($59.92 \mu\text{g}/\text{cm}^2 \pm 10.64$) was found to be highest in the skin followed by C12(A)-LAA-hexapeptide-3 ($33.06 \mu\text{g}/\text{cm}^2 \pm 3.70$) and acetyl hexapeptide-3 ($12.64 \mu\text{g}/\text{cm}^2 \pm 1.48$). This peptide accumulation data suggests that there is a strong interaction between the lip amino acid conjugates of the hexapeptide and lipidic bilayers of the skin as previously described by Schuetz *et al.*²¹⁵ Thus of the applied amount of each compound 2.99% of C12(B)-LAA-hexapeptide-3, 1.65% of C12(A)-LAA-hexapeptide-3 and 0.63% of acetyl hexapeptide-3 permeated into and remained in the epidermis over 48h.

To increase the transepidermal delivery of acetyl hexapeptide-3, C12-LAA was conjugated to the parent peptide. Drug delivery is always a delicate balance between adequate lipophilicity to cross lipid bilayers and water solubility to aid in formulation. An important challenge though, is delivery into skin because peptides are poorly penetrating, especially as the number of amino acid residues increases.²²² Because human skin functions as a physicochemical barrier, it has been historically assumed that molecules over 500 MW are unable to traverse the *stratum corneum*²²³ and this is further compounded if the molecule is polar in nature. An approach to this problem of poor

epidermal delivery is the addition of a lipophilic chain (eg, palmitate), which can increase skin penetration several fold over the underivatized peptide.²²⁴ However in our study, coupling of the peptide with individual diastereomers of C12-LAA-hexapeptide-3 did not increase their permeation across the human epidermis. Due to availability of limited quantity of peptides (only 18 mg of each was supplied) we were not able to assess the effect of donor concentration, skin hydration and other formulation parameters on the transdermal delivery of these compounds. The skin diffusion of acetyl hexapeptide-3 was found to be fairly low which may be due to the donor concentration used in the study. A study recently published in the International Journal of Cosmetic Science reported that acetyl hexapeptide-3 at a 10% concentration reduces the depth of wrinkles. Skin topography analysis was performed to determine the effectiveness of an O/W emulsion containing 10% acetyl hexapeptide-3 using silicon imprints from the lateral preorbital area in healthy women volunteers. A concentration of 10% acetyl hexapeptide-3 caused a 30% reduction in wrinkle depth in the lateral preorbital area of healthy human volunteers *in vivo* when applied topically.²²⁵ *In vitro* skin permeation of the peptide was also evaluated. It was reported that 30% of the applied amount was found in the receptor compartment but cumulative amount or transdermal flux have not been stated. This makes comparison with the present study difficult but it clearly indicates that higher amount of acetyl hexapeptide-3 was found traversing the skin which may be due to a higher applied concentration of the peptide. In the current study a donor concentration of 2 mg hexapeptide-3 and its lipoamino acid conjugates was used which is approximately 30 times less than the dose used by Blanes-Mira *et al.* This data is a preliminary indication of the effect lipoamino acid conjugation has on the transdermal delivery of acetyl hexapeptide-3. Even though, there was negligible permeation of the conjugates through the epidermis, C12-LAA-hexapeptide-3 retained in the skin was higher than acetyl hexapeptide-3. The amount in the skin was highest for C12(B)-LAA-hexapeptide-3 followed by C12(A)-LAA-hexapeptide-3 and the native hexapeptide. The poor permeation of the lipoamino acid conjugates may be attributed to its lipophilicity and chain length as discussed in earlier sections 3.3.3.4 and 3.3.3.5. Drugs with higher molecular weight are poor candidates for delivery by transdermal route. However, for topical drug delivery, accumulation of drug in the skin with minimal

permeation is desired. The target site for these peptides is the dermo-epidermal junction.¹⁹¹ Hence, drugs with moderate and low permeability can also be considered for topical use. Unlike transdermal delivery, an optimal accumulation in the skin with little or no flux through the skin to systemic uptake is desirable.

Koda *et al* reported a similar finding with C8 lipophilic chain conjugates of endomorphin.¹⁵⁹ An increase in apparent permeability of endomorphin was observed for N-terminus analogues bearing shorter LAA (C8 and C10) but the higher molecular weight of C12-LAA resulted in poor permeation across the human epidermis. A similar result was also observed for acyl tetragastrins where the permeation of tetragastrin across the intact skin was improved by chemical modification with acetic acid and butyric acid. However, caproyl-tetragastrin did not permeate across the intact skin up to the end of the experiment and a bell shaped profile between the permeability of acyl tetragastrins was observed.¹⁶⁴ We therefore speculate that similar to our previous study on AAPV, the permeability of C12-LAA- Glu-Glu-Met-Gln-Arg-Arg through human epidermis may be inhibited due to its high binding characteristics to the lipidic *stratum corneum* region. The higher lipophilicity of the conjugate and the effect of conjugation of lower chain length LAAs such C6 and C8 should be investigated.

4.4 Conclusions

In summary we demonstrated that the epidermal permeation of acetyl hexapeptide-3 was low. Detectable amounts of C12(A)-LAA-hexapeptide-3 and C12(B)-LAA-hexapeptide-3 were not found in the receptor solution but higher quantities of these conjugates were found to be retained in the skin. The amount of C12(B)-LAA-hexapeptide-3 in the epidermis was highest followed by C12(A)-LAA-hexapeptide-3 and acetyl hexapeptide-3. This might be due to higher lipophilicity of these conjugated peptides due to the longer chain length. Thus, chemical modification approach may be more useful for small peptides with fewer amino acid residues or by conjugating peptides to smaller chain length lipoamino acids.

Chapter 5.

Skin Permeation of an Anti-inflammatory Peptide and Analogues Exhibiting Improved Biological Efficacy and Specificity

5.1 Aim

Peptides hold considerable promise in the management of dermatological conditions if they can be delivered in active form to their target sites within the skin. Peptides consist of chains of amino acids which can be modified to increase receptor binding, increase specificity, decrease toxicity and increase skin penetration, stability and solubility. Technological advances have created newer peptides capable of targeting many aspects of dermal health.²²⁰ Psoriasis and contact dermatitis are skin disorders that are characterized by long-term inflammation. These disorders are commonly treated with topical corticosteroids that target a variety of pathways of the inflammation cascade.¹⁸⁹ However corticosteroid therapy is associated with local side effects and there is a need for new therapies and delivery systems to overcome some of the limitations imposed by chronic steroid therapy. The purpose of this study was to evaluate the skin permeability and in skin stability of an anti-inflammatory peptide (core peptide: CP) and two analogues that have demonstrated improved biological efficacy and specificity: a cyclic peptide sequence (C1) and its linear sequence counterpart (C1-L).

5.2 Materials and methods

5.2.1 Chemicals

Core peptide, CP (MW 1024), linear sequence of C1 (MW 1137) and cyclic peptide, C1 (MW 1119) sequences (Table 5-1) were synthesized by Dr Marina Ali from Associate Professor Manolios' group at Westmead Hospital, Sydney. Dimethyl sulphoxide (DMSO) was obtained from Ajax FineChem Pvt Ltd. HPLC grade acetonitrile and methanol was used and all other chemicals were of analytical grade. Phosphate buffered saline solution (PBS) was prepared according to the United States Pharmacopoeia.

Table 5-1 Peptide sequences and code

Sequence	Name	Code
L _D RL _D LL _D LL _D KV _D G	Cyclic peptide 1	CP1 or C1
L _D RL _D LL _D LL _D KV _D G	Linear sequence of C1	CP1-L or C1-L
GLRILLKLV	Core peptide	CP

5.2.2 HPLC instrumentation and conditions

The samples were analysed by reverse phase HPLC (Agilent 1200 system) on a Grace Vydac C18 column (4.6 mm×250 mm) using a mobile phase gradient and assay conditions were modified from an assay provided by Associate Professor Manolios' group. Calibration curves of CP, C1 and C1-L in PBS were obtained to ensure consistency with samples from the *in vitro* permeation experiments. Solvent A was 0.1% TFA, and solvent B was 0.1% TFA in acetonitrile. Elution was performed at a flow rate of 1.0 ml/min with the column temperature held at 25°C and the injection volume was 50 µL. The core peptide and its analogues were eluted using a combination of isocratic and linear gradient protocol; buffer B was held at 2.5 % for 2.5 min followed by a linear gradient from 2.5 to 60% B over 23.5 min. Each sample analysed was automatically followed by a post-wash for 5 min. Absorbance was simultaneously monitored at 210 and 220 nm using a photo diode array detector. All calculations were carried out in comparison with external standards using areas acquired at 220 nm.

5.2.3 HPLC analysis

5.2.3.1 Assay precision

Stock solutions were prepared by accurately weighing the peptides and dissolving in DMSO. Working solutions of the three peptides were freshly prepared from their stock solutions.

- Working solution for C1 was prepared by serially diluting the stock with PBS. Appropriate dilution of this working solution gave concentrations of 1.90 to 121.86 µg/mL.

- For C1-L working solution was prepared by serial dilution of the stock with PBS. Appropriate dilution of this working standard gave concentrations of 4 to 129 µg/mL.
- A core peptide working solution was prepared by serial dilution of the stock with PBS. Appropriate dilution of this working standard gave concentrations of 3.90 to 125 µg/mL

Calibration curves were obtained using these concentration ranges and linearity (quoted as R^2) was evaluated by linear regression analysis, which was calculated by the least square regression method. The precision of the assay was determined by injecting two standard concentrations (7.61 and 60.93 µg/mL C1, 8 and 64.5 µg/mL C1-L, 7.8 and 62.5 µg/mL CP) five times on the HPLC column. The intra-day repeatability was assessed by injecting the same standards six times at different times in a day. The inter-day repeatability was determined by injecting the same standards six times on 3 different days. The intra- and inter-day repeatability was quoted as the coefficient of variance.

5.2.3.2 Lower limit of detection (LOD) and quantitation (LOQ)

The minimum detectable and quantifiable limits (LOD and LOQ) were measured by diluting the stock solutions of C1, C1-L and core peptide in PBS to give a concentration range from 1.90 to 121.86 µg/mL, 4 to 129 µg/mL and 3.90 to 125 µg/mL respectively and then injected on the HPLC. The LOD was calculated as greater than 3 times the baseline noise level: $LOD = 3 \times \text{average peak height of noise} / \text{slope}$. The LOQ was calculated as 10 times the baseline noise level: $LOQ = 10 \times \text{average peak height of noise} / \text{slope}$

5.2.4 Skin stability study

The influence of human skin on the stability of the cyclised and core peptide was determined by placing the skin in a vial containing peptide solutions to provide an estimate of their stability during the skin diffusion experiments. Vials containing 2 mL of 100 µg/mL C1, C1-L and CP solutions were stored at 37°C. Samples (150 µL) were withdrawn at 0, 2, 4, 6, 8, 24 and 48h. The samples were analysed by HPLC to quantify

the amount of peptide remaining at the end of each test period. The results were expressed as the percentage of active peptide at the end of the test period and were calculated as follows:

$$\text{Intact peptide} = \frac{\text{Final amount of peptide}}{\text{Initial amount of peptide}} \times 100\%$$

5.2.5 Preparation of human skin

Full thickness human skin samples excised from female patients undergoing abdominoplasty at Perth hospitals were refrigerated immediately after surgery (42 and 50 year old female abdominal section was used in this study). Sampling was approved by the Human Research Ethics Committee of Curtin University (Approval numbers HR132/2001, HR 70/2007 and HR 129/2008) and was conducted in compliance with the guidelines of the National Health and Medical Research Council of Australia. Epidermal sheets were prepared and stored as previously described.

5.2.6 Formulation optimization

An appropriate amount of each of the three peptides was dissolved in 100% DMSO, 100% propylene glycol (PG) and 75:25 DMSO:PBS to test solubility in these solvents. In the biological efficacy studies conducted by the Manolios group, peptides were initially dissolved in 100% DMSO and then diluted to working concentrations due to the good solubility of the peptides in DMSO. Based on the solubility of the peptides in the different solvents, it was decided to use 100% DMSO as the donor vehicle. Solutions of peptides in 100% PG or 75:25 DMSO:PBS were cloudy in appearance with undissolved compound still present in solution. It was decided to use 90:10 PBS: DMSO as the receptor medium to aid in the solubility of the peptides in the receptor compartment and prevent salting out.

5.2.7 *In-vitro skin diffusion of C1, C1-L and CP*

Skin samples were allowed to thaw at room temperature. The heat separated epidermal membrane was mounted on a Franz-type diffusion cell (effective diffusion surface area approximately 1 cm² and receptor volume approximately 3 ml) with the *stratum corneum* facing the donor compartment. The receptor compartment was filled with 90:10 DMSO: PBS and allowed to equilibrate in a 35°C water bath with the receptor phase stirring continuously for approximately 24h before the addition of the peptide to the donor compartment. The conductivity across the epidermis was measured using a digital multimeter to determine membrane integrity. The donor compartment was loaded with 300 µL of 3 mg peptide (C1, C1-L and CP) and sealed. These amounts were completely soluble at these concentrations. The apparatus was maintained at 35°C throughout the duration (48h or 6 days) of the experiment. The duration of experiment was varied to assess the effect of time on skin permeation. Aliquots (200 µL) were taken from the receptor compartment at 0, 0.5, 1, 1.5, 2, 3, 4, 6, 8, 24 and 48 h or 6 days then replaced immediately with 200 µL of receptor medium pre-equilibrated at 35°C. At the termination of the experiment samples were also taken from the donor compartment and peptide content in all samples analysed. Samples collected were kept at 4°C in the injecting tray while awaiting analysis by reverse phase HPLC.

5.2.8 *Recovery of the peptides from the epidermis*

Human epidermal membranes were immersed in 2 mL of standard solution of peptides for 48h at 35°C. At the end of 48h, the skin samples were placed in 500 µL methanol in an Eppendorf tube and agitated for 2 mins. The sample was then transferred to a second Eppendorf containing 500 µL methanol and agitated for another 2 min. The skin sample was then extracted with 500 µL 75:25 DMSO: PBS for 2 hours with agitation. After 2 hours the methanolic and DMSO: PBS extracts with skin were centrifuged at 10,000 RPM for 10 mins. The supernatants were withdrawn, diluted appropriately and injected on HPLC to quantify the amount of peptides in the skin. This procedure was validated to determine the % recovery of peptide from the epidermal membrane.

For mass balance/recovery purposes, the donor solution was removed from the donor compartment and diluted appropriately to quantify the amount of peptide in the donor at the end of the experiment. The donor compartment with the skin was rinsed with 300 μ L PBS and the wash was collected. The receptor compartment was emptied and washed with 500 μ L PBS. Samples from both the washes were injected on HPLC to quantify the peptides present in the washes.

5.2.9 Statistical analysis

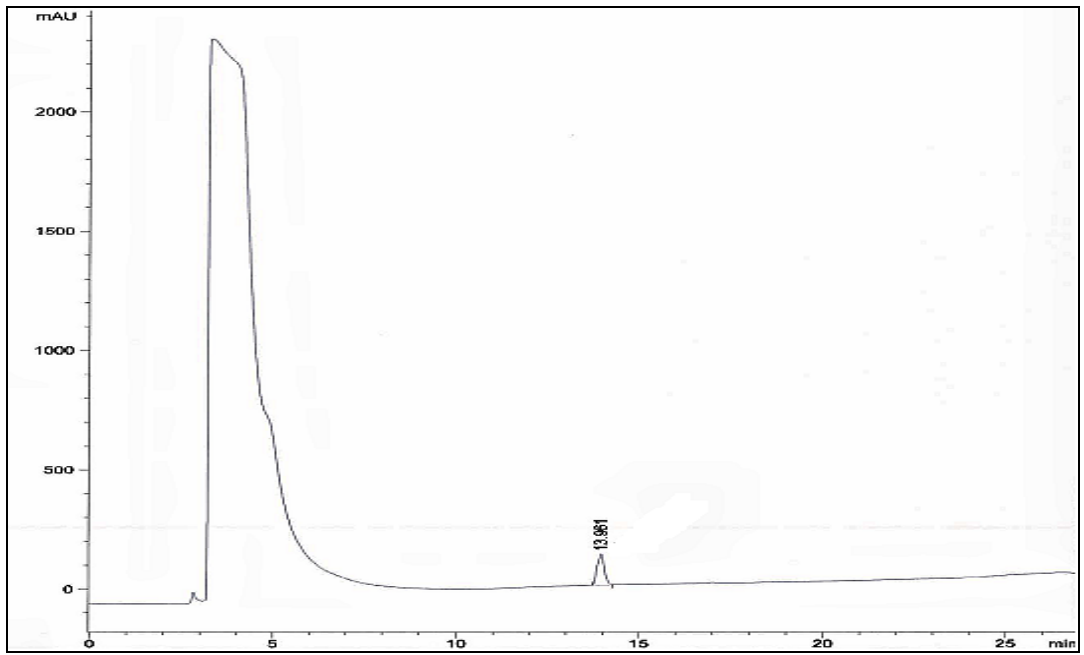
Differences between the permeation and stability of CP, C1 and C1-L were analysed for statistical significance ($p < 0.05$) using an Analysis of Variance (ANOVA) at each of the prescribed time points. The ANOVA model was implemented using the GENMOD procedure in the SAS software system, with the control group being the reference group in each model. Because of the skewness in the concentrations, the regression model was applied to the log-transformed data (in order to obtain the p-values for comparison of treatments). The overall p-values were found to be significant for most of the comparisons.

5.3 Results and discussion

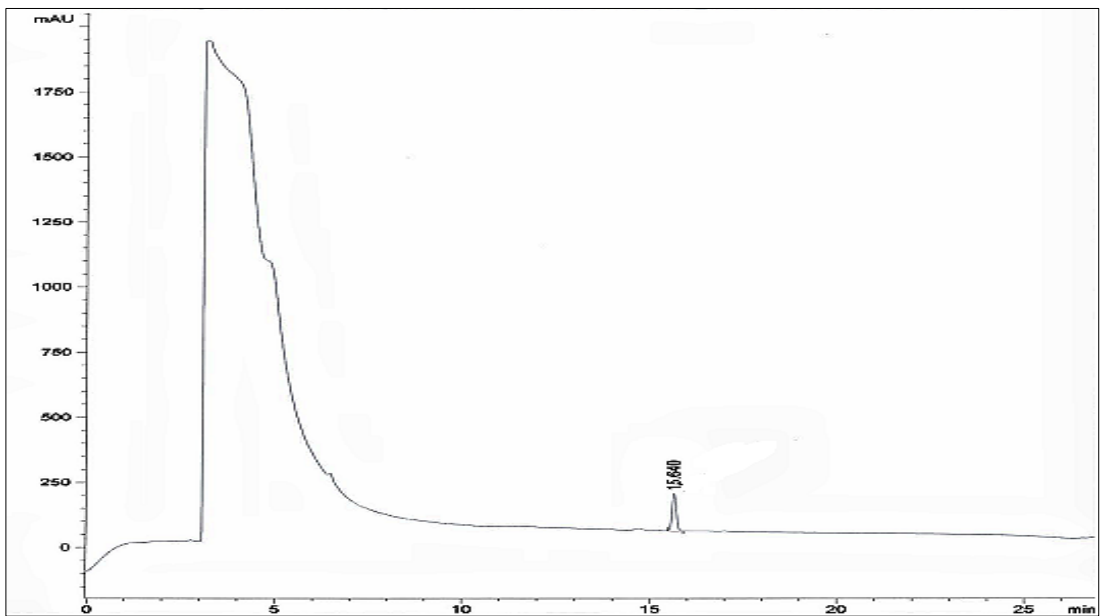
5.3.1 Chromatography

HPLC chromatograms of C1, C1-L and CP are shown in Figure 5.1. Good resolution of the peptides on the column was achieved and they eluted without any interfering peaks at 19.18, 15.64 and 13.9 mins for C1, C1-L and CP respectively.

(a)



(b)



(c)

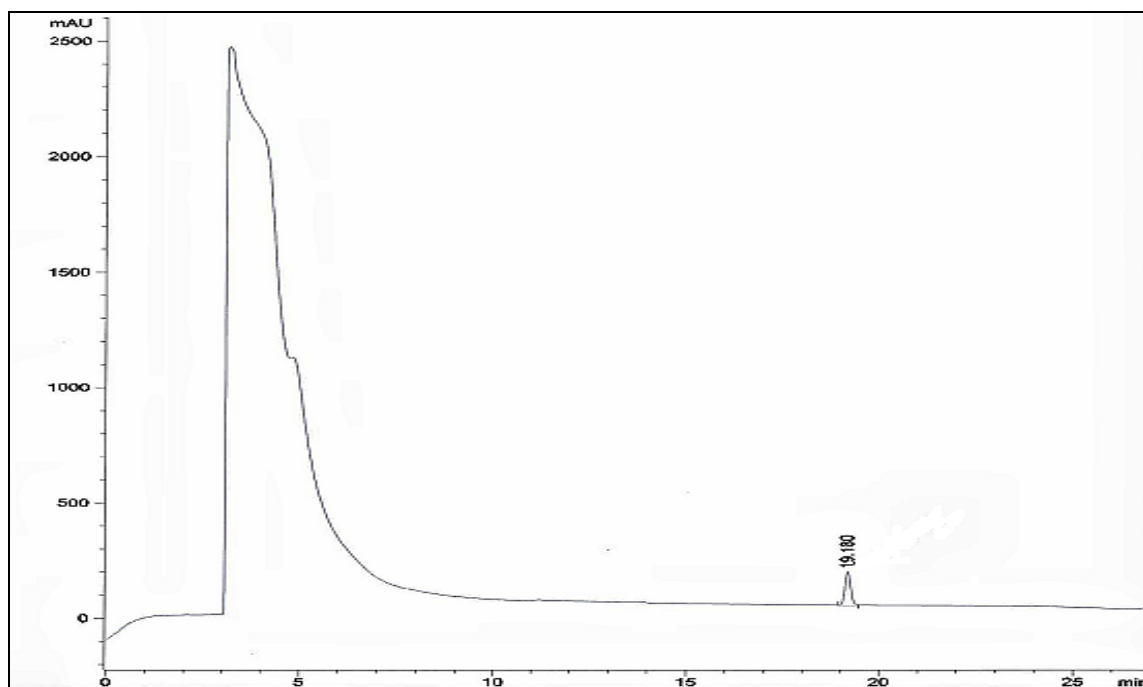


Figure 5.1 Chromatograms for (a) CP at 62.5 $\mu\text{g/mL}$, (b) C1-L at 64.5 $\mu\text{g/mL}$ and (c) C1 at 60.93 $\mu\text{g/mL}$

5.3.1.1 Linearity

A calibration curve was obtained by plotting the peak area versus concentration of standards injected. The best-fit straight lines were determined using the method of least squares. All plots passed through the origin. To obtain a satisfactory UV response for all peptides, the detection wavelength was selected at 220 nm. Table 5-2 reports the results for calibration curve linearity. Excellent linearity was obtained for all three peptides over the concentration range studied.

Table 5-2 Correlation coefficient of C1, C1-L and CP

Peptide	Correlation coefficient (r^2)	Linear range($\mu\text{g/mL}$)
C1	0.9991	1.90-121.86
C1-L	1.000	4-129
CP	0.9998	3.90-125

5.3.1.2 Assay precision

The coefficient of variation (CV) for precision was determined from the relative standard deviation ($n = 5$). The intra-day and inter-day precisions of the assay are summarised in Table 5-3. Intra and inter day coefficients of variation (C.V.) of the assay for the three peptides were below 5%

Table 5-3 Assay precision, Intra-day and Inter-day variations of C1, C1-L and CP

Peptide	Precision (n=5)		Intra-day variation (n=5)		Inter-day variation (n=9)	
	7.61 $\mu\text{g/mL}$	60.93 $\mu\text{g/mL}$	7.61 $\mu\text{g/mL}$	60.93 $\mu\text{g/mL}$	7.61 $\mu\text{g/mL}$	60.93 $\mu\text{g/mL}$
C1 C.V.(%)	0.82	0.94	1.93	1.83	2.0	1.83
	8 $\mu\text{g/mL}$	64.5 $\mu\text{g/mL}$	8 $\mu\text{g/mL}$	64.5 $\mu\text{g/mL}$	8 $\mu\text{g/mL}$	64.5 $\mu\text{g/mL}$
C1-L C.V. (%)	2.91	1.30	2.91	1.12	4.80	1.26
	7.8 $\mu\text{g/mL}$	62.5 $\mu\text{g/mL}$	7.8 $\mu\text{g/mL}$	62.5 $\mu\text{g/mL}$	7.8 $\mu\text{g/mL}$	62.5 $\mu\text{g/mL}$
CP C.V. (%)	1.86	1.24	2.39	3.89	1.89	1.18

5.3.1.3 Low limit of detection and low limit of quantitation

The LOD calculated as greater than 3 times the baseline noise in the assay was 240 ng C1, 270 ng for C1-L and 210 ng for CP. The LOQ calculated as greater than 10 times the baseline noise in the assay were 800 ng for C1, 930 ng for C1-L and 710 ng for CP.

5.3.2 Stability of C1, C1-L and CP

The degradation profile of C1, C1-L and CP is shown in Figure 5.2. The stability data was presented as the percentage of active peptide remaining over time when placed in contact with skin at 37°C. It was observed that when epidermal membrane was placed in a vial containing CP solution at 37°C about 75% of the peptide was lost in 8h and 80% in 24 h compared to 23 and 58% loss of C1-L in 8 and 24h and 30 and 50% loss of C1 in 8 and 24h (Figure 5.2). C1 and C1-L had significantly higher stability as compared to CP when incubated with skin at 37°C ($p < 0.001$ at 8h and $p < 0.05$ at 24h for C1 and C1L).

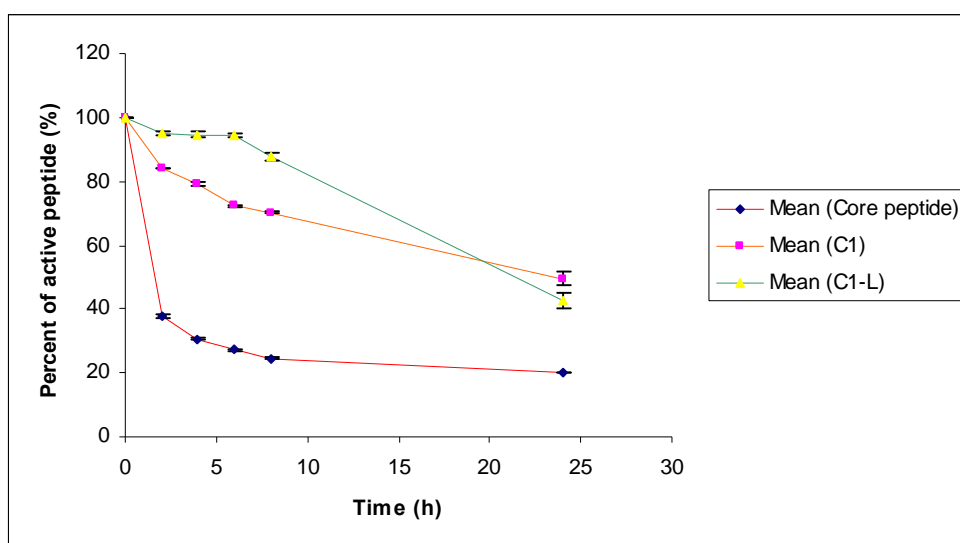


Figure 5.2 Degradation profiles of CP, C1 and C1-L

The amount of peptide remaining intact at the end of 24h was higher in the skin diffusion studies as compared to the stability study. One of the reasons may be because the samples in the permeation studies were collected from the receptor compartment

which has a lower concentration of the peptide and is affected by the skin permeability of the peptide.

Cyclisation of a peptide is a strategy often employed to enhance stability. For example, Kampi *et al* studied the solution stability of linear (Arg-Gly-Asp-Phe-OH; 1) versus cyclic (cyclo-(1,6)-Ac-Cys-Arg-Gly-Asp-Phe-Pen-NH₂; 2) RGD (Arg-Gly-Asp) peptides and found that the cyclic peptide 2 was 30-fold more stable than the linear peptide 1 at pH 7. The increase in stability of the cyclic peptide 2 compared to linear peptide 1, especially at neutral pH, may be due to decreased structural flexibility imposed by the ring.²²⁶ In another study, the cellular permeation, chemical and enzymatic stability of phenylpropionic acid-based cyclic prodrugs of opioid peptides [Leu⁵]-enkephalin (H-Tyr-Gly-Gly-Phe-Leu-OH) and DADLE (H-Tyr-D-Ala-Gly-Phe-D-Leu-OH) were investigated. When applied to the apical side of a Caco-2 cell monolayer both the cyclic prodrug and DADLE exhibited significantly greater stability against peptidase metabolism than [Leu⁵]-enkephalin.²²⁷ Cyclization can thus be used to synthesize more stable peptide analogues that mimic the biological activity of natural peptide structures, resulting in enhanced conformational stability when compared to their natural counterparts.²²⁸

5.3.3 In-vitro permeation of C1, C1-L and CP across human epidermis

The cumulative amount of C1, C1-L and CP penetrating the human epidermis to the receptor solution over 48h is demonstrated in Figure 5.3. The duration of the experiment was varied (48h and 6 days) to assess the effect of time on in-vitro diffusion of the peptides across the epidermis. The use of DMSO as donor vehicle is not ideal as it is capable of interacting with the skin to reduce the barrier properties. However with very limited compound and poor solubility of the peptides in aqueous vehicle, it was decided to use DMSO as the solvent.

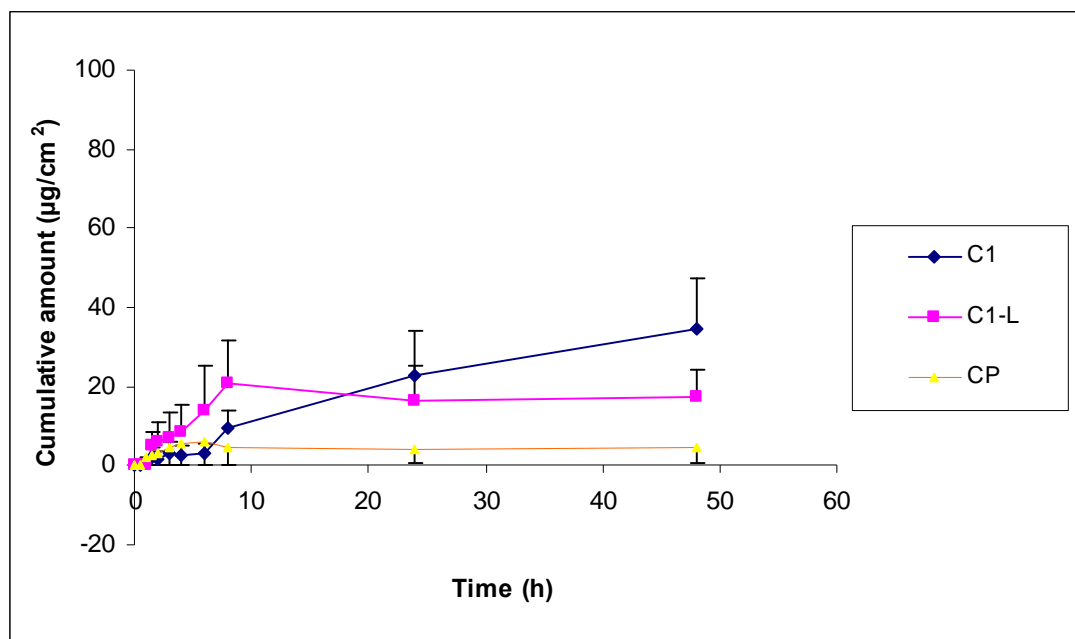


Figure 5.3 Permeation profiles for individual C1, C1-L and CP across human epidermis from 0-48h. Results are expressed as mean (\pm SEM: n=6 for C1, n=4 for C1-L and n=6 for CP)

The results indicated an increase in the amount and rate of permeation of C1 over 48h (Table 5-4). C1 and C1-L permeation was significantly increased compared to permeation of CP over the time period of the experiment ($p < 0.0001$ for C1 and $p < 0.05$ for C1-L) over 48h. The permeation of C1 was slow but a significant increase was observed at the 24 ($p < 0.05$) and 48h ($p < 0.0001$) time periods. On the other hand, the *in-vitro* diffusion of C1-L was more rapid initially but there was no substantial increase in the permeation after 8h. The estimated transdermal flux was $2.15 \mu\text{g}/\text{cm}^2/\text{h}$ for C1, $1.07 \mu\text{g}/\text{cm}^2/\text{h}$ for C1-L and $0.29 \mu\text{g}/\text{cm}^2/\text{h}$ for CP. The estimated permeability coefficient for C1 was $7.1 \times 10^{-4} \text{ cm}/\text{h}$, $3.5 \times 10^{-4} \text{ cm}/\text{h}$ for C1-L and $9.8 \times 10^{-5} \text{ cm}/\text{h}$ for CP. Based on the mean cumulative permeation graph the area under the curve (AUC, Sigma Plot 8.0) was calculated. AUC of the cumulative amount of C1, C1-L and CP in the receptor compartment verses time graph yielded values of 966.02, 779.41 and 212.90 $\mu\text{g}/\text{cm}^2/\text{h}$ for C1, C1-L and CP respectively. It was thus observed that there was an approximately 7.2-fold enhancement in the delivery of cyclic peptide as compared to the core peptide and 3.6 fold enhancement in the linear peptide as compared to the core peptide based on

the mean cumulative permeation over 48h . The skin permeation was affected by the stability of the parent peptide and the type of the analogue.

Table 5-4 Comparison of permeation parameters of C1, C1-L and CP over 48 h

Peptide	Cumulative amount ($\mu\text{g}/\text{cm}^2$)	AUC ($\mu\text{g}/\text{cm}^2/\text{h}$)	Transdermal flux ($\mu\text{g}/\text{cm}^2/\text{h}$)	Permeability coefficient (cm/h)
C1	34.48 (\pm 13.05)	966.02	2.15	7.1×10^{-4}
C1-L	17.19 (\pm 7.21)	779.41	1.07	3.5×10^{-4}
CP	4.73 (\pm 4.22)	212.90	0.29	9.8×10^{-5}

The 48h data showed that the permeation of the peptides was relatively slow so a longer duration experiment was undertaken to further assess *in vitro* skin diffusion. In the longer duration study (6 days) it was similarly observed that the permeation of C1 was higher than C1-L and core peptide though the absolute values were different from the 48h study due to the use of a skin sample from a different donor. C1 and C1-L permeation was significantly increased compared to permeation of CP over the time period of the experiment ($p < 0.0001$ for C1 and C1-L). The cumulative amount of C1, C1-L and CP penetrating the human epidermis to the receptor solution over 6 days is demonstrated in Figure 5.4 and Table 5-5. The relative permeation follows the same trend as that observed in the 48h study. The estimated transdermal flux calculated over 24h time period was $0.74 \mu\text{g}/\text{cm}^2/\text{h}$ for C1, $0.46 \mu\text{g}/\text{cm}^2/\text{h}$ for C1-L and $0.019 \mu\text{g}/\text{cm}^2/\text{h}$ for CP. The estimated permeability coefficient for C1 was 2.4×10^{-4} cm/h, 1.5×10^{-4} cm/h for C1-L and 6.4×10^{-6} cm/h for CP. The enhancement ratio of C1 and C1-L was greater for the longer duration experiment and there was an increase of approximately $4 \mu\text{g}/\text{cm}^2$ in the cumulative amount of C1 at the end of the experiment. Based on the mean cumulative permeation graph the area under the curve (AUC, Sigma Plot 8.0) was calculated. AUC of the cumulative amount of C1, C1-L and CP in the receptor compartment verses time graph yielded values of 3235.35, 2308.62 and 224.01 $\mu\text{g}/\text{cm}^2/\text{h}$ for C1, C1-L and CP respectively. Based on the mean cumulative permeation over 6 days, there was approximately a 38.2 fold enhancement in the delivery of the cyclic

peptide as compared to the core peptide and 23.9 fold enhancement in the linear peptide as compared to the core peptide.

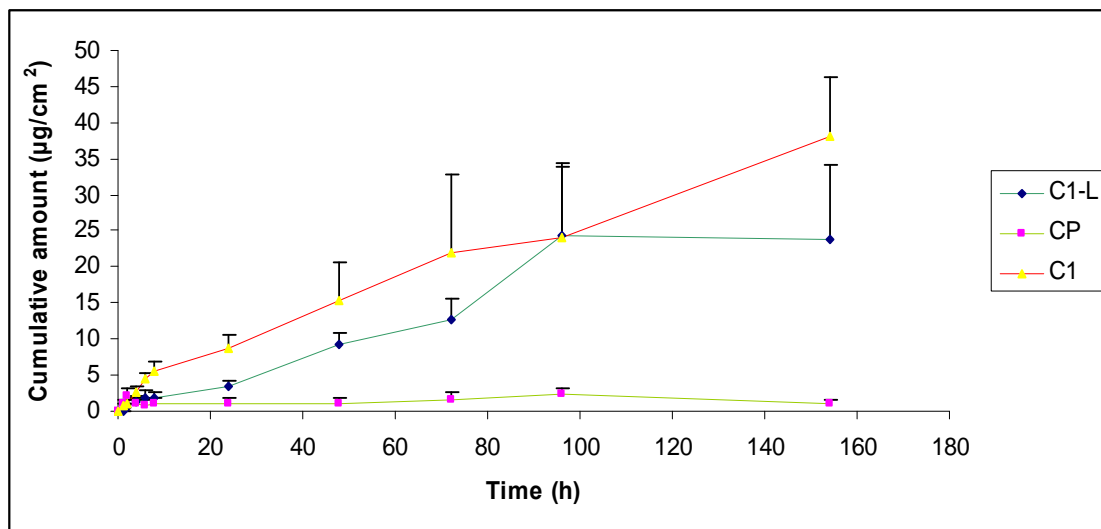


Figure 5.4 Permeation profiles for C1, C1-L and CP across human epidermis from 0-154h. Results are expressed as mean (\pm SEM: n=3 for C1-L and C1, n=4 for CP)

Table 5-5 Comparison of permeation parameters of C1, C1-L and CP over 6 days

Peptide	Cumulative amount ($\mu\text{g}/\text{cm}^2$)	AUC ($\mu\text{g}/\text{cm}^2/\text{h}$)	Transdermal flux ($\mu\text{g}/\text{cm}^2/\text{h}$)	Permeability coefficient, (cm/h)
C1	38.07 (\pm 8.16)	3235.35	0.74	2.4×10^{-4}
C1-L	23.86 (\pm 10.38)	2308.62	0.46	1.5×10^{-4}
CP	0.99 (\pm 0.62)	224.01	0.019	6.4×10^{-6}

A number of linear and cyclic peptides inhibit the immune response and inflammation in the skin; thereby have potential as novel therapeutic agents. Efficient delivery to the site of action following topical administration can offer opportunities for use of these peptides as novel and highly effective dermatologicals and cosmeceuticals. A number of cyclic peptides have activity in the skin. Cyclosporin A is a cyclic nonribosomal peptide of 11 amino acids produced by the fungus *Beauveria nivea*. It inhibits cytochrome C release and is of therapeutic value in conditions such as psoriasis, severe atopic

dermatitis and pyoderma gangrenosum.²²⁹ Melanin concentrating hormone (MCH) regulates skin colour by causing the aggregation of melanin granules and lightening the skin. Thus this cyclic peptide plays an important role in skin and hair pigmentation.²³⁰ Cyclic histatin is a potent wound healing peptide from human saliva. Cyclization of this peptide potentiated its activity at least 10-fold when compared to uncyclized histatin.²³¹

Cyclic peptides are of considerable interest as potential protein ligands. It has been postulated that cyclic molecules might be more cell permeable than their linear counterparts due to their reduced conformational flexibility.²³² Cyclic peptides are of considerable interest for a couple of reasons: their inherent limited conformational flexibility and their resistance to proteolytic hydrolysis and degradation. Recently Borchardt *et al* introduced the concept of making cyclic prodrugs of peptides as a way to modify their physicochemical properties sufficiently to allow them to permeate biological barriers (i.e., intestinal mucosa). Specifically, acyloxyalkoxy-, phenylpropionic acid- and 5 coumarinic acid-based cyclic prodrugs of [Leu]-enkephalin (H-Tyr-Gly-Gly-Phe-Leu-OH) and its metabolically stable analog DADLE (H-Tyr-D-Ala-Gly-Phe-D-Leu-OH) were prepared and their metabolic and biopharmaceutical properties determined. The cyclic prodrugs of these opioid peptides were shown to have: (i) favorable physicochemical properties (e.g., increased lipophilicity) for membrane permeation; (ii) unique solution structures (e.g., β -turns) that reduce their hydrogen bonding potential; and (iii) metabolic stability to exo- and endopeptidases. The phenylpropionic acid- and coumarinic acid-based cyclic prodrugs of [Leu]-enkephalin and DADLE were shown to have *significantly* better cell permeation characteristics through Caco-2 cell monolayers than the parent opioid peptides.²²⁸

In the present study we found that, the permeation of the cyclic peptides was higher than its linear counterpart and the core peptide though the permeation of C1-L was higher than C1 till 8h and then decreased. This may be due to the rate of partitioning of C1 into the epidermis and its conformational flexibility. We cannot directly compare the data in the present study with the apparent permeability coefficients observed by Borchardt *et al* because the experiments were conducted in Caco-2 cell layers. Cyclisation also improved the stability of the core peptide by 40%. The greater stability of the cyclic

peptide makes it possible to detect and quantify the intact peptide at the end of the skin diffusion experiments. Cyclization also led to increase in biological efficacy of the core peptide. The research group at Westmead Hospital has conducted biological activity studies in which the effect of these peptides on T cell function was examined *in-vitro*. They demonstrated improved and significant effectiveness by 80% of C1 compared to CP. To validate that the activity of C1 was not due to toxicity, antigen specific T-cell hybridoma cells (2B4) were incubated overnight with C1 at 50 μ M and examined by trypan blue exclusion staining to assess cellular membrane integrity, and [³H] thymidine uptake for cellular proliferation. The results showed that C1 at 50 μ M caused a decrease in cellular proliferation (62.56% \pm 14.25 SD), but only a marginal decrease in cell survival (viability = 86.63% \pm 8.14 SD), hence C1 was not toxic to cells.

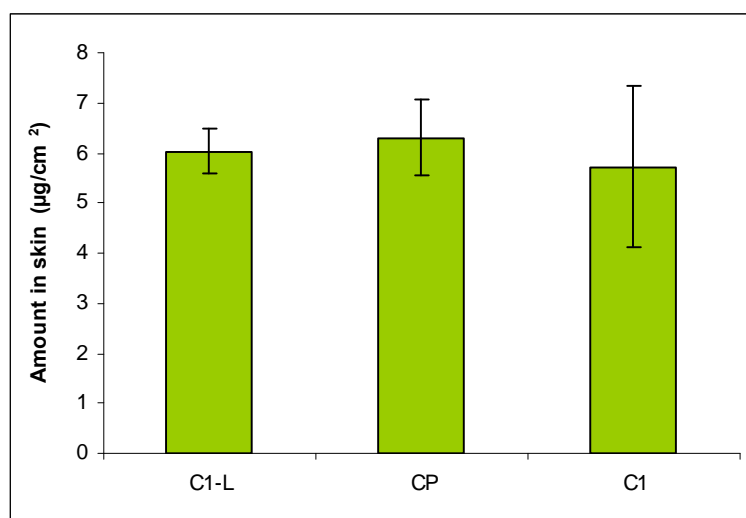
The effectiveness of C1 *in-vivo* was compared to commercially available cyclosporine. C1 given subcutaneously to rats had a comparable effect to cyclosporine in reducing inflammation in the adjuvant induced arthritis model. Significance between C1 and placebo treated rats was $p < 0.0001$ and no significance was observed between C1 and cyclosporine treated rats.

One major drawback of the study was the use of DMSO as the donor vehicle. Using DMSO as a donor vehicle was a compromise as we needed to solubilise the peptide and had very little compound to use for vehicle choice in this preliminary screening of permeability. Alternatively, we could have looked at essential oils such as eucalyptus oil, menthol or cineole as donor vehicles. Permeation data are therefore most relevant in relative terms rather than absolute terms as they may be an over-estimate due to the effect of DMSO on the skin barrier properties. It has been suggested that the skin penetration enhancement produced by DMSO not only involves changes in protein structure but may also be related to alterations in *stratum corneum* lipid organizations.²³³ Measurement of resistance of skin membranes was used as an integrity check and we found that there was a slight drop in resistance at the end of the test period. Also when using DMSO as a solvent it is important to consider the membrane used in the study. Actions of DMSO on animal tissue may be dramatically greater than the effects seen on a human skin membrane.

5.3.4 Recovery and mass balance

Figure 5.5 indicates the amounts of C1, C1-L and CP in the skin after the 8 and 48 h permeation experiments. The % recovery of C1, C1-L and CP from the skin using the extraction procedure described in Section 5.2.8 was 95%, 92.9% and 91% respectively.

(a)



(b)

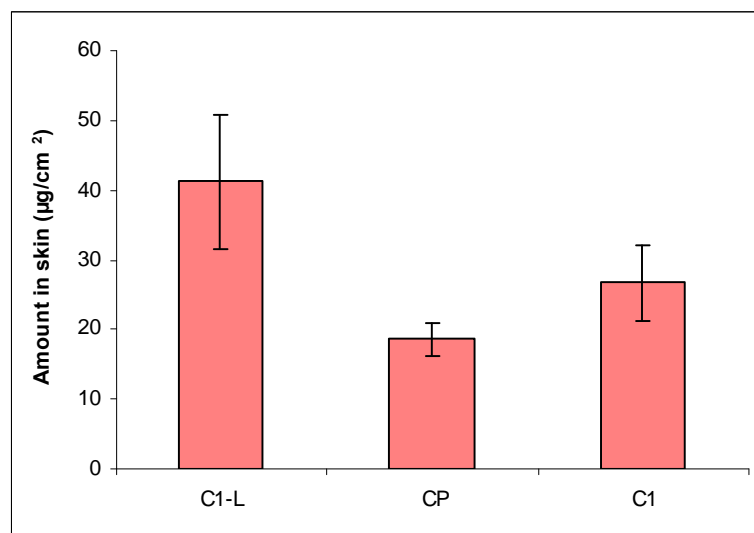


Figure 5.5 Amount of C1-L, CP and C1 in the skin after (a) 8 h (n=3) and (b) 48 h (n=4). Results are expressed as mean (\pm SEM)

The method for extraction of C1, C1-L and CP from the epidermis resulted in high recovery. The amount of the cyclic peptide (C1) and linear counterpart of the cyclic peptide (C1-L) in the skin was higher than the core peptide. The amount of peptide present in the skin was affected by the duration of the skin diffusion experiment with more present in the 48h study as compared to the 8h study. The amount in the epidermis did not vary much for all the three peptides in the 8h study because the duration of the experiment was short and peptide did not partition well into the epidermis at the earlier time points. As discussed in Section 5.3.3 the permeation and hence partitioning of C1 and CP into the epidermis was low during the initial time period. In case of the 48h study the amount of C1-L ($38.32 \mu\text{g}/\text{cm}^2 \pm 9.58$) retained in the skin was higher than C1 ($25.32 \mu\text{g}/\text{cm}^2 \pm 5.49$) and CP ($16.92 \mu\text{g}/\text{cm}^2 \pm 2.42$). This may be due to the higher molecular weight of C1-L or more importantly due to the structural and conformational differences between the linear counterpart and cyclic peptide of C1-L which might lead to stronger binding with the *stratum corneum* lipids.

5.4 Conclusions

In conclusion these results demonstrate that the epidermal penetration and stability of the core anti-inflammatory peptide improved after cyclisation. The order of permeation of the analogues was C1>C1-L>CP after 48h and 6 days. The amount of peptide retained in the skin was higher after 48h as compared to 8h due to greater partitioning of these peptides in the skin. This improved delivery to the skin and the previously demonstrated improvement in biological activity and specificity demonstrate the potential of cyclic peptides for skin therapeutics.

Chapter 6.

Summary and Conclusions

In recent years the revolutionary advances in biotechnology have increased interest in protein and peptide entities with therapeutic potential.²³⁴ However, unless these compounds can be administered efficiently, survive degradation by enzymes and be absorbed across cell membranes, they are unlikely to succeed as therapeutic moieties.¹⁰⁶ Proteins and peptides are generally delivered by the parenteral route because of their poor oral bioavailability, raising several issues such as poor patient compliance. Therefore, alternative non-invasive delivery techniques have been extensively studied.²³⁵ There has been an increasing recognition of the importance of skin as a route of administration of drugs.²³⁶ The advantages of TDD have been well documented. They include: therapeutic benefits such as sustained delivery of drugs to provide a steady plasma profile, particularly for drugs with short half-lives, and hence reduced systemic side effects; reducing the typical dosing schedule to once daily or even once weekly, hence generating the potential for improved patient compliance; and avoidance of the first-pass metabolism effect for drugs with poor oral bioavailability.²³⁷

Peptides and proteins are poor candidates for passive transdermal delivery as they are usually charged at physiological pH. Although transdermal delivery enables administration of these compounds, thus avoiding degradation in the gastrointestinal tract and first-pass metabolism associated with oral delivery, it requires special enhancement techniques. In this project we have assessed the potential of Dermaportation (Pulsed electromagnetic field technology), chemical conjugation of a therapeutic and cosmetic peptide with lipoamino acid and cyclisation of an anti-inflammatory peptide to enhance delivery across the skin. Figure 6.1 outlines the techniques and peptides investigated to optimize transdermal delivery.

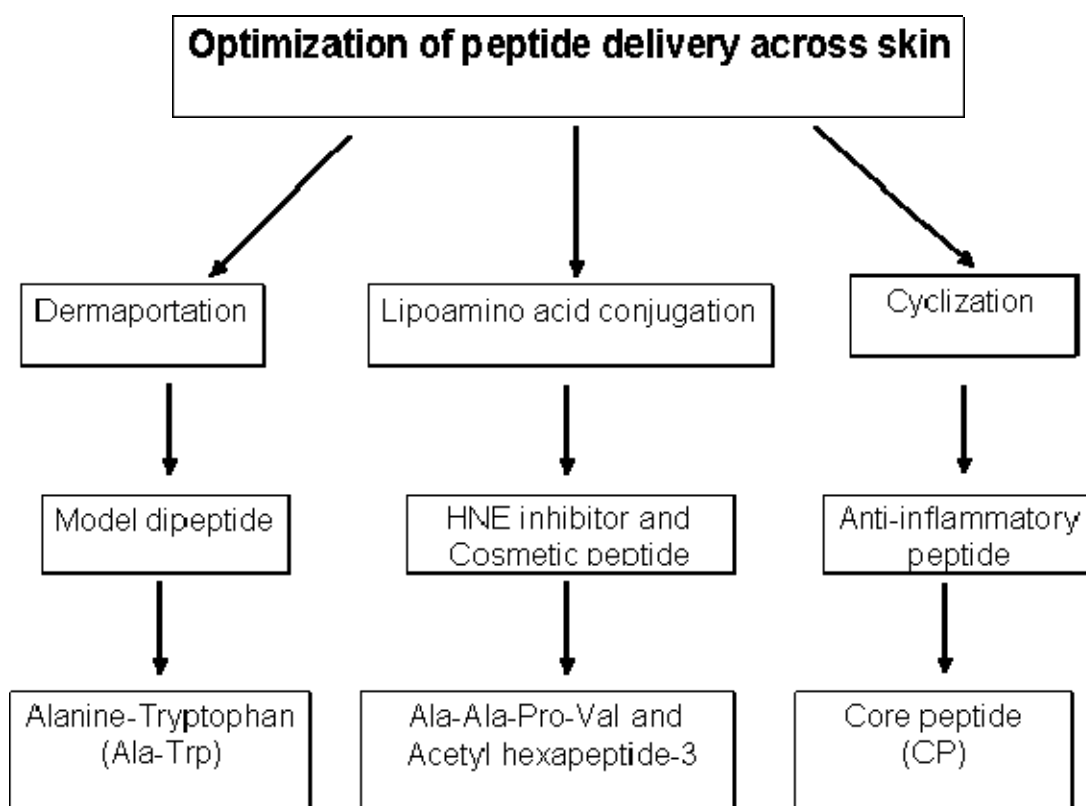


Figure 6.1 Optimization of peptide delivery

Chapter 2 describes the enhancement in percutaneous penetration of a model dipeptide, Ala-Trp across human epidermis with Dermaportation. The stability of this dipeptide was also assessed in different conditions with or without contact with skin. It was observed that Dermaportation *significantly* enhanced the delivery of Ala-Trp through human epidermis *in vitro* over an 8 h period when compared to passive diffusion. The dipeptide was found to be unstable on exposure to human epidermis with the amount of degradation product increasing steadily in the receptor compartment over 6h. Dermaportation may thus provide an effective means of delivering molecules which are highly susceptible to degradation like dipeptides, in higher amounts and in a relatively short duration of time.

In Chapter 3, enhanced delivery of the HNE inhibitor, Ala-Ala-Pro-Val was achieved by chemical modification by conjugation with lipoamino acids. C6, C8 and C10 LAAs were conjugated with AAPV and stability, *in vitro* epidermal permeability, skin

accumulation and biological activity of the resulting conjugated peptides was investigated and compared with the parent peptide. The stability of the lipoamino acid conjugates was *significantly* higher than the parent peptide with C8(D,L)-LAA-AAPV being the most stable conjugate. The addition of LAA generated two stereoisomers, D- and L-. It was observed that the skin permeability of the D- diastereomer was found to be higher as compared to the L- diastereomer. Permeation of C10(D,L)-LAA-AAPV was significantly greater at higher donor concentration and skin hydration. Overall the permeation of D-diastereomer of C6(D)-LAA-AAPV was found to be highest followed by C8(D)-LAA-AAPV. The racemic mixture of C6(D,L)-LAA-AAPV showed lower permeability as compared to C6(D)-LAA-AAPV and C8(D)-LAA-AAPV. Permeability of C10(D,L)-LAA-AAPV increased only after 8 h which may be due to the higher molecular weight of this conjugate which may have resulted in binding with the stratum corneum lipids resulting in slower release. The amount of the C10(D,L)-LAA-AAPV was found to be highest in the skin followed by C8(D,L)-LAA-AAPV and C6(D,L)-LAA-AAPV after in vitro diffusion studies. A preliminary study undertaken to investigate the surface activity of the peptides indicated that there was a decrease in the surface tension of the lipoamino acid conjugates as compared to control PBS. There was no significant difference in the biological activity of the lipoamino acid conjugates as compared to AAPV. We conclude that the degree of penetration enhancement of AAPV is associated with the lipophilicity, molecular weight and chain length of the LAA conjugates. Lower chain length conjugates (C6 and C8) of AAPV resulted in increase in delivery with lower lag time and donor concentration. Our studies suggest that LAA conjugation is a good technique to increase the permeation of AAPV across epidermis but further studies need to be undertaken to optimize the penetration and tissue distribution of the peptides to be able to effectively quantify them in the different layers of the skin. Studies should also be undertaken to ascertain the surface active properties of these peptides which will be an important step in understanding the mechanism of action of the native and conjugated peptides. This structural modification of the native peptide by conjugating it with LAA is a non-invasive technique for enhancing the delivery of peptides across the skin and does not have the disadvantages associated with

active technologies such as iontophoresis and electroporation that can cause skin irritation and may also decrease the stability of the peptide due to electrical pulses.

The permeation of C12 (A) and (B)-LAA conjugate of acetyl hexapeptide-3 is described in chapter 4. There was no permeation of either of the conjugates across the human epidermis. This may be due its high molecular weight and lipophilicity which may result in binding with the lipid bilayer components. The permeation of acetyl hexapeptide-3 by itself was very low and variable. The skin accumulation data showed that C12 (B)-LAA was found in the highest quantity in the skin followed by C12 (A)-LAA and acetyl hexapeptide-3. This may be useful from a cosmetic standpoint since topical application of a cosmetic agent should result in appreciable accumulation of the molecule of interest in the upper layers of skin to exert its effect. The delivery potential of actyl hexapeptide-3 could be increased with shorter chain length LAAs such as C6 and C8-LAA and also by increasing the concentration of the peptide in the donor.

In chapter 5 we investigated cyclisation strategy to improve the transdermal permeability of an anti-inflammatory peptide, core peptide (CP). Two analogues of CP were synthesized, cyclic peptide (C1) and a linear counterpart (C1-L). Stability of the cyclic peptide and C1-L was found to be significantly higher as compared to CP. Skin permeability was assessed over 48h and 6 days and it was observed that there was a steady increase in the cumulative amount of C1 permeating the receptor at the end of the test period. The mass balance studies indicate that higher amount C1-L was found in the skin when compared to C1 and CP after 48h. This may be due to the conformational differences between the two compounds. Future work should be directed at studying the solubility of these peptides in different vehicles which will make it possible to use a more polar solvent for skin permeation studies. We thus conclude that the cyclization strategy increased the stability, skin permeability and biological efficacy of an anti-inflammatory peptide.

Overall, it can be concluded that all the three strategies investigated in this project can modify the permeation characteristics of peptides after topical application. Further work needs to be undertaken to optimize the formulation strategies used to deliver these peptides across the skin so that the peptide can be made available to the site of action

without causing any irreversible damage to the barrier properties of the skin. Also optimization in terms of the chain length of LAA used is an important consideration and lastly more research needs to be undertaken to understand the stereo-selective permeation of these lipoamino acid conjugates across the skin since the activity of these peptides remains considerably unaffected by the stereochemistry.

Chapter 7.

References

1. Goebel A, Neubert RHH. Dermal peptide delivery using colloidal carrier systems. *Skin Pharmacology and Physiology*. 2008; 21(1):3-9.
2. Loffet A. Peptides as drugs: Is there a market? *Journal of Peptide Science*. 2001; 8(1):1-7.
3. Namjoshi S, Caccetta R, Benson HAE. Skin peptides: biological activity and therapeutic opportunities. *Journal of Pharmaceutical Sciences*. 2008; 97(7):2524-42.
4. Moody RP, Wester RC, Melendres JL, Maibach HI. Dermal absorption of the phenoxy herbicide 2,4-D dimethylamine in humans: effect of DEET anatomic site. *Journal of Toxicology and Environmental Health*. 1992; 36(3):241-250.
5. Guy RH, Maibach HI. Drug delivery to local subcutaneous structures following topical administration. *Journal of Pharmaceutical Sciences*. 1983; 72(12):1375-80.
6. Kikwai L, Babu J, Prado R, Kolot A, Armstrong CA, Ansel JC, et al. In Vitro and In Vivo Evaluation of Topical Formulations of Spantide II. *AAPS PharmSciTech*. 2005; 6(4):565-572.
7. Whitehouse MW, Roberts MS. *Drugs for pain and inflammation*. New York: Marcel Dekker; 1998.
8. Menon GK. New insights into skin structure: scratching the surface. *Advanced Drug Delivery Reviews*. 2002; 54(Supplement 1):S3-S17.
9. Kumar R, Philip A. Modified transdermal technologies: Breaking the barriers of drug permeation via the skin. *Tropical Journal of Pharmaceutical Research*. 2007; 6(1):633-644.
10. Williams AC. *Structure and function of human skin*. 2003.
11. Ong PY, Ohtake T, Brandt C, Strickland I, MLeung DY. Endogenous antimicrobial peptides and skin infections in atopic dermatitis. *New England Journal of Medicine*. 2002; 347(15):1151–1160.

12. Guy RH. Current status and future prospects of transdermal drug delivery. *Pharmaceutical Research*. 1996; 13(1765-1769).
13. Ting WW, Vest CD, Sontheimer RD. Review of traditional and novel modalities that enhance the permeability of local therapeutics across the stratum corneum. *International Journal of Dermatology*. 2004; 43(7):538-547.
14. Fearon DT, Locksley RM. The instructive role of innate immunity in the acquired immune response. *Science*. 1996; 272:50-53.
15. Izadpanah A, Gallo RL. Antimicrobial peptides. *Journal of the American Academy of Dermatology*. 2005; 52:381–390.
16. Niyonsaba F, Ogawa H. Protective roles of the skin against infection: Implication of naturally occurring human antimicrobial agents [beta]-defensins, cathelicidin LL-37 and lysozyme. *Journal of Dermatological Science*. 2005; 40:157-168.
17. Harder J, Schroder JM. Psoriatic scales: A promising source for the isolation of human skin derived antimicrobial proteins. *Journal of Leukocyte Biology* 2005; 77:476–486.
18. Harder J, Bartels J, Christophers E, Schroder JM. A peptide antibiotic from human skin. *Nature*. 1997; 387:861.
19. Frohm M, Agerberth B, Ahangari G. The expression of the gene coding for the antibacterial peptide LL-37 is induced in human keratinocytes during inflammatory disorders. *Journal of Biological Chemistry*. 1997; 272:15258–15263.
20. Nilsson MF, Sandstedt B, Sorensen O, Stahle-Backdahl M. The human cationic antimicrobial protein (hCAP18), a peptide antibiotic, is widely expressed in human squamous epithelia and colocalizes with interleukin 6. *Infection and Immunity*. 1999; 67:2561-66.
21. Leung DYM, Boguniewicz M, Howell MD, Nomura I, Hamid Q. New insights into atopic dermatitis. *Journal of Clinical Investigation*. 2004; 113(5):651-657.

22. Christophers E, Henseler T. Contrasting disease patterns in psoriasis and atopic dermatitis. *Archives of Dermatological Research*. 1987; 279(1):S48–S51.
23. Gallo RL, Ono M, Povsic T. Syndecans, cell surface heparan sulfate proteoglycans, are induced by a proline-rich antimicrobial peptide from wounds. *Proceedings of the National Academy of Sciences of the United States of America* 1994; 91(23):11035–9.
24. Howell MD, Jones JF, Kisich KO, Streib JE, LGallo R, Leung DY. Selective killing of vaccinia virus by LL-37: Implications for eczema vaccinatum. *The Journal of Immunology*. 2004; 172:1763–67.
25. Cooper KD. Atopic dermatitis: Recent trends in pathogenesis and therapy. *Journal of Investigative Dermatology*. 1994; 103(5):128-137.
26. Rieg S, Steffen H, Seeber S, Humeny A, Kalbacher H, Dietz K, et al. Deficiency of dermcidin-derived antimicrobial peptides in sweat of patients with atopic dermatitis correlates with an impaired innate defense of human skin in vivo. *The Journal of Immunology*. 2005; 174(12):8003–10.
27. Madsen P, Rasmussen HH, Leffers H, Honore B, Dejgaard K, Olsen E, et al. Molecular cloning, occurrence, and expression of a novel partially secreted protein "psoriasin" that is highly up-regulated in psoriatic skin. *Journal of Investigative Dermatology*. 1991; 97(4):701-712.
28. Ruzicka T, Simmet T, Peskar B, Ring J. Skin levels of arachidonic acid—Derived inflammatory mediators and histamine in atopic dermatitis and psoriasis. *Journal of Investigative Dermatology*. 1986; 86(2):105–108.
29. Watson PH, Leygue ER, Murphy LC. Psoriasin (S100A7). *The International Journal of Biochemistry & Cell Biology*. 1998; 30(5):567–571.
30. Tonel G, Conrad C. Interplay between keratinocytes and immune cells--Recent insights into psoriasis pathogenesis. *The International Journal of Biochemistry & Cell Biology*. 2009; 41(5):963-968.

31. Nonomura K, Yamanish K, Yasuno H. Upregulation of elafin/SKALP gene expression in psoriatic epidermis. *Journal of Investigative Dermatology*. 1994; 103(1):88–91.
32. Baumann H, Gauldie J. The acute phase response. *Immunology Today*. 1994; 15(2):74–80.
33. Tanaka N, Fujioka A, Tajima S, Ishibashi A, Hirose S. Elafin is induced in epidermis in skin disorders with dermal neutrophilic infiltration: Interleukin-1beta and tumour necrosis factor alpha stimulate its secretion in vitro. *British Journal of Dermatology*. 2000; 143(4):728–732.
34. Raychaudhri SK, Raychaudhri SP, Farber EM. Anti-Chemotactic activities of peptide-T: a possible mechanism of actions for its therapeutic effects on psoriasis. *International Journal of Immunopharmacology*. 1998; 20(111):661-667.
35. Wiedow O, Young J, Davison M, Christophers E. Antileukoprotease in psoriatic scales. *Journal of Investigative Dermatology*. 1993; 101(3):305–309.
36. Wiedow O, Harder J, Bartels J, Streit V, Christophers E. Antileukoprotease in Human Skin: An Antibiotic Peptide Constitutively Produced by Keratinocytes. *Biochemical and Biophysical Research Communications*. 1998; 248:904–909.
37. Baker BS, Fry L. The immunology of psoriasis. *British Journal of Dermatology*. 1991; 126(2):1-9.
38. Nanney LB, Stoscheck CM, Magid M, King LE. Altered epidermal growth factor binding and receptor distribution in psoriasis. *Journal of Investigative Dermatology*. 1986; 86(3):260–265.
39. Sticherling M, Bornscheuer E, Schroder JM, Christophers E. Localization of neutrophil-activating peptide-1/interlukin-8-immunoreactivity in normal and psoriatic skin. *Journal of Investigative Dermatology*. 1991; 96(1):26–30.
40. Horvath A, Olive C, Wong A, Clair T, Yarwood P, Good M, et al. A Lipophilic adjuvant carrier system for antigenic peptides. *Letters in Peptide Science*. 2002; 8:285-288.

41. Schroder JM, Harder J. Human beta-defensin-2. *The International Journal of Biochemistry and Cell Biology*. 1999; 31(6):645–651.
42. Raychaudhuri SP, Raychaudhuri SK. Relationship between kinetics of lesional cytokines and secondary infection in inflammatory skin disorders: A hypothesis. *International Journal of Dermatology*. 1993; 32(6):409–412.
43. Harder J, Schröder J-M. RNase 7, a Novel Innate Immune Defense Antimicrobial Protein of Healthy Human Skin. *Journal of Biological Chemistry*. 2002; 277(48):46779-46784.
44. Schroder JM, Harder J. Antimicrobial peptides in skin disease. *Drug Discovery Today: Therapeutic strategies*. 2006; 3(1):93–100.
45. Mckay IA, Leigh IM. Epidermal cytokines and their roles in cutaneous wound healing. *British Journal of Dermatology*. 1991; 124(6):513–518.
46. Barrandon Y, Green H. Cell migration is essential for sustained growth of keratinocyte colonies: The roles of transforming growth factor and epidermal growth factor. *Cell*. 1987; 50(7):1131-1137.
47. Meyer-Ingold W. Wound therapy: Growth factors as agents to promote healing. *Trends in Biotechnology*. 1993; 11(9):387–392.
48. Lynch SE, Colvin RB, Antoniades HN. Growth factors in wound healing. Single and synergistic effects on partial thickness porcine skin wounds. *The Journal of Clinical Investigation*. 1989; 84(2):640–646.
49. Sorensen OE, Cowland JB, Theilgaard-Monch K, Liu L, Ganz T, Borregaard N. Wound healing and expression of antimicrobial peptides/polypeptides in human keratinocytes, a consequence of common growth factors. *Journal of Immunology*. 2003; 170(11):5583–89.
50. Rennekampff H-O, Hansbrough JF, Kiessig V, Dore C, Sticherling M, Schroder J-M. Bioactive Interleukin-8 Is Expressed in Wounds and Enhances Wound Healing. *Journal of Surgical Research*. 2000; 93:41-54.

51. Vigor C, Rolfe KJ, Richardson J, Baker R, Grobbelaar A, Linge C. The involvement of the ECM and RGD peptides in apoptosis induction during wound healing. *Journal of Plastic, Reconstructive & Aesthetic Surgery*. 2006; 59(9):S4-S4.
52. Buckley CD, Pilling D, Henriquez NV, Parsonage G, Threlfall K, Scheel-Toellner D, et al. RGD peptides induce apoptosis by direct caspase-3 activation. *Nature*. 1999; 397:534–539.
53. Buffoni F, Pino R, Pozzo AD. Effect of tripeptide-copper complexes on the process of skin wound healing and on cultured fibroblasts. *Arch Int Pharmacodyn Ther*. 1995; 330(3):345–360.
54. Maquart FX, Pickart L, Laurent M, Gillery P, Monboisse JC, Borel JP. Stimulation of collagen synthesis in fibroblast cultures by the tripeptide-copper complex glycyl-L-histidyl-L-lysine- Cu^{2+} . *FEBS Letters*. 1988; 238(2):343–346.
55. Carraway JH. Using Aldara, copper peptide, and niacinamide for skin care *Aesthetic Surgery Journal* 2004; 24(1):83-84
56. Martinez A, Elsasser TH, Cacho CM, Cuttitta F. Expression of adrenomedullin and its receptor in normal and malignant human skin: A potential pluripotent role in the integument. *Endocrinology*. 1997; 138(12):5597–04.
57. Lundy FT, Orr DF, Gallagher JR, Maxwell P, Shaw C, Napier SS, et al. Identification and overexpression of human neutrophil [alpha]-defensins (human neutrophil peptides 1, 2 and 3) in squamous cell carcinomas of the human tongue. *Oral Oncology*. 2004; 40(2):139-144.
58. Zouki C, Ouellet S, Filep J. The anti-inflammatory peptides, antinflammins, regulate the expression of adhesion molecules on human leukocytes and prevent neutrophil adhesion to endothelial cells. *FASEB Journal*. 2000; 14:572–580.
59. Howell MD, Wollenberg A, Gallo RL, Flaig M, Streib JE, Wong C, et al. Cathelicidin deficiency predisposes to eczema herpeticum. *Journal of Allergy and Clinical Immunology*. 2006; 117(4):836-841.

60. Lai Y-P, Peng Y-F, Zuo Y, Li J, Huang J. Functional and structural characterization of recombinant dermcidin-1L, a human antimicrobial peptide. *Biochemical and Biophysical Research Communications* 2005; 328(1):243-50.
61. Molhuizen HO, Alkemade HA, Zeeuwen PL, Jongh GJd, Wieringa B, Schalkwijk J. SKALP/elafin: An elastase inhibitor from cultured human keratinocytes. Purification, cDNA sequence, and evidence for transglutaminase cross-linking. *Journal of Biological Chemistry* 1993; 268(12028–12032).
62. Raychaudhuri SP, Jiang WY, Raychaudhuri SK, Krensky AM. Lesional T cells and dermal dendrocytes in psoriasis plaque express increased levels of granulysin. *Journal of the American Academy of Dermatology*. 2004; 51(6):1006-1008.
63. Slominski A, Malarkey WB, Wortsman J, Asa SL, Carlson A. Human skin expresses growth hormone but not the prolactin gene. *Journal of Laboratory and Clinical Medicine*. 2000; 136(6):476-481.
64. Fulton C, Anderson GM, Zasloff M, Bull R, Quinn AG. Expression of natural peptide antibiotics in human skin. *The Lancet*. 1997; 350(9093):1750-1751
65. Toth I, Christodoulou M, Bankowsky K, Flinn N, Hornebeck W. Design of potent lipophilic - peptide inhibitors of human neutrophil elastase : in vitro and in vivo studies. *International Journal of Pharmaceutics*. 1995; 125:117 - 122.
66. Tsatmali M, Ancans J, Thody AJ. Melanocyte Function and Its Control by Melanocortin Peptides. *The Journal of Histochemistry & Cytochemistry*. 2002; 50(2):125–133.
67. Suzuki I, Cone RD, Sungbin IM, Nordlund JM, Abdel-Malek ZA. Binding of Melanotropic Hormones to the Melanocortin Receptor MC1R on Human Melanocytes Stimulates Proliferation and Melanogenesis. *Endocrinology*. 1996; 127(5):1627-1633.
68. Glaser R, Harder J, Lange H, Bartels J, Christophers E, Schroder JM. Antimicrobial psoriasin (S100A7) protects human skin from *Escherichia coli* infection. *Natural immunology*. 2005; 6(1):57-64.

69. Lucca AJD, Walsh TJ. Antifungal peptides: Origin, activity, and therapeutic potential. *Rev Iberoam Micol.* 2000; 17:116-120.
70. Mor A, Chartrel N, Vaudry H, Nicolas P. Skin peptide tyrosine-tyrosine, a member of the pancreatic polypeptide family: Isolation, structure, synthesis, and endocrine activity. *Proc Natl Acad Sci.* 1994; 91:10295-10299.
71. Falanga V, Gerhardt CO, Dasch JR. Skin distribution and differential expression of transforming growth factor beta1 and beta2. *Journal of Dermatological Science.* 1992; 3(3):131–136.
72. Choi CM, Berson DS. Cosmeceuticals. *Seminars in Cutaneous Medicine and Surgery.* 2006; 25:163-168.
73. Katyama K, Armendariz-Borunda J, Rachow R. A pentapeptide from Type I procollagen promotes extracellular matrix production. *Journal of Biological Chemistry.* 1993; 268:9941-9944.
74. Bascom CC, inventor; The Procter and Gamble Company, assignee. Compositions for treating wrinkles comprising a peptide. United States patent 5492894. 1993 June 25.
75. Quinn PJ, Boldyrev AA, Formazuyk VE. Carnosine: Its properties, functions and potential therapeutic applications. *Molecular aspects of Medicine.* 1992; 13:379-444.
76. Hipkiss AR. Carnosine, a protective, anti-ageing peptide? *The International Journal of Biochemistry and Cell Biology.* 1998; 30:863-868.
77. Conner K, Nern K, Rudisill J, O'Grady T, Gallo RL. The antimicrobial peptide LL-37 is expressed by keratinocytes in condyloma acuminatum and verruca vulgaris. *Journal of the American Academy of Dermatology.* 2002; 47(3):347–350.
78. Martinez A, Elsasser TH, Cacho CM-, Cuttitta F. Expression of adrenomedullin and its receptor in normal and malignant human skin : A potential pluripotent role in the integument. *Endocrinology.* 1997; 138:5597-5604.

79. Dureja H, Kaushik D, Gupta M, Kumar V, Lather V. Cosmeceuticals: An emerging concept. *Indian Journal of Pharmacology*. 2005; 37(3):155-158.
80. Lupo MP. Cosmeceutical peptides. *Dermatologic Surgery*. 2005; 31:832-836.
81. Togashi S-i, Takahashi N, Iwama M, Fukui T. Antioxidative collagen-derived peptides in human-placenta extract. *Placenta*. 2002; 23:497-502.
82. Yann M, inventor; Societe L' Oreal S.A., assignee. Modulating body/cranial hair growth with derivatives of the alpha type melanocyte stimulating hormone. France patent 5739111. 1996 April 29.
83. Kansci G, Genot C, Meynier A, Gandemer G. The antioxidant activity of carnosine and its consequences on the volatile profiles of liposomes during iron/ascorbate induced phospholipid oxidation. *Food Chemistry*. 1997; 60(2):165-175.
84. Schwartz RA, Centurion SA. Cosmeceuticals. 2006 [updated 27/04/2007]. Available
85. Fitzpatrick RE, Rostan EF. Reversal of photodamage with topical growth factors: a pilot study. *Journal of Cosmetic and Laser Therapy*. 2003; 5:25–34.
86. Linter K, inventor; Sederma, assignee. Cosmetic or dermopharmaceutical use of peptides for healing, hydrating and improving skin appearance during natural or induced ageing (Helioderma, Pollution). France. 2003.
87. Martin DC, inventor; L'Oreal Paris, assignee. Cosmetic compositions containing a lipid ceramide compound and a peptide having a fatty chain and their uses. France. 1998.
88. Amsden BG, Goosen MFA. Transdermal delivery of peptide and protein drugs: an overview. *Bioengineering, Food and Natural products*. 1995; 41(8):1972-1997.
89. Benson HAE. Transdermal drug delivery: Penetration enhancement techniques. *Current Drug Delivery*. 2005; 2:23-33.

90. Higuchi WI. Analysis of data on the medicament release from ointments. *Journal of Pharmaceutical Sciences*. 1962; 51(8):802-804.
91. Michaels AS, Chandrasekaran SK, Shaw JE. Drug permeation through human skin: Theory and in vitro experimental measurement. *American Institute of Chemical Engineers (AIChE) Journal*. 1975; 21(5):985–996.
92. Elias PM, Menon GK. Structural and lipid biochemical correlates of the epidermal permeability barrier. *Advances in Lipid Research*. 1991; 24:1-26.
93. Ogiso T, Iwaki M, Tanino T, Yono A, Ito A. In vitro skin penetration and degradation of peptides and their analysis using a kinetic model. *Biological and Pharmaceutical Bulletin*. 2000; 23(11):1346–51.
94. Shah PK, Borchardt RT. A comparison of peptidase activities and peptide metabolism in cultured mouse keratinocytes and neonatal mouse epidermis. *Pharmaceutical Research*. 1991; 8(1):70–75.
95. Steinstrasser I, Merkle HP. Dermal metabolism of topically applied drugs: Pathways and models reconsidered. *Pharmaceutica Acta Helvetiae*. 1995; 70(1):3–24.
96. Cross SE, Roberts MS. Physical enhancement of transdermal drug application: Is delivery technology keeping up with pharmaceutical developments? *Current Drug Delivery*. 2004; 1:81-92.
97. Magnusson BM, Runn P. Effect of penetration enhancers on the permeation of the thyrotropin releasing hormone analogue pGlu-3-methyl-His- Pro amide through human epidermis. *International Journal of Pharmaceutics*. 1999; 178(2):149-159.
98. Karande P, Jain A, Arora A, Ho MJ, Mitragotri S. Synergistic effects of chemical enhancers on skin permeability: A case study of sodium lauroylsarcosinate and sorbitan monolaurate. *European Journal of Pharmaceutical Sciences*. 2007; 31(1):1-7.

99. Karande P, Jain A, Ergun K, Kispersky V, Mitragotri S. Design principles of chemical penetration enhancers for transdermal drug delivery. *Proceedings of the National Academy of Sciences of the United States of America*. 2005; 102(13):4688-4693.
100. Foldvari M, Baca-Estrada ME, He Z, Hu J, Attah-Poku S, King M. Dermal and transdermal delivery of protein pharmaceuticals: Lipid-based delivery systems for interferon alpha. *Biotechnology and Applied Biochemistry*. 1999; 30(2):129-137.
101. Dkeidek I, Touitou E. Transdermal absorption of polypeptides. *AAPS PharmSci*. 1999; 1(S202).
102. Gupta PN. Non invasive vaccine delivery in transferosomes, niosomes and liposomes: a comparative study. *International Journal of Pharmaceutics*. 2005; 293(1-2):73-82.
103. Manconi M. Niosomes as carriers for tretinoin III. A study into the invitro cutaneous delivery of vesicle-incorporated tretinoin *International Journal of Pharmaceutics*. 2006; 311(1-2):11-19.
104. Benson HAE. Transferosomes for transdermal drug delivery. *Expert Opinion on drug Delivery*. 2006; 3(6):727-737.
105. Benson HAE, Namjoshi S. Proteins and peptides: Strategies for delivery to and across the skin. *Journal of Pharmaceutical Sciences*. 2008; 97(9):3591-10.
106. Blanchfield JT, Toth I. Modification of peptides and other drugs using lipoamino acids and sugars. *Methods in Molecular Biology*. 2005; 298:45-61.
107. Ali M, Manolios N. Peptide delivery systems. *Letters in Peptide Science*. 2002; 8:289-294.
108. Toth I. A novel chemical approach to drug delivery: Lipidic amino acid conjugates *Journal of Drug Targeting* 1994; 2(3):217-239.
109. Barry BW. Mode of action of penetration enhancers in human skin. *Journal of Controlled Release*. 1987; 6(1):85-97.

110. Roberts M, Walker M. The most natural penetration enhancer. In. New York: Marcel Dekker Inc; 1993.
111. Potts RD. Physical characterization of the stratum corneum: the relationship of mechanical and barrier properties to lipid and protein structure. New York: Marcel Dekker; 1989.
112. Barry BW. Novel mechanisms and devices to enable successful transdermal drug delivery. *European Journal of Pharmaceutical Sciences*. 2001; 14(2):101–114.
113. Delgado-Charro MB, Guy RH. Characterization of convective solvent flow during iontophoresis. *Pharmaceutical Research*. 1994; 11(7):929–935.
114. Schuetz YB, Naik A, Guy RH, Kalia YN. Effect of amino acid sequence on transdermal iontophoretic peptide delivery. *European Journal of Pharmaceutical Sciences*. 2005; 26(5):429–437.
115. Lau DT, Sharkey JW, Petryk L, Mancuso FA, Yu Z, Tse FL. Effect of current magnitude and drug concentration on iontophoretic delivery of octreotide acetate (Sandostatin) in the rabbit. *Pharmaceutical Research*. 1994; 11(12):1742–46.
116. Boinpally RR, Zhou SL, Devraj G, Anne PK, Poondru S, Jasti BR. Iontophoresis of lecithin vesicles of cyclosporin A. *International Journal of Pharmaceutics*. 2004; 274(1-2):185-190.
117. Pillai O, Kumar N, Dey CS, Borkute S, Nagalingam S, RPanchagnula. Transdermal iontophoresis of insulin. Part 1: A study on the issues associated with the use of platinum electrodes on rat skin. *Journal of Pharmacy and Pharmacology*. 2003; 55(11):1505-13.
118. Prausnitz MR, Bose VG, Langer R, Weaver JC. Electroporation of mammalian skin: A mechanism to enhance transdermal drug delivery. *Proceedings of the National Academy of Sciences of the United States of America*. 1993; 70(22):10504–08.
119. Prausnitz MR, Edelman ER, Gimm JA, Langer R, Weaver JC. Transdermal delivery of heparin by skin electroporation. *Biotechnology (NY)*. 1995; 13:1205-09.

120. Sen A, Daly ME, Hui SW. Transdermal insulin delivery using lipid enhanced electroporation. *Biochimica et Biophysica Acta (BBA) - Biomembranes*. 2002; 1564(1):5-8.
121. Gaudy C, Richard MA, Folchetti G, Bonerandi JJ, Grob JJ. Randomized controlled study of electrochemotherapy in the local treatment of skin metastases of melanoma
115–121. *Journal of Cutaneous Medicine and Surgery*. 2006; 10:115-121.
122. Pitt WG, Hussein GA, Staples BJ. Ultrasonic drug delivery—A general review. *Expert Opinion on Drug Delivery*. 2004; 1(1):37-56.
123. Alvarez-Roman R, Merino G, Kalia YN, Naik A, Guy RH. Skin permeability enhancement by low frequency sonophoresis: Lipid extraction and transport pathways. *Journal of Pharmaceutical Sciences*. 2003; 92(6):1138-46.
124. Park EJ, Werner J, Smith NB. Ultrasound mediated transdermal insulin delivery in pigs using a lightweight transducer. *Pharmaceutical Research*. 2007; 24(7):1396-01.
125. Katz NP, Shapiro DE, Herrmann TE, Kost J, Custer LM. Rapid onset of cutaneous anesthesia with EMLA cream after pretreatment with a new ultrasound-emitting device. *Anaesthesia and Analgesia*. 2004; 98(2):371-376.
126. Lee S, McAuliffe DJ, Kollias N, Flotte TJ, Doukas AG. Photomechanical delivery of 100-nm microspheres through the stratum corneum: Implications for transdermal drug delivery. *Lasers in Surgery and Medicine*. 2002; 31(3):207-210.
127. Lee S, McAuliffe DJ, Mulholland SE, Doukas AG. Photomechanical transdermal delivery of insulin in vivo. *Lasers in Surgery and Medicine*. 2001; 28(3):282-285.
128. Murthy SN. Magnetophoresis: an approach to enhance transdermal drug diffusion. *Pharmazie*. 1999; 54(5):377-409.
129. Santini JT, Cima MJ, Langer R. A controlled-release microchip. *Nature*. 1999; 397(28):335-338.

130. Mooney V. A randomized double-blind prospective study of the efficacy of pulsed electromagnetic fields for interbody lumbar fusions. *Spine*. 1990; 15(7):708-712.
131. Simko M, Mattsson MO. Extremely low frequency electromagnetic fields as effectors of cellular responses in vitro: possible immune cell activation. *Journal of Cellular Biochemistry*. 2004; 93(1):83-92.
132. Namjoshi S, Caccetta R, Edwards J, Benson HAE. Liquid chromatography assay for 5-aminolevulinic acid: Application to in vitro assessment of skin penetration via Dermaportation. *Journal of Chromatography B*. 2007; 852(1-2):49-55.
133. Benson HAE, Caccetta R, Eijkenboom M. 8th World Congress on Inflammation [2007. Copenhagen, Denmark:
134. Benson HAE, Caccetta R, Namjoshi S, Edwards J, Eijkenboom M. World Congress on Pain [2005. Sydney:
135. Prausnitz MR. Microneedles for transdermal drug delivery. *Advanced Drug Delivery Reviews*. 2004; 56(5):581-587.
136. Henry S, McAllister DV, Allen MG, Prausnitz MR. Microfabricated microneedles: A novel approach to transdermal drug delivery. *Journal of Pharmaceutical Sciences*. 1998; 88(9):922-925.
137. Martanto W, Davis SP, Holiday NR, Wang J, Gill HS, Prausnitz MR. Transdermal delivery of insulin using microneedles in vivo. *Pharmaceutical Research*. 2004; 21(6):947-952.
138. Nelson JS, McCullough JL, Glenn TC, Wright WH, Liaw LH, Jacques SL. Mid-infrared laser ablation of stratum corneum enhances in vitro percutaneous transport of drugs. *Journal of Investigative Dermatology*. 1991; 97(5):874-879.
139. Svedman P, Lundin S, Høglund P, Hammarlund C, Malmros C, Pantzar N. Passive drug diffusion via standardized skin mini-erosion; methodological aspects

and clinical findings with new device. *Pharmaceutical Research*. 1996; 13(9):1354-59.

140. Badkar AV, Smith AM, Eppstein JA, Banga AK. Transdermal delivery of interferon alpha-2B using microporation and iontophoresis in hairless rats. *Pharmaceutical Research*. 2007; 24(7):1389–95.

141. Barry BW. Breaching the skin's barrier to drugs. *Nature Biotechnology*. 2004; 22:165-167.

142. Srinivasan V, Su MH, Higuchi WI, Behl CR. Iontophoresis of polypeptides: Effect of ethanol pretreatment of human skin. *Journal of Pharmaceutical Sciences*. 1990; 79(7):588-591.

143. Choi EH, Lee SH, Ahn SK, Hwang SM. The pretreatment effect of chemical skin penetration enhancers in transdermal drug delivery using iontophoresis. *Skin Pharmacology and Applied Skin Physiology*. 1999; 12(6):326-335.

144. Blanchfield J, Toth I. Lipid, sugar and liposaccharide based drug delivery systems 2. *Current Medicinal Chemistry*. 2004; 11:2375-82.

145. Toth I, Christodoulou M, Bankowsky K, Flinn N, Gibbons WA, Godeau G, et al. Design of potent lipophilic-peptide inhibitors of human neutrophil elastase: In vitro and in vivo studies. *International Journal of Pharmaceutics*. 1995; 125(1):117-122.

146. Kellam B, Drouillat B, Dekany G, Starr MS, Toth I. Synthesis and in vitro evaluation of lipoamino acid and carbohydrate modified enkephalins as potential antinociceptive agents. *International Journal of Pharmaceutics*. 1998; 161(1):55-64.

147. Hughes RA, Toth I, Ward P, McColmn AM, Cox DM, Anderson GJ, et al. Lipidic peptides. V: Penicillin and cephalosporin acid conjugates with increased lipophilic character. *Journal of Pharmaceutical Sciences*. 1992; 81(8):845-848.

148. Toth I, Flinn N, Hillery A, Gibbons WA, Artursson P. Lipidic conjugates of luteinizing hormone releasing hormone (LHRH)+ and thyrotropin releasing hormone (TRH)+ that release and protect the native hormones in homogenates of human

intestinal epithelial (Caco-2) cells. *International Journal of Pharmaceutics*. 1994; 105(3):241-247.

149. Toth I, Malkinson JP, Flinn NS, Keri G. Novel lipoamino acid- and liposaccharide-based system for peptide delivery: application for oral administration of tumor-selective somatostatin analogues. *Journal of Medicinal Chemistry*. 1999; 42:4010-13.

150. Toth I, Danton M, Flinn N, Gibbons WA. A combined adjuvant and carrier system for enhancing synthetic peptides immunogenicity utilising lipidic amino acids. *Tetrahedron Letters*. 1993; 34(24):3925-3928.

151. Pignatello R, Puleo A, Puglisi G, Vicari L, Messina A. Effect of liposomal delivery on in vitro antitumor activity of lipophilic conjugates of methotrexate with lipoamino acids. *Drug Delivery*. 2003; 10(95-100).

152. Bergeon JA, Toth I. Enhancement of oral drug absorption--Effect of lipid conjugation on the enzymatic stability and intestinal permeability of l-Glu-l-Trp-NH₂. *Bioorganic & Medicinal Chemistry*. 2007; 15(22):7048-7057.

153. Koda Y, Del Borgo M, Wessling ST, Lazarus LH, Okada Y, Toth I, et al. Synthesis and in vitro evaluation of a library of modified endomorphin 1 peptides. *Bioorganic & Medicinal Chemistry*. 2008; 16(11):6286-6296.

154. Staffan T, Hashimoto K, Malkinson J, Lazorova L, Toth I, Artursson P. A new principal for tight junction modulation based on occludin peptides. *Molecular Pharmacology*. 2003; 64(6):1530-40.

155. Yamamoto A, Setoh K, Murakami M, Shironoshita M, Kobayashi T, Fujimoto K, et al. Enhanced transdermal delivery of phenylalanyl-glycine by chemical modification with various fatty acids. *International Journal of Pharmaceutics*. 2003; 250(1):119-128.

156. Uchiyama T, Kotani A, Tatsumi H, Kishida T, Okamoto A, Okada N, et al. Development of novel lipophilic derivatives of DADLE (leucine enkephalin analogue): intestinal permeability characteristics of DADLE derivatives in rats. *Pharmaceutical Research*. 2000; 17(12).

157. Rothbard JB, Garlington S, Lin Q, Kirschberg T, Kreider E, McGrane PL, et al. Conjugation of arginine oligomers to cyclosporin A facilitates topical delivery and inhibition of inflammation. *Nat Med.* 2000; 6(11):1253-1257.
158. Liang MT, Hennessy T, Toth I, Davies NM, Hook S. Synthetic lipopeptides formulated in liposomes: effect on their immune stimulatory capacity in vitro. *Nanoscience and Nanotechnology.* 2006:286-289.
159. Koda Y, Liang MT, Blanchfield JT, Toth I. In vitro stability and permeability studies of liposomal delivery systems for a novel lipophilic endomorphin 1 analogue. *International Journal of Pharmaceutics.* 2008; 356(1-2):37-43.
160. Sinha VR, Kumria R. Polysaccharides in colon-specific drug delivery. *International Journal of Pharmaceutics.* 2001; 224(1-2):19-38.
161. Liu Z, Wu XY, Ballinger JR, Bendayan R. Synthesis and characterization of surface-hydrophobic ion-exchange microspheres and the effect of coating on drug release rate. *Journal of Pharmaceutical Sciences.* 2000; 89(6):807 - 817.
162. Hashizume M, Douen T, Murakami M, Yamamoto A, Takada K, Muranishi S. Improvement of large intestinal absorption of insulin by chemical modification with palmitic acid in rats. *Journal of Pharmacy and Pharmacology.* 1992; 44:555-559.
163. Whittaker RG, Hayes PJ, Bender VJ. A gentle method of linking Tris to amino acids and peptides. *Peptide Research.* 1993; 6:125-128.
164. Setoh K, Murakami M, Araki N, Fujita T, Yamamoto A, Muranishi S. Improvement of transdermal delivery of tetragastrin by lipophilic modification with fatty acids *Journal of Pharmacy and Pharmacology.* 1995; 47(10):808-811.
165. Fujita T, Fujita T, Morikawa K, Tanaka H, Iemura O, Yamamoto A, et al. Improvement of intestinal absorption of human calcitonin by chemical modification with fatty acids: Synergistic effects of acylation and absorption enhancers. *International Journal of Pharmaceutics.* 1996; 134(1-2):47-57.

166. Linter K, Peschard O. Biologically active peptides: from a laboratory bench curiosity to a functional skin care product *International Journal of Cosmetic Science*. 2000; 22:207-218.
167. Osborne R, inventor; Personal care compositions. US patent 20070020220. 2006.
168. Lintner K, inventor; Lys-thr dipeptides and their use. France patent WO/2006/114657. 2006.
169. Marie-christine S, inventor; Exsymol S.A.M. (Monaco, MC), assignee. Citrullinylarginine dipeptide analogs and their dermatological uses as care and treatment agents US patent 7270824. 2007.
170. Acetyl-dipeptide-1 cetyl ester. 01/08/09]. Available from: <http://www.cosmeticsdatabase.com>.
171. Dipeptide-2. 05/08/09]. Available from: <http://www.truthinaging.com/ingredients/dipeptide-2/>.
172. Namjoshi S, Chen Y, Edwards J, Benson HAE. Enhanced transdermal delivery of a dipeptide by dermaportation. *Biopolymers Peptide Science*. 2008; 90(5):655-662.
173. Rose Li WA, Tuthill C, Pyles RB. An immunomodulating dipeptide, SCV-07, is a potential therapeutic for recurrent genital herpes simplex virus type 2 (HSV-2). *International Journal of Antimicrobial Agents*. 2008; 32(3):262-266.
174. Sidwell RW, Smee DF, Huffman JH, Bailey KW, Warren RP, Burger RA, et al. Antiviral activity of an immunomodulatory lipophilic desmuramyl dipeptide analog. *Antiviral Research*. 1995; 26(2):145-159.
175. Krivorutchenko YL, Andronovskaja IB, Hinkula J, Krivoshein YS, Ljungdahl-Ståhle E, Pertel SS, et al. Study of the adjuvant activity of new MDP derivatives and purified saponins and their influence on HIV-1 replication in vitro. *Vaccine*. 15(12-13):1479-1486.

176. Neu J, Grant MB, inventors; University of Florida Research Foundation, Inc., assignee. Arginyl-glutamine dipeptide for treatment of pathological vascular proliferation. US patent 7148199. 2006.
177. Kohler H, Klowik M, Brand O, Gobel U, Schroten H. Influence of glutamine and glycyl-glutamine on in vitro lymphocyte proliferation in children with solid tumors Supportive Care in Cancer. 2001; 9(4):261-266.
178. Yagasaki M, Hashimoto S-i. Synthesis and application of dipeptides; current status and perspectives Applied Microbiology and Biotechnology. 2008; 81(1):13-22.
179. Lin R-Y, Hsu C-W, Chen W-Y. A method to predict the transdermal permeability of amino acids and dipeptides through porcine skin. Journal of Controlled Release. 1996; 38(2-3):229-234.
180. Abla N, Naik A, Guy RH, Kalia YN. Effect of charge and molecular weight on transdermal peptide delivery by Iontophoresis. Pharmaceutical Research. 2005; 22(11):2069-78.
181. Babizhayev MA. Biological activities of the natural imidazole-containing peptidomimetics n-acetylcarnosine, carbinine and l-carnosine in ophthalmic and skin care products. Life Sciences. 2006; 78(20):2343-2357.
182. Alasbahi R, Melzig M. The In vitro Inhibition of human neutrophil elastase activity by some yemeni medicinal plants. Scientia Pharmaceutica. 2008; 76:471-483.
183. Steinbrecher T, Hrenn A, Dormann KL, Merfort I, Labahn A. Bornyl (3,4,5-trihydroxy)-cinnamate - An optimized human neutrophil elastase inhibitor designed by free energy calculations. Bioorganic & Medicinal Chemistry. 2008; 16(5):2385-2390.
184. Yasutake A, Powers JC. Reactivity of human leukocyte elastase and porcine pancreatic elastase toward peptide-4-nitroanilides containing model desmosine residues. Evidence that human leukocyte elastase is selective for crosslinked regions of elastin. Biochemistry. 2002; 20(13):3675-3679.

185. Hassal H, Johnson WH, Kennedy AJ, Roberts NA. A new class of inhibitors of human leucocyte elastase. *FEBS Letters*. 1985; 183:201-205.
186. Hornebeck W, Moczar E, Szecsi J, Robert L. Fatty acid peptide derivatives as model compounds to protect elastin against degradation by elastases. *Biochemical Pharmacology*. 1985; 34(18):3315-3321.
187. Rasoamanantena P, Moczar E, Robert L, Wei SM, Godeau G, Hornebeck W. Protective effect of oleoyl peptide conjugates against elastolysis by neutrophil elastase and kappa elastin-induced monocyte chemotaxis. *American Journal of Respiratory Cell and Molecular Biology*. 1993; 8(1).
188. Hrenn A, Steinbrecher T, Labahn A, Schwager J, Schempp CM, Merfort I. Plant phenolics inhibit neutrophil elastase. *Planta Medica*. 2006; 72(12):1127-31.
189. Wieczorek M, Gyorkos A, Spruce LW, Ettinger A, Ross SE, Kroona HS, et al. Biochemical Characterization of [alpha]-Ketoaxadiazole Inhibitors of Elastases. *Archives of Biochemistry and Biophysics*. 1999; 367(2):193-201.
190. Caccetta R, Blanchfield JT, Harrison J, Toth I, Benson HAE. Epidermal penetration of a therapeutic peptide by lipid conjugation; stereo-selective peptide availability of a topical diastereoisomeric lipopeptide. *International Journal of Peptide Research and Therapeutics*. 2006; 12(3):327-333.
191. Babu RJ, Kikwai L, Jaiani LT, Kanikkannan N, Armstrong CA, Ansel JC, et al. Percutaneous absorption and anti-inflammatory effect of a substance P receptor antagonist: Spantide II. *Pharmaceutical Research*. 2004; 21(1):108-113.
192. Christophers E, Sterry W. Psoriasis. In: *Dermatology in General Medicine*. New York: McGraw Hill; 1993. p. 489-514.
193. Manolios N, Collier S, Taylor J, Pollard J, Harrison LC, Bender V. T-cell antigen receptor transmembrane peptides modulate T-cell function and T-cell mediated disease. *Nature Medicine*. 1997; 3(1):84-88.
194. Manolios N, Ali M, Kurosaka N. 4th Australian Peptide Conference [2001. Lindeman Island, Queensland, Australia:

195. Luger TA, Brzoska T. Alpha MSH related peptides: a new class of anti-inflammatory and immunomodulating drugs. *Annals of the Rheumatic Diseases*. 2007; 66(3):52-5.
196. Kim J. In: Broad spectrum antimicrobial peptide for the treatment of acne and skin cancer. 2003 UCLA technology.
197. Mize NK, Buttery M, Ruis N, Leung I, Cormier M, Daddona P. Antiflammin 1 peptide delivered noninvasively by iontophoresis reduces irritant-induced inflammation in vivo. *Experimental Dermatology*. 1997; 6:181-185.
198. Christophers E, Kligman AM. Visualization of the cell layers of the stratum corneum. *Journal of Investigative Dermatology*. 1964; 42:407-409.
199. Egelrud T. Purification and preliminary characterization of stratum corneum chymotryptic enzyme: a proteinase that may be involved in desquamation. *Journal of Investigative Dermatology*. 1993; 101(2):200-204.
200. Horie N, Fukuyama K, Ito Y, Epstein WL. Detection and characterization of epidermal proteinases by polyacrylamide gel electrophoresis. *Comparative Biochemistry and Physiology*. 1984; 77B:349-353.
201. Choi H, Flynn GL, Amidon GL. Transdermal delivery of bioactive peptides: the effect of n-decylmethylsulfoxide, pH and inhibitors on enkephalin metabolism and transport. *Pharmaceutical Research*. 1990; 7 1099-05.
202. Niven GW. The characterization of two aminopeptidase activities from the cyanobacterium *Anabaena flos-aquae*. *Biochimica et Biophysica Acta* 1995; 1253(2):193-198.
203. Simat TJ, Steinhart H. Oxidation of Free Tryptophan and Tryptophan Residues in Peptides and Proteins. *Journal of Agricultural and Food Chemistry*. 1998; 46(2):490-498.
204. Altenbach M, Schnyder N, Zimmermann C, Imanidis G. Cutaneous metabolism of a dipeptide influences the iontophoretic flux of a concomitant uncharged permeant. *International Journal of Pharmaceutics*. 2006; 307(2):308-317.

205. Benson HAE, Caccetta R, Chen Y, Kearns P, Toth I. Transdermal delivery of a tetrapeptide: Evaluation of passive diffusion *Letters in Peptide Science*. 2003; 10(5-6):615-620.
206. Afouna MI, Fincher TK, Khan MA, Reddy IK. Percutaneous permeation of enantiomers and racemates of chiral drugs and prediction of their flux ratios using thermal data: A pharmaceutical perspective. *Chirality*. 2003; 15:456-465.
207. Brittain HG. Crystallographic consequences of molecular dissymmetry. *Pharmaceutical Research*. 1990; 7(7):683-690.
208. Heard CM, Brain KR. Does solute stereochemistry influence percutaneous penetration? *Chirality*. 1995; 7:305-309.
209. Benezra C, Stampf JL, Barbier P, Ducombs G. Enantiospecificity in allergic contact dermatitis. *Contact Dermatitis*. 1985; 13:110-114.
210. Suedee R, Brain KR, Heard CM. Differential permeation of propranolol enantiomers across human skin in vitro from formulations containing an enantioselective excipient. *Chirality*. 1999; 11:680-683.
211. Miyazaki K, Kaiho F, Inagaki A, Dohi M, Hazemoto N, Haga M, et al. Enantiomeric difference in percutaneous penetration of propranolol through rat excised skin. *Chemical and Pharmaceutical Bulletin*. 1992; 40:1075.
212. Ahmed S, Imai T, Otagiri M. Evaluation of stereoselective transdermal transport and concurrent cutaneous hydrolysis of several ester prodrugs of propranolol: mechanism of stereoselective permeation. *Pharmaceutical Research*. 1996; 13(10):1524-1529.
213. Asada H, Douen T, Waki M, Adachi S, Fujita T, Yamamoto A, et al. Absorption characteristics of chemically modified-insulin derivatives with various fatty acids in the small and large intestine. *Journal of Pharmaceutical Sciences*. 1995; 84:682-687.
214. E Touitou, Chow DD, Lawter JR. Chiral beta blockers for transdermal delivery. *International Journal of Pharmaceutics*. 1994; 104:19-28.

215. Schuetz YB, Naik A, Guy RH, Vuaridel E, Kalia YN. Transdermal iontophoretic delivery of vapreotide acetate across porcine skin in vitro. *Pharmaceutical Research*. 2005; 22(8):1305-12.
216. Walter K, Kurz H. Binding of drugs to human skin: influencing factors and the role of tissue lipids. *Journal of Pharmacy and Pharmacology*. 1988; 40(10):689-693.
217. Infante MR, Pérez L, Pinazo A, Clapés P, Morán MC, Angelet M, et al. Amino acid-based surfactants. *Comptes Rendus Chimie*. 7(6-7):583-592.
218. Surfactin. Wikipedia[24/10/09]. Available from: <http://en.wikipedia.org/wiki/Surfactin>.
219. Ashton P, Walters KA, Brain KR, Hadgraft J. Surfactant effects in percutaneous absorption I. Effects on the transdermal flux of methyl nicotinate. *International Journal of Pharmaceutics*. 1992; 87(1-3):261-264.
220. Baby AR, Lacerda ACL, Velasco MVR, Lopes PS, Kawano Y, Kaneko TM. Evaluation of the interaction of surfactants with stratum corneum model membrane from *Bothrops jararaca* by DSC. *International Journal of Pharmaceutics*. 2006; 317(1):7-9.
221. Rona C, Vailati F, Berardesca E. The cosmetic treatment of wrinkles. *Journal of Cosmetic Dermatology*. 2004; 3:26-34.
222. Bissett DL. Common cosmeceuticals. *Clinics in Dermatology*. 2009; 27:435–445.
223. Fields K, Falla TJ, Rodan K, Bush L. Bioactive peptides: signaling the future. *Journal of Cosmetic Dermatology*. 2009; 8:8-13.
224. Foldvari M, Attah-Poku S. Palmitoyl derivatives of interferon alpha: potent for cutaneous delivery. *Journal of Pharmaceutical Sciences*. 1998; 87:1203-8.
225. Blanes-Mira C, Clemente J, Jodas G. Australian Society of Cosmetic Chemists Annual Conference [In: A synthetic hexapeptide (Argireline) with antiwrinkle activity., 2003

226. Bogdanowich-Knipp SJ, Chakrabarti S, Williams TD, Dillman RK, Siahaan TJ. Solution stability of linear vs. cyclic RGD peptides. *Journal of Peptide Research*. 1999; 53(5):530-541.
227. Gudmundsson OS, Nimkar K, Gangwar S, SIAHAAN T, Borchardt RT. Phenylpropionic acid-based cyclic prodrugs of opioid peptides that exhibit metabolic stability to peptidases and excellent cellular permeation. *Pharmaceutical Research*. 1999; 16(1):16-22.
228. Borchardt RT. Optimizing oral absorption of peptides using prodrug strategies. *Journal of Controlled Release*. 1999; 62:231-238.
229. Borel JF. History of the discovery of cyclosporin and of its early pharmacological development. *Wien Klin Wochenschr*. 2002; 114(12):433-507.
230. Shi Y. Beyond skin color: emerging roles of melanin-concentrating hormone in energy homeostasis and other physiological functions. *Peptides*. 2004; 25:1605-11.
231. Oudhoff MJ, Kroeze KL, Nazmi K, Veerman ECI. Structure-activity analysis of histatin, a potent wound healing peptide from human saliva: cyclization of histatin potentiates molar activity 1000-fold. *The FASEB Journal*. 2009.
232. Kwon Y-U, Kodadek T. Quantitative comparison of the relative cell permeability of cyclic and linear peptides. *Chemistry & Biology*. 2007; 14:671-677.
233. Anigbogu ANC, Williams AC, Barry BW, Edwards HGM. Fourier transform raman spectroscopy of interactions between the penetration enhancer dimethyl sulfoxide and human stratum corneum. *International Journal of Pharmaceutics*. 1995; 125(2):265-282.
234. Schuetz YB, Naik A, Guy RH, Kalia YN. Emerging strategies for the transdermal delivery of peptide and protein drugs. *Expert Opinion on Drug Delivery*. 2005; 2(3):533-548.

235. Henchoz Y, Abla N, Veuthey J-L, Carrupt P-A. A fast screening strategy for characterizing peptide delivery by transdermal iontophoresis. *Journal of Controlled Release*. 2009; 137(2):123-129.

236. Wilkinson SC, Maas WJM, Nielson JB, Greaves LC, Sandt JJMVD, Williams FM. Interactions of skin thickness and physicochemical properties of test compounds in percutaneous penetration studies. *International Archives of Occupational and Environmental Health* 2006; 79(5):405-413.

237. Guy RH, Hadgraft J. *Transdermal drug delivery: developmental issues and research initiatives*. Marcel Dekker; 1989.

"Every reasonable effort has been made to acknowledge the owners of copyright material. I would be pleased to hear from any copyright owner who has been omitted or incorrectly acknowledged."

Chapter 8.

Appendix

Poster presentations

1. Sarika Namjoshi, Yan Chen, Joanne Blanchfield, Istvan Toth and Heather Benson, Skin permeability and biological activity of a therapeutic peptide and its lipoamino acid conjugates. Poster presentation at 36th annual meeting and exposition of the controlled Release Society, Bella Center, Copenhagen, Denmark, July 2009

2. Heather Benson, Sarika Namjoshi, Marina Ali and Nicholas Manolios, Cyclic peptides as potential therapeutic agents for skin disorders. Poster presentation at 1st International Conference On Circular Proteins, Herron island resort, Queensland, Australia, October 2009

3. Heather Benson, Sarika Namjoshi, Marina Ali and Nicholas Manolios, Skin permeation of an antiinflammatory peptide and analogues exhibiting improved biological efficacy and specificity. Poster presentation at 8th Australian Peptide Conference, Couran Cove, South Stradbroke Island, Queensland, Australia, October 2009

4. Sarika Namjoshi, Yan Chen, Jeffery Edwards and Heather Benson, Electromagnetophoresis: potential for enhanced skin permeation of peptides. Poster presentation at Skin and Formulation, 3rd Symposium and 10th Skin Forum, Versailles, France, March 2009

5. Heather Benson, Jeffery Edwards, Gayathri Krishnan and Sarika Namjoshi, Electromagnetophoresis: potential for enhanced skin permeation of drugs and cosmetics. Poster presentation at Skin and Formulation, 3rd Symposium and 10th Skin Forum, Versailles, France, March 2009

6. Sarika Namjoshi, Yan Chen, Jeffery Edwards and Heather Benson, Enhanced transdermal delivery of a dipeptide by Dermaportation. Poster presentation at 7th Australian Peptide Conference, Cairns, Queensland, Australia, October 2007.